Circulating MicroRNAs Associated to Solid Tumors : Study of their Potential as Biomarkers for Evaluation of Prognosis and Treatment Response

Nikiforos Ioannis Kapetanakis

université PARIS-SACLAY

UNIVERSITÉ PARIS SUD
Comprendre le monde, construire l'avenir

NNT : 2017SACLS245

THESE DE DOCTORAT
DE
L'UNIVERSITE PARIS-SACLAY
PREPAREE A
L'UNIVERSITE PARIS-SUD

ECOLE DOCTORALE N° 582
CBMS Cancérologie : biologie - médecine - santé

Spécialité de doctorat : Recherche clinique, innovation technologique, santé publique

Par

Nikiforos-Ioannis Kapetanakis

Circulating microRNAs associated to solid tumors: study of their potential as biomarkers for evaluation of prognosis and treatment response

Thèse présentée et soutenue à Villejuif, le 14 septembre 2017 :

Composition du Jury :

Pr François DAUTRY	ENS Cachan, Université Paris Sud/Paris-Saclay	Président
Dr Christophe GROSSET	U1035 INSERM, Université de Bordeaux	Rapporteur
Dr Eric BARREY	INRA, UMR 1313, Université Paris Sud/Paris-Saclay	Rapporteur
Dr Alexandra LEARY	Equipe Cancer Gynécologique, Gustave Roussy	Examinatrice
Dr Robin FAHRAEUS	UMR 1162, Hôpital Saint-Louis, Université Paris-Diderot	Examinateur
Dr Pierre BUSSON	CNRS UMR 8126, Gustave Roussy	Directeur de thèse

GUSTAVE ROUSSY
CANCER CAMPUS
GRAND PARIS

cnrs
dépasser les frontières

Signalisation Noyaux Innovations en Cancérologie
UMR 8126

Acknowledgements

In order to produce good work, one needs to be in a comfortable, motivating and "healthy" professional environment. From day 1 the research unit UMR8126 has made me feel that I am part of a team, part of a scientific family, equal among equals. So I would like to start by thanking the unit as a group, for welcoming me in a very warm way, for taking the best out of me for three and a half years, for generously giving me everything I could need to build a strong profile and succeed in the tough and demanding world of science. Feeling supported and surrounded by real friends should not be taken for granted in such a competitive domain. During my stay here I had the chance and the privilege of meeting extraordinary people, each in his/her own way, creating friendships that are not limited to the four walls of our laboratory and, hopefully, will last for a long time.

Every lab is a leaving organism; people come and go, leaving their work as a legacy, thus creating a highly dynamic situation. I will start my personal acknowledgements by the person of reference when it comes to my work: my thesis director and head of our team. Pierre, thank you for trusting me and giving me the chance to beat any pre-existing doubts, yours and mine. Thank you for taking the risk of this collaboration. I believe that it was a wise decision after all. Thank you for your patience, for your understanding, for the respect I have earned, which is not often seen at this level of collaboration. Thank you for this wonderful scientific journey, for the support and the guidance. Thank you as well for giving me the freedom to work in my own autonomous way and develop my own ideas, but also for being constantly there when I needed your advice or your point of view. A few lines are not enough to express my gratitude, but I hope that my attitude and my work throughout our collaboration were able to prove it.

Before I go deeper in the UMR8126, a big thank you to the members of my thesis committee. Dr Leary, Dr Dautry, Dr Grosset, Dr Barrey and Dr Fahraeus: thank you for accepting to evaluate my work. It is a privilege defending my thesis in front of you and an honor to receive (I hope) the title of Doctor in Cancerology by you. I will do my best not to disappoint you.

My dear Aurore, thank you for being my partner in crime, thank you for being my friend and my ally, but also a maternal figure to me. Thank you for your friendship, for your constant help and, of course for all the nice moments we shared together. Valentin and Tram, thank you for our collaboration, as well as for the moments of laughter that we shared. I'm really happy to know that this laboratory has PhD students with great potential and dedication. Julie, thank you for contributing to the last chapters of my projects, for adding a pleasant note in the

lab's routine. Time for the blond duo: Eugénie and Claire, my mentors. A huge thank you to both of you for welcoming me to this team and for doing everything so that I can feel comfortable at the beginning. Your absence during the second half of my PhD has been more than felt, both in a scientific and a human way. Thank you Natalie, Mathieu and Benjamin for our collaboration and help, whenever needed and for letting me contribute to your project as well. To Gaëlle, Delphine and Lydia, the interns who worked in our lab: thank you for giving me the chance to contribute to your scientific formation.

Jérémy, Caroline, Anamarija and Diego: I don't really know what to say here. You are my FRIENDS and I feel deeply honored for that. You opened your hearts and homes for me, as I did for you. We shared moments that we will remember forever, that we keep narrating, laughing every single time. There were tough and difficult moments, but I think that those moments made our friendship strong and genuine and I sincerely wish that we will stay in touch and keep seeing each other no matter where we work in the future. Because of this friendship, the feeling to be member of a strong team, I never felt alone during my PhD. You are all people of a rare quality and I am eager to see you shine in the future, as you are already shining.

Thank you Marc and Joëlle, for believing in me and giving me the chance to work in your unit. Thank you for your support and your guidance throughout this journey, but above all, thank you for creating the ideal professional conditions in the context of this unit. It has been an experience that I have thoroughly enjoyed.

Thank you Justine, Loëtitia, Carla, Eliana, Claire MJ, Yara, Rawan, Anastasia, Sergiu for all the nice and funny moments that we shared during that time. Thank you Aude for your kindness, your humor and your help.

Muriel: a huge thank you for your help, both inside and outside of this lab. Thank you for your rare kindness and your constant will to help and support. I am really grateful to you.

Thank you to all the lab directors of our unit, for our pleasant coexistence and your contribution to the great atmosphere of this unit. Thank you to the doctors of Gustave Roussy, as well to Gwénaël Le Teuff for kindly contributing to my work.

Last but not least: A big thank you to my family. Mom, Dad, Kimon. There may be several kilometers between us but I am extremely happy and relieved to know that you are always by my side, with your heart and soul. There are no words able to express my gratitude; I hope

that my actions do it, little by little. Thank you for giving me roots, to know where I come from and wings, to go wherever I want.

Statue of a mouse knitting a DNA double helix in Novosibirsk, Russia. Dedicated to all animals that have given and keep giving their life every day for the progress of scientific research. Their contribution and their blood tax should never be ignored by the science community. Without them, very little progress would have been achieved.

Table of contents

Summary

This doctorate thesis provides an insight into the biology and dynamics of circulating microRNAs, demonstrating their potential to become crucial biomarkers for a better surveillance and prognosis of cancer. MicroRNAs (miRNAs) are small, single-stranded non-coding RNAs, 19-25 nt long, with a key role in the post-transcriptional regulation of gene expression, repressing the translation of target mRNAs through partial base-pair complementarity with their 3'-UTR. They can be released in the extracellular medium, being protected from RNases by association with various transporters and reach body fluids and circulation, participating in intercellular communication. Their remarkable stability and manageable diversity in circulation, as well as the fact that they derive from both malignant and normal cells make them very attractive biomarker candidates, potentially reflecting tumor state and dynamics. We have been focusing on ovarian (OvCa) and nasopharyngeal (NPC) carcinomas, attempting to elucidate the relation between plasma miRNAs and the prognosis of OvCa after first-line treatment, as well as to evaluate their use in the detection of early response of NPC tumors to treatment. Serous epithelial ovarian carcinoma is the most frequent ovarian and the most aggressive gynecologic malignancy. The absence of early symptoms and the insufficiency of modern means to accurately map residual disease and assess treatment outcome highlight the need for new diagnostic and prognostic biomarkers. Using sequential plasma samples from OvCa patients before and after first-line treatment, we studied a pre-selection of miRNAs, comparing them to samples from benign pelvic lesions and healthy women. MiR-200b exhibited a distinct higher concentration in malignant samples before treatment compared to both non-cancerous groups. Pre- and post-treatment assessment of miR-200b in parallel with the standard biomarker CA125 revealed distinct variations and a significant correlation of miR-200b variation with the progression-free survival (PFS) of the patient. We suggest that miR-200b could eventually be used as a supplementary biomarker for estimation of the remission upon treatment completion. Nasopharyngeal carcinoma (NPC) on the other hand is a tumor consistently associated to latent Epstein-Barr virus (EBV) infection of the malignant cells, presenting a unique geographical incidence pattern. The deep position of the tumor makes it tough to access surgically, with biomarkers assessing different therapeutic approaches being greatly needed. Studying a new oral form of the demethylating agent 5-azacytidine, proven to be promising for one third of NPC patients receiving it as a monodrug, we attempted to identify impact of the drug on the expression of viral miRNAs and proteins. Despite the latent viral infection, viral miRNAs are abundantly expressed,

attracting interest in EBV-associated malignancies. Treating four in vivo developed NPC tumor models for two weeks, we observed clear response in two of them, in a dose-dependent manner. Protein analysis showed an induction of the immediate-early lytic protein BZLF1, solidifying previous evidence of partial activation of the viral lytic cycle by 5-azacytidine. MiRNA analysis confirmed robust expression of BART and absence of BHRF1 miRNAs at baseline status of NPC. Upon treatment, we observed an induction of BHRF1 miRNAs in both tumor and plasma of treated mice. This induction was successfully validated in a following one-week treatment and completed by a recorder de novo expression of the BHRF1 mRNA, transcribed within the BHRF1 miRNA loci. A weaker induction of BHRF1 miRNAs was also recorded after treatment with standard chemotherapeutic agents, suggesting a potential clinical utility of these miRNAs as circulating biomarkers for detection of early response to treatment. We are further working to confirm this induction by chemotherapy and extend our study to plasma samples derived from treated patients.

French Summary

Cette thèse de doctorat est une étude de la biologie et de la dynamique des microARN circulants, démontrant leur potentiel comme biomarqueurs pour l'amélioration de la surveillance et de l'évaluation pronostique dans le cancer. Il s'agit des ARN non codants simple-brin, d'environ 19-25 nt de longueur. Ils jouent un rôle clé dans la régulation de l'expression génomique au niveau post-transcriptionnel, en ciblant et réprimant la traduction des ARNm par complémentarité partielle avec leur 3'-UTR. Ils sont également libérés dans le milieu extracellulaire, la circulation et les liquides biologiques. Leur stabilité remarquable et leur diversité dans la circulation, ainsi que leur provenance maligne ou normale, en font des candidats biomarqueurs intéressants, reflétant potentiellement l'état et la dynamique d'une tumeur. Nous nous sommes focalisés sur les carcinomes ovariens (OvCa) et nasopharyngés (NPC), essayant d'élucider la relation entre les miARN plasmatiques et le pronostique des OvCa après une première ligne de traitement, ainsi que d'évaluer leur utilité dans la détection d'une réponse précoce des NPC au traitement. Le carcinome ovarien séreux est la malignité gynécologique la plus agressive. L'absence de symptômes précoces et l'insuffisance des moyens modernes pour détecter la maladie résiduelle et évaluer les résultats du traitement signalent le besoin de nouveaux biomarqueurs diagnostiques et pronostiques. En utilisant des prélèvements plasmatiques séquentiels OvCa avant et après traitement, nous avons étudié un groupe de miARN, en comparaison à des lésions pelviennes bénignes et des femmes en bonne santé. MiR-200b avait une concentration nettement plus élevée dans les échantillons malins avant traitement par rapport aux deux groupes non cancéreux. L'analyse pré- et post-traitement de miR-200b en parallèle avec le biomarqueur standard CA125 a révélé des variations distinctes et une corrélation significative de la variation de miR-200b avec le temps de rémission (PFS). Nous concluons que miR-200b pourrait éventuellement être utilisé comme biomarqueur supplémentaire pour l'estimation de la rémission à la fin du traitement. Le carcinome nasopharyngé (NPC) d'autre part est une tumeur constamment associée à une infection latente des cellules malignes par le virus d'Epstein-Barr (EBV), présentant une distribution géographique particulière. La position de la tumeur rend difficile l'approche chirurgicale, les biomarqueurs évaluant différentes approches thérapeutiques étant de grande importance. Etudiant une nouvelle forme orale de l'agent démethylant 5-azacytidine, démontrée prometteuse pour un tiers des patients NPC qui l'ont reçue, nous avons essayé d'évaluer son impact sur l'expression des miARN et des protéines virales. Malgré l'infection virale latente, les miARN viraux sont

abondamment exprimés. En traitant pendant deux semaines quatre modèles de tumeur NPC développés in vivo, nous avons observé une réponse nette dose-dépendante dans les deux. L'analyse protéique a montré une induction de la protéine activatrice du cycle lytique BZLF1, renforçant les preuves antérieures d'induction partielle du cycle lytique viral par la 5-azacytidine. L'analyse des miARN a confirmé l'expression robuste des miARN BART et l'absence des miARN BHRF1 dans les NPC sans traitement. Lors du traitement, nous avons détecté les miR-BHRF1 à la fois dans la tumeur et le plasma des souris traitées. Cette induction a été validée par un traitement ultérieur d'une semaine qui a aussi mis en évidence l'induction de l'expression de l'ARNm de BHRF1, transcrit par le locus situé parmi les miARN BHRF1. Une induction de ces miARN a été observée après traitement par des agents de chimiothérapie, suggérant une utilité clinique potentielle des miR-BHRF1 comme biomarqueurs pour l'évaluation précoce de l'efficacité du traitement. Notre objectif actuel est de valider cette induction par chimiothérapie et étendre nos études au plasma humain.

List of abbreviations

AML: acute myeloid leukemia

BART: BamHI-A region rightward transcript

BHRF1: BamHI fragment H rightward open reading frame 1

BL: Burkitt's lymphoma

BOT: borderline ovarian tumor

BRCA: breast cancer antigen

CA125: cancer antigen 125

CpG: cytosine-guanine dinucleotide

CRC: colorectal cancer

CT: computed tomography

Ct: cycle threshold

ddPCR: droplet-digital PCR

dsRNA: double-stranded RNA

EA: early antigen

EBER: Epstein–Barr virus-encoded small RNA

EBV: Epstein-Barr virus

EMT: Epithelial-to-Mesenchymal Transition

EV: extracellular vesicles

FRET: Förster resonance energy transfer or fluorescence resonance energy transfer

GTP: guanosine triphosphate

HBOC: hereditary breast-ovarian cancer (syndrome)

HDAC(i): histone deacetylase (inhibitors)

HGSC: high-grade serous carcinoma

HLA: human leukocyte antigen

HPV: human papilloma virus

IgA: immunoglobulin A

IMRT: intensity modulated radiation therapy

IP: intraperitoneal

IV: intravenous

LCL: lymphoblastoid cell lines

LGSC: low-grade serous carcinoma

LOH: loss of heterozygosity

MET: mesenchymal-to-epithelial transition

MHC: major histocompatibility complex

miRNA: microRNA

MRI: magnetic resonance imaging

mRNA: messenger RNA

MVBs: multivesicular bodies

NPC: nasopharyngeal carcinoma

OSE: ovarian surface epithelium

OvCa: ovarian cancer

PFS: progression-free survival

RT-(q)PCR: reverse-transcription (quantitative) polymerase chain reaction

SNP: single-nucleotide polymorphism

ssRNA: single-stranded RNA

TLR: Toll-like receptor

TNM: NPC tumor staging system (T for tumor, N for nodal metastases, M for distant metastases)

TR: terminal repeat

UTR: untranslated region

VCA: viral capsid antigen

List of Figures and Tables

INTRODUCTION

Chapter 1: The microRNAs

A doctoral thesis tells a story. It's the story of three or more years dedicated to the deep and analytical study of a specific scientific field. As every story, it has its own characters, others with a major and others with a minor role. Here, I will start by introducing the protagonists of the story I will be narrating: microRNAs. Their existence and function became widely known at the dawn of the new millennium, instantly attracting scientific attention and interest, due to their significance in the fine tuning of gene expression, their high degree of conservation among species and their potential therapeutic use. Their biology, biogenesis, regulation and action, as well as the association of altered miRNA profiles with malignant phenotypes are thoroughly presented in the beginning of this thesis. However, the core of this work and what has been fueling our research lies in a surprising finding that followed later: their extracellular liberation, remarkable stability and detection in body fluids and especially in circulation. These features, along with their potential to reflect an abnormal phenotype in terms of unusual kinetics outside of the cells and the relatively easy procedure to obtain and analyze blood and other fluids, promoted miRNAs to top candidate biomarkers for the diagnosis and surveillance of various diseases, with cancer having a central spot. With numerous advances taking place every day in the field of cancer treatment, the need of strong reliable biomarkers for the assessment of their efficacy grows exponentially, in the context of an emerging tailor-made, personalized approach of a patient's cancer. Our work extends on two highly different types of cancer, ovarian and nasopharyngeal, linked by the difficulty to evaluate tumor evolution under a selected treatment. The following work is an attempt to explore how circulating extracellular miRNAs could be used in order to achieve a more accurate understanding of tumor dynamics and evolution under various therapeutic modalities, leading to the selection of the best possible approach. Therefore, the first chapter introduces the reader into the biology of miRNAs and their extracellular existence, while chapters 2 and 3 present the molecular basis, as well as the major challenges of ovarian and nasopharyngeal carcinomas respectively. Concerning nasopharyngeal carcinoma, its strong association with the persistent presence of the Epstein-Barr virus in the malignant cells prompted us to explore the potential of viral miRNAs to reflect the state of a tumor. As a consequence, a fourth and final chapter stands alone, in order to secure a sufficient understanding of the biology of this malignancy's viral component…

History

MicroRNAs (abbreviated as miRNAs) are a distinct class of small single-stranded non-coding RNAs, with an average length of 21-25 nucleotides (nt) [1]. The term small RNAs refers to a broader group of RNAs with a length inferior to 200 nt, containing transfer RNAs (tRNAs), ribosomal RNAs (rRNAs), small interfering RNAs (siRNAs), small nucleolar RNAs (snoRNAs) and of course miRNAs. These groups share the common characteristic of not coding for proteins (like long non-coding RNA besides). They can be distinguished and classified by their structure and function, as well as their pathway of maturation. The only exception is found between miRNAs and siRNAs, which are biochemically and functionally indistinguishable, as they have the same length, with 5'-phosphate and 3'-hydroxyl ends and they interact with the same proteins, playing the same role [2]. The difference is found in their biogenesis, as miRNAs derive from the double-stranded region of 60-70 nt RNA hairpin precursors, whereas siRNAs are generated from long double-stranded RNA (dsRNA) [3]. The first miRNA was reported in the nematode Caenorhabditis elegans, in 1993, and was named lin-4 [4]. It was found to regulate the expression of lin-14 mRNA in a way later characterized as the miRNA-mediated post-transcriptional regulation of genomic expression. To date, 35828 mature microRNAs have been identified, according to the latest updates in miRBase, in 223 species including animals, plants and even viruses. Registered mature human miRNAs have exceeded 2000 (2588 in the 21st release of the database, http://www.mirbase.org/).

Structure and biogenesis

MiRNA precursors are commonly found in clusters through many different genomic loci, most frequently emerging from intergenic regions and introns of protein-coding genes [5]. Rare cases of exon-derived miRNAs have also been reported, like miR-198, emerging from the 3' untranslated region (3' UTR) of the gene coding for FSTL1 (follistatin-like 1 protein) [6]. They serve, thus, as a first-class proof that non-coding genomic regions are far from being "junk DNA", a term previously used to describe them. Precursors in the context of the same cluster are often tandemly co-transcribed (figure 1A). Furthermore, precursors of the same miRNA can be found in more than one locus and in different clusters throughout the genome. Their generation and maturation is a complex enzymatic procedure, partially depending on their origins. The microRNA precursors which are localized in introns of protein-coding genes are transcribed from the same promoter as the primary mRNA, while precursors found in intergenic regions might have their own promoters [7]. The former are transcribed by RNA polymerase II (pol II), the polymerase responsible for the DNA to mRNA transition, as part of

the pre-mRNA transcript [8]. The latter have been shown to be transcribed either by RNA pol II, or by RNA pol III, involved in the transcription of various small non-coding RNAs [9, 10].

In animals, primary microRNAs, also called pri-miRNAs, transcribed from intergenic regions are long RNAs (several kilobases) that fold back on themselves to form stem-loop structures, also called hairpins, with single stranded ends in both extremities (figure 1B). The following double-stranded stem ends in a single-stranded 10-bp loop. The first step of miRNA maturation is the enzymatic cleavage of pri-miRNAs, resulting to the liberation of the 60-70 nt hairpin structures, named pre-miRNAs (miRNA precursors). The recognition and cleavage of pre-miRNAs from the pri-miRNA is conducted by the so-called "microprocessor complex", comprised of the RNase III endonuclease Drosha and the double-stranded RNA-binding protein DiGeorge syndrome Critical Region gene 8 (DGCR8) [11, 12]. DGCR8 recognizes the ssRNA-dsRNA junction across the pri-miRNA, guiding Drosha towards these sites. Drosha cuts the stem, approximately 11 bp from the junction, liberating the 60-70bp pre-miRNAs with a 5′-phosphate group and an approximately 2 nt 3′ overhang [13]. Pre-miRNAs are subsequently exported to the cytoplasm by association with the nucleocytoplasmic transporter factor Exportin-5 (EXP5) and RanGTP [14, 15]. According to the proposed model, recognition of the hairpin structure by EXP5 leads to co-operative binding to both the precursor and the GTP-associated co-factor Ran. The formed complex is transported outside of the nucleus through the nuclear pore complex and reaches the cytoplasm. There, the pre-miRNA is released from the complex by hydrolysis of the GTP [16] (maturation pathway shown in figure 1C).

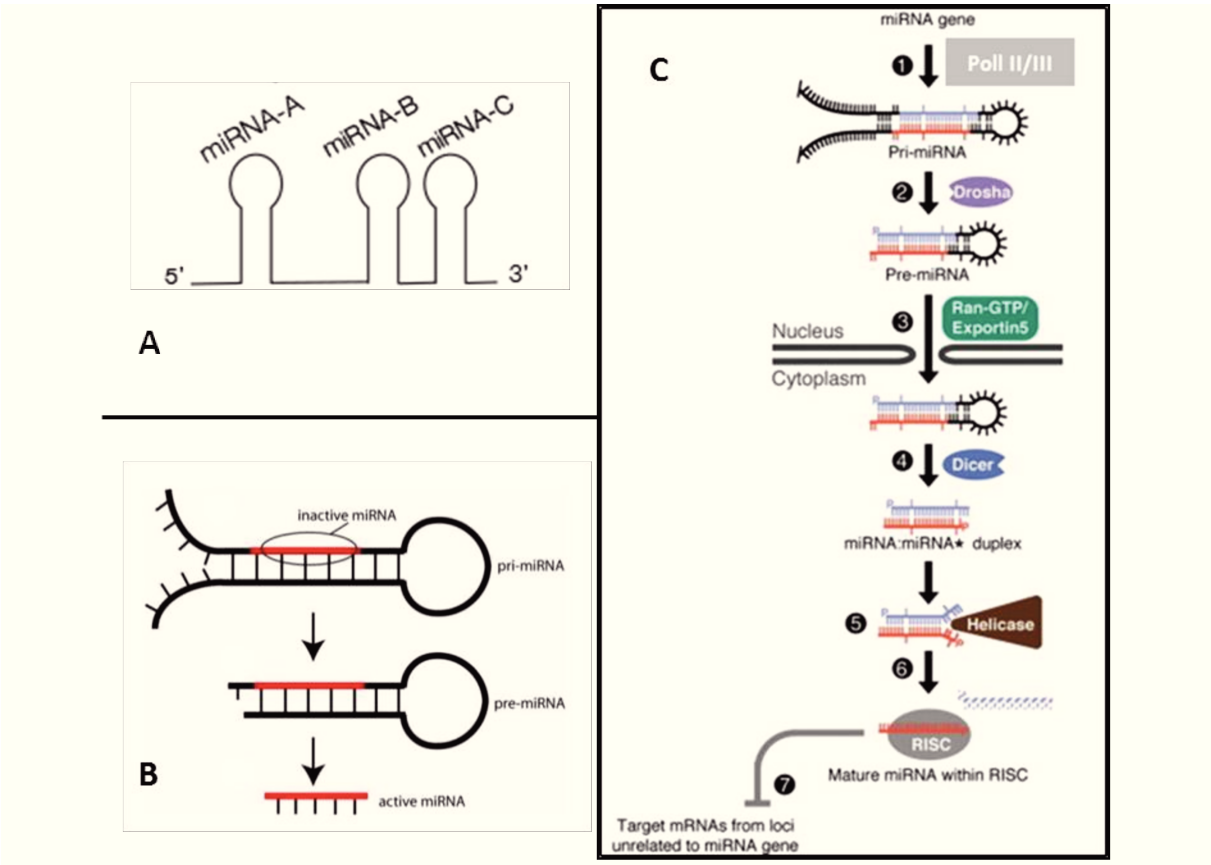

Figure 1: A) Tandemly co-transcribed pri-miRNAs, B) Forms of miRNA during maturation and C) Biogenesis of miRNAs (supplemented, from D. Bartel Cell 2004 [3]).

For miRNAs produced by intronic regions, the procedure has not been entirely elucidated. MiRNA-including introns (mirtrons) are released from the pre-mRNA transcript following splicing by the spliceosomal components, but it is not clear if this step generates directly hairpin structures, or a pri-miRNA which is further processed by the "microprocessor" in order to generate pre-miRNAs. Upon reaching the cytoplasm, pre-miRNAs are further processed by the cytoplasmic endonuclease RNase III Dicer-1 (Dicer-2 for siRNAs [17]), which specifically recognizes and cuts the stem approximately 22 nt from the pre-miRNA end [18, 19]. Mature, functional miRNAs can be derived from either the 5' or the 3' arm of a pre-miRNA and are denoted 5p or 3p, based on their origin [1]. Dicer is a highly conserved protein among most eukaryotic organisms and in humans it is closely associated with two proteins: the trans-activation response RNA-binding protein (TRBP) and the protein kinase interferon-inducible double-stranded RNA-dependent activator (PRKRA or PACT). Dicer-mediated cleavage eliminates the loop-containing part and leaves the mature miRNA attached to its complementary strand, named passenger strand. Following Dicer-catalyzed cleavage, the double-stranded miRNA is incorporated to the assembled RNA-induced silencing

complex (RISC), mainly containing one of the 4 members of the Argonaute (AGO) protein family (AGO1, AGO2, AGO3, AGO4) [20]. The RISC can be found either diffusely in the cytoplasm, or in dense cytoplasmic structures called P-bodies, where mRNAs undergo decapping, deadenylation and degradation [21]. TRBP and PRKRA seem to contribute to the formation of RISC. Once incorporated to the complex, the two strands are separated, by a helicase-member of the complex, and the strand with the less thermodynamically stable 5' end (guide strand) stays attached to AGO and eventually to RISC, as the mature miRNA. The passenger strand is removed by the endonucleolytic activity of the AGO protein, leading to its degradation [22, 23]. AGO binds the 3' end of the mature miRNA through a PAZ domain, while interacting with the 5' end through another RNA-binding domain called PIWI. All 4 human AGO proteins described so far have the ability to mediate both translation repression of mRNA on ribosomes and mRNA decay in P-bodies. However, only AGO2 is capable of directly cleaving mRNA in the cytoplasm [24]. Further details will not be presented here, but can be found reviewed by MacFarlane and Murphy (2010) [25], as well as by Wahid et al (2010) [26].

Role

MicroRNAs may be tiny molecules, but they possess a major power: the ability to specifically regulate gene expression at the post-transcriptional level. Associated with the RISC complex (miRISC format), miRNAs target and repress the translation of a vast number of mRNAs, via base complementarity [27, 28]. This RNA-mediated inhibition of gene expression and translation is widely known as RNA interference, or RNAi, having been the object of the 2006 Nobel Prize in Physiology or Medicine. Acting like a navigator, miRNAs guide the activated RISC towards an mRNA, forming Watson-Crick base-pairs with the 3'UTR of the coding transcript or, rarely, with a sequence located in the 5'UTR or even inside the coding region. In animals, most miRNA-binding sites are found in multiple copies in the 3'UTR of the target mRNAs. This complementarity is crucial for the recognition of the target and its binding by the RISC complex and in most cases is a partial complementarity. More specifically, it relies heavily on the perfect complementarity between the nucleotides 2-8 from the 5' end of the miRNA and the target mRNA. This sequence is called the "seed" and its 100% complementary with the target sequence in animals. "Seed-like" regions have also been identified in more recent studies, at the nucleotides 13-16 from the 3' end of the miRNA, having the same role as the 5' dominant "seed" regions, but being less frequent in mammalians. A single base difference in the sequence of this seed region may completely

change the miRNA's target. For instance, miR-96 and miR-182 share the same seed sequence from the second until the seventh nucleotide, but their eighth nucleotide is different. This difference is enough to prevent them from targeting the same mRNA, as miR-96 downregulated Glypican-3, a heparan-sulfate proteoglycan frequently upregulated in liver malignancies such as hepatocellular carcinoma (HCC), but miR-182 was unable to do so [29]. In most cases, the AGO-containing complex scans the mRNA sequence and, upon recognition of the "seed" sequence, establishes an initial hybridization with the nucleotides 2-4 of the guide miRNA, eventually resulting to a full hybridization until the 8^{th} nucleotide. The fixation of the RISC complex on mRNAs inhibits their translation either by blocking a step of the initiation or elongation procedure, or by destabilizing their structure, leading to the 5' decapping and the deadenylation of their poly(A) tail. The final step in this case is the degradation of the target RNA, performed by exonucleases located at the P-bodies. P-bodies (from processing bodies) are distinct foci in the cytoplasm, where mRNA decay takes place. They consist of the main enzymes catalyzing their decapping and degradation, mainly GW182, Argonaute (AGO), decapping enzymes and RNA helicases. The first two interact with each other by domains rich in glycine/tryptophan repeats, linking the RISC complex to the P-bodies. Apart from decay, mRNAs can be also temporarily stocked in these foci, awaiting re-initiation of translation.

Base pairing and type of regulation

The mechanisms of miRNA gene regulation are not very clear yet, although different models have been proposed. As a brief reminder regarding the initiation of translation, the process is started when a subunit of the eIF4F complex, eIF4E recognizes the 5' terminal cap of the mRNA. Two other subunits of the complex, eIF3 and eIF4G interact to assemble the 40S ribosomal subunit at the 5' end of the mRNA and the formation of the preinitiation complex. The same two subunits interact with the polyA-binding protein PABP1, resulting to the circularization of the mRNA. The elongation process begins upon joining of the preinitiation complex with the 60S ribosomal subunit at the AUG codon of the mRNA. According to one of the proposed models of miRNA-mediated translational repression, miRISC promotes early ribosome dissociation from mRNAs [30]. It has been suggested that it may inhibit the joining of the 60S subunit to the preinitiation complex. Furthermore, some evidence shows that miRISC competes with eIF4E for binding to the 5'cap of the mRNA, thus blocking the initiation of translation [31]. Another model suggests that miRISC prevents mRNA circularization, while a fourth one proposes that miRNA-guided accumulation of ribosome-

free mRNAs in P-bodies lacking translation machinery may cause translation repression [32, 33].

The degree of miRNA-mRNA base complementarity defines the fate of the latter and the nature of gene silencing (figure 2). When the complementarity is partial, primarily limited to the "seed" region of the miRNA, the translation of the mRNA is reduced or inhibited in a reversible way. On the other hand, an extensive base complementarity approaching perfect results in direct mRNA degradation, by an initial cleavage of the mRNA by AGO2. RISC complexes containing other members of the Argonaute family are associated to translational repression. AGO2 cleaves the mRNA into two, followed by subsequent deadenylation by enzyme complexes comprised of Pop2, Ccr4 and Not1 and decapping, catalyzed by Dcp1 and Dcp2. The target is thus left exposed to nuclease action and undergoes both 3' to 5' and 5' to 3' degradation by the exosome complex and the Xrn1p exonuclease respectively.

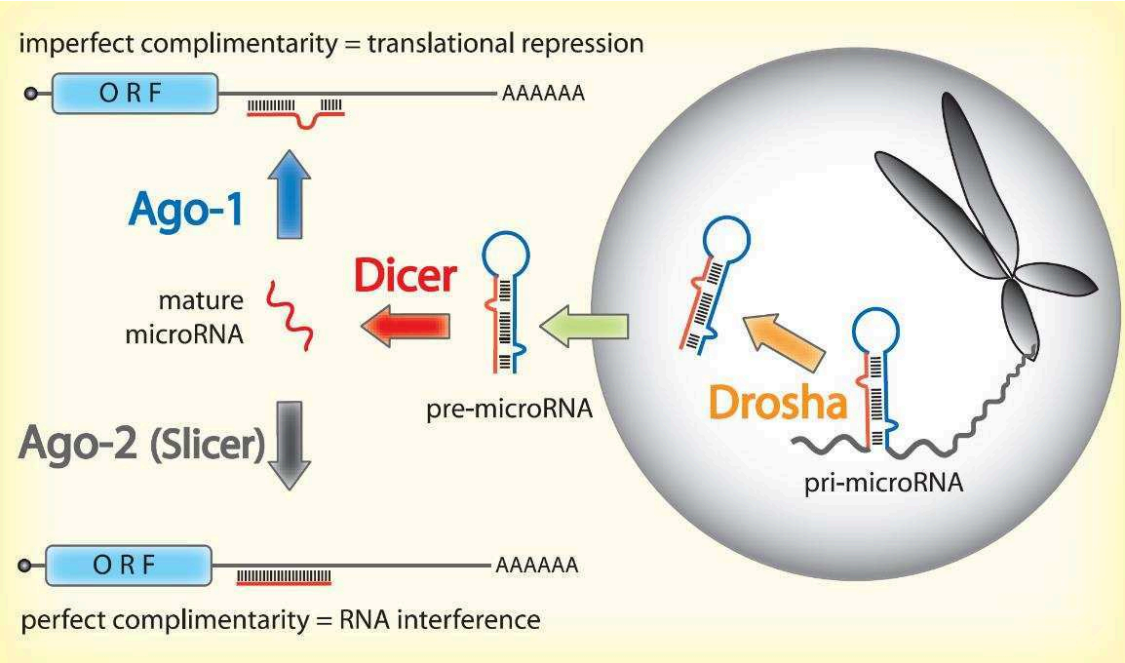

Figure 2: Mechanisms of miRNA-mediated post-transcriptional regulation, depending on the degree of base complementarity between miRNA and mRNA, as well as the member of the AGO family associated with the miRNA.

Since most target sites on the mRNA have only partial base complementarity with their corresponding microRNA, individual microRNAs may target as many as 100 different mRNAs. Moreover, individual mRNAs may contain multiple binding sites for different microRNAs, resulting in a complex regulatory network. In a 2005 study, Lewis et al analyzed the 3' UTRs of four different human genomes and found that approximately 13000

regulatory relationships were detected above the estimate of false-positive predictions, thereby implicating as miRNA targets more than 5300 human genes, which represented 30% of our gene set [34]. More recent bioinformatic analyses predict a capability of all known miRNAs up until now to regulate up to 60% of the transcriptome [35]. Here, we underline another significant distinction between miRNAs and siRNAs: whether they silence their own expression. Almost all siRNAs (regardless of their viral or other origin) silence the same locus from which they were derived. On the other hand, most miRNAs do not silence their own loci, but other genes instead.

MiRNAs and mitochondria

It is worth noting that the presence of miRNA precursors and mature miRNAs has been also confirmed in mitochondria. In a 2011 study, Barrey et al used a miRBase search tool in order to align the human mitochondrial genome to potential miRNAs, finding 33 matches for pre-miRNAs, as well as 25 mature miRNAs [36]. In situ hybridization proved the localization of the mature miR-365 and two miRNA precursors, while RT-qPCR analysis confirmed the presence of other miRNAs in the mitochondria of human myotubes. In silico analysis revealed 80 potential target sites in the mitochondrial genome, mainly concerning genes as ND6, CYTB and ND1. This work coincided with the work of Mercer et al (2011), who showed the abundant expression of small RNAs (sRNAs) in human mitochondria, constituting 3.1% of the total cellular RNAs of a length inferior to 30 nt [37]. They also proved that such small mtRNAs (mitochondrial RNAs) can derive from enzymatic cleavage of tRNAs encoded by the mitochondrial genome. During the last years, the presence of miRNAs in the mitochondria has been confirmed in other mammalian species, including rat, mouse and horse [38, 39]. Ro et al (2013) provided more evidence concerning the production of miRNAs in these organelles, further showing that small mitochondrial non coding RNAs are not products of RNA turnover, but they are the result of Dicer activity, even though not entirely [38]. One year earlier, tested cancer cell lines (HEK293 and HeLa) had also proved to produce mitochondrial miRNAs after deep sequencing of mitochondrial RNA extracts and qPCR validation [40]. Again, bioinformatic analyses supported that these miRNAs might control the expression of genes involved in apoptosis, cell cycle and nucleotide metabolism among others, mechanisms often deregulated in cancer. Last, in a recent publication, two detected mitochondrial miRNAs (miR-4485 and miR-1973) were found to be produced by enzymatic cleavage of a long ncRNA which is present in the organelles [41]. Furthermore, works indicate a deeper involvement of the mitochondria in RNA interference, through a synergistic

cooperation with the P-bodies, as reviewed by Ernoult-Lange et al (2012) [42]. More specifically, P-body formation is stimulated by accumulation of RNAi-repressed mRNAs. As explained, P-bodies contain the RNAi machinery, miRNA-repressed mRNAs and their dynamics is sensitive to the efficiency of the RNAi pathway. Huang et al (2011) reported that P-bodies establish frequent and prolonged contacts with mitochondria. Disrupting P-bodies did not affect mitochondrion morphology and function. However, disturbing mitochondrial activity strongly repressed a P-body-associated function, the silencing by small RNAs [43]. The group suggested that these findings are linked to a potential important role of the mitochondria in the assembly of the RISC complex, thus enhancing RNAi efficiency, probably by locally fueling the procedure with ATP.

MicroRNAs and Cancer

Because of their abundance, stability and tissue-specific expression, miRNAs are involved in almost all biological processes and pathways. Depending on their target, these powerful regulatory tools participate in various physiological functions. Their action has mostly been studied using the knockout gene strategy. Studies on various animal models, like Drosophila melanogaster, C. elegans or mouse, have shed a significant amount of light on the multifaceted action of miRNAs. Major functions regulated by miRNAs include early and late stages of development, cell fate and differentiation, growth and apoptosis, as well as participation in fat metabolism, hematopoiesis, secretion of hormones and various immune responses to pathogens. Interestingly, some miRNAs have been found to play a significant role in more than one cellular functions, not necessarily linked to each other. Inevitably, their misregulation is linked to the development of various diseases [44] and their implication in innovative therapeutic strategies is under extensive evaluation. Concerning their therapeutic utility, two are the fundamental ideas. The first is the so-called “miRNA replacement therapy”, involving introduction of synthetic miRNAs in a targeted tissue, in order to alter genomic expression and restore a specific function which is found defective in a certain disease. The second lies on the inhibition of some miRNAs, thus allowing an increase in the production of a protein which could have a therapeutic effect. One example is the use of an antagomiR for miR-122, meaning a synthetic miRNA with perfect complementarity, in order to block the replication of the HCV virus, responsible for human hepatitis C. As it has been shown, HCV acts as a sponge, attracting the liver-specific miR-122 produced by the host cell, in order to facilitate its replication via binding of the miRNA to two target sites of the viral genome. This leads to the de-repression of the expression of various host mRNAs targeted by

miR-122, thus providing an environment fertile for the long-term oncogenic potential of HCV [45]. Various therapeutic programs have been launched and miRNA-based approaches are currently under development and clinical evaluation, showing great potential in diagnosis and therapy.

As one can easily understand, cancer is not an exception. Microarray expression data from various different types of cancer have proven that aberrant miRNA expression is a common phenomenon in cancer. Depending on the genetic and epigenetic profile of the malignant cell, miRNAs can be found downregulated or overexpressed due to numerous alterations. A general downregulation of miRNA abundance in the context of a cancerous cell can be often the result of defects in their biogenesis pathway and the tools taking part in this complex procedure. Different human tumors have exhibited reduced Dicer1 expression levels [46-48], as a consequence of genetic loss, epigenetic silencing or frame-shift mutations. Mutations in Drosha or Exportin-5 have also been mentioned to result in reduced levels of miRNAs in cancer, trapping miRNA transcripts in the nucleus. Both Drosha and Dicer1 have been characterized as haplo-insufficient tumor suppressors, as in vitro and in vivo studies revealed that their partial deletion has the ability to propel tumorigenesis and cancer progression, although knockout of both alleles inhibits this procedure [49, 50]. On the other hand, upregulation in the levels of Drosha and Dicer has also been identified in oesophageal and prostate cancer, correlating with increased levels of miRNAs and disease progression [51, 52]. Aberrant expression of the tumor suppressor p53 has also been linked to altered miRNA expression, as it influences the miRNA biogenesis mechanism by interacting with Drosha in a transcription independent manner [53]. Furthermore, things can get more complicated by some miRNAs that have been shown to target the miRNA processing pathway itself and their misregulation may reduce the global miRNA levels in some cancers. Such an example has been highlighted by Martello et a1 (2010) for the miR-103/107 family, whose upregulation in some breast cancers targets and reduces Dicer1 function, enhancing their aggressivity and metastatic potential [54].

Apart from defects altering their general biogenesis and maturation, miRNAs can have specifically aberrant profiles in cancer due to selective genetic and epigenetic alterations or regulation by transcription factors related to a malignant phenotype. Evidence shows that the dysregulation of the miRNA expression plays a fundamental role in the onset, progression and dissemination of cancers. Many miRNAs have been shown to have oncogenic or tumor suppressor functions [55]. Depending on the oncogenic or tumor suppressive nature of their

protein-coding targets, miRNAs can function as tumor suppressors or "oncomirs" respectively. Previous works have shown that, in some cases, miRNA clusters are located at fragile sites of some chromosomes and cancer susceptibility loci [56, 57]. Mapping of miRNA genes revealed a strong association with cancer-specific translocation breakpoints and repetitive sequences. In addition, single-nucleotide polymorphisms (SNPs) have been also suspected to bear an impact on miRNA expression and function in a dual way. SNPs in mature miRNA sequences may alter their regulatory potential, either enhancing it or decreasing it. Depending on the nature of the target mRNA in cancer-related pathways, SNPs in miRNAs may act allowing oncogenes to escape miRNA-mediated degradation, or increase the expression of a miRNA with an oncogenic activity.

Epigenetic mechanisms have been proven to be severely modulated in malignant phenotypes, influencing not only the expression of protein-coding genes, but also miRNA-producing loci. Hyper- and hypomethylation are believed to be an early event in cancer establishment and can have the form of DNA hypermethylation, affecting tumor suppressor genes, extensive DNA hypomethylation with oncogenic consequences, or even an altered histone modification pattern of methylation and acetylation [58]. Weber et a1 (2007) showed that a great number of miRNA genes are located near CpG islands, thus being susceptible to cancer-related epigenetic modifications [59]. An example was shown in colorectal cancer presenting upregulated DNA methylation, directly suppressing the expression of miR-127, miR-9-1, miR-200c/141 and the tumor suppressor miRNA cluster miR-34b/c, with a significant impact on cancer motility and invasive capacity [60-63]. The miR-34 family targets cyclin D, cyclin E2, CDK4 and 6, Myc and Bcl2, all of which play a major role in promoting cell proliferation and apoptosis evasion [64]. MiR-200c has also been shown in non-small cell lung cancer (NSCLC) to have a hypermethylated promoter, leading to a suppressed expression and poor differentiation, as well as a reduced E-cadherin expression, promoting metastatic ability [65]. Apart from DNA methylation status, histone hypermethylation or deacetylation has been proven sufficient to diminish the expression of anti-oncogenic miRNAs. In bladder cancer cells, treatment with 5-aza-2′-deoxycytidine and histone deacetylase (HDAC) inhibitor 4-phenylbutyric acid (PBA) was enough to upregulate various miRNA, including miR-127, with the latter inducing significant apoptosis in tested cancer cell lines. Scott et a1 (2006) also showed that HDAC inhibition applied to breast cancer cells resulted in severely altered miRNA levels [66].

Nevertheless, oncogenic transcription factors have also been mentioned to act by suppressing numerous miRNAs. The Myc oncogene was shown to upregulate the oncogenic miR-17-92 cluster [67], while it downregulates let-7, miR15a/16-1, miR26a and the miR-34 family, attenuating their known anti-proliferative, tumor-suppressive and pro-apoptotic effects [68]. In KRAS mutant pancreatic cancer, Ras oncogene activation directs the RREB1 protein towards the promoter of miR-143/145. Its binding leads to transcriptional repression. Interestingly, there is a two-way interaction, as this miRNA cluster appears to be targeting KRAS and RREB1 [69]. In contrast, p53, responsible for the response to DNA damage and crucial in cell cycle regulation and apoptosis, controls in a positive manner the expression of miR-34 family members. As this transcription factor is found mutated or epigenetically silenced in approximately half of human cancers, it is clear that its altered expression may reflect a downregulation of these anti-oncogenic miRNAs [70]. In an early 2017 review on circulating miRNAs and cancer, J. Matsuzaki and T. Ochiya (2017) carried out a systematic research for works regarding extracellular miRNAs and cancer, summarizing the 10 most frequently documented miRNAs, shown to be abnormally expressed in cancer [71]. These miRNAs, along with their top target genes and the concerned types of cancer are listed in the table below (table 1).

Various works are being carried out in the context of using miRNAs for therapeutic purposes in cancer treatment. First-class examples are provided by the works of C. Grosset's group, focused on the expression of the previously mentioned Glypican-3 (GPC3) in hepatocellular carcinoma (HCC). Screening for miRNAs with aberrant profiles in HCC samples compared to control samples, they found that miR-96, miR-129-1-3p, miR-1271, miR-1291, and miR-1303 differentially control GPC3 expression in HCC cells [72]. More precisely, miR-1271 and miR-4510 were found downregulated in HCC, inversely correlating with GPC3 mRNA expression. Restoration of their expression in vitro inhibited cell growth in a GPC3-dependent manner and induced cell death [72, 73]. Furthermore, miR-1291 was found to positively regulate GPC3 expression by targeting the expression of IRE1a, a stress sensor that cleaves GPC3 mRNA. Restoration of normal IRE1a expression downregulated GPC3 levels [74]. Vectorization of such miRNAs and in vivo delivery to the tumor is a challenging step.

miRNA	**Cancer site**	**Representative targets***
hsa-miR-21-5p	Hepatocellular, colorectal, breast, lung, pancreatic, nasopharyngeal	*PTEN*, *PDCD4*, *RPS7*
hsa-miR-221-3p	Hepatocellular, colorectal, lung, sarcoma	*CDKN1B*, *KIT*, *TMED7*
hsa-miR-155-5p	Lung, breast, colorectal, pancreatic, laryngeal	*CEBPB*, *SOCS1*, *TP53INP1*
hsa-miR-223-3p	Hepatocellular, colorectal, lung, esophageal, pancreatic, sarcoma	*IGF1R*, *FBXW7*, *NFIA*
hsa-miR-92a-3p	Colorectal, hepatocellular, breast, gastric, endometrial	*BCL2L11*, *FOXN2*, *SOX4*
hsa-miR-16-5p	Breast, esophageal, gastric, lung, melanoma, pancreatic, ovarian	*BCL2*, *VEGFA*, *CCNE1*
hsa-miR-20a-5p	Lung, colorectal, gastric, hepatocellular, pancreatic	*CCND1*, *TGFBR2*, *E2F1*
hsa-miR-141-3p	Colorectal, hepatocellular, breast, lung	*ZEB2*, *ZEB1*, *YRDC*
hsa-miR-145-5p	Colorectal, hepatocellular, lung, breast, gastric, ovarian	*IRS1*, *FSCN1*, *POU5F1*
hsa-miR-210-3p	Colorectal, breast, lung, pancreatic, glioma, hepatocellular, melanoma, renal, bladder	*EFNA3*, *ISCU*, *E2F3*
*The top 3 reported genes according to miRTarBase		

Table 1: The 10 most frequently documented miRNAs in cancer (Matsuzaki and Ochiya, 2017 [71])

Circulating microRNAs

During the last years, miRNAs have also been detected in the extracellular medium. Less than ten years ago, pioneering works by many different research groups brought to light the presence of miRNAs in blood plasma and serum [75-77]. These findings came to solidify the hypothesis of extracellular miRNA release, derived one year before from the results of Valadi et a1 (2007), indicating the liberation of intracellular miRNAs in the culture medium of different cell cultures [78]. Their existence has subsequently been confirmed in most body fluids and more precisely in tears, urine, semen, breast milk, saliva, cerebrospinal and

amniotic fluid (reviewed by Turchinovich et al (2012) [79]). From the early works on circulating miRNAs, it was shown that these molecules exhibit a surprising level of stability in an RNase-enriched environment such as circulation. Other RNA species like mRNA, rRNA and tRNA are rapidly degraded within seconds when exposed to such enzymes. Nevertheless, circulating miRNAs survived a variety of extreme experimental conditions, like low pH, temperatures reaching the boiling point, multiple freeze-thaw cycles and extended storage [80, 81].

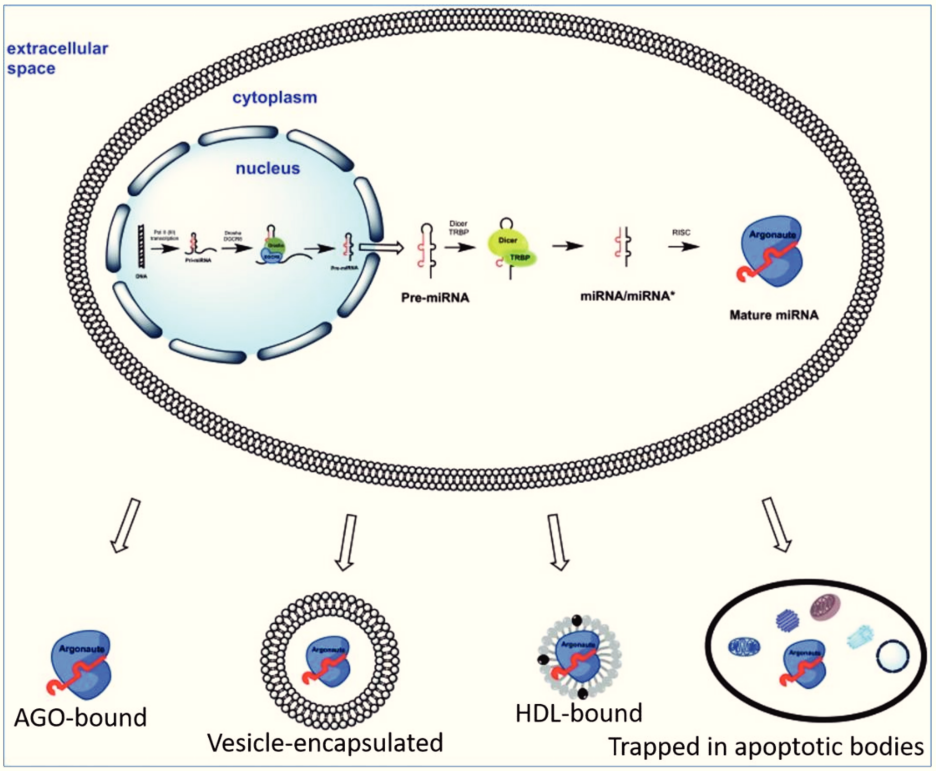

Figure 3: Modes of miRNA transport and protection in the extracellular system (taken and modified from Turchinovich et al, 2013 [82])

The main questions deriving from these data were two: 1) how intracellular miRNAs are exported to the extracellular medium and 2) how they are able to retain such a remarkable stability upon exposure to hostile conditions. A first evidence came from the same work of Valadi et al, showing a mechanism of extracellular transport of miRNAs by encapsulation into exosomes and membrane-formed microvesicles [78]. Hunter et al (2008) came to confirm these findings one year later, raising the hypothesis of active miRNA secretion by the cells and cell-cell communication by exchange of circulating miRNAs, protected by transporter-vehicles [83]. The encapsulation of miRNAs into such vesicles proved to be only a partial explanation of their stability in circulation. A fundamental work by Arroyo et al a few years later (2011) focused on plasma and serum miRNAs and revealed that a relative minority of

them is carried in vesicles. Starting by proving that miRNAs alone are not resistant to circulation-localized RNases, this group performed differential centrifugation and size exclusion chromatography in order to analyze all compartments of cell-free blood fluid, confirming that vesicle-associated miRNA transport is indeed a fact. Analysis of vesicle-free compartments led to the discovery of a whole ribonucleoprotein complex-based binding and transportation of extracellular miRNAs [84]. More precisely, they are shielded from RNase-linked degradation by packaging in apoptotic bodies, shedding vesicles and exosomes, but also by association with AGO proteins (at least with AGO2), high-density lipoproteins (HDL) and nucleophosmin 1 (NPM1), although the in vivo existence of the last one remains unclear (figure 3) [79, 85-87]. These works provided significant proof that miRNAs can be either actively secreted, or passively liberated by cells, or even be released upon cell lysis [81]. MiRNA liberation as a result of cell death has been confirmed, as applied toxicity in certain tissues led to an increase in the concentration of miRNAs in the blood, many of them remaining stable even after the death of their parental cells [88, 89]. Vesicle-based secretion reflects a more selective release of miRNAs, while AGO2-associated carrying seems to be a form of non-selective liberation, linked to physiological cell activity or cell death. No significant uptake of AGO2-bound miRNAs or HDL-associated miRNAs was shown to take place [87]. However, miRNAs in secreted microvesicles and exosomes were found to co-localize with AGO2, also contained in these vesicles. Such vesicles, as well as apoptotic bodies, were found to be transferred and recognized by recipient cells, where carried miRNAs are able to target host mRNAs and regulate their expression. Selective packaging of mature miRNAs in vesicles for their export was further supported by evidence that miRNAs, GW182 and AGO proteins co-localize with endosomes and multivesicular bodies (MVBs) [90]. This was not the case for mRNAs found in exosomes, as their patterns did not correlate with the donor cells, indicating that there might be a selective packaging of miRNAs in exosomes and microvesicles for active secretion [91, 92]. Exosomes are 30-100 nm in diameter, formed within the MVBs and released by fusion of MVBs with the plasma membrane [93]. On the other hand, microvesicles span from 100 nm to 1 μm of diameter, being produced upon outward budding and fission of the plasma membrane ([94] and figure 4). Both exosomes and microvesicles can be isolated by different techniques based on differential ultracentrifugation. Because of their similar size and the fact that vesicles even smaller than exosomes can bud from the cellular membrane, it remains quite challenging to achieve absolute purification of each type of extracellular vesicle. However, differential floatation velocity in a sucrose gradient can allow a relatively efficient separation upon ultracentrifugation [95].

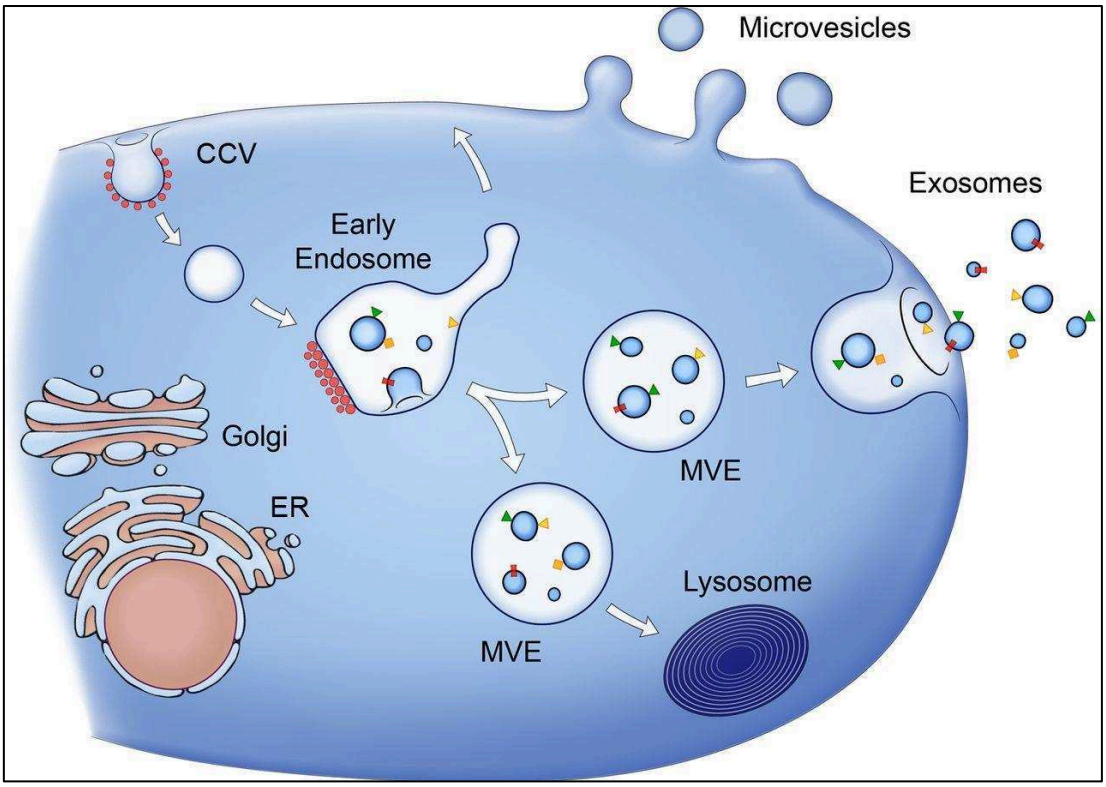

Figure 4: Formation and release of microvesicles and exosomes from the cell to the extracellular medium (taken from [95])

The secretion of stable, protected miRNAs in the extracellular environment, along with their direct protein partners AGO2 and GW182 raised the hypothesis of an intercellular communication and regulation via circulating miRNAs. Indeed, successive works provided strong examples of regulation mediated by delivery of vesicular miRNAs to recipient cells. In 2010, it was shown in vitro that microvesicles containing miRNAs had the ability to be uptaken by murine tubular epithelial cells (mTEC) and increased the intracellular miRNA abundance in a dose-dependent manner. Furthermore, the administered enriched miRNAs went on to downregulate the expression of known targets, like PTEN for miR-21, cyclin D1 for miR-99a, miR-100 and miR-223 and Bcl-2 for miR-16, the miR-34 family and miR-181b [96]. A year later, Yang et al showed that in IL-4-stimulated macrophages, there was an induced secretion of miR-223-rich exosomes, which were able to target breast cancer cells. Once introduced to the cancer cells, these miRNAs affected the Mef2c mRNA levels, leading to an increase in the nuclear β-catenin levels and an enhanced cellular invasiveness [97]. Another work from Kosaka et al (2010) highlighted the transport of vesicle-encapsulated miR-146a from a fibroblast-like cell line derived from monkey kidney (COS-7) to metastatic prostate cancer cells (PC-3M), where it repressed its known target ROCK1, provoking a

decrease in cellular proliferation [98]. Finally, an interesting discovery by Pegtel et a1 (2010) implicated viral miRNAs, in Epstein-Barr virus-infected B-lymphoblastoid cells. More analytically, following infection of these cells with the virus, this group reported the secretion of exosomes containing viral miRNAs, which targeted co-cultured but not infected B-cells, altering the expression of C-X-C motif chemokine 11 (CXCL-11), a small chemokine targeted by viral miRNAs [99]. This result was also confirmed in vivo and provided evidence that viral miRNAs can use host exosomes and circulate, thus promoting viral infection. An impressive load of publications came to confirm the cell-cell distant communication via extracellular miRNA trafficking, in a paracrine way. Among those, two groups indicated an interaction of secreted miRNAs with the Toll-like receptors (TLRs) of recipient cells, inducing a response of the innate immune system [100, 101]. However, the concentration of miRNAs in biofluids is drastically lower than in the medium of cell cultures, leaving the in vivo significant effect of circulating miRNA-mediated gene regulation to be further elucidated. Extracellular miRNA transfer and gene regulation is not limited in the context of cancer. Various examples have been studied in depth. One fascinating and groundbreaking work published in 2012 by Zhang et a1 brought to light not only the existence of this mechanism in plants, but also the possibility of cross-kingdom gene regulation by transfer of circulating miRNAs [102]. This work showed that plant miRNAs and more precisely rice-derived miRNAs, can be found in human circulation following oral food intake. Furthermore, an abundantly expressed rice miRNA, miR-168a, was found to diffuse to human serum, being associated with AGO2. Last, this miRNA was uptaken by recipient cells and effectively targeted and downregulated the expression of the low-density lipoprotein receptor adapter protein 1 (LDLRAP1) in the liver, thus decreasing LDL removal from the plasma.

Tumor-derived circulating miRNAs

As it was mentioned above, tumor cells are equally capable of releasing miRNAs into the circulation, altering extracellular miRNA profiles in biofluids like plasma, serum, saliva, urine, etc [103]. Studies have shown that different miRNA expression profiles are associated with tumor development, progression and response to therapy. In addition, specific aberrant miRNA profiles are often linked to specific types of cancer. These profiles are reflected in the circulation, as tumor-derived miRNAs can be detected and quantified, depicting a malignant phenotype at the extracellular level. Tumor-derived extracellular vesicles (EVs) impact the local and distal environment, aiding in tumor progression, angiogenesis and metastasis [104]. Taken together, these data indicate that blood plasma and serum, along with other biofluids,

could be a useful source of biomarkers for cancer diagnosis and prognosis, suggesting an easy and non-invasive way to have access to miRNA expression monitoring. These results, as well as promising results from the study of other tumor-derived circulating macromolecules like long non-coding RNA, DNA fragments bearing cancer-specific mutations or polymorphisms and proteins gave birth to the notion of the liquid biopsy. As defined from the National Cancer Institute of USA (NCI), a liquid biopsy is "a test done on a sample of blood to look for cancer cells from a tumor that are circulating in the blood or for pieces of DNA or RNA from tumor cells that are in the blood (figure 5). A liquid biopsy may be used to help find cancer at an early stage. It may also be used to help plan treatment or to find out how well treatment is working or if cancer has come back. Being able to take multiple samples of blood over time may also help doctors understand what kinds of molecular changes are taking place in a tumor". From 2009 until now, hundreds of works have been carried out regarding circulating miRNAs, associated or not to EVs, and their potential to serve as predictive, diagnostic, or prognostic biomarkers in almost all types of cancer. Various groups have analyzed the miRNA expression profiles using comprehensive high-throughput approaches, like microarrays and next-generation sequencing, from cancerous cell lines, subsequently comparing them to blood plasma or serum samples coming from patients suffering from the same type of cancer. Circulating DNA-based approaches seem to be a step more advanced, as in June of 2016, Roche's ctDNA-based detection of EGFR mutations in lung cancer patients was the first liquid biopsy to garner FDA approval, as a highly specific companion diagnostic for a certain treatment [105].

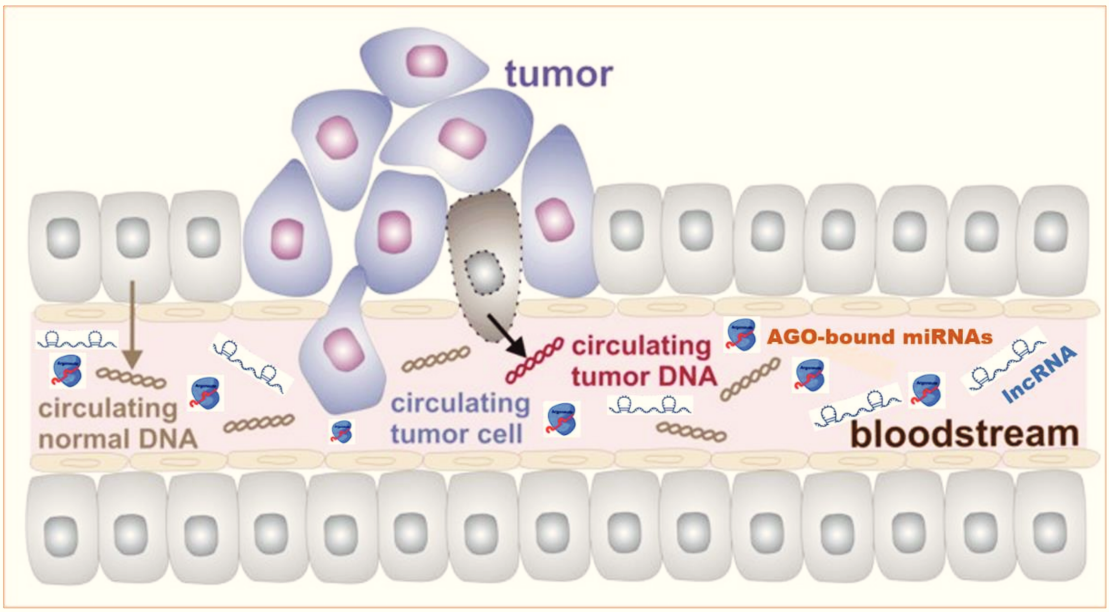

Figure 5: Circulating nucleic acids and cells, derived from tumors

Toiyama et al (2013) screened miRNA expression in culture medium from two distinct cell lines of colorectal cancer (CRC) by quantitative RT-PCR, focusing on two miRNAs, miR-21 and miR-31, with a well-defined oncogenic activity, frequently overexpressed in CRC tissues and shown to be associated with poor survival and response to chemotherapy, as well as with tumor prognosis respectively. After establishing the secretory potential of these miRNAs in vitro, they analyzed their expression in the serum of 12 CRC patients, versus 12 control subjects and validated the results in a series of 186 preoperative CRC patients, compared to 60 postoperative patients, 43 patients with benign colonic adenoma, often a precursor of colorectal cancer, and 53 control subjects. MiR-21 was found to be abundantly expressed and secreted from CRC cell lines, while it is upregulated in the serum of preoperative CRC and adenoma cases, having a significant association with tumor burden, distant metastasis and poor survival. Thus, miR-21 could be a potential prognostic biomarker for CRC [106]. Another three-stage study was published by Lin et al (2015), indicating the utility of serum miRNAs in clinical diagnosis of hepatocellular carcinoma (HCC) [107]. This group studied individuals with HCC, chronic hepatitis B, hepatitis B-induced liver cirrhosis, as well as healthy subjects, performing microarray analysis and RT-qPCR and identifying 19 miRNAs differentially expressed in HCC compared to non-cancerous conditions. Validation in a training cohort and two more validation cohorts reduced the miRNA signature to 7 (miR-29a, miR-29c, miR-133a, miR-143, miR-145, miR-192 and miR-505), allowing consistent detection of HCC. Furthermore, they went on to compare this miRNA signature to α-fetoprotein (AFP20), a plasma protein used as a biomarker in HCC [108]. The signature exhibited a higher accuracy than AFP20, distinguishing individuals with HCC more efficiently in fixed time periods before clinical diagnosis, as well as detecting small-size and early-stage cancer. Similarly, Schultz et al (2014) studied whole-blood samples from patients with pancreatic cancer, along with chronic pancreatitis patients and healthy participants. Pre-treatment expression profiles of miRNAs in whole-blood were analyzed, indicating the dysregulation of 38 miRNAs in cancer patients. Further analysis of these miRNAs in additional training cohorts led to the development of two diagnostic panels of 4 and 10 miRNAs respectively [109]. The group tested the panels in parallel with the cancer antigen 19-9 (CA19-9), used in the clinic as a biomarker for pancreatic and other cancers, but with questionable accuracy [110]. Although the panels alone did not show a higher specificity and sensitivity than CA19-9, when used in combination with the biomarker, they gave a significantly improved performance than the biomarker alone. Additional works including

studies on circulating long non-coding RNAs and circulating EV-associated proteins are presented in a very recent review by J. Matsuzaki and T. Ochiya [71].

Many other miRNA signatures (specific groups of aberrantly expressed miRNAs) have been proposed as tests for the early detection or better surveillance of cancers, with their lack of reproducibility being for now the major factor hampering their introduction to the clinic. However, the volume of the newly produced data, as well as the constant improvement of the available analysis tools, point towards their progressive establishment as informative cancer biomarkers. Newly proposed circulating miRNA biomarkers gather an increasing amount of interest, as they are showing significant capacity in distinguishing malignant and benign pathologies. Furthermore, their emergence coincides with a period where protein-based biomarkers extensively used for cancer detection and surveillance present considerable limitations in specificity and sensitivity. Accumulating results from the analysis of circulating nucleic acids suggest that newly developed non-protein biomarkers could replace some of them, or used in combination, improving diagnostic efficacy and prognostic predictivity, as well as assessing response to treatment.

Pre-analytical requirements for the detection of circulating miRNAs

Among the body fluids used for the study and discovery of circulating biomarkers, the most common are serum and plasma, both coming from centrifugation and elimination of all cell types from total blood. Their composition is practically the same, with the exception of fibrinogens, the protein precursors responsible for blood clotting, which are not included in the serum. The serum is collected by centrifugation of coagulated total blood in dry tubes, while plasma is obtained by centrifugation of blood placed in special tubes containing anti-coagulation factors, like EDTA or heparin, immediately after collection. As heparin has the potential to inhibit subsequent PCR amplification, EDTA-covered tubes are generally preferred in quantitative studies. Comparative studies have pointed out that there is no significant difference between serum and plasma's miRNA concentrations, although serum might contain slightly more miRNAs as individual analyses suggest [111]. Plasma isolation requires one or two steps of centrifugation, depending on the selected protocol, in order to eliminate all types of cells. As blood platelets have been shown to contain RNAs [112], potentially affecting subsequent analyses, the aim of the second centrifugation, which is much faster, is their complete elimination. When a single centrifugation step is chosen, the abundance of platelets in the stored plasma depends on the speed of the centrifugation. As Cheung et al (2013) explain, centrifugation of whole blood at 600g for 10 minutes provides

platelet-rich plasma, whereas centrifugation at 3400g for the same duration results in a platelet-poor plasma [113]. After extensive bibliographic research, we chose an intermediate protocol, based on a one-step isolation centrifugation at 1400g, for a slightly longer duration of 15 minutes. Blood samples were processed within an hour from collection, in order to avoid as much as possible, contamination of the plasma with hemolysis-derived molecules. Hemolysis is a major issue, not to be ignored in circulating miRNA studies. Like all cell types, red blood cells express miRNAs which can selectively alter the global miRNA profile of plasma or serum upon lysis of these cells. To assure optimal results, we excluded miRNAs that are known to be very abundant in those cells, like miR-16 and miR-451. Apart from rapid separation of the plasma, we followed the indications by Kirschner et al (2011), measuring the optical density of plasma samples at a wavelength of 414 nm (corresponding to globulin absorption) and selecting those with values not exceeding 0.2 [114]. An additional way to evaluate the degree of hemolysis in plasma samples, according to the same group, is the assessment of the abundance of miR-451 (abundant in red blood cells) and miR-23a (absent or poorly expressed in red blood cells) by RT-qPCR and the elimination of the samples with ΔCt values superior to 5.

Chapter 2: Ovarian Cancer

Definition and epidemiology

Ovarian cancer is a general term for a series of molecularly and etiologically distinct diseases, resulting in the formation of cancer in tissues of the ovary. The ovaries are the twin organs that produce a woman's ovules and the main source of the female hormones estrogen and progesterone. The vast majority of ovarian cancers are carcinomas (ie epithelial cancers) and most of them are adenocarcinomas. They arise from the surface of the ovarian gland. In contrast, a small minority of ovarian cancers derive from internal ovarian cells, either the female gamete cells or follicular supporting cells. The histogenesis of ovarian carcinomas remains somehow controversial. In some cases, the tumor seems to be the result of a local transformation process directly affecting cells of the ovarian surface epithelium (OSE). However, there is growing evidence that in most cases, surface ovarian adenocarcinomas derive from epithelial cells lining the fimbriae of fallopian tubes [115]. There is pathological and experimental evidence that these tubal epithelial cells undergo a complex two-stage process: progressive in situ transformation resulting in an in situ carcinoma and secondary migration and engraftment on the surface of the OSE. Regardless of the oncogenic scenario, one distinctive characteristic of ovarian adenocarcinomas is their invasive behavior with penetration in the underlying ovarian stroma across the basal membrane. In 2010, approximately 160.000 women died from ovarian cancer, which is more common in industrialized countries. In the USA, ovarian cancer is the sixth most common cancer as well as the second most common gynecologic cancer, after endometrial cancer [116]. In France, it is the fifth most common cancer in women, while being the fourth in terms of mortality, after breast, colon and lung cancer. In most cases, ovarian cancer is diagnosed at a late stage, thus followed by a poor prognosis.

Evolution and prognosis

The cancer starts silently and early signs are hard to come by. When they are present, most symptoms are non-specific, making the diagnosis very difficult during stages I and II. Ovarian cancer staging uses information obtained after surgery, in order to describe the extent of the primary tumor, the absence or presence of metastasis to nearby lymph nodes and the absence or presence of distant metastasis (Figure 6). Thus, stage I depicts a tumor limited to one or both ovaries. Stage II is a more advanced stage of cancer. In this case, the tumor has grown in one or both ovaries and has spread to the uterus, fallopian tubes or other pelvic tissues. In

stage III implants can be found outside of the pelvis, in the peritoneum, or extend to the small bowel. This stage allows the measurement of the size of the metastatic tumors. Even very small tumors can be visible under the microscope. These three stages are divided into three subcategories (a, b, c) according to the extent of the findings. In stage IIIc, metastatic tumors have a size that exceeds 2 cm. In stage IV, the patient shows distant metastases to the liver or outside the peritoneal cavity, to other organs like lungs for example. Apart from the stage, ovarian cancer diagnosis also defines its histological grade, estimating the cells' level of malignancy and abnormality after microscopic study of tumor fragments. There are four distinct grades (0, 1, 2, 3) assessing the level of differentiation of the tumor cells and their invasiveness (table 2). The higher the grade, the less the cells are differentiated and the more they look different than normal cells. Grade 3 is accompanied by the worst prognosis, exhibiting poorly differentiated, abnormal cells.

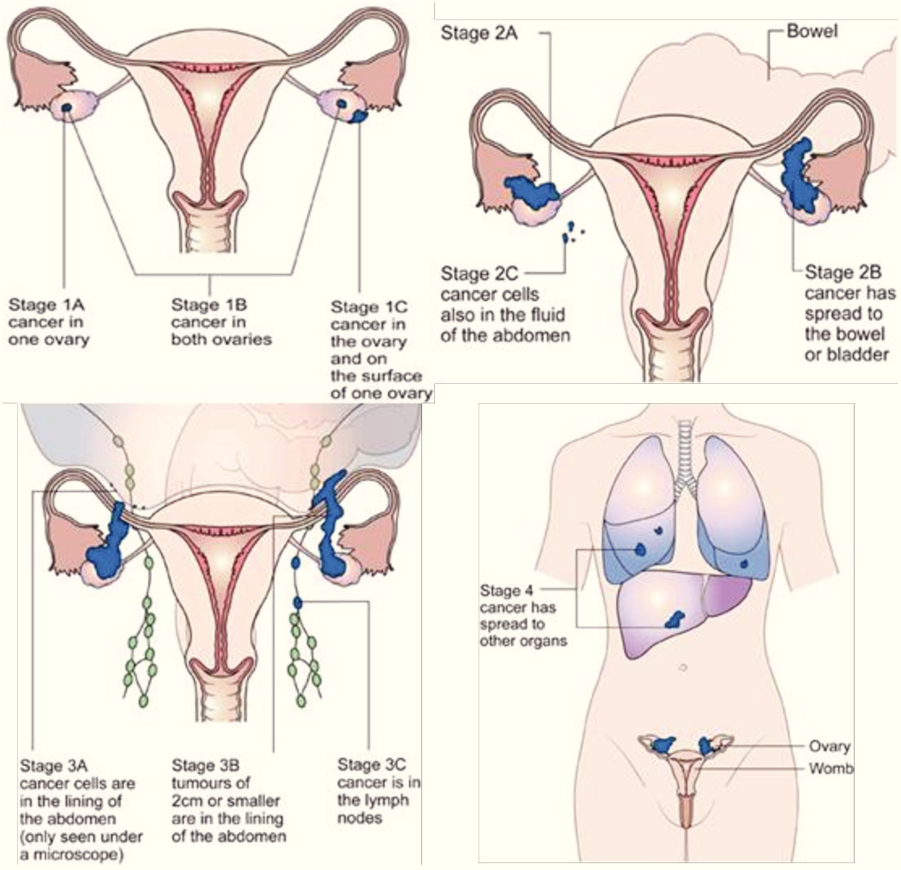

Figure 6: Stages and evolution of ovarian cancer (CancerHelp UK, Cancer Research UK, http://www.cancerresearchuk.org/cancer-help/type/ovarian-cancer/treatment/stages-of-ovarian-cancer)

Grade	Description
0	Grade of differentiation cannot be assessed
1	Well differentiated or low grade – slow growing, less likely to spread
2	Moderately well differentiated or moderate grade
3	Poorly differentiated, undifferentiated or high grade – tend to grow quickly, more likely to spread

Table 2: Grading of ovarian cancer (Canadian Cancer Society, www.cancer.org)

Because of its late diagnosis, roughly only 20% of cases are found in an early stage, where the cancer is limited to the primary site. The absence of an anatomic barrier blocking the dissemination of tumor cells in the abdominal cavity results in early metastasis. At stage I, the possibility of complete curability can be higher than 70%. Ovarian cancer can be a frightening diagnosis with five-year relative survival rates ranging from 89% to 18% for epithelial ovarian cancer, depending on the stage when it was detected. For stage I cancer, five-year survival rate is 92.7%. On the other hand, women diagnosed with an advanced ovarian cancer (stages III, IV) have a five-year survival rate inferior to 30% [117]. Unfortunately, more than 60% of the women found to have ovarian carcinomas are already on stage III or IV, placing it among the deadliest cancers, with an overall five-year survival rate of 47%, while for all cancers combined it has improved to 68% (American Cancer Society, 2013).

Histology - Types of ovarian cancer

Clinical treatment, management and prognosis of ovarian cancer are strongly related to the histological analysis of the tumor, defining its classification. The main points taken into consideration in the classification of ovarian tumors are the cellular type, reflecting the state of differentiation and the degree of malignancy. At the cellular and molecular level, ovarian cancers can be quite heterogeneous. The vast majority of all ovarian cancers are epithelial carcinomas, also known as surface epithelial-stromal tumors or simply adenocarcinomas. There are four types of adenocarcinoma (Figure 7): serous (50%), endometrioid (20%), mucinous (15%) and clear cell (5%), each one presenting distinct morphologic abnormalities [118]. Another 8% consists of rare histologies. Approximately 70% of deaths due to ovarian cancer are cases of advanced-stage, high-grade serous ovarian carcinomas (HGSC) [119]. Ovarian cancer can be often the result of metastasis of another primary tumor, elsewhere in

the body, most commonly in the breast or in the gastrointestinal region. A distinct entity within epithelial ovarian tumors is the group of the so-called borderline ovarian tumors (BOTs). Borderline tumors remain a controversial issue, because of their uncertain malignant potential. They are mostly noninvasive tumors, with a characteristic histology, either mucinous, or in most cases serous. Based on molecular studies, some mucinous borderline tumors of the ovary may actually represent metastasis from the intestinal appendix. Borderline tumors, as with other ovarian tumors, are difficult to detect clinically until they are advanced in size or stage. In general, these tumors occur in younger women compared to malignant tumors, are found at an earlier stage and have a favorable prognosis. However, in some cases, symptomatic recurrence and death may occur, even years after treatment. Although these tumors mainly exhibit molecular linkage to low-grade tumors, they can host more invasive implants, confusing diagnosis [120]. Detailed histological analysis of these tumors is a crucial factor for the definition of the optimal treatment modalities.

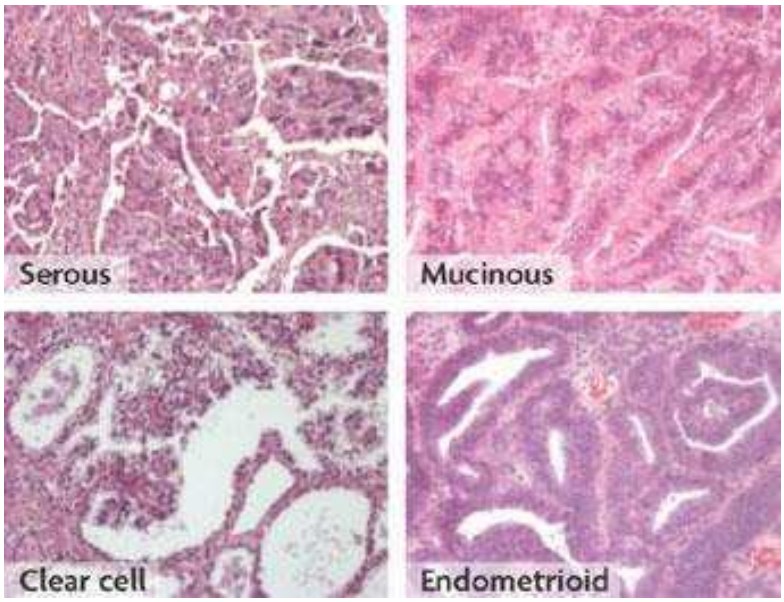

Figure 7: The four histological subtypes of epithelial ovarian cancer (from Nature Reviews/Cancer)

Causes - Risk factors

The exact causes of ovarian cancer development are unknown, but there are several factors, genetic and environmental, related to its occurrence. The strongest risk factor is age, as after menopause, a woman is more likely to develop ovarian cancer. The risk of ovarian carcinoma depends closely on pre-menopausal operations of the endocrine system and of the reproductive apparatus. There is indirect evidence that the risk increases with the overall

number of ovulations ("incessant ovulation hypothesis"). Disruption and subsequent repair of the ovarian epithelium, taking place during ovulation, can lead to the acquisition of genetic damage in ovarian epithelial cells [121]. The fact that women who have been taking birth control pills for at least five years have about half the risk of developing ovarian cancer is congruent with the idea that the reduction, either natural or artificial, of ovulations plays a significantly protective role against ovarian cancer. Estrogen stimulation especially when not compensated by concomitant stimulation by progesterone increases the risk of ovarian carcinoma. Symptomatic estro-progestative imbalance increases the risk by two-fold. Infertile women and women with a condition called endometriosis are at increased risk [122]. In contrast, women who undergo complete pregnancy have generally lower possibilities to get ovarian cancer than women who have never given birth, as it appears that the risk decreases after every pregnancy. A strong impregnation by progesterone for several months is believed to reduce the risk. Breastfeeding is also thought to provide supplementary protection. Postmenopausal hormone therapy may increase the risk, especially when women take estrogen without progesterone for at least 5 to 10 years.

Genetic familial predisposition

Genetic factors are also important, as women who are carriers of various germinal mutations in the BRCA1 or BRCA2 genes are at high risk of developing either breast or ovarian cancer. Mutations in these two genes are responsible for 5%-13% of total ovarian cancers [123]. Women carrying BRCA1/2 mutations have a lifetime risk of 20-50% of developing ovarian cancer. A combined analysis of 22 studies showed that the average cumulative risks in BRCA1-mutation carriers by age 70 years were 39% for ovarian cancer, with corresponding estimates for BRCA2 being at 11% [124]. The BRCA genes play a crucial role in the maintenance of genome integrity, leading the system which repairs double-strand breaks occurring in the DNA after during the phase of replication. In the classical conception, the germinal mutation of a single allele has no deleterious effect. According to the Knutson "two-hit" model, cellular dysfunction occurs only when the other allele is affected by the random occurrence of a somatic mutation. On the contrary, there is growing evidence that germinal mutations of single alleles in the BRCA1/BRCA2 genes often result in haplo-insufficiency in various tissues or organs, including the cardiac muscle [125]. The most notable consequence of harmful mutations in BRCA1 or BRCA2 cis a very high rate of breast or ovarian cancer in families that bear a mutant allele, a phenomenon better known as hereditary breast-ovarian cancer syndrome (HBOC). Mutations in other genes have also been reported to create

predisposition to breast or ovarian cancer, like CDKN2, while approximately 45% of HBOC cases involve unidentified genes or multiple genes [126].

Genomic alterations in ovarian cancer

Genomic investigations performed by the American cooperative group called TCGA (The Cancer Genome Atlas) have provided the most comprehensive and synthetic view of genetic and epigenetic alterations observed in ovarian carcinomas. As in other malignancies, genetic alterations can be classified as point mutations, gene deletions and gene amplifications. In sporadic, non-hereditary ovarian cancer cases, a great number of genes are found mutated or differentially expressed, even in very early tumorigenesis stages. High-grade serous carcinomas (HGSC) are often characterized by mutations or loss of heterozygosity of p53. Exome sequencing on DNA isolated from 316 HGSC cases revealed approximately 61 somatic mutations per tumor, with TP53 bearing mutations in 96% of cases. Germline mutations in BRCA1 and BRCA2 were found mutated in 9% and 8% respectively, with another 3% of the tumors bearing sporadic somatic mutations in these genes. Frequent mutations were also identified in genes FAT3, NF1, CSMD3, RB1 and GABRA1. The mutated genes whose role has been well described are divided into two categories: tumor suppressor genes and oncogenes. TP53 and BRCA1/2 are paradigms of well-known tumor suppressors, as well as CDK12, frequently mutated in HGSCs, which is involved in the regulation of RNA splicing and has already been associated to other cancer types [127]. Comparative studies have revealed mutations in potential oncogenes, like BRAF, KRAS, NRAS and PIK3CA, which are rare but have transforming activity. Copy number analysis showed extended chromosome aberrations, with at least 5 gains and 18 losses present in more than 50% of the examined tumors. Focal aberrations were also identified, with CCNE1, MYC, MAPK1 and MECOM being frequent targets of amplification (>20% of tumors). Meanwhile, already identified tumor suppressor genes like PTEN and genes that are often found mutated, like the previously mentioned RB1 and NF1, are targets of focal deletions, resulting in loss of expression. Epigenetic events also play a significant role, as DNA methylation analysis has brought to light an extended hypermethylation in the promoters of at least 168 genes, being responsible for their reduced or even silenced expression. AMT, CCL21 and SPARCL1 are among the most noteworthy cases of epigenetic silencing, while BRCA1 is also a frequent target. Transcriptome and DNA methylation analyses indicated 4 distinct clusters of genomic alterations, dividing HGSC in 4 different expression subtypes (table 4). On the basis of their transcription profile, they were named “immunoreactive”, “differentiated”, “proliferative” and

"mesenchymal" [127]. Other histotypes correlate with different mutations, as K-ras, BRAF and ERBB2 genes are usually mutated in low-grade serous carcinomas (LGSC) (table 3). More than 70% of LGSC cases have mutations in the RAS pathway [128]. In addition, clear cell ovarian cancers usually exhibit PIK3CA activation and amplification of tyrosine kinases like MET and ERBB2, while CTNNB1 and PTEN mutations are commonly seen in endometrioid cancers.

Cancer Grade	**Mutation Analysis**
High-Grade Serous Ovarian Cancer	Frequent mutations in TP53 Rare mutations in KRAS, BRAF and ERBB2
Low-Grade Serous Ovarian Cancer	Rare mutations in TP53 Frequent mutations in KRAS, BRAF and ERBB2

Table 3: Relation between mutation pattern and serous cancer grade

A global study of the totality of the genetic and epigenetic aberrations identified in ovarian cancer indicates that central, cancer-associated pathways are altered, harboring more than one alterations. Mutations and epigenetic inactivation of BRCA1/2, along with mutations in PTEN, RAD51C, ATM, ATR and other genes result in a defective homologous recombination system in approximately half of the cases. The RB1 and PI3K/RAS pathways are deregulated in 67% and 45% of cases respectively. NOTCH signaling pathway is altered in 22% of HGSC samples. Finally, the multiple roles of p53 in various cell metabolic pathways are confirmed by the fact that TP53 mutations lead to the overexpression of genes that do not present copy number alteration, like FOXM1 and its target genes, normally repressed by p53 [129]. These commonly deregulated pathways provide opportunities for more efficient, individual therapeutic treatment and will continue to be a field of deep research in the following years, as there are encouraging findings, like the good response to PARP inhibitors, seen in patients with defective homologous recombination (BRCA1/2 mutations) [130]. PARP is a family of proteins with enzymatic or scaffolding properties and recruiting ability for other necessary DNA repair proteins. They are activated by DNA strand breaks and carry vital roles for survival of cells and organisms, contributing to DNA damage repair. As a consequence, their activity might block apoptosis induction in the context of defective BRCA1/2 phenotypes.

Somatic mutations of BRCA1 or BRCA2, especially if occurring in the context of germinal mutations are regarded as the best indications for a treatment by PARP inhibitors. Patients with BRCA1/2 mutations are heterozygous for the abnormality, as a germline homozygous deactivation is not viable. On the other hand, the genotype of the tumor can be homozygous after a second hit occurs. This class of agents is thought to augment cytotoxic therapy without increasing side effects and to kill cancer cells with DNA repair defects as a single agent. The genomic instability of tumor cells based on this homozygous pattern confers to PARP inhibitors selectivity for the tumor cells over normal cells [131].

HGSC molecular subtypes	Genomic Alterations
Immunoreactive	CXCL11, CXCL10 and CXCR3 activity (T cell ligands and receptor)
Proliferative	High expression of HMGA2, SOX11, MCM2 and PCNA Low expression of MUC1 and MUC16
Differentiated	High expression of MUC1, MUC16 and SLPI
Mesenchymal	High expression of HOX genes, FAP and ANGPTL1/2

Table 4: Molecular subtypes of high-grade serous ovarian carcinomas according to mRNA, miRNA expression and DNA methylation analysis patterns [127]

Diagnosis and Treatment

The diagnosis of ovarian cancer is done by a physical examination of the pelvis, followed by a blood test for the measurement of CA125 levels and a transvaginal ultrasound. However, the cancer cannot be confirmed without microscopic analysis of a tissue biopsy requiring a coelioscopy and/or a laparotomy. Over the past few years the response of ovarian cancer to chemotherapy has been improved, thanks to the combined use of cisplatin or carboplatin and other genotoxic drugs that target the malignant cells more effectively, like the previously mentioned PARP inhibitors. In addition, Avastin (also known as Bevacizumab), a monoclonal antibody inhibiting angiogenesis by targeting the vascular endothelial growth factor A (VEGF-A), enhanced overall survival when administered to platinum-sensitive recurrent ovarian cancer along with chemotherapy [132]. Surgery is a key step in the treatment of ovarian carcinoma. The complete ablation of the tumor mass is a necessary condition for cure

or at least for a long remission. This is relatively easy in the case of tumors at stages I or II where malignant lesions are restricted to the ovaries and genital organs. These patients undergo bilateral ovariectomy, salpingectomy and hysterectomy “de principio”. For patients with stages III and IV, performing complete surgery often represents a major challenge, especially when the intestine is entrapped in the tumor mass or when hundreds of tumor nodules are disseminated into the peritoneal cavity. In most French cancer care centers, when upfront surgical ablation of the tumors is regarded as impossible, the patient is subjected to initial chemotherapy usually called “neo-adjuvant chemotherapy”. If significant tumor reduction is achieved under chemotherapy, the patient can benefit of surgical tumor ablation a few months later. Once upfront or delayed debulking surgery has been performed, even when tumor exeresis has been complete, the patient is subjected to complementary chemotherapy often called “adjuvant chemotherapy”. It usually includes 6 monthly cycles. In summary, the primary treatment of OvCa is usually structured by the following sequences: either upfront surgery followed by adjuvant chemotherapy or neo-adjuvant chemotherapy, followed by surgery and adjuvant chemotherapy. Sometimes, surgical tumor reduction is not possible at any stage of the treatment, for example because of poor general condition or insufficient tumor response to neo-adjuvant chemotherapy. Surgery “renunciation” is a major factor of poor prognosis. The response to neo-adjuvant chemotherapy can be evaluated during the tumor cytoreduction surgery. A significant response is of good prognosis. The residual tumor mass is assessed at the end of the adjuvant chemotherapy by medical imaging and most often by a secondary coelioscopy or exploratory laparotomy. A complete remission is of better prognosis than persistence of malignant lesions. However, even in case of complete remission, relapse occurs in more than 50% of the cases. Unfortunately, so far, there is no means – clinical index or biomarker – allowing estimation of the risk of relapse and the duration of the remission at the end of the primary treatment.

Recurrent ovarian cancer and need of early detection

Despite recent improvements, in approximately 75% of the women who were operated for ovarian cancer and followed chemotherapy, remission is short and in most cases the cancer relapses, accompanied by a very poor prognosis, as the cancer develops resistance to previously effective chemotherapy [133]. As in the majority of cases, symptoms are absent until the cancer has spread to other tissues, it is detected at a late stage, making it very hard to completely remove the malignant cells with surgery. It is, therefore, obvious that the earlier

the cancer is detected, the better the prognosis will be, as well as the chances of completely eliminating the tumor with the first surgery.

CA125

Up to now detection of early ovarian carcinogenesis remains a major unsolved issue. The only standard of care biomarker, approved and used for ovarian cancer monitoring is CA125, a cancer antigen [134]. CA125, also known as MUC16 is a glycoprotein of the mucin family, present in the epithelium of the reproductive tract. Women who are at risk or who have been operated for ovarian cancer are advised to repeatedly measure the concentration of CA125 in their blood, as an increase in its expression could be linked to the evolution of ovarian cancer. However, CA125 has limited ability to the detection of cancer in asymptomatic women, because of its low specificity and poor sensitivity. Elevated numbers of CA125 have been linked to many benign conditions, as well as to other types of cancer. In parallel, there are many women who bear ovarian tumors and do not have increased levels of CA125 [135]. It is found to be elevated in 69-88% of ovarian cancers, depending on histology, while only 50% of stage I cases show higher levels (normal levels are supposed to be lower than 30-35 units per ml of serum). However, when initially contributive to the diagnosis, CA125 monitoring in patients who are in remission can be really useful for early detection of tumor relapses. CA125 levels tend to rise at least 3 months before recurrence, preceding findings on imaging studies, with a sensitivity of 62-94% and a specificity of 91-100%, making it a valuable tool for detection of relapse after a successful primary treatment followed by remission [136]. In the absence of a non-invasive method to accurately detect early-stage ovarian cancer, it is of great importance to search blood biomarkers, useful in early detection, allowing a better prognosis.

MiRNAs in the tumorigenesis of ovarian cancer

The implication of microRNAs in cancer is based on their role in cell differentiation, as they act as switches, repressing key genes in organismal development. There is accumulating evidence showing that miRNAs are involved in tumorigenesis and progression of ovarian cancer, with many of them being aberrantly expressed in ovarian carcinomas. Their expression patterns can be associated even to tumor subtypes and clinical outcomes. The dysregulation of miRNAs can be a result of different mechanisms, including point mutations or chromosomal alterations affecting the miRNA genes, epigenetic modifications or transcriptional modulation, all of them influencing the miRNA production machinery [137].

Their cancer-related functions can be either oncogenic, or tumor suppressive. Numerous miRNAs are found to target and repress oncogenes, thus acting like tumor suppressors, while others can repress tumor suppressor genes or even contribute to the overexpression of oncogenes. MiR-21 is among commonly altered miRNAs in various cancer types, including ovarian cancer. It can be induced by IL6 or GF1alpha and it targets mostly tumor suppressor genes, like PTEN and TPM1. In contrast, let-7a-2 has been identified as a tumor suppressor molecule, as it targets KRAS, IL6, MYC and other potential oncogenes and is often found downregulated in breast, lung, colon and ovarian cancer.

Studies from Bendoraite et al (2010) and Mateescu et al (2011) have revealed interesting information about the miR-200 family and its complex involvement in ovarian tumorigenesis. This group comprises miR-200a, miR-200b, miR-200c, miR-141 and miR-429. There is a very high sequence affinity among all of them, however they are generated from two different loci, one in chromosome 1 and one in chromosome 12. MiR-141 and miR-200a have proven to regulate response to oxidative stress by targeting the protein kinase p38a, a MAPK protein which, in contrast to other MAPKs, acts as a tumor suppressor by blocking cell proliferation and inducing apoptosis. MicroRNA expression can be altered by oxidative stress, hypoxia or radiation, having the ability to regulate stress response. Accumulation of these two miRNAs has been shown to have the same result as p38a deficiency, promoting malignancy and tumor growth. Interestingly, their accumulation has the opposite results during chemotherapy, enhancing sensitivity to chemotherapeutic drugs like paclitaxel, known to increase the reactive oxygen species (ROS) in the cell, improving the survival of patients [138]. The majority of publications show that the members of miR-200 family are significantly elevated in ovarian cancer, while they are detected at very low levels in normal epithelial cells of the ovaries. The transcriptional repressors ZEB1 and ZEB2 exhibit the opposite pattern, being substantially underexpressed in ovarian cancer. ZEB2 is a target of both subgroups of the miR-200 family, miR-141/200a and miR-200b/c/429 and ZEB1, which is a ZEB2 homolog, is a target of miR-141/200a. The loss of their function boosts the levels of E-cadherin and Lgl-2, critical adhesion molecules of epithelial cells. The increase of these proteins can potentially transform mesenchymal cells, giving them the characteristics of epithelial cells. This mesenchymal-to-epithelial transition (MET) is thought, according to other studies, to be one aspect of the development of ovarian cancers in the surface of the ovary [139].

Chapter 3: Nasopharyngeal carcinoma

Definition and epidemiology

Nasopharyngeal carcinoma (NPC) is a malignancy arising from the upper epithelial part of the pharyngeal cavity, most commonly in the pharyngeal recess (Rosenmüller's fossa), posteromedial to the medial crura of the Eustachian tube opening in the nasopharynx. The pharynx can be divided in three distinct parts: the superior part or nasopharynx, the intermediate part behind the oral cavity (oropharynx) and the lower part or hypopharynx. The nasopharynx is localized behind the nasal cavity, spanning from the oral cavity to the base of the skull (figure 8). Nasopharyngeal carcinoma belongs to the family of "Head and Neck" cancers of the upper aerodigestive tract. This cancer exhibits a unique geographical pattern of distribution, as it is rare in European and North American countries, but vastly more common in endemic areas of Southeast Asia and North Africa. Its incidence is probably underestimated in some other countries considered as non-endemic, especially in Central Africa (N. Berthet, Pasteur Institute, personal communication). It reaches a maximum frequency of 25-50 diagnosed cases per 100000 habitants in the Guangdong Province of Southern China. In the neighboring city of Hong Kong, nasopharyngeal carcinoma is the 7th most prevalent cancer. In 2014, NPC was the sixth commonest cancer in men and thirteenth in women. It accounted for 2.8% of all new cancer cases (Hong Kong Center for Health Protection, http://www.chp.gov.hk). The incidence of NPC reportedly remains high among people native of Southern China, even those who have migrated to North America (incidence lower than in their country of origin but higher than in other ethnic groups) [140]. Its occurrence is approximately two to three times higher in male subjects than in females. In Northern African countries, approximately 20% of newly diagnosed patients are younger than 30 years-old, while diagnosis at a young age is much rarer in Chinese territories. The general peak age for disease occurrence is between 50 and 60 years [141].

Symptoms and diagnosis

Symptoms related to NPC depend on the extent of primary and nodal disease and can originate from three regions: the nose, the ears and the neck. The first sign in most cases is a swelling of the lymph nodes in the neck and the diagnosis of NPC is often made by lymph node biopsy. NPC has the tendency to affect lymph nodes at an early stage [142]. Nasal symptoms include epistaxis, meaning bleeding from the nose, blocked nose or a feeling of stuffiness and discharge and facial numbness or even pain. Ear symptoms refer mostly to

recurrent infections, unilateral hearing loss, ringing in the ear, or feeling of fullness in the ear (especially on one side only). Apart from neck swelling, other symptoms repeatedly reported are blurred or double vision, trouble opening the mouth and frequent headaches [143].

The main tool for NPC diagnosis is nasendoscopy, meaning the introduction of a flexible fiber-optic tube into the nose for internal viewing, allowing a biopsy from the mass in the nasopharynx. CT and MRI scans at the head and neck area also contribute to the definition of the tumor burden, while PET-CT is used to indicate the extent of the disease to the whole body in advanced stages. Regarding circulating biomarkers, one should keep in mind that the first correlation of EBV with NPC dates back to 1966, when it was reported that patients with nasopharyngeal carcinoma presented an increased titer of these EBV-specific antibodies in their serum [144]. Numerous studies following this discovery showed that 80-92% of the patients had a dramatically higher titer of EBV antibodies – especially IgA - compared to healthy subjects, even from the early stages, reaching 100% at stage IV [145, 146]. More recently, in the late nineties, detection of circulating EBV DNA has emerged as another promising EBV-related biomarker. However the implementation of these biomarkers for population screening and early detection has been slowed by considerable difficulties. In endemic regions, detection of anti-EBV IgA has very good sensitivity but poor specificity. Detection of circulating EBV DNA has average sensitivity and specificity. However, combination of serum VCA-IgA antibody and circulating EBV DNA had an overall sensitivity of 99% [147].

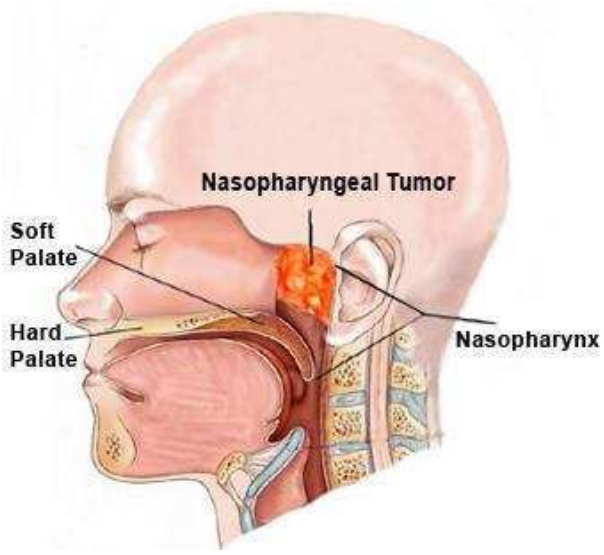

Figure 8: Anatomy of the pharynx and position of nasopharyngeal carcinoma (taken from the International Medical University of Malaysia)

Histological subtypes, staging and treatment

Morphologically, nasopharyngeal carcinoma is regarded to be squamous in origin, as under light microscopy it shows signs of squamous differentiation (intercellular bridges, keratinization), although in most cases with a low degree of differentiation [148]. Squamous epithelial cells are a flat type of cell found in the skin and the membranes that line some body cavities and they are wider than their height (flat and scale-like). Differentiation refers to the degree of difference between the cancer cells and the normal cells of the same tissue. Thus, undifferentiated cells are cells that lack their mature features or functions. The tumor grows in irregular islands separated by desmoplastic stroma and with variable numbers of lymphocytes, plasma cells, neutrophils, and eosinophils. Heavy lymphocyte infiltration among malignant epithelial cells is a characteristic of NPC, as mentioned by Li et al (2017) [149]. On the basis of the World Health Organization criteria (WHO), NPC is categorized into three pathological subtypes, depending on the degree of cellular differentiation. Type I refers to differentiated tumor with extracellular keratin, produced by the cancer cells. Types II and III contain differentiated and undifferentiated tumors respectively, both not keratinized. According to more recent nomenclature (since 2005), types II and III tend to be fused into a new type II, leaving type III for a newly defined and very rare basaloid squamous carcinoma, as shown in figure 9. Non-keratinized NPC types are predominant in endemic regions, whereas keratinized tumors are more common in other parts of the world [142, 150].

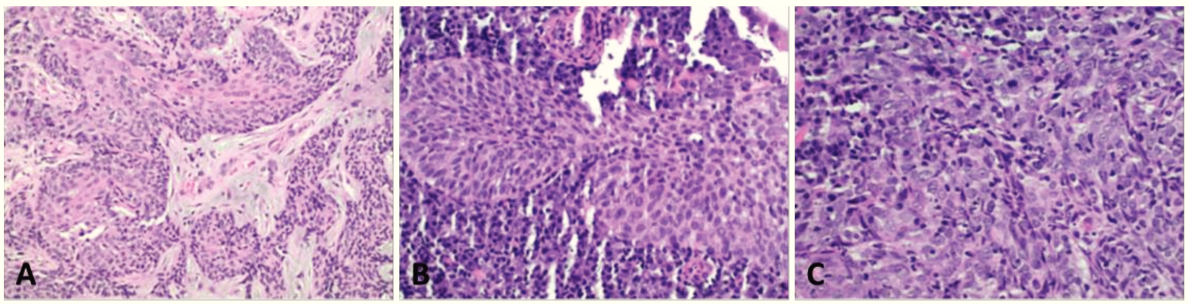

Figure 9: Haematoxylin and eosin-stained light microscopic appearance of nasopharyngeal carcinomas of the keratinizing squamous type (A), non-keratinizing differentiated type (B) and non-keratinizing undifferentiated type (C), as provided by Chua et al, 2015 [142].

Staging of nasopharyngeal cancer is crucial for treatment selection and prognosis. The spread of NPC is determined by physical exam, imaging (CT or MRI scan, etc.) and other tests and is defined according to the TNM system (American Joint Committee on Cancer, AJCC). This system contains 3 key pieces of information. Briefly, T refers to the primary tumor size, N to lymph node metastases and M to metastases at distant organs of the body (figure 10). The

spread for each category is further described with numbers 0-4. More analytical information is provided in the 7th edition of the TNM classification system [151].

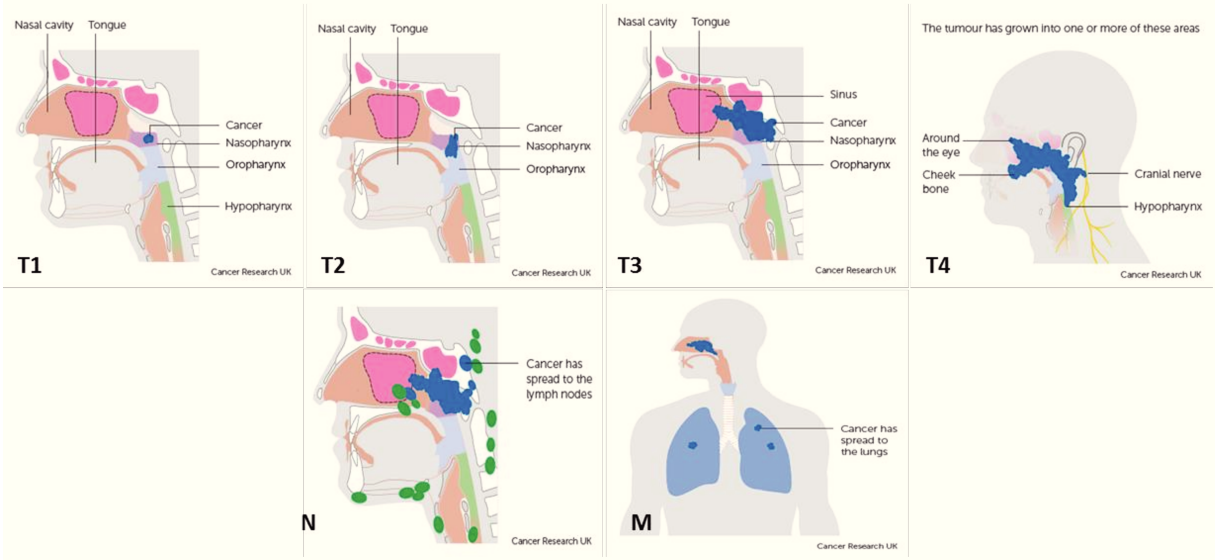

Figure 10: Stages of nasopharyngeal carcinoma indicating primary tumor progression (T1-T4), nodal metastasis (N) and distant metastasis to other parts of the body (M) (from Cancer Research UK)

As its deep-seated anatomic location limits a surgical approach, radiotherapy is the golden standard in the treatment of primary nasopharyngeal carcinoma. The progress and evolution of the radiotherapy technique is mainly responsible for the improved efficacy of NPC treatment and control over the years. Conventional two-dimensional (2D) and three-dimensional (3D) radiotherapy tend to be replaced by intensity-modulated radiotherapy (IMRT). This technique further improved the therapeutic index, delivering tumoricidal doses of radiation to tumor cells, while sparing adjacent normal tissues. Thus, the undesired toxic side-effects of previous techniques are avoided. Studies have shown an impressive improvement in 3-year local control and survival rates, even for more advanced stages, reaching 80-90% [152]. The combination of radiotherapy and chemotherapy for locally advanced NPC is another pivotal factor in the improvement of the outcome, as many trials have proved its benefits in disease control and survival [153]. In most cases, cisplatin is the chemotherapeutic agent of choice, although alternative drugs with similar efficacy are also used, such as uracil plus tegafur (a prodrug of fluorouracil) and oxaliplatin. Although more effective, chemoradiotherapy is associated with higher incidences of hematological and non-hematological acute toxic effects, compared to radiotherapy alone [154]. A combination of taxane-containing induction chemotherapy with concurrent chemoradiotherapy recently proved to further improve to short-term control of locally advanced NPC [155]. Overall, the

advances in tumor mapping and treatment of NPC have led to significant improvement of the outcome during the last years, with high cure rates for early-stage NPC. The 5-year survival for these cases has risen to 90%. However, half of the newly diagnosed cases concern metastasized carcinomas, with 5-year survival rates declining to 50-70% (reviewed by Tan et a1 in 2016 [156]). Finally, where lasting cure is achieved, the aggressiveness of the therapeutic approach may often leave severe consequences, influencing the quality of life. Common acute radiotherapy-related effects include mucositis, dysphagia, dermatitis, and xerostomia [142]. Other examples include neurological symptoms, such as temporal lobe injury, cranial neuropathies, Lhermitte's syndrome, and brachial plexopathy, as well as non-neurological effects, such as auditory and visual complications, soft-tissue fibrosis, feeding difficulties and endocrinopathies related to thyroid and pituitary dysfunction [157]. Clinical symptoms typically improve within weeks after treatment cessation, but in instances of grade 3 or 4 reactions, these can persist, leading to consequential late effects. Recurrence also remains a challenging issue, highlighting the need to further develop more efficient evaluation and therapeutic approaches.

Nasopharyngeal carcinoma, a multifactorial disease

Like most human malignancies, NPC is a multifactorial disease resulting from environmental factors, genetic susceptibility and EBV infection. The role of environmental factors, mainly nutritional habits, and the role of genetic susceptibility will be introduced briefly in the next two paragraphs. Obviously EBV is only a co-factor since NPC is frequent only in restricted geographical areas whereas EBV infection is ubiquitous in the human genus. However, the role of EBV should not be neglected since the presence of the EBV genome in malignant NPC cells is a constant characteristic of NPC regardless of patient geographic origin. The contribution of EBV to NPC oncogenesis will be thoroughly discussed in the next chapter. The infection is mainly latent, meaning that there is no production of viral particles. Works have suggested another viral cause for nasopharyngeal carcinoma, mostly concerning its non-endemic form, implicating infection by the human papillomavirus (HPV). However, as discussed during the GRC conference on nasopharyngeal carcinoma (Hong Kong, June 2016), HPV is mostly associated with oropharyngeal carcinoma, while EBV infection is linked to nasopharyngeal carcinoma.

Environmental factors

As reviewed by Bruce et al (2015), various environmental factors are key factors in the etiological basis of NPC, mainly traditional dietary habits, including frequent consumption of salt-preserved fish and meat, particularly in infancy and childhood [158]. This preservation technique has been shown to allow partial decomposition, resulting in the accumulation of carcinogenic nitrosamines, leading to an approximately 2-fold higher incidence of NPC in regions of frequent consumers. Better conservation methods like the use of refrigerators are considered to contribute to the decrease of NPC incidence. Other environmental risk factors of lower importance include tobacco smoking, wood-fire smoke inhalation, occupational exposures and some herbal medicines [159]. On the other hand, high consumption of fruits and vegetables is thought to decrease the risk of NPC, being rich in fiber, vitamins, folate and carotenoids, which are believed to protect from cancer [159].

Genetic susceptibility

Familial predisposition is a major risk factor in NPC. In endemic regions it is obvious that the risk is much higher for members of families where a case has been previously reported [160]. However, there are no major susceptibility genes like the previously mentioned BRCA1/2 for breast and ovarian carcinomas. Most if not all susceptibility genes have low penetrance, even in endemic regions and their identification requires genetic surveys on very large series. Most investigations – especially extensive association studies like genome-wide association studies (GWAS) – have pointed the importance of genetic polymorphisms mapping within the MHC region (major histocompatibility complex) of the sixth chromosome (6p21), coding for the HLA genes (human leukocyte antigens). Such studies examine a genome-wide set of genetic variants in different individuals to see if any variant is associated with a trait. GWASs typically focus on associations between single-nucleotide polymorphisms (SNPs) and traits like major human diseases. The MHC complex produces the set of cell membrane proteins which are responsible for foreign molecule recognition and T-cell-mediated antigen recognition. This locus contains 6 HLA genes (HLA-A, HLA-B, HLA-C, HLA-DQ, HLA-DR, HLA-F) and certain HLA haplotypes are associated with a reduced or increased risk for NPC. The affinity of their products for EBV antigens seems to be capable of influencing tumor immunoediting, thus promoting or thwarting recognition and elimination of EBV-associated NPC cells by infiltrating lymphocytes [161]. GWAS on Southern Chinese, Taiwanese and Tunisian NPC patients and comparison with healthy subjects revealed consistent association of NPC with certain HLA alleles, as SNP variations (single-nucleotide polymorphisms) were

extensively analyzed [162]. All HLA genes mentioned above were found to play a role in genetic susceptibility for NPC development, but the one gene being presented in most if not all analyses is HLA-A [163, 164]. Notably, the allele HLA-A*1101 was strongly associated to a reduced risk for NPC [165]. HLA-A*1101 was shown to present immunodominant EBV epitopes and to induce cytotoxic T-lymphocyte responses against EBV-infected cells, which might explain the decreased risk of NPC among individuals with HLA-A*1101. Similarly, the HLA-A*0207 allele predisposes individuals to developing NPC, whereas the HLA-A*0201 allele is protective [166]. Interestingly, the strong association between HLA gene variants and cancer susceptibility has also been demonstrated in non-Hodgkin lymphoma [167], another malignancy related to EBV infection, suggesting that HLA-mediated immune responses play an important role in virus infection–related cancers. Taken together, these data clearly indicate that HLA alleles define a stronger or weaker immune response to viral antigens, leading to a reduced or increased risk of developing EBV-associated neoplasms respectively. Other, non-HLA, genes in the 6p21 locus have also been shown to confer susceptibility to NPC, like GABBR1 and HCG9 [168]. Distinct loci also linked to NPC susceptibility through SNP variation include mainly TNFRSF19 in 13q12, ITGA9 (3p21), MECOM (MDS1 and EVI1 Complex Locus) in 3q26, as well as the tumor suppressor genes CDKN2A and CDKN2B (9p21) [162, 169]. Interestingly, the last two were also found with a homozygous deletion or a promoter hypermethylation in about 40% of NPC primary tumors [170]. Taken together, the identification of TNFRSF19, MECOM and CDKN2A-CDKN2B as susceptibility loci suggest an important role for the TGF-β and JNK signaling pathways in the pathogenesis of NPC. It is also noteworthy that TNFRSF19, MECOM and CDKN2A-CDKN2B are all involved in leukemogenesis, suggesting that there could be a partially shared pathogenic mechanism between hematological malignancy and NPC. Finally, altered genes involved in the DNA double-strand repair pathway, such as RAD51L1, have been shown to be relevant, whereas a large-cohort validation analysis based on Hong Kong population confirmed that this pathway can be a potential risk factor for NPC [171].

Histogenesis

Comparative investigations made on pieces of nasopharyngeal mucosa obtained from Chinese donors living in endemic or non-endemic regions of China have shown striking differences. These differences are not related to EBV whose genome is consistently undetectable in non-malignant nasopharyngeal mucosa regardless of the endemic or non-endemic context. The major difference is the detection of genetic alterations in nasopharyngeal epithelial cells from

individuals leaving in endemic regions. These alterations are mainly losses of heterozygosity (LOH) for tumor suppressor genes like CDKN2a (9p21.3) and RASSF1 (3p21.3). These alterations occur in a context of limited alterations of cell morphology (except the usual metaplasia from cylindric to squamous epithelial differentiation). Another remarkable observation is that nasopharyngeal carcinomas in situ are rarely observed, especially carcinomas in situ with EBV infection, although a few cases have been reported. Overall, these observations have suggested a scenario characterized by a long stage of premalignant genetic alterations of the nasopharyngeal mucosa with LOH of tumor suppressor genes followed by a rapid progression towards invasive carcinoma following the infection of a unique cell affected by genetic alterations. Strong arguments in favor of this scenario have come from recent investigations on the in vitro alterations required for establishment of a permanent latent infection in primary epithelial cells.

Today, EBV has been well described to contribute to the establishment of a malignant state under favorable conditions. In EBV-positive tumors, the virus has been found exclusively in all tumor cells, but not in normal nasopharyngeal epithelium surrounding the tumor, suggesting that EBV activation is involved in the pathogenesis of NPC. Analysis of pre-invasive lesions showed that EBV is present even during the initial phases of the transformation [172]. Southern blot-based experiments back in 1986 showed that EBV-associated epithelial malignancies are clonal expansions of a single EBV-infected progenitor cell [173]. Another study dating back to 1993 screened 26 nasopharyngeal biopsies from EBV-carrying Chinese Malaysians who had presented with clinical symptoms possibly indicative of NPC, but in whom histological analysis of an adjacent biopsy had revealed no evidence of tumor, finding out that 23 showing normal nasopharyngeal histology were consistently negative for EBV markers, while the other 3 cases were all positive and their biopsies revealed NPC cells [174]. This study concluded that EBV infection of the normal nasopharynx is not a regular feature of the virus carrier state. However, as mentioned by A. Hildesheim and C.-P. Wang, since EBV infection is nearly ubiquitous and NPC development rare, it is widely acknowledged that EBV infection is not sufficient to induce cancer and that other cofactors play an important role in NPC pathogenesis [161]. It seems that EBV infection is not the first step in the process of carcinogenesis, although being a very early one. This suggestion is further supported by the fact that, in areas with high frequency of NPC, 80-100% of NPC cases present chromosomal losses in the 3p and 9p loci. These losses are found with the same frequency in EBV-related low-grade dysplastic lesions and in normal

nasopharyngeal epithelia negative for EBV markers in the same geographical areas [175, 176]. These data indicate that chromosomal losses precede viral infection, maybe even predisposing to it, in the process of NPC malignant transformation. This is further supported by in vitro experiments demonstrating that stable EBV infection of epithelial cells requires an altered, undifferentiated cellular environment and that p16 deletion on chromosome 9p and amplification of the cyclin D1 (CCND1) locus on chromosome 11q facilitate persistent EBV infection of immortalized nasopharyngeal epithelial cells [177, 178] (reviewed L. Young and C. Dawson in 2014 and presented in figure 11). The biology of the virus and the relation between infection and development of NPC will be further analyzed in the following pages.

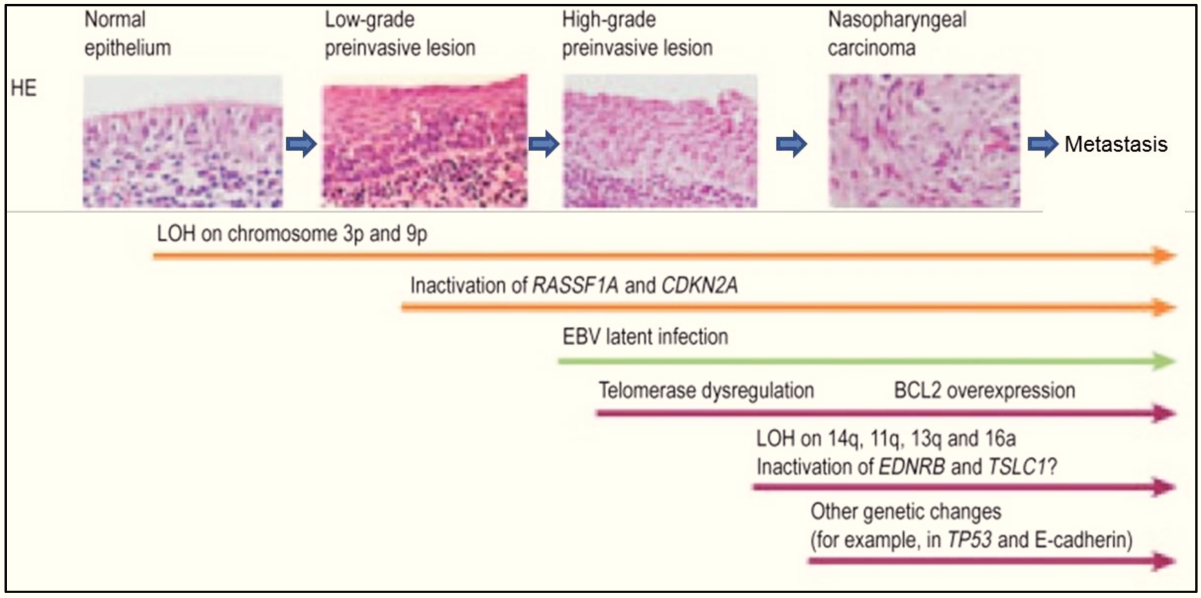

Figure 11: Schematic presentation of NPC pathogenesis, as proposed by L. Young and C. Dawson (taken and modified from [179])

A brilliant study by Li et al (2006) compared artificially immortalized normal cells taken from nasopharyngeal epithelia with NPC cells and revealed interesting facts linking nasopharyngeal carcinogenesis and cell immortalization [180]. By transducing the expression of human telomerase catalytic subunit (hTert), they managed to generate, after two senescence periods, immortalized EBV-negative nasopharyngeal cells. Molecular analysis of immortalized cells showed a unique chromosomal gain (17q21.32-q25.2) located in the 11p15 site, present universally in immortalized cells and also observed in 40-50% of NPC. Gene expression analysis showed a progressive upregulation of Id1 and activation by nuclear translocation and progressive increase in the expression of p-IκB and NF-κB. On the other hand, there was a downregulation of RASSF1A and a homozygous deletion of the $p16^{INK4A}$ locus. Ras association domain family member 1 (RASSF1) was found frequently deleted in

NPC, an event suggested to promote mitotic progression and chromosomal instability [181, 182]. This study highlighted these alterations as early events of immortalization, eventually turning premalignant nasopharyngeal epithelial susceptible to EBV infection and establishment of viral latency, as many of these genes are also targets of viral proteins, like LMP1 [183, 184].

Somatic genetic and epigenetic alterations

Apart from the already mentioned chromosomal losses, gene misregulations and genetic variation predisposing for NPC development, genomic analyses during the last 3 years have shed significant light on the extensive genomic alterations found in NPC and playing a role in disease establishment, immune evasion and progression. These works were based on whole-exome sequencing, targeted deep sequencing and SNP arrays [185]. Additional chromosomal events include focal losses in regions 11q, 13q, 14q and 16q. Genes CDKN2A and CDKN2B previously mentioned to be lost (9p21.3), code for three tumor suppressors: $p16^{INK4A}$, ARF and $p15^{INK4B}$. Deletion of the first was demonstrated to be involved in NPC progression, as its forced re-expression resulted in cell-cycle arrest and blocked the tumorigenic interaction between cdk4/cdk6 and cyclin D1 [186]. The $p16^{INK4A}$ is a cyclin-dependent kinase inhibitor which inhibits the function of cyclin-dependent kinase and prevents phosphorylation of RB, resulting in the blockage of cell cycle progression from G1 to S phase. The p16 protein is largely responsible for the onset of replicative senescence in many types of human epithelial cells. Several genomic translocations have also been found in NPC, although at low frequencies, creating gene fusions and are summarized by Bruce et al (2015) [158]. Small-scale genomic alterations like single-nucleotide variants (SNV) or small insertions and deletions (indels) exhibit a low frequency in NPC, nevertheless affecting key genes and pathways. Major examples include TP53, rarely mutated in NPC in contrast to most cancers, but found altered at the somatic level in one fifth of cases and genes implicated in chromatin modification pathways (ARID1A) and the oncogenic pathways related to PI3K and receptor tyrosine kinase [185]. Genomic aberrations at the level of the MHC class I genes in NPC were already discussed, but they were also found to correlate with a worst prognosis and poorer disease-free and overall survival [149].

Epigenetic events further contribute to deactivation of various tumor-suppressing genes, including some of the above mentioned (RASSF1, CDKN2A). The Wnt inhibitory factor 1 is reported to have a hypermethylated promoter in 85-90% of studied NPC cases, an event shown to promote clonogenic survival [187]. Cell adhesion molecule 1 (TSLC1) and Thy-1

cell surface antigen, found in the same locus (11q23) have also been identified as frequent targets of hypermethylation in NPC, with their inactivation concurring with enhanced metastatic potential, as found in lymph node metastases [188, 189]. NPC-related aberrant methylation patterns affect a variety of metabolic pathways, like cell invasion/migration, response to DNA damage, apoptosis and cell cycle regulation/proliferation. Interestingly, among the influenced gene targets implicated in these pathways we also find miRNAs, such as miR-148a (cell invasion/migration) and miR-218 (apoptosis) [190, 191]. MiR-31, a miRNA encoded within the same region (9p21.3) as CDKN2A/p16, was also recently found to be inactivated by promoter hypermethylation in NPC, promoting tumorigenesis [192]. Under normal conditions, this miRNA was shown to control cell growth by directly targeting FIH1 and MCM2, involved in p53 inhibition and DNA replication licensing respectively. Finally, apart from DNA methylation aberrancies, histone modification is also altered in NPC, affecting various target genes. EZH2, a gene coding for a histone-lysine N-methyltransferase, is found upregulated in NPC, bearing an impact on angiogenesis, cell motility and survival [193, 194]. A recently published study by Ye et al (2016) shed significant light to the contribution of tumor miRNAs in tumor evasion via exosome-mediated delivery [195]. This group reproduced in vitro the microenvironment of an NPC tumor, by mixing malignant NPC cells with T-cells from healthy donors. In a paradoxal way, although NPC tumors are characterized by a highly inflammatory phenotype, with a heavy infiltration by non-malignant leucocytes, mainly T- but also B-lymphocytes as well as macrophages, dendritic cells and neutrophils, the immune escape is a fact. This is supported by the rapid proliferation of malignant cells, despite the consistent expression of EBV proteins known to induce an immune response, such as EBNA1 and LMP1 and 2, targets of CD4+ and CD8+ cytotoxic T-cells [196]. The works of this group revealed a secretion and delivery of tumor exosomes carrying immunosuppressive factors which altered the behavior of T-cells. Most notably, exosomes delivered to T-cells miR-24-3p, which were internalized and decreased the expression of FGF11, conferring subsequent modifications in the ERK and STAT phosphorylation, reducing the proliferation of these cells. An observed decrease in the expression of interferon-γ and IL-17 also provided evidence of a blocked differentiation.

On the other hand, focal amplifications in some loci, such as 3q26.1, 11q13 and 12p13, lead to copy-number gains for genes with oncogenic potential [158]. Related oncogenes often amplified in NPC include CCND1, as mentioned above, in more than 90% of studied cases increasing proliferation, PIK3CA activating the PI3K/Akt pathway with reflection on cell

growth and survival in 70-75% of primary NPC [197, 198]. Furthermore, the lymphotoxin-β receptor (LTBR) is often a target of amplification, directing towards an activation of the NF-κB pathway for enhanced tumor growth and cell survival [199]. NF-κB pathway aberrations were studied in depth in a recently published work by the group of Kwok-Wai Lo in Hong Kong, China. This work demonstrated the pivotal role of the pathway in NPC pathogenesis, revealing consistent downregulation of multiple negative regulators of the pathway, as CYLD, TRAF3, NFKBIA and NLRC5, in 41% of studied cases [149]. Particularly mutations in CYLD were shown to play a substantial driver role in cell growth, as ectopic expression of the wild-type gene blocked cell proliferation and reduced NF-κB transcriptional activity, inhibiting nuclear translocation of Bcl-3.

Biological resources for NPC study

The difficulty to derive tumor cell lines permanently propagated in vitro is variable depending on the type of malignancies. In contrast with other EBV-negative Head and Neck carcinomas, obtention of NPC cell lines propagated in vitro has proven to be extremely difficult especially when starting directly from clinical specimens. Even when some of these cells can grow in vitro, they tend to lose their EBV episomes after a few passages, although this type of event has never been well documented [200]. Currently there is only one in vitro EBV-positive NPC cell line, which was secondarily derived from an NPC PDX (C666-1). Patient-derived xenografts (PDX) as opposed to CDX (cell-derived xenografts) are xenografts serially passaged on immunocompromised mice. These xenografts are obtained directly from clinical tumor specimens without having been passaged in vitro. In the recent years, PDX have become very popular in the pharmaceutical industry and academic labs because they mostly retain the principal histological and genetic characteristics of their donor tumor and display the same sensitivity to therapeutic agents. They often remain stable across passages. These models have been shown to be predictive of clinical outcomes and are being used for preclinical drug evaluation, biomarker identification, biological studies, and personalized medicine strategies. In the case of NPCs, like for some other types of human malignancies, it is somehow easier to derive PDX than cell lines directly implemented in vitro. However, so far the success rate has been very low; one successful graft for about 100 attempts from primary tumors and 1 for 2 attempts from metastatic lesions. Therefore, so far, all existing NPC PDX have been concentrated in only two labs: KW Lo's lab in Hong Kong and our lab in Villejuif. In addition, so far, it has proven very difficult to derive cell lines permanently propagated in vitro from these PDX. The C666-1 cell line is a remarkable exception. Very

recently, another cell line has been derived from C17 but is not yet available for all investigators (Pr G. Tsao personal communication). In this context, several authors have proposed another approach: they perform in vitro artificial EBV infections of EBV-negative cell lines which are presumed to be derived from NPC tumors (example of SUNE1). Our group is not enthusiast of this approach because these cell lines do not reproduce the phenotype of NPC cells. Both before and after EBV infection, they rather have the phenotype of differentiated squamous epithelial cells without the typical inflammatory markers of NPC cells (constitutive MHC class II expression, CD54, CD48, CD70, etc). This is in contrast with what is observed for C666-1. In the context of our work, we used the only globally used cell line of NPC, C666-1, that retains the viral genome independently of the number of passages, developed from a primary NPC tumor in Honk Kong [201]. Three PDX of poorly differentiated NPC developed in Gustave Roussy in the late '80s by Pierre Busson and colleagues were also used, all tested positive for EBV serological markers [202]. The first, named C15, was developed from a primary locally advanced tumor, characterized by a wild-type p53 phenotype and bearing approximately 30 copies of the EBV genome per cell. The other two xenografts derived from metastases of NPC tumors, the C18 from a lymph node metastasis and the C17 from a cutaneous secondary tumor, previously treated for 2 months and 2 years respectively. The first is characterized by a p53 mutation, while the second lacks both alleles of the gene [203]. C18 bears 12 copies of the viral genome, whereas C17 only 3. The spectrum of EBV gene expression is not identical in these 3 cell lines. They have in common expression of EBNA1 and EBERs. The LMP1 protein is detected only in C15. EBV infection is tightly latent in C15 and C17 whereas lytic proteins, especially the BZLF1 protein are consistently detected in C18, although at a low level in baseline conditions [204]. Constitutive activation of NF-κB p50/p50/Bcl3 and p50/relB complexes is a characteristic feature of NPC cell phenotype. It is achieved in two different ways in C15 and C17; by expression of the viral LMP1 protein in C15 and by a missense mutation of the gene encoding TRAF3 in C17 [205]. The status of NF-κB in C18 is not yet known.

Chapter 4: EBV and NPC pathogenesis

- Historic data on EBV biology

As previously said, the first etiological factor, distinguishing nasopharyngeal carcinoma among other types of cancer, is its consistent association with the presence of the Epstein-Barr virus (EBV). EBV was discovered in 1964, as Tony Epstein and Yvonne Barr identified herpesvirus particles by electron microscopy in a subpopulation of Burkitt's lymphoma (BL) tumor cells in vitro. Old et al, two years later described BL antigen-specific antibodies in the serum of African patients, which recognized BL cell line-derived antigens [206]. Similar antibodies were subsequently detected in patients with post-nasal carcinomas, leading to the suspicion that similar viral particles might be found in those carcinomas as well. Immunofluorescence assays confirmed the presence of such antibodies against the viral capsid antigen (VCA) and the membrane antigen (MA) of EBV in NPC, as further serological analysis and DNA hybridization also confirmed these findings. Interestingly, Wolf et al in 1973 found that EBV is detected exclusively in NPC cells and not in tumor-infiltrating lymphocytes [207], although their interaction with adjacent malignant cells appears to be crucial for tumor growth [179]. In 1985, a massive serological screening in Southern China showed that elevated titers of EBV antibodies can be found up to 41 months prior to clinical diagnosis of NPC, while there is an association between their levels and tumor stage, demonstrating their utility in early diagnosis [208]. This work was preceded by the full sequencing of the genome of EBV in 1984. In fact, EBV can be found in the vast majority of healthy people worldwide, exceeding 90% in adults, as the virus is not fully eliminated after a previous infection (American National Center for Infectious Diseases). It can be easily transferred by saliva, through kissing, use of eating equipment, as well as sharing food and drinks, or through genital secretions. Although infants can get infected by EBV within the first two years of their life, they rarely present symptoms of infection or, if present, the symptoms are mild and subclinical until the age of 8 months. Studies have revealed that, during that time, infants have persisting levels of maternal antibodies, containing the infection [209]. When infection by EBV occurs during adolescence, it abruptly causes infectious mononucleosis in approximately half of the cases. EBV is a member of the viruses of the herpes family, among the most common human viruses, mainly infecting B cells and epithelial tissues. Among other diseases, EBV was the first virus shown to cause cancer in humans and is associated with a wide range of human cancers originating from epithelial cells, lymphocytes and mesenchymal cells. Examples of EBV-related malignancies are

nasopharyngeal carcinomas, several types of lymphomas (endemic Burkitt's Lymphoma (BL), more rarely Hodgkin lymphomas, centro-facial NK-T lymphoma, post-transplant lymphomas and AIDS-associated lymphomas), and approximately 10% of gastric cancers worldwide [210-213].

- Viral and genomic structure

EBV, also named Human Herpesvirus 4 (HHV-4), is one of the 8 members of the human Herpesviridae viral family, belonging to the subfamily of γ-herpesvirinae and the genus of lymphocryptoviruses. Its genome consists of a linear double-stranded DNA of approximately 172 kilobase pairs (kbp), with a 60% Guanine (G) + Cytosine (C) composition, containing around 80 protein-coding genes. Both ends of the viral DNA contain a variable number of repeated non-coding sequences of 500 bp (called TR for terminal repeats). In addition, there are internal repeated sequences called internal repeats (major IR1 and minor IR 2–4). Ori-P is the replication origin of the viral genome used in the latent state of infection. The Ori-lyt are two replication origins used during the lytic infection. The genome is surrounded by a viral envelop. Apart from causing infectious mononucleosis and contributing to the development and proliferation of various cancers, EBV is also linked to some autoimmune diseases, like multiple sclerosis and lupus erythematosus [214, 215].

- Virus-cell interactions

Like other herpesviruses, EBV causes lifelong infection following the primary infection. As mentioned above, the vast majority of adult humans (>90%) are healthy carriers of EBV regardless of their geographic origin. Its persistence in healthy subjects relies on three key features: (1) its capacity to continuously induce bursts of productive infections in various tissues, especially in the upper aerodigestive tract and more specifically in the tonsils, the salivary glands and possibly gingiva; (2) its capacity to achieve latent infection mainly in B-lymphocytes, especially memory B cells in blood, bone marrow and lymphoid organs; (3) its sophisticated strategies of immune evasion [216]. The distinction between two major modes of virus-cell interactions is a key to understanding EBV biology [217]. (1) Latent infections are cellular infection modalities characterized by the absence of viral particle production, a restricted expression of viral genes (often less than 10 out of 80) and a circular configuration of the viral genome (Figure 12). (2) Lytic/productive infections are characterized by sequential or concomitant expression of most viral genes, abundant synthesis of linear viral

genomes and finally extracellular release of viral particles or virions in a context of mandatory cell death.

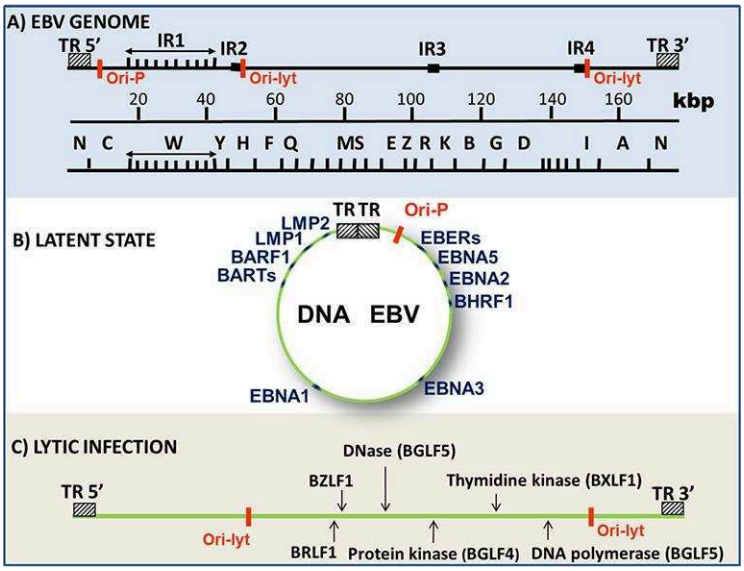

Figure 12: The structure and configuration of the genome of the Epstein-Barr virus in connection with the latent and lytic forms of infection (graphic representation done and published by our group [218]).

When the infected cell enters a state of latent infection the viral DNA is circularized by homologous recombination of the TRs (terminal repeats). Fused TRs with an identical number of repeats denote expansions of a single infected progenitor cell, thus used as measure of EBV clonality in EBV-positive tumors [173]. This circular form of the genome called episome is contained in the nucleus in combination with cellular chromatin but apart from chromosomes. The episomes are passively replicated by cellular DNA polymerases starting from the Ori-P origin of replication. During latent infection, most viral genes are silent. However, about 10% of them are consistently expressed (in blue in figure 12). Most of these genes encode final products — viral non-coding RNAs or proteins — with transforming properties. They are called “latent genes” whereas genes expressed only during lytic infection are called “lytic genes”. There is no topographical separation between the two categories of genes. As usual in virology, the phase of the lytic cycle which precedes viral DNA replication is called the early phase. As soon as the viral DNA pol starts the autonomous replication of the viral genome, lytically infected cells enter the late phase. Newly synthesized viral genomes are in a linear configuration. Viral proteins expressed at the very beginning of the early phase of the lytic cycle like BZLF1 and BRLF1 are encoded by immediate early genes. Early viral proteins are expressed at a more advanced stage. Many of them are involved in DNA metabolism, for

example, the viral thymidinekinase, DNAse and DNA polymerase. The EBV protein kinase (BGLF4; protein encoded by the Bam G leftward open reading frame 4) can phosphorylate various substrates. It is also one component of the viral particle (reviewed by Oker et al in 2016 [218]).

- Types of EBV latency

A crucial aspect in EBV-related malignancies is the predominance of viral latency in the interaction between EBV and the host cells. This means that most viral genomes are silent in the vast majority of malignant cells. However, a small fraction of them are consistently expressed, coding for a handful of viral products and untranslated RNAs, most of them with proven oncogenic properties. Different patterns of expression of these products among EBV-positive tumors have led to the definition of three types of EBV latency. Lymphoblastoid cell lines (LCLs), meaning peripheral B lymphocytes in vitro infected by EBV, are a model extensively used for the study of carcinogen sensitivity and DNA repair and their development demonstrated in an emphatic way the ability of EBV to immortalize human resting B cells and give rise to an actively proliferating B cell population [219]. In LCLs, every cell carries multiple copies of EBV episomes, expressing a 6 nuclear antigens (EBNAs 1, 2, 3A, 3B, 3C and LP) and 3 latent membrane proteins (LMPs 1, 2A and 2B) [220, 221]. In addition to latent proteins, LCLs also exhibit robust expression of viral non-coding RNAs. These include the non-polyadenylated EBV-encoded small RNAs (EBERs) 1 and 2, expressed in all forms of EBV infection and EBV microRNAs. Up to date, 44 EBV-derived microRNAs have been identified, produced by two distinct loci of the viral genome. Transcripts from the BamHI-A region, originally referred to as BamHI-A rightward transcripts (BARTs), along with transcripts from the BamHI H rightward reading frame 1 (BHRF1) region encode miRNAs. This pattern of latency is referred to as the type III of viral EBV latency and is characteristic in the majority of EBV-associated lymphomas arising from immunosuppressed patients. However, Burkitt's lymphoma (BL) biopsies revealed another pattern of expression, named type I. In this type, EBNA1 is the only protein expressed in a consistent manner, along with the EBERs and the BART transcripts (table 5). Variations in this type appear in 5-10% of BLs, concerning the additional expression of the BHRF1 transcripts and the nuclear antigens EBNA3A, 3B and 3C [222]. The remaining type (type II) is an intermediate type of expression, identified in NPC and EBV-associated Hodgkin lymphoma (HL) biopsies [223-226]. In this type, apart from the expression of EBNA1, BART and EBER transcripts, there is a detection of LMP1 and LMP2A/2B. Although consistent in

HL, LMP1 detection is reserved to approximately one fifth of NPC biopsies tested at the protein level [221]. EBERs and BART miRNAs are generally expressed in all types of EBV latency, at an abundant level. Most particularly, BARTs can account for up to one third of the cells produced miRNAs. However, in B cell malignancies BART are often expressed at a modest level, while BHRF1 miRNAs are abundant. In NPC the predominant pattern is the exact opposite: there is almost no detection of BHRF1 miRNAs, whereas BARTs are massively produced (see figure 13).

Gene Expressed	EBNA1	EBNA2	EBNA3A	EBNA3B	EBNA3C	EBNALP	LMP1	LMP2A	LMP2B	EBERs
Product	Protein	Protein	Protein	Protein	Protein	Protein	Protein	Protein	Protein	ncRNAs
Latency I	+	–	–	–	–	–	–	–	–	+
Latency II	+	–	–	–	–	+	+	+	+	+
Latency III	+	+	+	+	+	+	+	+	+	+

Table 5: Expression pattern of viral genes in every type of EBV latent infection

These different forms of viral latency reflect “the cellular environment and the complex interplay between host regulatory factors and viral promoters that drive EBV latent gene expression” [179]. A characteristic example is the transcription of EBNA and LMP genes and their differences between latency III and latency II. In type III, the EBNAs are encoded by different mRNAs, produced via differential splicing of the same long transcript expressed from promoter Cp or Wp, located close to each other in the BamHI-C and BamHI-W regions respectively. A switch from Wp to Cp occurs early in B-cell infection as a consequence of the transactivating effects of both EBNA1 and EBNA2 on Cp. LMP transcripts are expressed from separate promoters in the BamHI-N region of the EBV genome, with the leftward LMP1 and rightward LMP2B mRNAs apparently controlled by the same bidirectional promoter sequence (ED-L1) that also responds to transactivation by EBNA2 [220]. The LMP2A promoter is also regulated by EBNA2. Both LMP2A and LMP2B transcripts cross the TRs into the U1 region, thus requiring the circularization of the genome for transcription. In type

II, EBNA1 transcription is driven from the TATA-less Qp promoter [227], and an alternative promoter, L1-TR, located in the terminal repeats is responsible for LMP1 expression [228].

- Contribution of viral proteins to carcinogenesis and immune evasion

In the context of NPC, the few expressed viral proteins are crucial for maintenance of the viral episomes and contribute to tumorigenesis. EBNA1, the only protein expressed in all types of EBV infection and consequently in all EBV-associated tumors, is responsible for the maintenance of EBV episomes in dividing cells by interacting with their OriP. Furthermore, it can induce the expression of other viral genes by transcriptional activation of the Cp and the LMP promoters [229]. Besides, EBNA1 has an oncogenic function, as its knockdown in NPC cell lines reduced proliferation, while its ectopic expression in xenografts promoted tumor growth and expansion. It was also shown to modulate various signaling cascades, like tumor growth factor β (TGF-β), signal transducer and activator of transcription 1 (STAT1) and NF-κB, favoring growth, survival, metastasis and angiogenesis. In NPC cells, EBNA1 induced the production of reactive oxygen species, in a way they caused DNA damage, as shown in B-cells [230]. Finally, evidence suggests that it can also downregulate p53 through interaction with the ubiquitin-specific protease USP7, thus destabilizing p53 and reducing its accumulation in response to DNA damage [229].

LMP1, although presenting a very heterogeneous expression pattern in NPC, has a multifaceted tumorigenic activity. This protein acts as a mimic of the tumor necrosis factor α (TNFα) receptor family members TNFR1 and CD40, altering TNF-responsive signaling proteins like TRAFs and the TNFR-associated death domain protein [231]. LMP1 expression achieved immortalization of rodent cells, while inhibiting differentiation in human epithelial cells [232]. It was shown to induce the expression of mitogenic receptors, such as the epidermal growth factor receptor (EFGR) and c-Met, as well as activating pro-growth and anti-apoptotic mediators, like survivin, NK-κB, PI3K/Akt and MAPK pathways [231]. These interactions promote cell proliferation and survival, while LMP1 was further shown to decrease expression of p16, already mentioned as often defective in NPC, by cytoplasmic sequestration of E2F4/5 and Ets2 transcription factors [233]. In addition, it was shown to promote angiogenesis through induction of hypoxia-induced factor 1α (HIF1α) and vascular endothelial growth factor (VEGF) [231]. Finally, numerous works have demonstrated the contribution of LMP1 to the tumor's metastatic potential through a variety of mechanisms. Most notably, it increases epithelial-to-mesenchymal transition (EMT), increases the expression and release of matrix metalloproteinases through activation of NF-κB, specificity

protein 1, activator protein 1 and extracellular regulated kinase (ERK)-MAPK pathways, while it also induces the expression of DNA methyltransferases 1, 3a and 3b, resulting in an increased promoter methylation, one of which for E-cadherin [231, 234].

LMP2A is consistently expressed in NPC, while LMP2B appears to be expressed in the absence of LMP1. Both proteins contribute to the oncogenic activity of infected cells, although their expression is not enough to transform normal cells alone. Transfection of human epithelial cells with LMP2A led to activation of several signaling cascades, including Notch, ERK, Syk, PI3K/Akt and Wnt/β-catenin [231]. Interestingly, LMP2A has also been suggested to block the switch from the latent to the lytic replicative cycle of EBV [235]. LMP2B on the other hand, also activates PI3K/Akt signaling and promotes cell motility by disrupting cellular adhesion. It also shares with LMP2A the ability to confer resistance to antiviral interferon (IFN) signaling in NPC cells through degradation of IFN-α, -β and -γ receptors [236].

A product of the BART-coding region (BamHI-A fragment) is the protein BARF1. BARF1 is considered to be a lytic gene, since its expression is induced upon induction of the lytic cycle in Burkitt's lymphoma cell lines. However, it has been shown that, in epithelial pharyngeal cells, EBV undergoes brief lytic replication [237]. Seto et a1 (2015) detected its expression in NPC cells and described its rapid secretion to the extracellular medium [238]. It was later found to be a homolog of the human colony stimulating factor 1 (CSF-1) receptor, with tumorigenic potential through its effect on apoptosis inhibition, as it induces Bcl-2.

Upon viral reactivation in NPC, several other lytic proteins have been detected and suggested to play a certain role in cell proliferation, migration and tumorigenicity. The EBV DNase (BGLF5) is an alkaline nuclease contributing to the generation and processing of linear viral genomes. Evidence shows that BGLF5 is involved in the repression of DNA repair mechanisms, enhancing genomic instability in human epithelial cells [239, 240]. The protein encoded in the same transcript coding for the BHRF1 miRNAs has also been detected in NPC biopsies and is another homolog of the human Bcl-2 protein, sharing its antiapoptotic properties [241].

- Viral non coding RNAs

The fact that EBV ncRNAs are produced in all latency stages, while EBV protein expression is limited, suggests that ongoing expression of these RNAs contributes to the maintenance of viral latency. Exact functions for many of them remain unknown but emerging studies during

the last years progressively unveil their contribution. EBERs 1 and 2, the non-coding viral small RNAs of 167 and 172 nucleotides respectively, are less studied regarding their function. These transcripts can account for up to 1 million copies per NPC cell. Takada and colleagues have shown that their expression in the EBV-positive NPC line C666-1 promotes favors cell growth. This is done by interaction with the double-stranded RNA sensing toll-like receptor 3 (TLR3) and consequently the transcriptional activation of the promoter of insulin-like growth factor-1 (IGF-1), thus leading to its release. IGF-1 expression has been confirmed in NPC in vivo [242]. EBV microRNAs are also very abundant in NPC, although the 4 miRNAs of the BHRF1 open reading frame are practically not detected in primary NPC [243]. BART transcripts were originally identified in the C15 NPC xenograft tumor (presented and used in the article 2) [244]. In the B95-8 strain of the virus, a big deletion is responsible for the absence of almost the entire BART region (figure 13C). However, this strain fully retains the ability to immortalize primary B cells in culture, implying that BARTs are not necessary for B cell transformation [245]. However, the fact that they are consistently highly abundant in latency II NPCs despite their dramatic variation in other cell types points towards a contributing role in NPC pathogenesis [246]. The entire BART locus is approximately 20 kbp, coding for longer ncRNAs (the BART transcripts family). For some of them their coding or non-coding potential remains controversial. The locus contains seven exons. BART miRNAs arise from the first four introns [246]. They are organized in two large clusters, encoding for the totality of BART miRNAs, except for the more isolated miR-BART2, which lies antisense to BALF5 gene, encoding for the viral DNA polymerase (figure 13C). Two TATA-less promoters, P1 and P2, upstream of exon 1 are responsible for the transcription of the BART RNAs. They are subject to regulation by a number of transcription factors, including Jun family members for P1 and C/EBP proteins for P2. Extensive promoter methylation has been shown to correlate with BART miRNA abundance in different types of cells [247] and the hypomethylation observed in NPC tumors may explain their increased abundance in this specific tissue [248]. Some of the studied BART microRNAs have been found to act complementarily to viral proteins, enhancing survival and proliferation, as well as immune evasion. Accumulating evidence on EBV miRNAs is constantly revealing their contribution to the establishment of viral latency by targeting viral and cellular factors involved in host cell growth, survival, signaling pathways, as well as host mechanisms inducing anti-viral immune response. BART miRNAs downregulate pro-apoptotic and tumor-suppressor genes of the host cell, promoting growth transformation of EBV-infected epithelial cells, also enhancing the metastatic potential of such carcinomas [249, 250]. BART miRNAs appear to target host

proteins p53 [251], Bcl-2 [252] and the outer mitochondrial membrane 22 homolog [253], thus acting in an anti-apoptotic way. Some of them are suggested to further influence immune response by targeting MHC class I-related chain B (MICB) [254], importin 7 [253] and Dicer [255]. Apart from host genes, BART miRNAs target a variety of viral proteins, thus regulating its expression in infected cells. LMP1 is targeted by ebv-miR-BART-1, -9, -16 and -17 [256], whereas ebv-miR-BART-22 targets LMP2A [257]. Other examples of viral targets of BARTs include BHRF1, BALF5, BZLF1/BRLF1, BNRF1 and BALF2, some of them targeted by more than one BARTs. It has been proposed that this self-regulation secures stabilization, maintenance and establishment of latency.

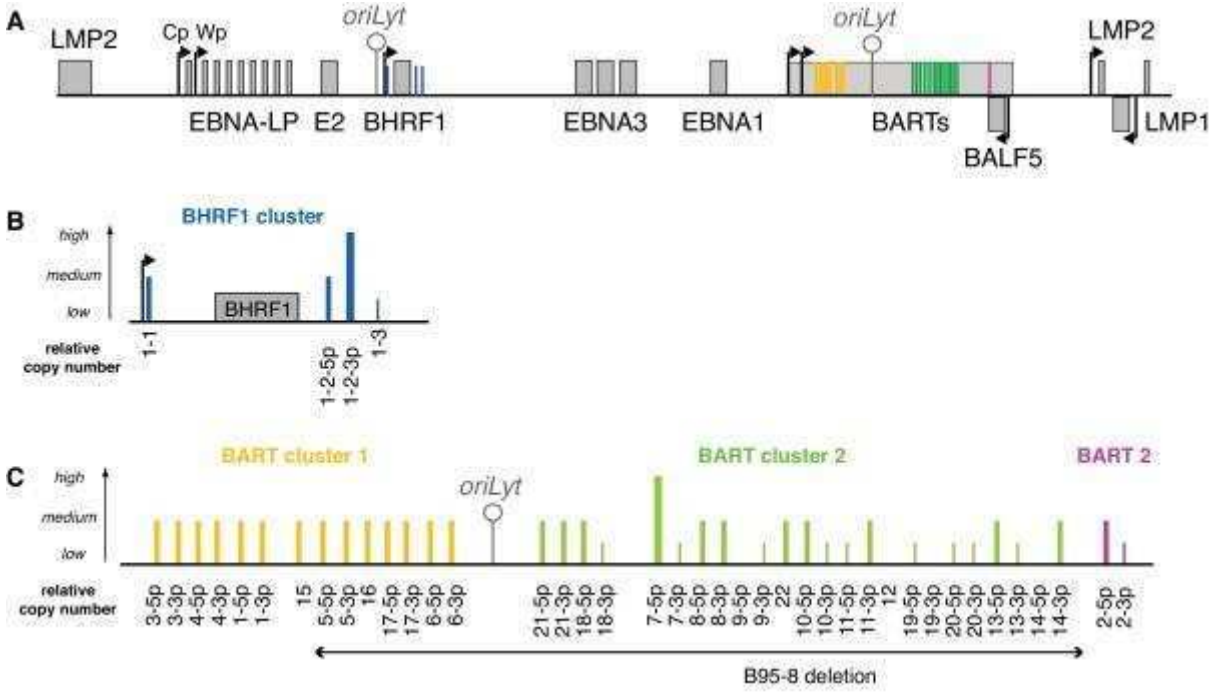

Figure 13: Location and expression pattern of EBV miRNAs (from [258]).

BHRF1 miRNAs on the other hand derive from introns of the BHRF1 locus, transcribed by the major latency promoters Cp and Wp (figure 13A). Latent Cp/Wp transcripts are alternatively spliced, leading to the production of the 4 BHRF1 miRNAs [259]. During the lytic cycle of EBV, an alternative promoter (BHRF1p) drives BHRF1 mRNA transcription, with studies showing a same kinetic behavior for miR-BHRF1-2 (5p and 3p) and BHRF1-3 [259]. These findings suggest that these miRNAs can also be generated by Drosha-mediated cleavage of the BHRF1 lytic transcript. MiR-BHRF1-1, in the contrary, overlaps the lytic promoter, thus depending entirely on the Cp/Wp activity [260]. Both BART and BHRF1 miRNAs have been shown to be upregulated upon viral lytic reactivation [261]. Studies on B cells showed that the loss of function of BHRF1 miRNAs negatively affects LCL outgrowth

and B cell immortalization, as well as cell cycle progression [262, 263]. In a recent publication, the group of Henri-Jacques Delecluse provided interesting information regarding the interaction between BHRF1 and the members of the miR-BHRF1 cluster, demonstrating their contribution to the inhibition of apoptosis. According to the model they proposed, miR-BHRF1-3 facilitates the abundant expression of BHRF1 in the early stages of viral infection by negatively regulating PTEN. As a double consequence of this, there is an increase in cell cycle entry, thus allowing the creation of a cellular reservoir for the virus, while expression of BHRF1 favors the establishment of the virus in the cell, blocking apoptosis. On the other hand, after the establishment of transformation, miR-BHRF1-2 targets BHRF1 and downregulates it, facilitating long-term persistence of the virus in the host [264]. Preceding this work, Milian et a1 (2015) used murine cells and showed that BHRF1 locates in the mitochondria in normal growing conditions and under apoptosis-triggering conditions. Under glutamine starvation, BHRF1 upregulated the endogenous Bcl-2 and increased the G1 phase of the cell cycle. In the mitochondria, BHRF1 blocked the modulator pro-apoptotic BH3-only protein Bim, preserving mitochondrial integrity [265]. An extensive list of BART miRNA targets, as well as additional information regarding their biology and dynamics are presented by Rebecca Skalsky and Bryal Cullen in their chapter “EBV Noncoding RNAs”, published in Epstein Barr Virus Volume 2, by Springer [266].

- EBV biomarkers for NPC

The ubiquity of EBV in nasopharyngeal carcinoma and the consistent expression of some viral genes have made EBV a valuable source of biomarkers for diagnosis and monitoring of the disease. Apart from the already mentioned EBV antibodies, EBV DNA is released by cancer cells and can be detected in serum and plasma of NPC patients [267]. It is found in the form of linear fragments, likely reflecting apoptotic processes [268]. Its abundance in the circulation of NPC patients before treatment, as well as its rapid decrease following surgery, radiation or chemotherapy make it an attractive potential biomarker, more and more used complementarily for diagnosis and screening for NPC in high-risk populations. Post-treatment re-ascension of EBV DNA correlates with disease recurrence, thus qualifying it as a contributive tool for NPC surveillance (presented by Dennis Lo in the 2016 International GRC NPC Congress held in Hong Kong). However, a better harmonization of laboratory methods has to be achieved before EBV DNA becomes a standard NPC biomarker. Furthermore, some EBV-encoded factors detected in the circulation of patients with NPC, are also under investigation for their potential use. These include LMP1 and Bam H1 reading

frame proteins, as well as noncoding RNA molecules EBER1, EBER2, and BART microRNAs. RT-qPCR analyses from NPC patients versus healthy control subjects already suggest a correlation between the serum levels of miR-BART2-5p, miR-BART6-5p and miR-BART17-5p and the status of the tumor, providing potential solutions for non-invasive monitoring and assessment of the disease. Our group has already published a study on plasma samples from NPC patients and control subjects, confirming the significant upregulation of miR-BART17-5p in NPC, while interestingly it co-purifies with a protein-rich fraction but not with exosomes [269].

Results

Article 1

Plasma miR-200b in ovarian carcinoma patients: distinct pattern of pre/post-treatment variation compared to CA-125 and potential for prediction of progression-free survival.

Introductory comment

The EXO-PLASMA project

This work was published in September 2015 in the journal Oncotarget and is the result of the first year of this PhD, inspired by preliminary encouraging results obtained during the previous semester, in the context of my MSc internship in the same laboratory. Having set up a project named EXO-PLASMA, IGR2009/1501 from 2009, in collaboration with the Head and Neck Surgery Department and the Gynecological Surgery Department of Gustave Roussy, our group managed to create a collection of whole blood and plasma samples from patients operated and treated at Gustave Roussy for an ovarian or a nasopharyngeal carcinoma. Besides, this collection also includes patients who underwent surgery for a benign pelvic lesion and patients who benefited of a prophylactic ovariectomy or annexectomy, after having been tested positive for ovarian cancer predisposition. At the time of the article's publication we had been able to enroll more than 200 patients in the EXO-PLASMA project, after securing a signed letter of consent by each one of them, mainly in collaboration with Dr Catherine Uzan. In this study, we used samples coming from patients bearing an ovarian carcinoma, patients with benign pelvic pathologies, such as fibroma, fibrothecoma, teratoma or ovarian cysts, as well as a control group consisted by healthy, disease-free women. The latter are not part of the EXO-PLASMA project, constituting a novel collection that I was able to create, in collaboration with Dr Busson and the Head of the Genetic Oncology department of Gustave Roussy, Dr Olivier Carron. This collection, numbering 100 subjects, includes plasma and, to a certain extent, whole blood from clinically healthy, cancer-free people (90% women) who were checked for mutations in the genes BRCA1 and BRCA2, predisposing, among others, for a breast and/or ovarian cancer, because of a charged family history. This collection aims to provide material for a future circulating miRNA analysis of a diagnostic nature. In the context of the present work, we used plasma samples from women tested negative for such mutations (wild-type BRCA1/2) and without any clinical signs of disease.

Treatment of ovarian cancer

As explained in the introduction, the major problem concerning the treatment of ovarian cancer is its diagnosis at a late stage, accompanied by existence of multiple metastatic lesions in the peritoneum, making its complete surgical excision almost impossible and leading to a poor prognosis. In the great majority of cases, epithelial ovarian cancer is detected at stages III and IV, where immediate debulking surgery is often not an option due to the extent of

cancer dissemination. Gustave Roussy, in contrast to many other health institutions, has included in the therapeutic strategy for the treatment of ovarian cancer the use of upfront chemotherapy. This feature, named neo-adjuvant chemotherapy, consists of a few (three to four in most cases) monthly cycles of chemotherapy, on the purpose of limiting the extent of the disease to a degree where complete macroscopic removal becomes possible. Following the initial onset of the symptoms and the results of an intravaginal echography and a CA125 measurement pointing towards the existence of a malignant tumor at the level of the ovaries, a diagnostic coelioscopy is performed in order to provide the best possible assessment of the tumor burden, as well as a definitive diagnosis. Depending on its results, the doctors conclude on the number of neo-adjuvant chemotherapy cycles that will be administered to the patient and a treatment plan is set. Every cycle is accompanied by new imaging tests and CA125 measurement for the evaluation of the response to the treatment. Following the completion of the neo-adjuvant cycles, an "evaluation" coelioscopy is performed in order to confirm a positive response and give the green light for a cytoreductive surgery. After the surgery and depending on its outcome (complete or incomplete macroscopic removal), the doctors set the number of "adjuvant" chemotherapy cycles to be administered. Depending on the type, the initial extent of the tumor and the outcome of the surgery, different combinations of chemotherapy can be selected. Chemotherapy for ovarian cancer is most often a combination of 2 or more drugs, given intravenously (IV) or, in some cases, intraperitoneally (IP) every 3 to 4 weeks. Giving combinations of drugs rather than just one drug alone seems to be more effective in the initial treatment of ovarian cancer. The standard approach is the combination of a platinum compound, such as cisplatin or carboplatin, and a taxane, such as paclitaxel (commercially Taxol) or docetaxel (Taxotere). For IV chemotherapy, carboplatin is often favored over cisplatin because it has fewer side effects and is just as effective. After the end of the adjuvant chemotherapy, patients with epithelial ovarian cancer may benefit from maintenance chemotherapy, instead of observation alone. This term refers to the chemotherapy given to women who have achieved remission after initial surgery and subsequent adjuvant chemotherapy. The aim of maintenance chemotherapy is to prolong the duration of remission and improve the overall length of survival. Some studies indicate that maintenance chemotherapy can improve the time without cancer progression, while others do not show any effect. Although there is no solid evidence from clinical trials suggesting that this method is significantly beneficial for the patients, at Gustave Roussy maintenance chemotherapy was often selected for patients treated during the time of the EXO-PLASMA collection (2010-2015) and it mainly consisted of bevacizumab (sold as Avastin).

Bevacizumab is a recombinant humanized monoclonal antibody acting as an angiogenesis inhibitor, targeting the human vascular endothelial growth factor A (VEGF-A) [270]. When associated with platinum- and taxane-based adjuvant chemotherapy, this drug has been found to have a positive impact on the progression-free survival (PFS) of patients with advanced disease, although an impact on the overall survival (OS) has not been confirmed yet [271]. In case of a confirmed relapse, the patient has to restart platinum-based chemotherapy, which is often proved ineffective at that point.

Major challenges in the treatment of ovarian cancer

Today's numbers suggest that 75% of the women may not have any evidence of disease at the end of this treatment. However, 75% of the women who respond to initial treatment will relapse within 18 to 28 months and only 20% to 40% of all women will survive beyond five years [133]. These data highlight the two major challenges emerging from the treatment of ovarian cancer: early diagnosis and post-treatment prognosis. The importance of early diagnosis can be depicted by the probability of complete cure compared to the degree of cancer dissemination. Stage I ovarian cancer, meaning that the tumor is limited at the ovaries, is completely cured in approximately 90% of cases [272]. In contrast, less than 20% of women with advanced ovarian cancer (stages III and IV) are cured. The cancer is generally diagnosed at stage IIIc, with an average 5-year survival of 39% (see table 6 below). At this point, there are large deposits of cancer cells on the surface of the spleen or the liver, having also spread to the lymph nodes. Although the disease responds to cytoreductive surgical resection and chemotherapy in 70% of such cases, less than 20% of women with advanced ovarian cancer can be cured (reviewed by P. Das and R. Bast Jr [273]).

FIGO Stage	5-year survival rate
I	90%
IA	94%
IB	92%
IC	85%
II	70%
IIA	78%
IIB	73%
III	39%
IIIA	59%
IIIB	52%
IIIC	39%
IV	17%

Table 6: Invasive epithelial ovarian cancer survival rates (American Cancer Society, www.cancer.org)

CA125 is the only tumor marker recommended for clinical use in the diagnosis and management of ovarian cancer. Although initially used to monitor patients previously diagnosed with ovarian cancer and not for screening, serum levels of CA125 can contribute to early diagnosis, as they were found elevated in up to 5 years prior to diagnosis of ovarian cancer in population-based studies [274]. Although it is elevated in 80-90% of women with epithelial ovarian cancer (EOC) after stage II, its sensitivity remains low for stage I EOC, ranging from 50% to 60% [275]. Another major issue of this biomarker is its limited specificity for EOC and ovarian cancer in general, as elevated concentrations can occur in several non-malignant and even non-gynecological diseases, such as peritoneal, pleural, and musculoskeletal inflammatory disorders as well as pelvic inflammatory disease, liver, and renal as well as cardiac disease [276]. CA125 levels can be elevated in the context of an inflammatory state, thus raising the probability of a false-positive diagnosis. Furthermore, CA125 is not expressed in pure mucinous tumors and is not useful among patients with this histological type of epithelial ovarian cancer [277]. These factors indicate the severe insufficiency of CA125 as a diagnostic biomarker in ovarian cancer and highlight the need for new, diagnostic tools. However, CA125 can be valuable for the detection of a relapse following treatment and temporary remission, as re-ascending levels in the serum correlate with disease recurrence in >90% of cases. Sadly, there is also a risk of a false remission

diagnosis, as up to 50% of patients with normalized levels of CA125 following chemotherapy (less than 35 U/ml) were found to have small volumes of persistent disease at second look operations (reviwed by R. Bast Jr [278]). The constant, often spectacular decrease of the biomarker after treatment makes it really difficult to accurately assess the quality of the response and to make a secure prognosis for the patient. Until now, an alternative to CA125 has not been identified for screening and monitoring ovarian cancer or for use as a prognostic indicator.

Goals of the study

This study aimed to gather information from the few, for now, published works on circulating miRNAs and ovarian cancer, attempting to assess the potential of proposed miRNAs in reflecting a malignant state. Towards this direction, we compared the plasma concentration of miRNAs in ovarian cancer before treatment with healthy donor samples and benign pelvic cases, studying their sensitivity and specificity for cancer. Taking advantage of sequential samples, before and after treatment, we analyzed for the first time the evolution of circulating miRNAs during primary treatment, attempting a parallel assessment with the kinetics of CA125 and demonstrating the vast differences in their patterns of variation. Last, we went through an exhaustive analysis of clinical data, for a better evaluation of the diagnostic and predictive value of plasma miRNAs. Our results suggest that miR-200b exhibits particular specificity for the malignant phenotype, as well as significant correlation of its evolution through treatment with the progression-free survival (PFS) of the patient, demonstrating potential to complement CA125 for a more precise evaluation of the treatment outcome and the duration of remission, eventually allowing a faster intervention and better adapted follow-up modalities. A surprising, paradoxal finding, worth further studying, is the fact that in some cases a reduction of the overall tumor burden caused by the treatment was accompanied by an increased plasma concentration of miR-200b.

Plasma miR-200b in ovarian carcinoma patients: distinct pattern of pre/post-treatment variation compared to CA-125 and potential for prediction of progression-free survival

Nikiforos-Ioannis Kapetanakis[1], Catherine Uzan[2], Anne-Sophie Jimenez-Pailhes[1], Sébastien Gouy[2], Enrica Bentivegna[2], Philippe Morice[2], Olivier Caron[3], Claire Gourzones-Dmitriev[1], Gwénaël Le Teuff[4,5] and Pierre Busson[1]

[1] UMR8126 CNRS, Univ. Paris-Sud, Université Paris-Saclay, Gustave Roussy, F-94805, Villejuif France

[2] Gustave Roussy, Department of Surgery, F-94805, Villejuif France

[3] Gustave Roussy, Department of Oncological Medicine, F-94805, Villejuif France

[4] Gustave Roussy, Department of Biostatistics and Epidemiology, F-94805, Villejuif France

[5] U1018 INSERM, CESP, Univ. Paris-Sud, Université Paris-Saclay, F-94085, Villejuif France

Correspondence to: *Pierre Busson*, ***email***: *pierre.busson@gustaveroussy.fr*

Keywords: ovarian cancer, plasma, microRNA, miR-200b, progression-free survival

Received: *August 05, 2015* ***Accepted***: *September 12, 2015* ***Published***: *September 21, 2015*

ABSTRACT

Ovarian carcinomas (OvCa) are highly heterogeneous malignancies. We investigated four circulating plasma microRNAs (miR-21, miR-34a, miR-200b and miR-205) as candidate biomarkers. Using qPCR, we assessed the plasma concentration of these markers in 101 women, including 51 previously untreated OvCa patients, 25 healthy women and 25 patients bearing benign pelvic lesions. For a subset of 33 OvCa patients, the assay was repeated at the end of the primary treatment. The pattern of variations (post- minus pre-treatment) of concentration was compared to that of CA-125. A Cox regression model was used to study the association between variations and the progression-free survival (PFS). Plasma miR-200b proved to have a greater average concentration in OvCa samples (median $2^{-\Delta\Delta Ct}$ = 15.18) than in samples linked to non-malignant lesions (median $2^{-\Delta\Delta Ct}$ = 1.26, *p*-value = 0.0004). Its concentration was highly heterogeneous among OvCa patients, without any correlations with the FIGO stage and the pre-treatment CA-125 level. The decrease in CA-125 concentration was constant and often dramatic, while the variations of miR-200b concentration were much more diverse. The variation of miR-200b was marginally associated with the PFS (hazard ratio=2.95 95%CI=[0.94; 9.28], *p*=0.06) while miR-200b as a continuous time-dependent variable was significantly associated (HR=1.06 [1.02; 1.10], *p*=0.003). This study is the first direct empirical evidence that miR-200b can provide additional information, independent of CA-125 in OvCa patients.

INTRODUCTION

In developed countries, ovarian carcinoma (OvCa) is the most lethal gynecologic cancer. High-grade serous ovarian carcinoma (HGSOC) is the most frequent (60%) and aggressive type of ovarian malignancies [1, 2]. Its bad prognosis is the result of late-stage discovery and unpredictable, as well as heterogeneous, response to treatment. At present, conventional imaging remains insufficient for the management of ovarian tumors, lacking sensitivity for the detection of small tumors and minimal residual disease. That is why the evaluation of treatment response often requires a surgical approach - second-look laparotomy or laparoscopy - to allow direct observation of the lesions.

Most ovarian carcinomas are found in stage III

(extension to the peritoneum and/or lymph nodes) or IV, with a five-year survival rate inferior to 30% [1]. Surgical cytoreduction (debulking) is a key component of any curative therapeutic strategy. Standard chemotherapy protocols combine a platinum salt and a taxane. Between 10% and 20% of ovarian tumors are initially resistant to this combination. The addition of Avastin to the platinum-taxane combination improves the tumor response in some cases [3]. The need for new biomarkers for OvCa is acute not only for early detection but also for the assessment of prognosis and response to treatment. CA-125 and other protein biomarkers have limited prognostic value [4].

MicroRNAs are small, single-stranded non-coding RNAs, about 19-25 nt long, which play key roles in the regulation of gene expression at the post-transcriptional level [5]. Multiple alterations of tumor microRNAs have been reported in most ovarian malignancies [6]. They are often released in the extracellular medium by healthy and malignant cells, associated to various carriers [7-9]. They are protected from RNases and can diffuse from the tumor interstitial fluid to the blood stream [10]. Several investigators, starting from 2008, published data on circulating microRNAs in the context of ovarian carcinomas [9, 11, 12]. However, despite a number of subsequent publications, so far no microRNA or set of microRNAs has been introduced in the clinics as biomarkers for ovarian carcinomas.

Our initial aim was the reproduction of previous findings on 4 circulating miRNAs in 51 women hospitalized for primary ovarian cancer. High concentrations in plasma samples from OvCa were found only for miR-200b. In contrast, the distribution of the 3 other selected miRNAs was highly similar in samples from untreated patients bearing OvCa or benign tumors. A longitudinal study (pre/post-treatment) was conducted, assessing the plasma levels of miR-200b. Our findings show that circulating miR-200b can provide additional information to that provided by CA-125. In contrast to CA-125, variations of miR-200b (post- minus pre-treatment) are marginally significantly associated with progression-free survival (PFS).

RESULTS

Patients' characteristics

From 72 OvCa patients initially included in this study, 21 were excluded for various reasons. In

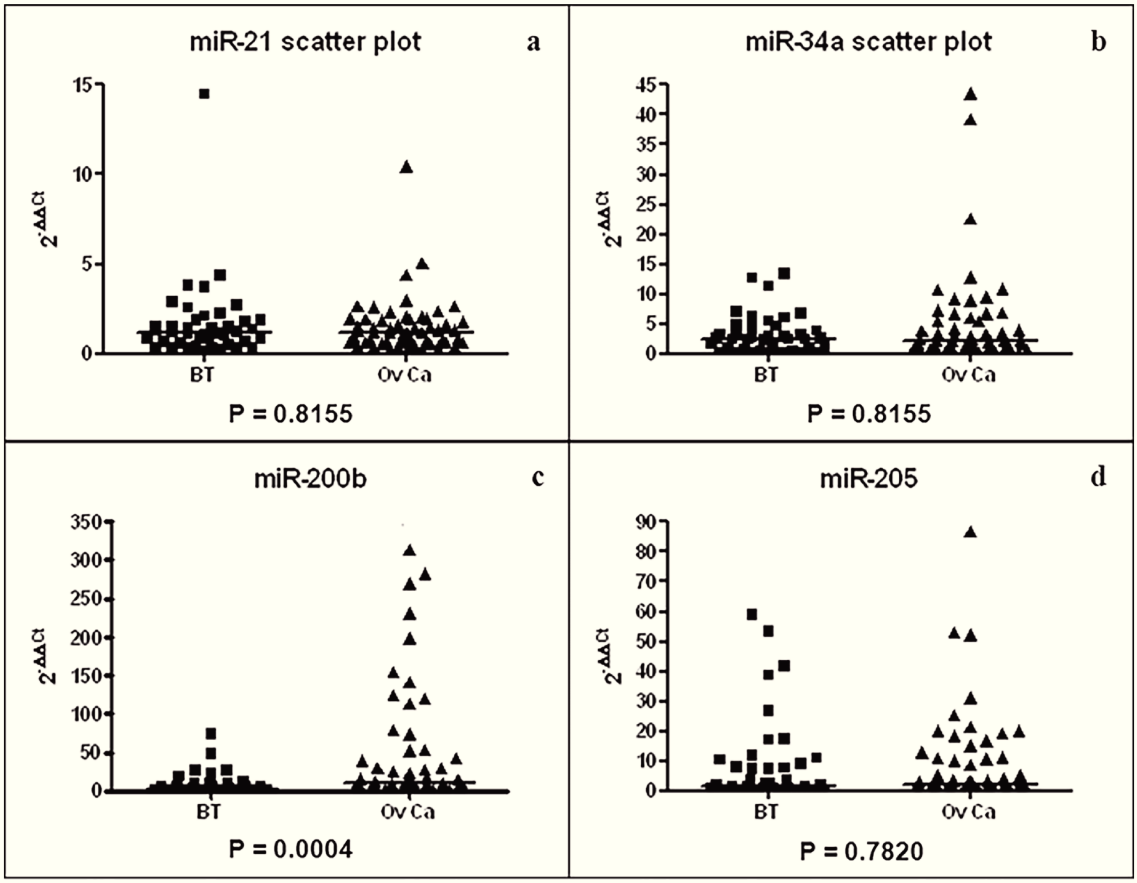

Figure 1: Scatter plots of miR-21 (a), miR-34a (b), miR-200b (c) and miR-205 (d) plasma concentrations for BT (N = 25) and OvCa (N = 51) patients. Median $2^{-\Delta\Delta Ct}$ (horizontal lines) is 1.17 (0.62; 1.85) (BT) and 1.18 (0.64; 1.91) (OvCa) for miR-21, 2.50 (0.83; 4.57) (BT) and 2.33 (1.01; 6.41) (OvCa) for miR-34a and 1.76 (0.34; 8.84) (BT) and 3.01 (0.86; 12.46) (OvCa) for miR-205.

Table 1: Variations (post- minus pre-treatment) of the plasma concentrations of CA-125 and miR-200b (median [Q1; Q3]) by primary treatment category and overall (*N*=33).

	Primary treatment categories*	Patients	Pre-treatment	Post-treatment	Pre/post-treatment variation (Δ)
CA-125	1) Unresectable tumor	9	2819.0 [1264.0; 8455.0]	31.6 [20.0; 57.0]	-2778.0 [-6855.0; -1254.0]
	2) Debulking after chemo	14	573.3 [235.0; 2858.0]	10.5 [7.4; 26.0]	-557.3 [-2645.0; -227.0]
	3) Direct debulking	10	200.5 [39.0; 230.0]	11.0 [7.0; 16.0]	-187.5 [-225.0; -27.0]
	Total	33	521.5 [184.0; 2819.0]	14.0 [8.0; 31.6]	-499.6 [-2645.0; -166.0]
miR-200b	1) Unresectable tumor	9	52.4 [14.4; 165.7]	136.8 [32.4; 239.6]	+7.7 [-1.0; 78.6]
	2) Debulking after chemo	14	16.1 [4.9; 53.1]	7.0 [1.3; 67.7]	-4.2 [-25.8; 5.1]
	3) Direct debulking	10	69.3 [17.5; 202.7]	22.7 [13.2; 54.6]	-20.9 [-157.4; 34.7]
	Total	33	30.3 [11.8; 93.4]	24.9 [4.4; 104.9]	0 [-49.4; 34.7]

*1: Non-resectable tumor at all stages of the treatment treated exclusively by chemotherapy; 2: Initially non-resectable tumor, treated by neo-adjuvant chemotherapy for tumor reduction, debulking surgery and adjuvant chemotherapy; 3: Initial debulking surgery followed by adjuvant chemotherapy.

consequence, 51 OvCa patients were included with a median follow-up of 39.7 months (range: 1.8; 56.6). The mean age was 62 years (min: 32; max: 81) with 7.8% FIGO stage I (*N* = 4), 3.9% stage II (*N* = 2), 82.4% stage III (*N* = 42) and 5.9% stage IV (*N* = 3). The 2 control groups were 25 HW and 25 BT (Supplemental data, Figure 1). According to the modalities of the primary treatment, the 33 sequentially studied OvCa patients were classified in 3 categories, as seen in Table 1 (thereafter designated as "primary treatment categories"). Category 1 represents tumors which remained non-resectable at all stages of the follow-up and were treated exclusively with chemotherapy. Category 2 included tumors which were initially non-resectable and firstly treated with neo-adjuvant chemotherapy for tumor reduction, followed by debulking surgery and adjuvant chemotherapy. In category 3, the patients' tumors allowed a direct debulking surgery completed by adjuvant chemotherapy.

Circulating miR-200b is significantly more abundant in patients bearing ovarian cancer than benign pelvic lesions

Out of the 4 candidate microRNAs (miR-21, miR-34a, miR-200b and miR-205) suspected to have a frequent high concentration in plasma samples from OvCa patients compared to BT patients, only miR-200b was found with a distinct pattern of distribution in these patients. The concentration median $2^{-\Delta\Delta Ct}$ was 15.18 (Q1: 3.47; Q3: 68.64) in OvCa compared to 1.26 (0.48; 5.73) in BT (*p*-value = 0.0004, Figure 1c). We observed no significant difference of the concentration of miR-21 (*p*-value = 0.82, Figure 1a), miR-34a (*p*-value = 0.82, Figure 1b) and miR-205 (*p*-value = 0.78, Figure 1d) between BT and OvCa groups.

Table 2: Prognostic effect of miR-200b and CA-125 in ovarian carcinoma patients according to different statistical approaches. First approach: the initial value of marker (*N*=51, 30 progressions); second approach: the variation (ΔmiR-200b and ΔCA-125); third approach: the initial value plus the variation, fourth approach: the marker as a continuous time-dependent covariate.

Models	Univariate	Multivariable¶
	HR [95%CI] (*p*-value) §	**HR 95%CI (*p*-value) §**
miR-200b		
Initial value* (*N*=51)	1.00 [0.960;1.042] (0.983)	1.007 [0.962;1.053] (0.775)
†Variation (Δ) (*N*=24) Negative Positive	 1.00 3.122 [1.130;8.625] (0.028)	 1.00 2.326 [0.828;6.535] (0.109)
†Initial value* Variation (Δ) Negative Positive	1.007 [0.935;1.085] (0.849) 1.00 3.143 [0.967;10.216] (0.057)	1.05 [0.968;1.139] (0.2397) 1.00 2.953 [0.939;9.281] (0.064)
Time-dependent*‡ (*N*=33)	1.063 [1.026;1.101] (<0.001)	1.057 [1.020;1.096] (0.003)
CA-125		
Initial value * (*N*=51)	1.00 [0.999; 1.001] (0.518)	1.000 [0.999; 1.001] (0.423)
†Variation (Δ) (*N*=24) Negative Positive	NE	NE
Initial value* Variation (Δ) Negative Positive	NE	NE
Time-dependent*‡ (*N*=33)	1.001 [0.999; 1.004] (0.198)	1.001 [0.999; 1.003] (0.402)

†: landmark analysis at 10 months. 9 patients were excluded. The variation represents the difference of the concentration of one marker between post- and pre-treatment (noted Δ=sample B – sample A)
¶: Multivariable Cox model adjusted on FIGO stage (I, II vs III, IV) and primary treatment categories described in patients' characteristics (1 vs 2, 3)
‡: We used the counting process for time-dependent marker. This allows reclaiming 9 patients excluded when using the landmark analysis
*: Hazard ratios reported for 10 units of change in the continuous marker
NE: not evaluable because only one patient has an increase of CA-125
§: HR for Hazard Ratios and CI for confidence interval

Independent distribution of plasma concentrations for miR-200b and CA-125 (*N* = 51)

As shown in Figure 1, the plasma concentrations of miR-200b were highly heterogeneous among OvCa patients. Since we knew that the same was true for CA-125, the standard-of-care biomarker for OvCa, we undertook to make a parallel assessment of CA-125 and miR-200b in the 51 OvCa patients. As shown in Figure 2, we observed no correlation in the distribution of plasma concentrations for CA-125 and miR-200b: many patients had a concentration of CA-125 above the average and a low concentration of miR-200b and vice-versa (R^2 = 0.0974, supplemental Figure 3). In addition, there was no significant correlation between both markers and the patients' age (Supplemental data, Table 3). When compared to the FIGO stage, CA-125 showed a significant correlation with the tumor stage (p = 0.01), which was not observed for miR-200b (p = 0.93). Regarding the four cases of early disease (stages Ia-Ic), CA-125 was very low in all of them whereas the concentration of miR-200b was above its average concentration for three of them.

Distinct patterns of variation for CA-125 and miR-200b concentrations prior and after the primary treatment ($N = 33$)

For 33 of the 51 OvCa patients, we were able to collect a second blood sample, at the end of their primary treatment (sample B in addition to the previously mentioned sample A collected prior to any treatment). The variations of CA-125 and miR-200b were designated ΔCA-125 and ΔmiR-200b (concentration of sample B minus concentration of sample A for CA-125 and miR-200b respectively). In almost every case, CA-125 was returning to normal plasma concentrations within the first months of the treatment, even among patients of category 1 (bearing unresectable tumors). At the end of the treatment, CA-125 was either normal (24 patients) or slightly above the limit (5 patients). This is illustrated in Figure 3a by a series of line segments with a negative slope. Consistently, the median CA-125 had the same similar decreasing pattern across the 3 primary treatment categories. The only specific feature of category 1 (unresectable tumors) was a much higher median for the initial concentration of CA-125 (Table 1). When looking at miR-200b, we get a very different picture with generally no variation (median: 0 (Q1: -49.4; Q3: 34.7). There was a remarkable mix of decreasing (16 patients) and increasing (17 patients) variations (Figure 3b). However, the proportion of patients with decreasing concentrations of miR-200b was different depending on the category of tumors: 3/9 (33%) for category 1 (unresectable tumors) versus 13/24 (54%) for categories 2 and 3 (tumors resectable immediately or after

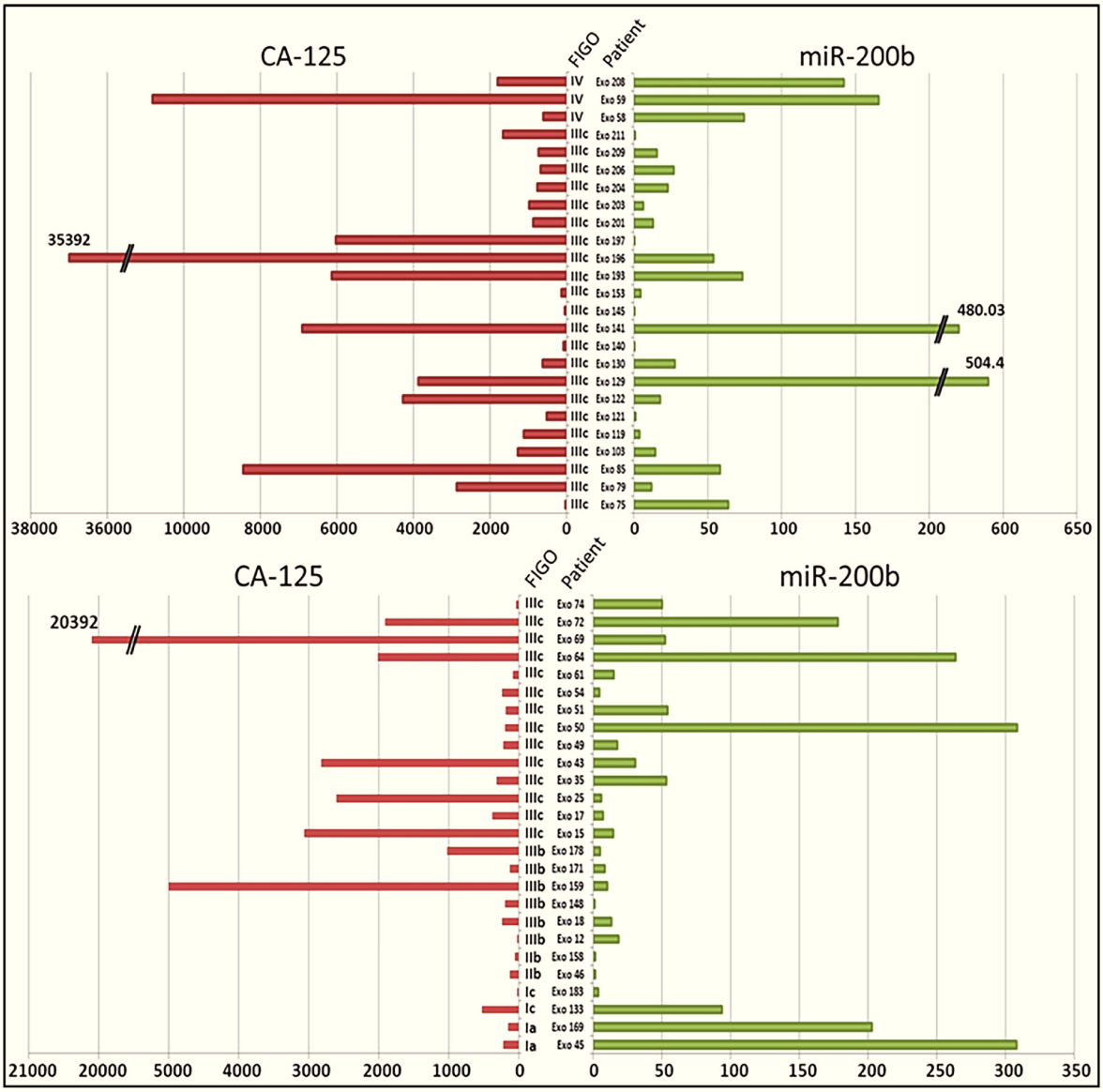

Figure 2: Individual profiles of the pre-treatment concentrations of CA-125 (U/ml) and miR-200b in plasma samples from each OvCa patient ($N = 51$). The concentration of miR-200b was assessed by the $2^{-\Delta\Delta Ct}$ method. The FIGO stages are mentioned between the two histograms, as well as the patients' code.

neo-adjuvant chemotherapy). Consistently, the median variation was positive for type 1 (median ΔmiR-200b at +7.7) and negative for types 2 and 3 (median ΔmiR-200b at -4.2 and -20.9 respectively) (Table 1).

Pre/post-treatment variation of plasma miR-200b (ΔmiR-200b) associated with progression-free survival (PFS) ($N = 33$)

To investigate the association between ΔCA-125 (< or ≥ 0) and ΔmiR-200b (< or ≥ 0) with the PFS, a landmark analysis at 10 months was used. This time space represents the highest time interval between evaluation of sample A and sample B. We imputed, for patients without evaluation of sample B at 10 months, the value before this time. Nine patients with an event recorded within the first 10 months had to be excluded from this analysis. Figure 4 shows that among the 24 remaining patients those with a negative ΔmiR-200b had a longer PFS (median: 50.5 months [15.21; NE] than patients with a positive variation (median: 17.3 months [11.2; 24.1] (p-value = 0.018).

In order to confirm this observation and to investigate whether the prognostic value of ΔmiR-200b was independent from some major clinical characteristics like tumor extension and the possibility of tumor resection, we used a multivariable analysis based on a Cox model adjusted on tumor stage (I, II vs III, IV) and primary treatment category (1 vs 2, 3). The univariate and multivariable hazard ratios (HR) were 3.12, 95% confidence interval = [1.13; 8.63] ($p = 0.03$), and 2.33, [0.83; 6.54] ($p = 0.11$) to the detriment of ΔmiR-200b≥0. When also adjusting on the initial plasma concentration of miR-200b prior to any treatment as a continuous covariate, univariate and multivariable, HR for the variation were 3.14 [0.97; 10.22] ($p = 0.06$) and 2.95 [0.94; 9.28] ($p = 0.06$), respectively. In other words, the risk of progression was marginally significantly higher in patients with a positive variation of miR-200b compared to patients with a negative variation. It is interesting to note that the initial value of plasma miR-200b was not associated with PFS ($p = 0.24$). The extension of the Cox regression model including miR-200b as a time-dependent covariate ($N = 33$ patients, 25 progressions) showed that the association was now statistically significant ($p < 0.003$ for multivariable analysis). We recorded a 5.7% higher risk of progression for a 10 unit increase of miR-200b concentration. No significant association between CA-125 and PFS was observed when considering the initial value of the marker ($p = 0.42$) or when taking it as a time-dependent covariate ($p = 0.40$).

DISCUSSION

So far, research on circulating microRNAs in OvCa patients has not resulted in clinical applications, apparently due to a lack of reproducibility [9, 12]. To our knowledge, none of the previous investigators has reported a simultaneous assessment of CA-125, or attempted a sequential assessment of plasma microRNAs to refine the prognosis of OvCa patients.

Our study was focused on 4 microRNAs previously described as often more abundant in the plasma of OvCa patients than in healthy donors or patients bearing benign pelvic tumors [13, 14]. A link with the presence of OvCa was confirmed only for miR-200b. One explanation might be our choice of distinct primers based on LNA technology, which are probably more specific. The

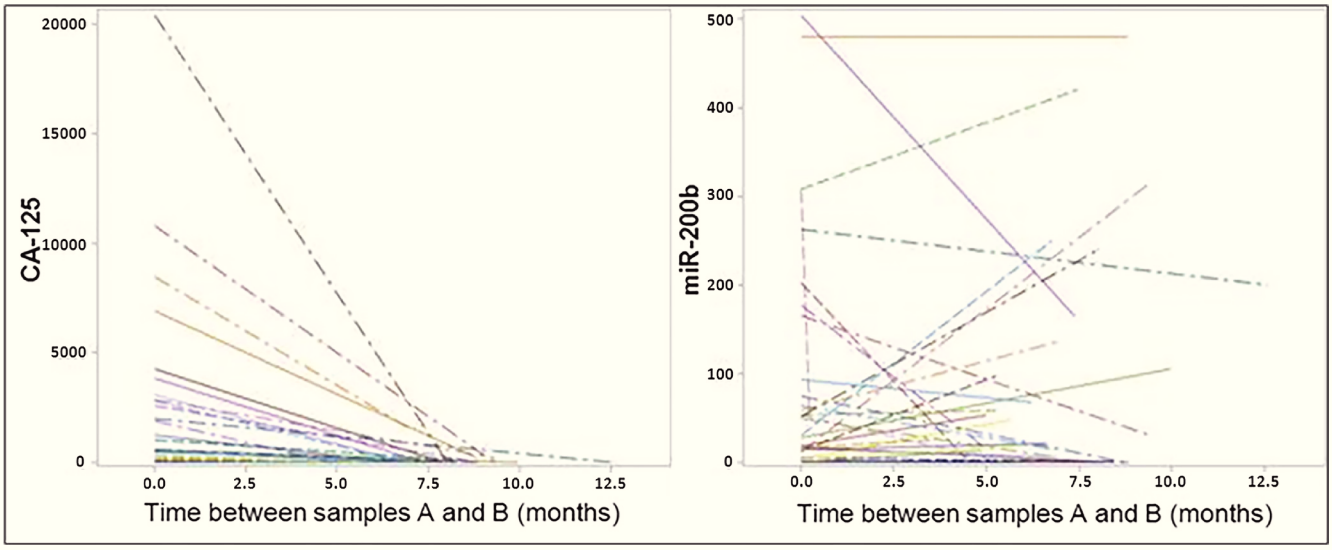

Figure 3: Variations of the plasma concentrations for CA-125 and miR-200b in samples collected prior and after the primary treatment. Left: CA-125 exhibits a reduction in its concentration for practically all the cases. Right: Variations in the concentrations of miR-200b are much more diverse; ΔmiR-200b was either negative or positive in about 50% of the cases (16 and 17 patients respectively).

distribution of miR-200b concentrations in OvCa plasma samples was highly heterogeneous and not correlated to CA-125 concentrations. Using plasma samples collected from 33 OvCa patients before and after the primary treatment, we made two remarkable observations. Firstly, the patterns of variations from sample A to sample B were much more diverse than for CA-125. Secondly, the sense of variation, increasing or decreasing concentration, was correlated to the PFS.

Markers of this type are eagerly awaited for patients who benefit from tumor resection either immediately or following neo-adjuvant chemotherapy (in contrast to patients with non-resectable tumors expected to have a very short PFS regardless of any biological parameter). If the variation of miR-200b is validated by future studies as a novel biomarker, it will be a tool of major interest for the management of patients on remission assessed by imaging or second-look surgery. Determining the patients at high risk of relapse could lead to the tailoring of more efficient adjuvant therapy approaches. The confirmation of the predictive value of miR-200b will require the investigation of new series of OvCa patients with greater numbers of sequential samples through the primary treatment. This will allow a better assessment of the kinetics of variation for miR-200b.

MiR-200b should not be regarded as a possible substitute of CA-125 but rather as a complementary marker. Two major advantages of CA-125 in the management of OvCa are its contribution to the initial diagnosis and the post-treatment surveillance. On the one hand, in the presence of a pelvic mass, the detection of the CA-125 strengthens the suspicion of ovarian carcinomas prior to laparoscopy or laparotomy [15]. On the other hand, following a complete remission accompanied by CA-125 normalization, its reascension raises the alarm for a relapse which is often confirmed by medical imaging and diagnostic surgery. However, the CA-125 has several limitations; its pattern and kinetics of decrease following the primary treatment are not always correlated to the amplitude and duration of the tumor response [16, 17]. For reasons which are not entirely elucidated, even with a partial tumor response there is often a dramatic decrease in the plasma concentration of CA-125. Because of its poor sensitivity, many patients with normal CA-125 levels after chemotherapy are found to have persistent disease [18, 19]. Therefore CA-125 and miR-200b could co-exist in the management of OvCa patients. CA-125 will be used for the initial diagnosis or for early detection of relapse whereas miR-200b will be used for the prediction of the PFS duration following clinical remission.

The miR-200 family contains five distinct members: miR-141, miR-200a, miR-200b, miR-200c and miR-429 [20]. A number of publications have shown that they are very abundant in ovarian carcinoma cells [21-23], suggesting that miR-200b detected in the plasma of OvCa patients is derived from material released by the malignant cells. However, at least a fraction of this circulating microRNA may derive from cells of the tumor micro-environment. Expression of miR-200b has been reported in proliferative fibroblasts and in a subset of human monocytes [24, 25]. In future studies, it would be necessary to investigate the variation of all the members

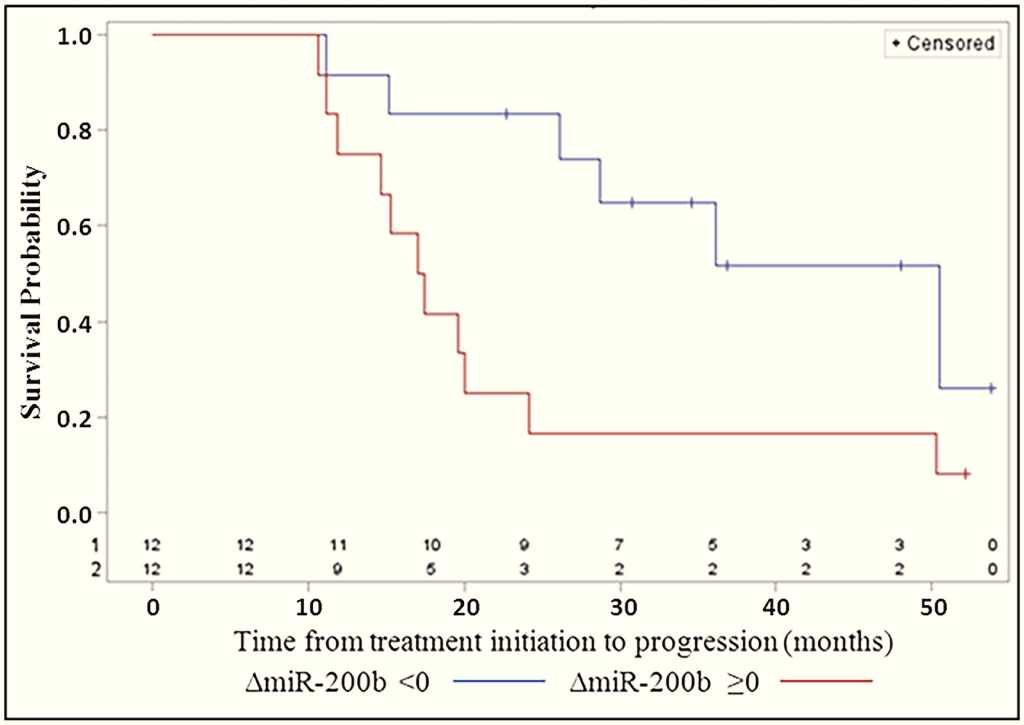

Figure 4: Progression-free survival according to the pre/post-treatment variation (< 0, ≥0) of the concentration of plasma miR-200b (ΔmiR-200b).

of the miR-200 family.

It is puzzling to observe that plasma miR-200b can rise in some patients in parallel with a substantial reduction of the tumor mass or even a complete remission. The elucidation of this paradox will be important for its future use as a prognostic marker. At this stage, one can only speculate on the role of hidden tumor cells not easily seen by medical imaging or second-look surgery, or a change of phenotype in cells resistant to the chemotherapy and likely to be involved in tumor relapse.

MATERIALS AND METHODS

Biological Material

Blood samples were collected prospectively from female patients admitted at Gustave Roussy, with written informed consent under the agreement of the ethical committee (CPP Tarnier-Cochin N°2746, 2010). The blood (10-20 ml) was collected in EDTA tubes and kept at room temperature for less than 2 hours, until plasma separation. Subsequently, it was centrifuged at 1700 g at 20°C for 15 minutes to separate plasma from blood cells. The plasma was homogenized, aliquoted and stored at -80°C, for 6-36 months. As controls, we used 25 samples from healthy women (HW), proved to be free of BRCA1/BRCA2 mutations detected in their family. Besides, we used 2 sets of pathological samples: one obtained from 25 women operated for benign pelvic tumors or lesions (BT hereafter) and a second set obtained prior to any treatment, before a diagnostic coelioscopy, from 72 women treated for malignant ovarian tumors (samples A). Among them, 33 women donated a second sample (samples B) at the end of the primary treatment (treatment including chemotherapy and debulking surgery when feasible), 4-8 months after the initial coelioscopy. For all patients, the follow-up time was at least 6 months from the diagnosis.

Small RNA extraction

The extraction of all small RNAs was done using the miRCURY RNA isolation kit of Exiqon, optimized for miRNA extraction from biofluids. For each extraction we used 200 µL of undiluted plasma, supplemented with 1 µg of carrier RNA (MS2 phage genomic RNA, Roche) per sample, in order to improve microRNA yield, according to the manufacturer's manual. The total RNA concentration was assessed using a Nanodrop2000 spectrophotometer.

Reverse transcription to total cDNA

Prior to retrotranscription, the samples were diluted to a final concentration of 5 ng/µl, including the carrier RNA. To exclude immature forms of miRNAs, we used Exiqon's Universal cDNA Synthesis kit II, which adds a poly-A tail to the extracted RNAs before the cDNA synthesis. Two microliters of diluted microRNA extract were mixed with 5 µl of RNase-free water, 2 µl of 5X Reaction buffer and 1 µl of a 10X enzyme mix, containing the reverse transcriptase and a poly-T primer with a 3' degenerate anchor and a 5' universal tag. The tubes were incubated at 42°C for 1 hour and at 95°C for 5 minutes, in order to heat-inactivate the enzyme and then stored at -20°C immediately after.

Selection of microRNA candidates and reference genes

Four microRNAs, hsa-miR-21-5p, hsa-miR-34a-5p, hsa-miR-200b-3p and hsa-miR-205-5p, were selected as candidate biomarkers for OvCa patients on the basis of literature data and MiRandola (the extracellular/circulating microRNAs' online database; http://atlas.dmi.unict.it/mirandola/). Each of them has been reported in at least two publications as exhibiting a high plasma or serum concentration in OvCa patients (Supplemental data, Table 1). MiR-191 was chosen as an endogenous reference for data normalization (see section of Figure 2 in the Supplemental data).

qPCR (quantitative Polymerase Chain Reaction)

The cDNA templates were amplified using Exiqon's miRNA-specific, LNA-enhanced primers (Table 3 in supplemental data). After optimization, we fixed the cDNA dilution to 1/40 or 1/20, depending on the specificity of each primer set and the abundance of the target miRNA in the plasma. We used Exiqon's ExiLENT SYBR Green Master Mix, containing the thermostable DNA polymerase, dNTPs and the Mg^{2+} ions needed for DNA replication. We also used ROX, an internal passive fluorescence standard dye, used to correct optical variations. Samples were amplified in triplicates, each well containing 4 µl of the diluted cDNA, 5 µl of SYBR Green Master Mix, 1 µl of the selected primer set and 0.1 µl of ROX dye. The assays were carried on 96-well plates, on a StepOnePlus Real-Time PCR System device, by Applied Biosystems. The amplification protocol was determined according to standard guidelines (supplemental data, Table 2) [26].

Samples of all the samples' sets were systematically mixed in the qPCR plates, in order to avoid technical variation. To determine the relative abundance of a given miRNA in a sample, we used the $2^{-\Delta\Delta Ct}$ value [27]. Every Ct for a studied miRNA was normalized with the Ct of the endogenous reference miRNA (ΔCt) and every patient from the BT or OvCa groups was normalized with the average value of the HW group (ΔΔCt value).

CA-125 quantification

Plasma CA-125 was assayed using the "Access OV-monitor" immunoassay system from Beckman Coulter. The limit of a normal concentration is generally set to 30-35 U/ml.

Data analysis

Patients' characteristics and treatment modalities were retrieved from Gustave Roussy medical files. The distribution of the concentrations ($2^{-\Delta\Delta Ct}$) of the candidate microRNAs was compared between BT and OvCa using the Kruskal-Wallis test. We used the false discovery rate adjustment to control for multiple testing. We studied the correlation between the selected miRNA and CA-125 plasma concentrations through a linear regression and R^2 after log transformation. The pre/post-treatment variations (noted Δ = sample B - sample A and defined as $<$ or ≥ 0) of CA-125 and miRNA plasma concentrations were reported (median [Q1, Q3]) by category of primary treatment and overall. Progression-free survival (PFS) was defined as the time from the start of the treatment to the first progression, as defined according to GCIG criteria [28]. Patients without event were censored at the date of the last follow-up examination. The cut-off date was April 30, 2015. We used the Kaplan-Meier method to estimate PFS curves and the log-rank test to compare PFS curves according to status of ΔCA-125 and ΔmiRNA concentrations. We used the Cox regression model to investigate the association between variation (Δ) and PFS and extended this model in considering the biomarkers as a continuous time-dependent covariate. The multivariable analyses were adjusted on stage (I, II versus III, IV) and treatment type (1 vs 2, 3). The Firth's approach was used because of the small sample size. We used the landmark method to assess the prognosis effects of ΔCA-125 and ΔmiRNA changes [29]. *P*-values were two-tailed. We used Graph Pad Prism 4 for the figures and SAS 9.3 for statistical analyses.

Abbreviations

OvCa: ovarian carcinoma, HGSOC: high-grade serous ovarian carcinoma, BT: benign pelvic lesions or tumors, miRNA: microRNA, PFS: progression-free survival, HW: healthy women

ACKNOWLEDGMENTS

Special thanks go to all the women who agreed to take part in this study. We sincerely thank Dr Alexandra Léary and Dr Fréderic Troalen for their scientific advice, as well as Eugénie Mussard and Aurore Gelin, for their help in the optimization of several experiments.

FUNDINGS

This work was supported by a grant for translational research from the Institut National du Cancer (n°2010-1-RT-05-IGR-1). Nikiforos-Ioannis Kapetanakis is the recipient of a PhD scholarship from the French Ministry of Higher Education and Research (MESR).

CONFLICTS OF INTERESTS

The authors declare no conflict of interests.

REFERENCES

1. Siegel RL, Miller KD and Jemal A. Cancer statistics, 2015. CA Cancer J Clin. 2015; 65:5-29.
2. Romero I and Bast RC, Jr. Minireview: human ovarian cancer: biology, current management, and paths to personalizing therapy. Endocrinology. 2012; 153:1593-1602.
3. Oza AM, Cook AD, Pfisterer J, Embleton A, Ledermann JA, Pujade-Lauraine E, Kristensen G, Carey MS, Beale P, Cervantes A, Park-Simon TW, Rustin G, Joly F, Mirza MR, Plante M, Quinn M, et al. Standard chemotherapy with or without bevacizumab for women with newly diagnosed ovarian cancer (ICON7): overall survival results of a phase 3 randomised trial. Lancet Oncol. 2015.
4. Scholler N and Urban N. CA125 in ovarian cancer. Biomark Med. 2007; 1:513-523.
5. Garofalo M and Croce CM. microRNAs: Master regulators as potential therapeutics in cancer. Annu Rev Pharmacol Toxicol. 2011; 51:25-43.
6. Integrated genomic analyses of ovarian carcinoma. Nature. 2011; 474:609-615.
7. Hunter MP, Ismail N, Zhang X, Aguda BD, Lee EJ, Yu L, Xiao T, Schafer J, Lee ML, Schmittgen TD, Nana-Sinkam SP, Jarjoura D and Marsh CB. Detection of microRNA expression in human peripheral blood microvesicles. PLoS One. 2008; 3:e3694.
8. Gibbings DJ, Ciaudo C, Erhardt M and Voinnet O. Multivesicular bodies associate with components of miRNA effector complexes and modulate miRNA activity. Nat Cell Biol. 2009; 11:1143-1149.
9. Mitchell PS, Parkin RK, Kroh EM, Fritz BR, Wyman SK, Pogosova-Agadjanyan EL, Peterson A, Noteboom J, O'Briant KC, Allen A, Lin DW, Urban N, Drescher CW, Knudsen BS, Stirewalt DL, Gentleman R, et al. Circulating microRNAs as stable blood-based markers for cancer detection. Proc Natl Acad Sci U S A. 2008; 105:10513-10518.
10. Chen X, Ba Y, Ma L, Cai X, Yin Y, Wang K, Guo J, Zhang Y, Chen J, Guo X, Li Q, Li X, Wang W, Wang J, Jiang X, Xiang Y, et al. Characterization of microRNAs in serum: a novel class of biomarkers for diagnosis of cancer and other

diseases. Cell Res. 2008; 18:997-1006.

11. Zavesky L, Jandakova E, Turyna R, Langmeierova L, Weinberger V, Minar L and Kohoutova M. New perspectives in diagnosis of gynaecological cancers: Emerging role of circulating microRNAs as novel biomarkers. Neoplasma. 2015.
12. Taylor DD and Gercel-Taylor C. MicroRNA signatures of tumor-derived exosomes as diagnostic biomarkers of ovarian cancer. Gynecol Oncol. 2008; 110:13-21.
13. Suryawanshi S, Vlad AM, Lin HM, Mantia-Smaldone G, Laskey R, Lee M, Lin Y, Donnellan N, Klein-Patel M, Lee T, Mansuria S, Elishaev E, Budiu R, Edwards RP and Huang X. Plasma microRNAs as novel biomarkers for endometriosis and endometriosis-associated ovarian cancer. Clin Cancer Res. 2013; 19:1213-1224.
14. Shapira I, Oswald M, Lovecchio J, Khalili H, Menzin A, Whyte J, Dos Santos L, Liang S, Bhuiya T, Keogh M, Mason C, Sultan K, Budman D, Gregersen PK and Lee AT. Circulating biomarkers for detection of ovarian cancer and predicting cancer outcomes. Br J Cancer. 2014; 110:976-983.
15. Gagnon A and Ye B. Discovery and application of protein biomarkers for ovarian cancer. Curr Opin Obstet Gynecol. 2008; 20:9-13.
16. Clarke-Pearson DL. Clinical practice. Screening for ovarian cancer. N Engl J Med. 2009; 361:170-177.
17. Gupta D and Lis CG. Role of CA125 in predicting ovarian cancer survival - a review of the epidemiological literature. J Ovarian Res. 2009; 2:13.
18. Martignetti JA, Camacho-Vanegas O, Priedigkeit N, Camacho C, Pereira E, Lin L, Garnar-Wortzel L, Miller D, Losic B, Shah H, Liao J, Ma J, Lahiri P, Chee M, Schadt E and Dottino P. Personalized ovarian cancer disease surveillance and detection of candidate therapeutic drug target in circulating tumor DNA. Neoplasia. 2014; 16:97-103.
19. Bast RC, Jr. CA 125 and the detection of recurrent ovarian cancer: a reasonably accurate biomarker for a difficult disease. Cancer. 2010; 116:2850-2853.
20. Feng X, Wang Z, Fillmore R and Xi Y. MiR-200, a new star miRNA in human cancer. Cancer Lett. 2014; 344:166-173.
21. Vilming Elgaaen B, Olstad OK, Haug KB, Brusletto B, Sandvik L, Staff AC, Gautvik KM and Davidson B. Global miRNA expression analysis of serous and clear cell ovarian carcinomas identifies differentially expressed miRNAs including miR-200c-3p as a prognostic marker. BMC Cancer. 2014; 14:80.
22. Nam EJ, Yoon H, Kim SW, Kim H, Kim YT, Kim JH, Kim JW and Kim S. MicroRNA expression profiles in serous ovarian carcinoma. Clin Cancer Res. 2008; 14:2690-2695.
23. Cao Q, Lu K, Dai S, Hu Y and Fan W. Clinicopathological and prognostic implications of the miR-200 family in patients with epithelial ovarian cancer. Int J Clin Exp Pathol. 2014; 7:2392-2401.
24. Tong J, Fu Y, Xu X, Fan S, Sun H, Liang Y, Xu K, Yuan Z and Ge Y. TGF-beta1 stimulates human Tenon's capsule fibroblast proliferation by miR-200b and its targeting of p27/kip1 and RND3. Invest Ophthalmol Vis Sci. 2014; 55:2747-2756.
25. Liu Y, Li J, Xia W, Chen C, Zhu H, Chen J, Li S, Su X, Qin X, Ding H, Long L, Wang L, Li Z, Liao W, Zhang Y and Shao N. MiR-200b modulates the properties of human monocyte-derived dendritic cells by targeting WASF3. Life Sci. 2015; 122:26-36.
26. Bustin SA, Benes V, Garson JA, Hellemans J, Huggett J, Kubista M, Mueller R, Nolan T, Pfaffl MW, Shipley GL, Vandesompele J and Wittwer CT. The MIQE guidelines: minimum information for publication of quantitative real-time PCR experiments. Clin Chem. 2009; 55:611-622.
27. Livak KJ and Schmittgen TD. Analysis of relative gene expression data using real-time quantitative PCR and the 2(-Delta Delta C(T)) Method. Methods. 2001; 25:402-408.
28. Rustin GJ, Vergote I, Eisenhauer E, Pujade-Lauraine E, Quinn M, Thigpen T, du Bois A, Kristensen G, Jakobsen A, Sagae S, Greven K, Parmar M, Friedlander M, Cervantes A and Vermorken J. Definitions for response and progression in ovarian cancer clinical trials incorporating RECIST 1.1 and CA 125 agreed by the Gynecological Cancer Intergroup (GCIG). Int J Gynecol Cancer. 2011; 21:419-423.
29. Anderson JR, Cain KC and Gelber RD. Analysis of survival by tumor response. J Clin Oncol. 1983; 1:710-719.

Plasma miR-200b in ovarian carcinoma patients: distinct pattern of pre/post-treatment variation compared to CA-125 and potential for prediction of progression-free survival

Supplementary Material

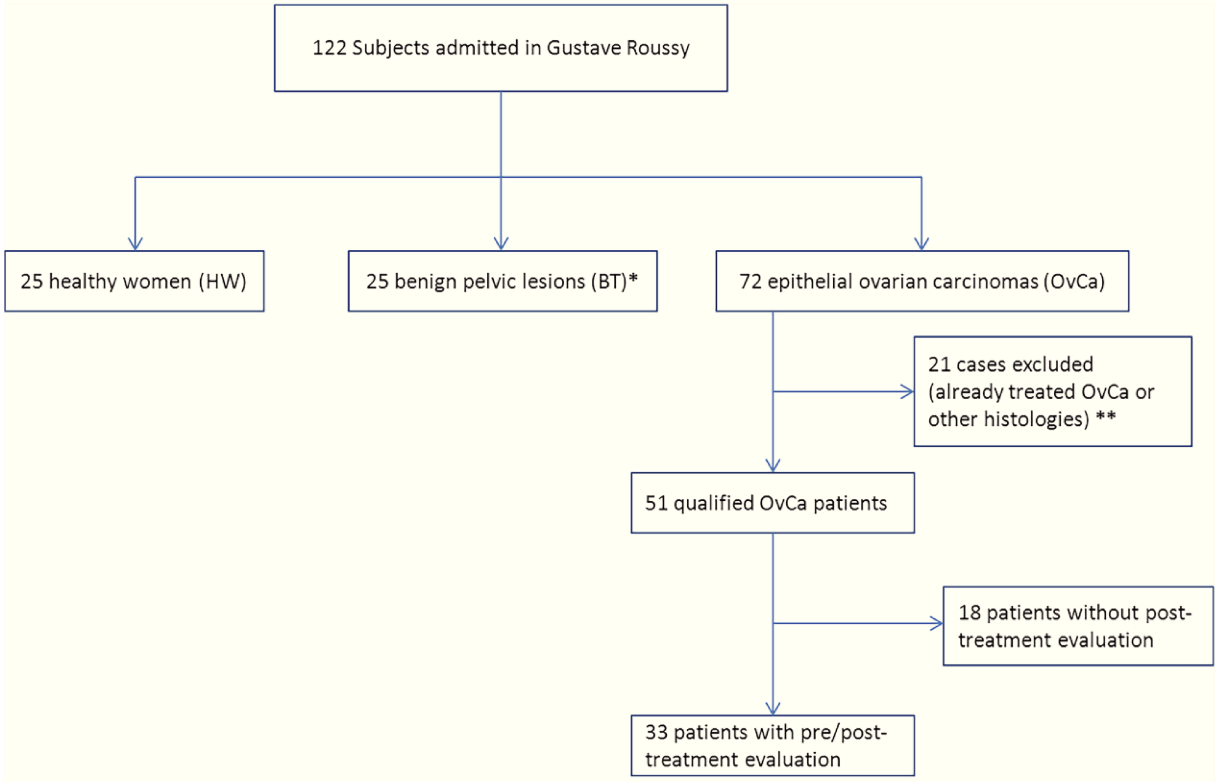

Figure 1: Flow-chart of the subjects included in the study.

*Most cases of BT were ovarian cystadenofibromas, leiomyomas, teratomas, fibrothecomas or various cysts which, after microscopical analysis of the biopsies, were shown to be non-malignant.

**Sixteen cases had received a treatment prior to the first coelioscopy or suffered a cancer within the two last years before the detection of the OvCa. Two patients were excluded, as the tumor was classified as borderline upon histopathological examination. Finally, 3 cases of ovarian tumors were proven to be the result of breast or colon cancer metastases.

Table 1: Candidate miRNAs selected for our experimental procedure.

microRNA	**Material**	**Type of aberration**	**Reference**
miR-21	Plasma, Serum	Increased	[1, 2]
miR-34a	Serum	Increased	[1, 3]
miR-200b	Serum	Increased	[3, 4]
miR-205	Plasma	Increased	[3, 5]

Introduction to Figure 2 - Selection of endogenous reference

Quantitative assessment of microRNAs by real-time PCR requires endogenous references to avoid biases due to RNA extraction and reverse transcription efficiency. Therefore, during preliminary studies, we investigated the potential of 3 miRNAs – hsa-miR-132-3p, hsa-miR-23a-3p and hsa-miR-191-5p – already used for normalization of plasma microRNAs in published studies [1, 6]. Our main selection criteria were their detection at a substantial and consistent level among our 3 groups of plasma samples (HW, BT, OvCa). The consistency of their concentration was evaluated by comparison of the median Ct value using the Kruskal-Wallis test. MiR-132 was rapidly eliminated because of being poorly detected in the majority of the control as well as OvCa subjects (data not shown). MiR-23a was readily detected in most plasma samples but was in fact dependent on the disease state (p-value = 0.036). In contrast, the average level of miR-191 was consistent in plasma samples from all 3 categories of donors (median values 31.91, 32.54 and 32.46 for HW, BT and OvCa respectively, p-value = 0.13). Therefore, miR-191 was chosen for data normalization (see Figure 2 below).

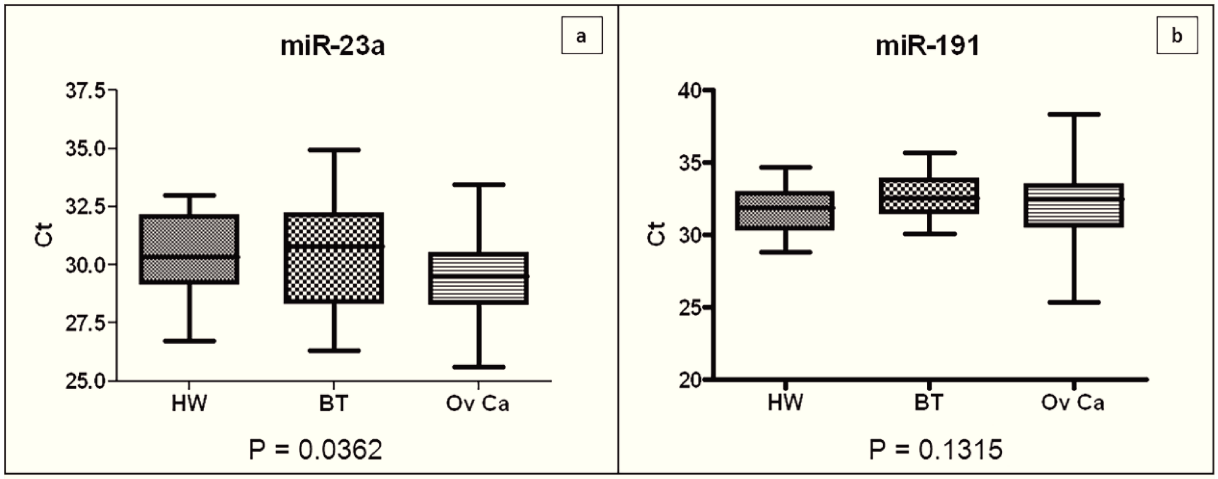

Figure 2: Comparison of miR-23a (a) and miR-191 (b) Ct values in the series of plasma samples from healthy women (HW), women with benign tumors or lesions (BT) and ovarian cancers (OvCa) (N_{HW}=25, N_{BT}=25, N_{OvCa}=51). Ct (cycle threshold) reflects the concentration of targeted miRNAs in each plasma sample (high Ct - low abundance). For miR-23a, the median values for HW, BT and OvCa were significantly different with 30.35, 30.80 and 29.49 respectively. For miR-191, they were not significantly different with 31.91, 32.54 and 32.46 respectively. The reported p-values are corrected for multiple testing. The horizontal line in the box interior represents the median.

Table 2: Real-time PCR cycle conditions

Process step	**Settings**
Polymerase Activation/Denaturation	95°C, 10 minutes
Amplification	40 cycles at 95°C for 10 seconds and 60°C for 1 minute, with a ramp-rate of 1.6°C/s
Melting Curve	Included

Table 3: Full name, accession number and Exiqon primers' reference number of each of the studied microRNAs.

microRNA	miRBase Accession Number	Exiqon Product Number
hsa-miR-21-5p	MIMAT0000076	204230
hsa-miR-23a-3p	MIMAT0000078	204772
hsa-miR-34a-5p	MIMAT0000255	204486
hsa-miR-132-3p	MIMAT0000426	204129
hsa-miR-191-5p	MIMAT0000440	204306
hsa-miR-200-3p	MIMAT0000318	206071
hsa-miR-205-5p	MIMAT0000266	204487

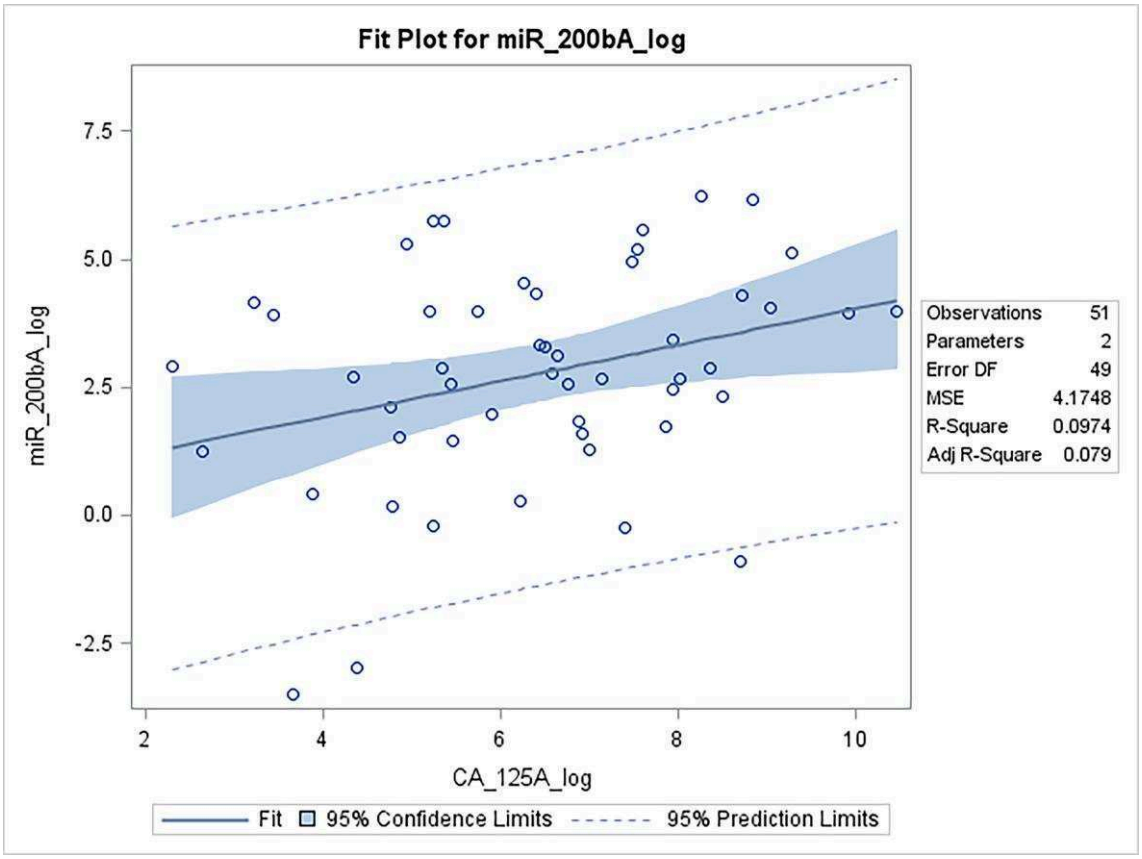

Figure 3: Plot of miR-200b versus CA-125 after log transformation: $R^2 = 0.0974$ (N=51).

Table 4: Correlation between CA-125, miR-200b measured prior to treatment and age, FIGO stage in ovarian cancer patients (N=51). Reported p-values (Kruskal-Wallis test) are not corrected for multiple testing.

			CA-125 Median [Q1; Q3]	miR-200b Median [Q1; Q3]
Age (years)	<65	(N=29)	600.0 [190.0; 1652.0]	17.7 [10.0; 53.8]
	≥65	(N=22)	1038.0 [119.0; 3058.0]	16.0 [1.5; 73.6]
			p-value= 0.6345	p-value= 0.4936
Stage FIGO	I, II	(N=6)	130.0 [49.0; 212.0]	48.5 [1.5; 202.7]
	III, IV	(N=45)	865.0 [211.0; 2858.0]	17.5 [6.3; 53.8]
			p-value= 0.0119	p-value=0.9301

Table 5: Individual fold changes in the concentrations of CA-125 and miR-200b in the samples collected before and after the primary treatment of OvCa patients (N=33).

Patient	CA-125 (U/ml)		miR-200b ($2^{-\Delta\Delta Ct}$)	
	Concentration	Fold change	Concentration	Fold change
Exo 12*	10→34	x 3.4	18.4→53.1	x 2.9
Exo 15	3058→20	1/153	14.5→6.7	1/2.2
Exo 18	90→5	1/18	13.1→97.8	x 7.5
Exo 25	2600→9.2	1/283	5.6→0.01	1/560
Exo 35	313→6	1/52	53.1→58.2	x 1.1
Exo 43	2819→41	1/69	30.3→250.0	x 8.3
Exo 45	212→11	1/19	308.0→54.6	1/6
Exo 49	211→7	1/30	17.5→24.9	x 1.4
Exo 50	190→16	1/12	308.5→420.3	x 1.4
Exo 51	184→18	1/10	53.8→3.0	1/18
Exo 54	235→8	1/29	4.3→19.5	x 4.5
Exo 58	600→30	1/20	74.6→0.04	1/1865
Exo 59	10816→26	1/416	165.7→32.4	1/5
Exo 64	2009→20	1/101	263.5→199.6	1/1.3
Exo 69	20392→57	1/358	52.4→239.6	x 4.6
Exo 72	1900→7	1/271	177.9→20.6	1/9
Exo 74	31,4→6.7	1/5	50.0→7.3	1/7
Exo 75	25→4	1/6	64.0→14.6	1/4.4
Exo 79	2858→213	1/13	11.8→311.8	x 26.4
Exo 85	8455→1600	1/5	58.2→136.8	x 2.4
Exo 103	1264→10	1/126	14.4→22.0	x 1.5
Exo 121	507→7.4	1/69	1.32→1.32	x 1
Exo 122	4269→40	1/107	17.65→1.31	x 13.5
Exo 129	3861→6	1/644	504.4→166.0	1/3.0
Exo 130	625→3.2	1/195	27.7→104.9	x 3.8
Exo 133	521.5→26	1/20	93.4→67.7	1/1.4
Exo 140	81→8	1/10	0.1→0.3	x 3
Exo 141	6900→41.6	1/166	480.0→480.6	x 1
Exo 145	39→12	1/3	0.03→13.2	x 440
Exo 153	130→31.6	1/4	4.6→48.2	x 10.5
Exo 158	49→14	1/4	1.52→0.51	1/3.0
Exo 169	141→8.2	1/17	202.7→4.4	1/46
Exo 178	1015→110.3	1/9	4,89→2.06	1/2.4

*The patients are named according to their order of induction in the project.

References

1. Suryawanshi S, Vlad AM, Lin HM et al. Plasma microRNAs as novel biomarkers for endometriosis and endometriosis-associated ovarian cancer. Clin Cancer Res 2013; 19: 1213-1224.
2. Resnick KE, Alder H, Hagan JP et al. The detection of differentially expressed microRNAs from the serum of ovarian cancer patients using a novel real-time PCR platform. Gynecol Oncol 2009; 112: 55-59.
3. Taylor DD, Gercel-Taylor C. MicroRNA signatures of tumor-derived exosomes as diagnostic biomarkers of ovarian cancer. Gynecol Oncol 2008; 110: 13-21.
4. Kan CW, Hahn MA, Gard GB et al. Elevated levels of circulating microRNA-200 family members correlate with serous epithelial ovarian cancer. BMC Cancer 2012; 12: 627.
5. Zheng H, Zhang L, Zhao Y et al. Plasma miRNAs as diagnostic and prognostic biomarkers for ovarian cancer. PLoS One 2013; 8: e77853.
6. Shapira I, Oswald M, Lovecchio J et al. Circulating biomarkers for detection of ovarian cancer and predicting cancer outcomes. Br J Cancer 2014; 110: 976-983.

Article 2

EBV-encoded BHRF1 microRNAs in nasopharyngeal carcinomas: Rare baseline expression and consistent induction in response to treatment

Introductory comment

5-azacytidine and cancer

This work is the result of collaboration with the American pharmaceutical company Celgene. Celgene has developed a new form of 5-azacytidine (or just azacytidine), which can be taken orally (commercially named CC-486). 5-azacytidine was first synthesized in 1964 [279]. It is a chemical analog of cytidine, a DNA and RNA nucleoside (figure 14). It was demonstrated to have a wide range of anti-metabolic activities when tested against cultured cancer cells and to be an effective chemotherapeutic agent for acute myelogenous leukemia (AML), along with its deoxy-derivative, 5-aza-2′deoxycytidine (commercially known as decitabine) [280].

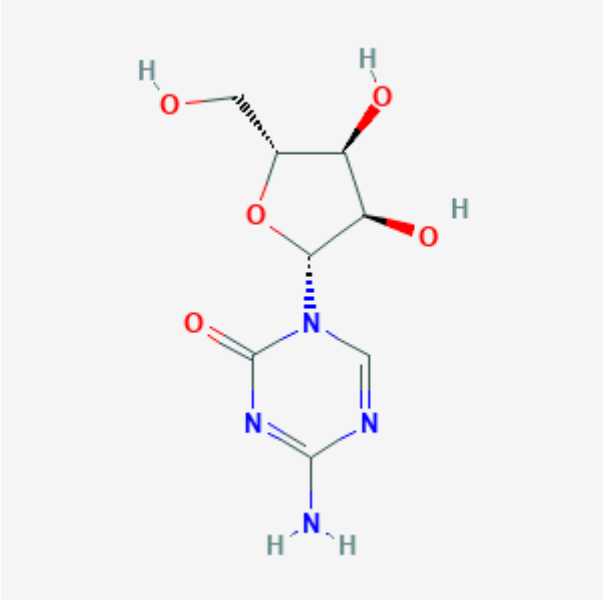

Figure 14: 2D chemical structure of 5-azacytidine

They belong to the category of chemotherapeutic agents called antimetabolites. Antimetabolites are very similar to normal substances within the cell. When the cells incorporate these substances into the cellular metabolism, they interact with a number of targets within the cell to produce a direct cytotoxic effect that causes death of rapidly dividing cancer cells. At high doses, by its direct cytotoxicity to rapidly proliferating cells, 5-azacytidine can result in cell death. Application of this feature has been confirmed in the case of rapidly proliferating abnormal hematopoietic cells in the bone marrow, while it has no toxic effects to cells which are under normal cell growth control. As a ribonucleoside, it is incorporated into RNA way more than into DNA. In contrast, 5-aza-2'-deoxycytidine is a

deoxyribonucleoside, so it can only be incorporated into DNA [281]. Thus, 5-aza-2'-deoxycytidine has been shown to be at least 10-fold more cytotoxic than 5-azacytidine for cultured cells and animals [282, 283]. 5-azacytidine is an inducer of chromosome breakage and a mutagen, but also leads to inhibition of DNA, RNA and protein synthesis. In addition, enzymatic deamination of 5-azacytidine and 5-aza-2'-deoxycytidine yields 5-azauridine and 5-aza-2'-deoxyuridine respectively. These compounds interfere with de novo thymidylate synthesis, adding to cytotoxicity [284].

Nevertheless, azacytidine's anticancer effects are believed to be twofold. 5-azacytidine is a member of a class of drugs known as DNA "demethylating" agents. The other side of its action is demethylation, or more correctly interfering with the methylation of DNA. Methylation of DNA is a major mechanism that regulates gene expression in cells. In mammals, DNA methylation is almost exclusively restricted to the CG, or CpG dinucleotide, with the cytosines on both strand being usually methylated. Increased methylation of CpG-rich regions (the so-called CpG islands) in gene promoters results in the blockage of their expression, hampering their transcription. Extensive methylation in these regions impedes binding of transcription factors, while it promotes binding of other proteins, known as methyl-CpG-binding domain proteins (MBDs), which recruit other proteins, thus resulting in the "heterochromatinization" of the affected loci [285]. At dose levels low enough to avoid triggering cell death, incorporation of 5-azacytidine or 5-Aza-2'-deoxycytidine into DNA of cultured cells leads to rapid loss of DNA (cytosine-C5) methyltransferase (DNMT1) activity because the enzyme becomes irreversibly bound to 5-azacytidine residues in DNA [286]. After aza-nucleosides such as azacytidine have been metabolized to 5-aza-2′-deoxycytidine-triphosphate, they can be incorporated into DNA and azacytosine can replace cytosine. Azacytosine-guanine dinucleotides are recognized as substrate by the DNA methyltransferases, instead of cytosine-guanine. This results in a covalent bond between the carbon-6 atom of the cytosine ring and the enzyme. The bond is normally resolved by beta-elimination through the carbon-5 atom, but this latter reaction does not occur with azacytosine because its carbon-5 is substituted by nitrogen, leaving the enzyme covalently bound to DNA and blocking its DNA methyltransferase function [287]. In addition, the covalent protein adduction also compromises the functionality of DNA and triggers DNA damage signaling, resulting in the degradation of trapped DNA methyltransferases. As a consequence, methylation marks become lost during DNA replication [288]. Incorporation of 5-azacytidine into tRNA was also shown to inhibit tRNA methyltransferases [289], and to interfere with

tRNA methylation and processing leading to defective acceptor function of transfer RNA [290]. Since methylation also plays an important role in ribosomal RNA processing [291, 292], effects of incorporation of 5-azacytidine on RNA function and stability are likely to account for much of its effect on protein synthesis. In cancer, high degrees of methylation are often observed, affecting promoters of "tumor suppressor genes" that regulate cell division and growth. When suppressor genes are blocked, cell division becomes unregulated, allowing or promoting cancer (examples of such genes and pathways are cited in the introduction). Cancers can be classified according to their degree of promoter DNA methylation (CpG island methylator phenotype, CIMP) [293]. By this process of demethylation, normal function to the tumor suppressor genes with hypermethylated promoters can be restored, thus restoring control over cell growth. The implications of both drugs in cancer treatment are further reviewed by Judith Christman [294].

Celgene's CC-486 is being tested as an easier to administer treatment for AML [295]. Since 2014, there is an ongoing clinical trial (phase 2) for the use of CC-486 in patients with locally advanced or metastatic nasopharyngeal carcinoma having failed one to two previous regimens, including platinum-based chemotherapy. According to results presented at the 2016 ASCO Annual Meeting, single-agent CC-486 was well tolerated in patients with recurrent locally advanced/metastatic NPC, with encouraging initial efficacy results [296]. Unofficial data suggest that approximately one third of enrolled patients had a positive response or at least stabilization of the disease. For Celgene, a major challenge is to predict at an early stage of the treatment, if the patient will eventually benefit from the drug, or if it will have no particular effect on the disease.

5-azacytidine and EBV

On the other hand, 5-azacytidine has been long suspected to induce, among other chemical compounds, the lytic/replicative cycle of the Epstein-Barr virus (EBV). In 2004, an original work by Chan et a1 (2004) provided evidence of extensive CpG demethylation in the genome of EBV, following administration of 5-azacytidine to biopsies from patients with EBV-associated tumors, including NPC [297]. As the authors conclude: "the occurrence of demethylation at several loci and the hint that lytic gene expression may have been activated in one instance points to possible future therapeutic maneuvers. In particular, evidence that modest reversal of dense CpG methylation can facilitate promoter activation with histone deacetylase inhibitors (HDACi) suggests the possibility that combinations of DNA methyltransferase inhibitors and histone deacetylase inhibitors might bring about expression

of silenced genes". Another work from Rodriguez et al (2001) suggested that 5-azacytidine treatment may partially cause a switch towards the lytic cycle by inducing the expression of the immediate-early lytic gene BZLF1, producing the Zta protein (also called "Z," "ZEBRA," or "EB1") [298]. The transition from viral latency to productive lytic infection is actually orchestrated by two 'immediate-early' genes [299], BZLF1 and BRLF1, which encode the transcription factors Zta and Rta (also called "R"), respectively. The former is a homolog of the activating protein 1 (AP-1) transcription factor family [300] and is a master regulator of the switch needed to induce the lytic phase of the EBV life cycle in latently infected B cells [301]. BZLF1 plays a key role in the switch from latent infection to lytic cycle producing new virions. It acts as a transcription factor, inducing early lytic cycle genes, and as an origin binding protein for genome replication. It activates the promoter of another EBV gene (BSLF2 + BMLF1). During latency, the viral lytic genes presumably are repressed by host-driven methylation of viral DNA, heterochromatin formation, and/or cellular transcriptional repressors [302]. In the switch from the latent to the lytic phase of the EBV life cycle, BZLF1 overturns this epigenetic silencing of the latent EBV genome. BZLF1 and BRLF1 activate one another's promoter and their cooperation is required for optimal activation of many lytic viral promoters [303]. BZLF1 preferentially activates these promoters when they are methylated, whereas BRLF1 is more active on unmethylated promoters [304]. Therefore, they cooperate to induce lytic activation, no matter if the viral genome is methylated or unmethylated.

The concept of cytolytic viral activation in the treatment of EBV-associated NPC is not a recent idea, dating back to the 1970s. Like for all Herpesviridae, production of viral particles is automatically associated with the death of cells infected by EBV. This is the reason why the productive cycle - as opposed to the state of latent infection - is often called the lytic cycle [217]. One hurdle for that strategy was the fact that the state of latent infection is generally very stable. In addition, in most cases it is difficult to go beyond partial reactivation with expression of some proteins of the lytic cycle like the immediate-early BZLF1 transactivator. On the other hand it was recognized that, in many cases, even partial reactivation is sufficient to block cell growth [305]. This intrinsic cytotoxic effect of partial reactivation, the possible induction of the expression of viral enzymes capable to of metabolizing a pro-drug and the wish to enlarge the range of viral targets for the immune system are currently the main incentives to investigate the induction of the viral lytic activation as a therapeutic approach [306].

Aims of this project

One key question regarding CC-486 is how to select at a very early stage of the treatment the patients who will benefit from this drug. In other words, how to set up a companion assay that will help to predict the likelihood and magnitude of the clinical response after only a few days of treatment. Our group had a strong belief that circulating viral microRNAs might be useful to progress towards this goal. Several publications suggest that malignant cells sensitive to demethylating agents undergo substantial changes in the profile of their microRNAs. For example, in collaboration with KW Lo's group in Hong-Kong, the group has demonstrated that 5-aza-2′deoxycytidine restores the expression of the cellular tumor suppressor microRNA, miR-31. This microRNA is silenced in most NPC tumors by hypermethylation of the promoter of its host gene LOC554202 [192]. Another group has shown that 5-aza-2′deoxycytidine triggers or enhances expression of viral microRNAs in latently EBV-infected B-cells [247]. On the other hand, we have demonstrated in xenografted mice as well as in NPC patients that at least a fraction of tumor microRNAs is released by malignant cells in the extracellular medium and can diffuse to the blood stream [269, 307]. Our hypothesis was that profiling of tumor microRNAs in the blood of NPC patients treated with CC-486 could become a useful approach for an early assessment of the tumor response. We believe that microRNAs encoded by the Epstein-Barr virus genome – BHRF1 and BART clusters - are of special interest because they are almost 100% specific of the tumor cells. Thus, the aims of this project were:

1) To investigate whether treatment of NPC cells with CC-486 induces a switch towards the lytic cycle or ectopic expression of latency III proteins (western blot detection of BZLF1, EBNA1, EBNA2 and LMP1 in NPC cells or tumor extracts),

2) To investigate the changes in the profile of BART and BHRF1 microRNAs potentially induced by treatment of NPC cells and tumors with CC-486,

3) To investigate the changes in the profile of BART and BHRF1 microRNAs in plasma samples from mice bearing C15, C17, C18 and C666-1 tumors or from NPC patients under treatment with CC-486.

4) To extend this study on other chemotherapeutic drugs, already used in clinic, in order to see their potential effect on the expression of viral microRNAs and assess the potential of the latter to be used as response-sensitive biomarkers in these types of treatment.

Note: The following is a provisional version of the article that will be submitted in a few months. As it is cited in its discussion, we are currently working on supplementary assays, both in vitro and in vivo, aiming to validate induction of BHRF1 miRNAs by various therapeutic approaches and not only 5-azacytidine. In addition, we have established communication with the Head and Neck department of Gustave Roussy, which will provide blood samples from NPC patients receiving chemotherapy or combined chemoradiotherapy, in order to directly assess this hypothesis in real patients.

EBV-encoded BHRF1 microRNAs in nasopharyngeal carcinomas: Rare baseline expression and consistent induction in response to treatment

Nikiforos-Ioannis Kapetanakis[1], Aurore Gelin[1], Aaron Nguyen[2], Julie Six[1], Pierre Busson[1,a]

[1]CNRS UMR8126 and Gustave Roussy, 114 rue Edourd-Vaillant, 94805 Villejuif, France and Université Paris-Sud and Paris-Saclay

[2]Celgene Corporation, 86 Morris Avenue, Summit New Jersey, 07901 United States

[a]Correspondence to: Dr Pierre Busson, CNRS UMR8126, Pavillon de Recherche 1, Gustave Roussy, 114 rue Edouard-Vaillant, 94805 Villejuif, France, telephone number: +33(0)142114583, e-mail: pierre.busson@gustaveroussy.fr

Keywords: nasopharyngeal carcinoma, Epstein-Barr virus, plasma, microRNA, 5-azacytidine

Abstract

Nasopharyngeal carcinoma (NPC) is a disease with a unique geographical distribution, consistently associated with latent EBV infection. Although its viral and non-viral mechanisms of oncogenesis are not fully understood, significant improvements have been achieved in its management. However, biomarkers are urgently needed for better assessment of the treatment efficacy. Currently in trials, 5-azacytidine has shown promising results in a subset of patients. Looking for potential biomarkers to assess early response, we focused on its impact on viral proteins and miRNAs in NPC-xenografted mice. We discovered an early de novo induction of BHRF1 miRNAs, detected in both tumor and plasma, proportionally correlated with drug dose and clinical response. A post-treatment induction of the BHRF1 mRNA was also recorded. A modest concomitant increase in the expression of the BZLF1 protein was observed in only one case, suggesting that the induction of the BHRF1 miRNAs is somehow independent of lytic viral reactivation. BHRF1 miRNAs were also detected in tumor and plasma of mice treated with standard therapeutic agents. Overall, our data indicate that de novo expression of BHRF1 miRNAs can be induced in NPC cells by various treatment modalities and their detection in the plasma could become a biomarker indicative of a favorable outcome early after the onset of a novel treatment. This is one of the first illustrations of the concept of using changes in plasma microRNAs as surrogate markers of the early tumor response to therapeutic agents.

Introduction

Nasopharyngeal carcinoma (NPC) is an epithelial tumor mostly poorly differentiated, arising from the epithelial lining of the superior part of the pharynx. It belongs to the group of head and neck cancers, exhibiting however a unique geographical pattern of distribution. It is a rare malignancy in most parts of the world [1], but with a high prevalence in Southeast Asia and North Africa, reaching a maximal incidence of 25 cases in 100000 people in the province of Guangdong, in China [2]. The principle causative factors of NPC are environmental, genetic and viral. Nasopharyngeal carcinomas are constantly associated with EBV infection,

regardless of their geographic origin [145]. The viral genome is conserved at a latent episomal form, expressing only a handful of proteins, but with a robust production of non-coding viral RNAs, like the small RNAs EBER1 and EBER2 and EBV miRNAs. Up to date, 44 miRNAs have been identified to be produced by EBV. They emerge from two distinct loci of the EBV genome, BART (40 miRNAs) and BHRF1 (4 miRNAs). Viral miRNAs present different patterns of expression, varying among EBV-associated malignancies and viral latency types [4]. In epithelial malignancies (NPC and EBV-related gastric carcinomas), the BART miRNAs are very abundant, accounting for at least 10% of the infected cell's miRNAs [5]. On the contrary, there is a consensus about the absence of BHRF1-derived miRNAs in EBV-infected epithelial cells. In contrast, in EBV-infected cells of lymphoid origin, BHRF1 miRNAs are usually well detected whereas expression of the BART microRNAs is at a lower level [5-8]. BHRF1 miRNAs are located within the 5′ and 3′ untranslated regions of the BHRF1 gene that lies downstream of the Cp/Wp and upstream of the Qp promoter [9]. Prompted by ongoing clinical trials with 5-azacytidine for relapsed nasopharyngeal carcinoma, we attempted a study of the impact of the drug on the viral miRNome. 5-azacytidine is a demethylating agent, already used in cases of acute myeloid leukemia (AML) and has been previously suspected to induce the lytic cycle of the virus via upregulation of the immediate-early lytic gene BZLF1 in EBV-positive Burkitt's lymphoma cells (reviewed in [10]). We treated 4 NPC in vivo models (3 patient-derived xenografts and the culture-derived derived xenograft C666-1) with 5-azacytidine and we assessed the expression of tumor and plasma EBV miRNAs, in parallel with treatment efficacy. Some markers related to the entry in the lytic cycle were investigated in the same experimental setting. Finally, treatments based on conventional chemotherapy were carried out, both in vitro and in vivo, to compare their effects to those of the demethylating agents. Our results revealed a de novo expression of the BHRF1 miRNAs, detected in both tumor and plasma of mice, following treatment with 5'azacytidine and standard chemotherapeutic components. The degree of induction reflected drug dose and clinical response, suggesting that detection of these 4 miRNAs in the plasma could be a very early sign of positive response. In at least one NPC model (C15), the induction of the BHRF1 microRNAs was observed in the absence of any modification suggestive of an entry in the lytic cycle.

Materials and Methods

Cells and xenografts

We developed 4 distinct tumor models, using a cell culture of the EBV-positive NPC cell line C666-1, derived from a biopsy of a primary tumor, consistently harboring approximately 12 copies of the EBV genome per cell [11, 12] and 3 patient-derived xenografts (PDX) from patients bearing nasopharyngeal carcinoma. The cell line was cultured in RPMI-1640 medium (Gibco, Life Technologies, Inc), supplemented with 7.5% fetal calf serum (FCS), 25 mM of HEPES, 2mM of glutamine and 5 µg/mL of gentamycin, at 37°C and 5% CO2. The cells were resuspended in culture medium, mixed with an equal volume of Engelbreth-Holm-Swarm (EHS) mouse

sarcoma-derived Matrigel (Sigma-Aldrich) and injected subcutaneously into Swiss nude immunocompromised mice at a load of 2 million cells in 200 µL total load per mouse (project number 1605-201509021649, approved by the ethics' committee). The mice were purchased from the Gustave Roussy pre-clinical evaluation platform, after validation of the project by the ethical committee of Gustave Roussy. The 3 PDX models used were developed and characterized by Busson et al (1988) [13] and are designated as C15, C17 and C18. They host approximately 30, 3 and 12 copies of the EBV genome per cell and were obtained from a primary advanced nasopharyngeal tumor before treatment, a cutaneous metastasis of a NPC after 2 years of treatment by radiotherapy and systemic polychemotherapy and a cervical lymph node after 2 months of polychemotherapy respectively. They had been conserved as tumor fragments in liquid nitrogen and an amount of 150 mg was engrafted into each mouse. Both xenografts and cells needed a mean time of 2-3 weeks following tumor engraftment or cell injection respectively in order to give tumors eligible for treatment.

Treatment

Oral 5-azacytidine, commercially named CC-486, was provided by Celgene (San Francisco, CA, USA) in glass vials containing the drug in powder, protected from light. All tumor models were treated by everyday intraperitoneal (IP) injections of CC-486 dissolved in sterile PBS. Three treatment conditions were applied (PBS alone, 1 mg/kg and 2 mg/kg of 5-azacytidine), each one on 5 mice for every tumor model. The body weight and the tumor dimensions were measured for each mouse every 3 days. Tumor burden was defined by measuring the bigger dimension (L) and the smaller (l) and applying the type: $L(l^2)/2$. Tumor progression was defined in comparison to the initial burden. At day 15, 1 ml of blood was taken by direct intracardiac puncture under general anesthesia (isoflurane inhalation) and transferred to EDTA tubes (KABE Labortechnik) and the mice were sacrificed right after. From each treatment condition, among the 5 mice, 3 were used for subsequent analysis: the one with the largest tumor, the one with the smallest and a third with an intermediate size. The tumors were dissected into small macroscopically non-necrotic fragments and immediately stored in liquid nitrogen. The blood was directly processed for plasma isolation by centrifugation at 1700g and at 4°C for 15 minutes. The plasma was transferred in Cryotube vials and stored at -80°C. Plasma samples were used for circulating microRNA extraction and tumor fragments for separate extractions of total RNA and proteins. For every tumor model, the treatment was later repeated following the exact same procedure, this time for one week (sacrifice at day 8), for validation of selected targets. Other treatments used include cisplatin and paclitaxel administered by intraperitoneal injections every 3 days, at 2 mg/kg and 15 mg/kg respectively for two weeks. For the mice which received a combination, paclitaxel was administered one hour after cisplatin. In the in vitro treatment we also tested 0.1 µM and 0.3 µM of 5-aza-2′deoxycytidine (5azaD), the deoxy-derivative of 5-azacytidine, as well as 0.3 µM, 1 µM, 3 µM and 10 µM of 5-azacytidine (5aza).

RNA extraction

Circulating microRNAs were extracted from 200 µl of plasma, using the miRCURY RNA Isolation Kit for Biofluids (Exiqon). During the procedure, the plasma was supplemented with 1 µg of carrier MS2 phage genomic RNA (Roche) per sample, in order to improve microRNA yield, according to the manufacturer's protocol. Total RNA was extracted from tumor fragments of 50-70 mg following the TRI Reagent® protocol (Molecular Research Center, Inc.), an improved version of the classic single-step method using phenol, guanidine thiocyanate and chloroform. Every tumor fragment was immediately placed in 1 ml of cold TRI Reagent® and homogenized with Qiagen's TissueRuptor (handheld rotor-stator homogenizer). The final RNA concentration of plasma and tissue RNA extracts was measured with a Nanodrop2000 spectrophotometer. All RNA extracts were eluted in 50 µL of nuclease-free H_2O and stored at -80°C.

RT-qPCR and data analysis

Viral microRNAs from tumor and plasma extracts were assessed by two-step RT-qPCR on Exiqon's custom-made qPCR plates with pre-fixed primers (Pick-&-Mix microRNA PCR Panels), including some human miRNAs as a pool of candidate endogenous references (hsa-miR-103a-3p, hsa-miR-190a-5p, hsa-miR-31-5p, hsa-miR-191-5p, hsa-miR-429-3p and hsa-miR-200b-3p). The global EBV miRNA analysis was performed at Exiqon headquarters, in Vedbaek, Denmark. After data analysis, the qualified miRNA candidates were validated in Gustave Roussy by two-step RT-qPCR. MicroRNAs were reverse-transcribed to cDNA with Exiqon's Universal cDNA Synthesis kit II, designed for selective reverse transcription of mature miRNAs, while reverse transcription of mRNAs was performed with Eurogentec's Reverse Transcriptase Core Kit 300. In both cases, we used 10 ng of RNA per 10 µl reaction. For miRNA detection and quantification we used SYBR-based qPCR, with Exiqon's ExiLENT SYBR® Green Master Mix kit, supplemented with ROX passive reference dye (Sigma-Aldrich), as well as Exiqon LNA primer sets for viral and human miRNAs. Mean values of three human miRNAs (miR-103a-3p, miR-191-5p and miR-200b-3p) and the snRNA U6 were used as endogenous references for results' normalization in the two-week treatment and the one-week treatment assays respectively. For the detection of viral mRNA transcripts we used a TaqMan-based approach, with Eurogentec's Takyon ROX Probe 2X MasterMix dTTP blue. Primers and probes for the detection of EBNA1, BZLF1 and latent BHRF1 transcripts were designed as shown in the supplementary data of Kelly et al (2009) [14] and bought from Eurogentec. For the normalization of the results we used the GAPDH Control kit Yakima Yellow® - Eclipse Dark Quencher® of Eurogentec.

Every reaction generates a Ct value, reflecting the cycle threshold of the detection of a given target, meaning the amplification cycle during which the detected SYBR fluorescence exceeds the background noise. We performed 40 amplification cycles and the number 40 was attributed as the Ct of the reactions where the target was not detected at the end. The higher the value of the generated Ct, the lower is the expression of the

target, as the detected fluorescence emerges later due to the lower initial abundance of the target. All sample reactions were carried out in duplicates and the mean Ct value of every sample was normalized with the ΔCt method, using the reference targets mentioned above. To determine the relative abundance of a given miRNA in a sample, compared to a control group we used the $2^{-\Delta\Delta Ct}$ value [15]. Baseline expression of the viral miRNAs (figure 1b) is presented in $2^{-\Delta Ct}$ values, as the Ct of every target miRNA was normalized for a given sample by the mean Ct of miR-103a-3p, miR-191-5p and miR-200b-3p. Upon analysis of the treatment results, the data are presented as expression changes compared to the control group. For each sample, plasma or tumor, the ΔCt generated by the above mentioned normalization was further normalized by the ΔCt of the control group (PBS alone). The final $2^{-\Delta\Delta Ct}$ value represents the fold-change in the expression compared to the control. The presented $2^{-\Delta Ct}$ and $2^{-\Delta\Delta Ct}$ values have been rounded up to two decimals.

Protein analysis and Western blotting

For protein analysis, tumor fragments of the same samples were homogenized as described for RNA extraction, in 1 ml of RIPA buffer supplemented with Complete Protease Inhibitor cocktail (Roche). After homogenization, the samples were sonicated and the protein concentration was defined using the Bradford assay. Western blot analysis was done for the expression of BZLF1, BHRF1, EBNA1, EBNA2, LMP1 and GAPDH using B95-8 marmoset-derived cells infected by EBV and treated with phorbol-ester (TPA) for induction of the lytic cycle as a positive control. 20 µg of total protein extract were charged per sample. We used mouse monoclonal antibodies, which are listed below: for BZLF1, Santa Cruz Biotechnology, catalog number sc-53904 (1:200 dilution), for BHRF1 Millipore, catalog number MAB8188 (1:500 dilution), for EBNA1 Santa Cruz Biotechnology, catalog number sc-81581 (1:200 dilution), for EBNA2 Abcam, catalog number ab90543 (1.5µg/mL dilution), for LMP1 Abcam, catalog number ab78113 (1.5µg/mL dilution) and for GAPDH Santa Cruz Biotechnology, catalog number sc-47724 (1:10000 dilution). A sheep anti-mouse antibody from GE Healthcare linked with horseradish peroxidase was used as a secondary antibody at a final dilution of 1:10000. Analysis and quantification of the blots was done with ImageJ, calculating the optical density of the protein of interest and the GAPDH and generating their ratio.

Results

Viral miRNA expression in NPC

Before testing the effects of 5-azacytidine, we evaluated the baseline expression of EBV microRNAs in the 4 NPC tumor models. For each tumor model, the abundance of viral microRNAs was assessed in tumor extracts and plasma samples from the corresponding tumor-bearing mice, first in the absence of any treatment. As endogenous references, we used three cellular microRNAs with minimal variations through all 4 tumor models (miR-191-5p, miR-103a-3p and miR-200b-3p). As expected, we detected all 40 BART microRNA species in the 4 NPC models with a particularly intense expression in C15 and C666-1 and a lower expression in C18 and C17. In contrast, the BHRF1 miRNAs were undetectable except

a.

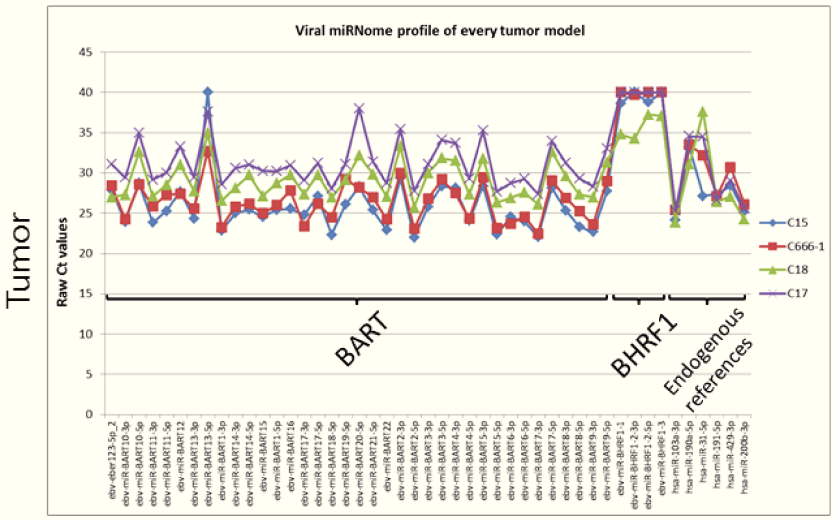

b.

Tumor

Tumor $2^{-\Delta Ct}$	C15	C666-1	C18	C17
ebv-eber123-5p_2	0,20	0,21	0,23	0,03
ebv-miR-BART10-3p	3,13	3,92	0,19	0,08
ebv-miR-BART10-5p	0,11	0,19	0,00	0,00
ebv-miR-BART11-3p	3,34	1,29	0,21	0,10
ebv-miR-BART11-5p	1,25	0,48	0,08	0,06
ebv-miR-BART12	0,23	0,44	0,01	0,01
ebv-miR-BART13-3p	2,37	1,59	0,13	0,08
ebv-miR-BART13-5p	0,00	0,01	0,00	0,00
ebv-miR-BART1-3p	6,73	7,79	0,31	0,15
ebv-miR-BART14-3p	1,49	1,32	0,10	0,04
ebv-miR-BART14-5p	1,08	1,04	0,03	0,03
ebv-miR-BART15	2,04	2,32	0,21	0,05
ebv-miR-BART1-5p	1,11	1,15	0,07	0,05
ebv-miR-BART16	1,03	0,33	0,03	0,03
ebv-miR-BART17-3p	1,71	7,16	0,18	0,11
ebv-miR-BART17-5p	0,35	1,00	0,03	0,02
ebv-miR-BART18-5p	9,69	3,43	0,23	0,22
ebv-miR-BART19-5p	0,70	0,13	0,05	0,03
ebv-miR-BART20-5p	0,15	0,26	0,01	0,00
ebv-miR-BART21-5p	1,14	0,59	0,03	0,02
ebv-miR-BART22	6,38	3,92	0,22	0,14
ebv-miR-BART2-3p	0,07	0,07	0,00	0,00
ebv-miR-BART2-5p	12,29	9,04	0,54	0,27
ebv-miR-BART3-3p	0,84	0,66	0,03	0,03
ebv-miR-BART3-5p	0,14	0,13	0,01	0,00
ebv-miR-BART4-3p	0,17	0,41	0,01	0,00
ebv-miR-BART4-5p	2,83	3,73	0,18	0,09
ebv-miR-BART5-3p	0,14	0,11	0,01	0,00
ebv-miR-BART5-5p	9,24	8,14	0,36	0,29
ebv-miR-BART6-3p	2,09	5,59	0,24	0,14
ebv-miR-BART6-5p	2,99	3,12	0,15	0,09
ebv-miR-BART7-3p	11,42	13,53	0,42	0,35
ebv-miR-BART7-5p	0,17	0,14	0,00	0,00
ebv-miR-BART8-3p	1,16	0,61	0,04	0,02
ebv-miR-BART8-5p	4,81	1,97	0,18	0,09
ebv-miR-BART9-3p	7,49	5,96	0,23	0,19
ebv-miR-BART9-5p	0,22	0,15	0,01	0,01
ebv-miR-BHRF1-1	0,00	0,00	0,00	0,00
ebv-miR-BHRF1-2-3p	0,00	0,00	0,00	0,00
ebv-miR-BHRF1-2-5p	0,00	0,00	0,00	0,00
ebv-miR-BHRF1-3	0,00	0,00	0,00	0,00

Plasma

Plasma $2^{-\Delta Ct}$	C15	C666-1	C18	C17
ebv-eber123-5p_2	0,00	0,00	0,01	0,00
ebv-miR-BART10-3p	3,56	8,19	0,16	0,06
ebv-miR-BART10-5p	0,01	0,03	0,00	0,00
ebv-miR-BART11-3p	3,66	1,92	0,25	0,13
ebv-miR-BART11-5p	0,01	0,01	0,00	0,00
ebv-miR-BART12	0,11	0,09	0,00	0,00
ebv-miR-BART13-3p	11,55	6,06	0,09	0,29
ebv-miR-BART13-5p	0,00	0,00	0,00	0,00
ebv-miR-BART1-3p	0,12	0,54	0,01	0,00
ebv-miR-BART14-3p	0,44	0,36	0,01	0,01
ebv-miR-BART14-5p	0,93	1,31	0,01	0,02
ebv-miR-BART15	9,57	11,20	0,18	0,17
ebv-miR-BART1-5p	0,37	0,23	0,01	0,01
ebv-miR-BART16	0,00	0,00	0,00	0,00
ebv-miR-BART17-3p	0,17	0,81	0,00	0,00
ebv-miR-BART17-5p	0,01	0,05	0,00	0,00
ebv-miR-BART18-5p	0,10	0,14	0,00	0,00
ebv-miR-BART19-5p	1,33	0,28	0,02	0,03
ebv-miR-BART20-5p	0,28	0,77	0,00	0,00
ebv-miR-BART21-5p	0,01	0,03	0,00	0,00
ebv-miR-BART22	0,02	0,00	0,00	0,00
ebv-miR-BART2-3p	0,25	0,12	0,00	0,01
ebv-miR-BART2-5p	28,38	17,88	1,28	0,54
ebv-miR-BART3-3p	5,31	4,29	0,13	0,08
ebv-miR-BART3-5p	0,01	0,01	0,00	0,00
ebv-miR-BART4-3p	0,55	1,23	0,00	0,00
ebv-miR-BART4-5p	1,73	1,97	0,06	0,04
ebv-miR-BART5-3p	0,12	0,20	0,00	0,01
ebv-miR-BART5-5p	17,52	19,45	0,04	0,09
ebv-miR-BART6-3p	1,27	3,48	0,01	0,04
ebv-miR-BART6-5p	0,07	0,31	0,00	0,00
ebv-miR-BART7-3p	77,28	54,79	0,28	0,29
ebv-miR-BART7-5p	0,06	0,06	0,00	0,00
ebv-miR-BART8-3p	1,23	0,43	0,01	0,03
ebv-miR-BART8-5p	0,04	0,09	0,00	0,00
ebv-miR-BART9-3p	0,48	0,35	0,01	0,01
ebv-miR-BART9-5p	0,74	0,44	0,01	0,02
ebv-miR-BHRF1-1	0,00	0,00	0,01	0,00
ebv-miR-BHRF1-2-3p	0,00	0,00	0,01	0,00
ebv-miR-BHRF1-2-5p	0,00	0,00	0,00	0,00
ebv-miR-BHRF1-3	0,00	0,00	0,00	0,00

Detection	Very strong	Strong	Weak	Absent

Figure 1a: Raw Ct values of the tested miRNAs in the tumors of the 4 different NPC models. Undetected miRNAs were attributed the arbitrary Ct value of 40, as mentioned above. Viral miRNAs seem to be overlapping among the 4 models, although every model revealed a different level of their global general expression. Figure 1b: Heatmaps showing the compared baseline expression of EBV miRNAs in tumor fragments and plasma of mice bearing the 4 different NPC models. Each Ct for a given miRNA target was normalized with the mean Ct of the 3 selected endogenous references (miR-191-5p, miR-103a-3p and miR-200b-3p), generating a ΔCt, thus the relative expression of the miRNA in equivalence to the reference. The lower the ΔCt value, the higher the expression of the target. The shown $2^{-\Delta Ct}$ value depicts the difference between the target and the reference in a proportional manner (the higher the $2^{-\Delta Ct}$, the higher the expression). A stable expression of BHRF1 miRNAs was seen only in C18 tumors (mainly miR-BHRF1-1 and miR-BHRF1-2-3p).

at a very low concentration in the C18 tumor extract (Figure 1a). The plasma analysis confirmed previous works of the group, proving the liberation and detection of EBV BART miRNAs in the plasma of individuals or animals bearing NPC tumors [16]. Their abundance in plasma samples was congruent with the one in tumor extracts, with high concentrations in the circulation of C15 and C666-1-bearing mice and a low concentration for C17- and C18-engrafted mice. Again, the BHRF1 miRNAs were undetectable except at a low level in plasma samples from C18 mice (figure 1b). Interestingly, there seems to be a correlation between the expression of BART miRNAs and the stage of the tumor, with a much stronger expression of BART miRNAs in primary NPC tumors, as compared to metastatic disease.

Changes in miRNA profiles related to treatment efficacy

We tested the effect of 2 doses of 5-azacytidine (1 mg/kg and 2 mg/kg), administered daily, versus PBS alone. After 2 weeks of treatment, C15, C666-1 exhibited a visible positive response to 5-azacytidine, showing either a stabilization of the tumors, in the case of C15, or even a regression during the second week, as seen in the case of C666-1 tumors (figure 2a). C18 exhibited a decrease in the tumor progression, but to a much lesser extent. On the other hand, C17 tumors proved to be resistant to the drug, with no change in tumor progression. The clinical image of the tumors revealed a response in a dose-dependent manner, as 2 mg/kg were more effective than 1 mg/kg. Analysis of the miRNA panels revealed a mild impact of the treatment on the expression of the BART miRNAs. We observed no significant upregulation or downregulation of their expression superior to 5-fold or inferior to 0.2-fold respectively, as compared to their baseline profiles (see figures 1a-1d in supplementary data). Most notable changes in BARTs were a progressive and substantial decrease in the expression of miR-BART20-5p, seen in treated C15, C666-1 and C17, as well as a spectacular decrease of miR-BART13-5p in treated C666-1 and C17. Interestingly, C15 presented a robust upregulation of this miRNA (superior to 150-fold for both doses). Overall, C15 and C666-1 exhibited a discreet but general reduction in the expression of BART miRNAs. C18 tumors had the opposite response, as the majority of BART miRNAs were upregulated between 2- and 4-fold in both treatment modalities. On the other hand, C17 tumors,

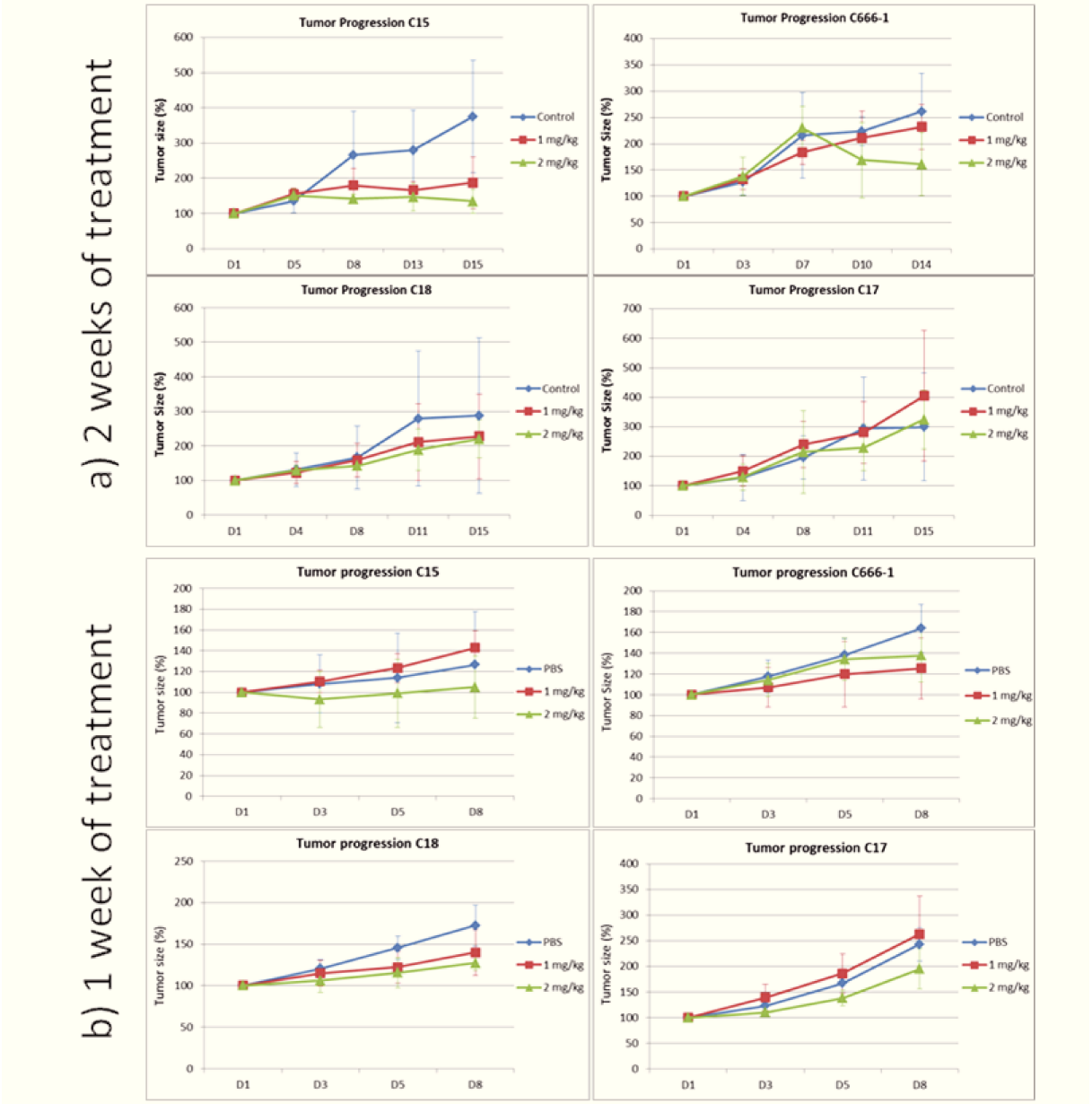

Figure 2: Clinical response in terms of tumor growth compared to the initial burden in mice xenografted with the 4 NPC models and treated with 5-azacytidine for a) two weeks and b) one week. C15 and C666-1 showed the most substantial responses over two weeks, with stabilization and regression of the tumors respectively, although they were not seen after only one week of treatment.

apart from a 10-fold downregulation of miR-BART13-5p, as already mentioned above, showed no visible change in the BART profiles. However, the most notable finding was a consistent induction of the 4 BHRF1 miRNAs following treatment. As presented in figure 3, there was a correlation between the clinical response to the drug and the induction degree of BHRF1 miRNAs. C15 and C666-1 presented a de novo expression of these miRNAs, which were also detectable in the blood of the animals (figure 3a). C18 on the other hand had the unique aspect of consistent baseline detection of BHRF1 miRNAs, which were very discreetly upregulated post-treatment. C17 exhibited no production of BHRF1 miRNAs in all treatment modalities, correlating with the absence of clinical response to the drug.

a.

Tumor

C15 Tumor $2^{-\Delta\Delta Ct}$ values	Control	1 mg/kg	2 mg/kg
ebv-miR-BHRF1-1	1	0,82	2,90
ebv-miR-BHRF1-2-3p	1	3,39	31,20
ebv-miR-BHRF1-2-5p	1	1,06	5,33
ebv-miR-BHRF1-3	1	3,15	9,40

C666-1 Tumor $2^{-\Delta\Delta Ct}$ values	Control	1 mg/kg	2 mg/kg
ebv-miR-BHRF1-1	1	66,59	120,79
ebv-miR-BHRF1-2-3p	1	36,65	33,81
ebv-miR-BHRF1-2-5p	1	6,93	20,65
ebv-miR-BHRF1-3	1	9,85	33,12

C18 Tumor $2^{-\Delta\Delta Ct}$ values	Control	1 mg/kg	2 mg/kg
ebv-miR-BHRF1-1	1	1,25	2,79
ebv-miR-BHRF1-2-3p	1	2,09	5,01
ebv-miR-BHRF1-2-5p	1	4,05	2,41
ebv-miR-BHRF1-3	1	9,60	15,53

C17 Tumor $2^{-\Delta\Delta Ct}$ values	Control	1 mg/kg	2 mg/kg
ebv-miR-BHRF1-1	1	1	1
ebv-miR-BHRF1-2-3p	1	1	1
ebv-miR-BHRF1-2-5p	1	2,43	1
ebv-miR-BHRF1-3	1	1	1

Plasma

C15 Plasma $2^{-\Delta\Delta Ct}$ values	Control	1 mg/kg	2 mg/kg
ebv-miR-BHRF1-1	1	1,64	0,30
ebv-miR-BHRF1-2-3p	1	1,42	1,38
ebv-miR-BHRF1-2-5p	1	0,58	1,17
ebv-miR-BHRF1-3	1	1,00	2,29

C666-1 Plasma $2^{-\Delta\Delta Ct}$ values	Control	1 mg/kg	2 mg/kg
ebv-miR-BHRF1-1	1	47,59	197,96
ebv-miR-BHRF1-2-3p	1	5,52	12,14
ebv-miR-BHRF1-2-5p	1	2,81	2,25
ebv-miR-BHRF1-3	1	2,27	31,11

C18 Plasma $2^{-\Delta\Delta Ct}$ values	Control	1 mg/kg	2 mg/kg
ebv-miR-BHRF1-1	1	3,25	2,05
ebv-miR-BHRF1-2-3p	1	0,53	1,22
ebv-miR-BHRF1-2-5p	1	2,75	1,29
ebv-miR-BHRF1-3	1	3,56	3,48

C17 Plasma $2^{-\Delta\Delta Ct}$ values	Control	1 mg/kg	2 mg/kg
ebv-miR-BHRF1-1	1	2,32	2,07
ebv-miR-BHRF1-2-3p	1	1	1
ebv-miR-BHRF1-2-5p	1	1,89	2,13
ebv-miR-BHRF1-3	1	1	1

Detection	Unchanged	Mild increase	Strong increase

b.

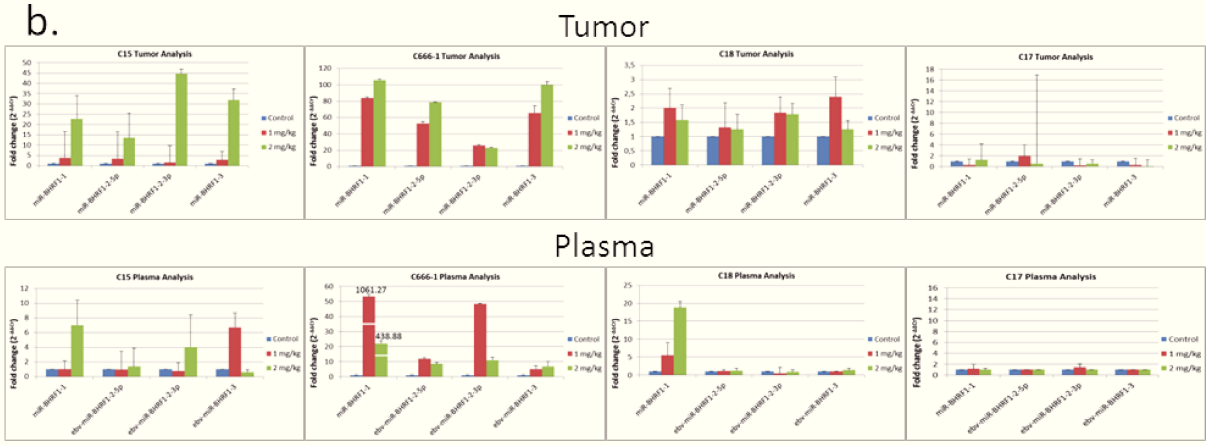

Figure 3a: Relative expression of BHRF1 miRNAs ($2^{-\Delta\Delta Ct}$, fold-change compared to Control) in tumor fragments and plasma of mice bearing the 4 different NPC models treated for 2 weeks with 5-azacytidine.The Ct of every BHRF1 miRNA was normalized with the mean Ct of the 3 reference miRNAs for a given sample (ΔCt) and every sample was compared to the control sample for a given tumor model (ΔΔCt). Figure 3b: Relative expression of BHRF1 miRNAs in tumor fragments and plasma of mice treated with the same conditions for one week. The same procedure was followed for data processing, but for this assay the snRNA U6 was used as an endogenous reference.

In order to validate these results, we repeated the treatment, with the same conditions, but only for one week, focusing on the expression of BHRF1 miRNAs in the tumor and the plasma. The outcome was very interesting, as the clinical impact was much weaker than the one after two weeks, but the pattern of BHRF1 induction was identical to the one seen before. More precisely, C15 exhibited stabilization after 7 days of daily treatment, but only for the tumors receiving 2 mg/kg (figure 2b). C666-1 exhibited a decrease in progression for both modalities, but not in a dose-dependent manner, without regression. C18 had a similar progression to the one seen in the initial treatment, presenting a decreased but continuous and steady progression, while C17 showed no stabilization at all. RT-qPCR analysis in the tumor and the plasma of the treated mice revealed BHRF1 kinetics reflecting the clinical impact observed at the two-week treatment. C15 had a discreet induction of BHRF1 miRNAs with 1 mg/kg of daily treatment, but a robust expression with 2 mg/kg, above 10-fold at the level of the tumor and detected in the

plasma (3b). C666-1 had a brutal induction of BHRF1, even with the low dose of 5-azacytidine, also reflected in plasma analysis. The induction was very weak for C18 and only miR-BHRF1-1 was detected in the plasma after one week of treatment, while C17 expressed no BHRF1 miRNA at all. These results suggest a clinical utility of these 4 miRNAs, as a signature of very early response of nasopharyngeal carcinoma tumors to treatment by 5-azacytidine. Screening for their detection in the plasma of patients initiating treatment could predict the outcome even before the onset of a clinical impact of the drug.

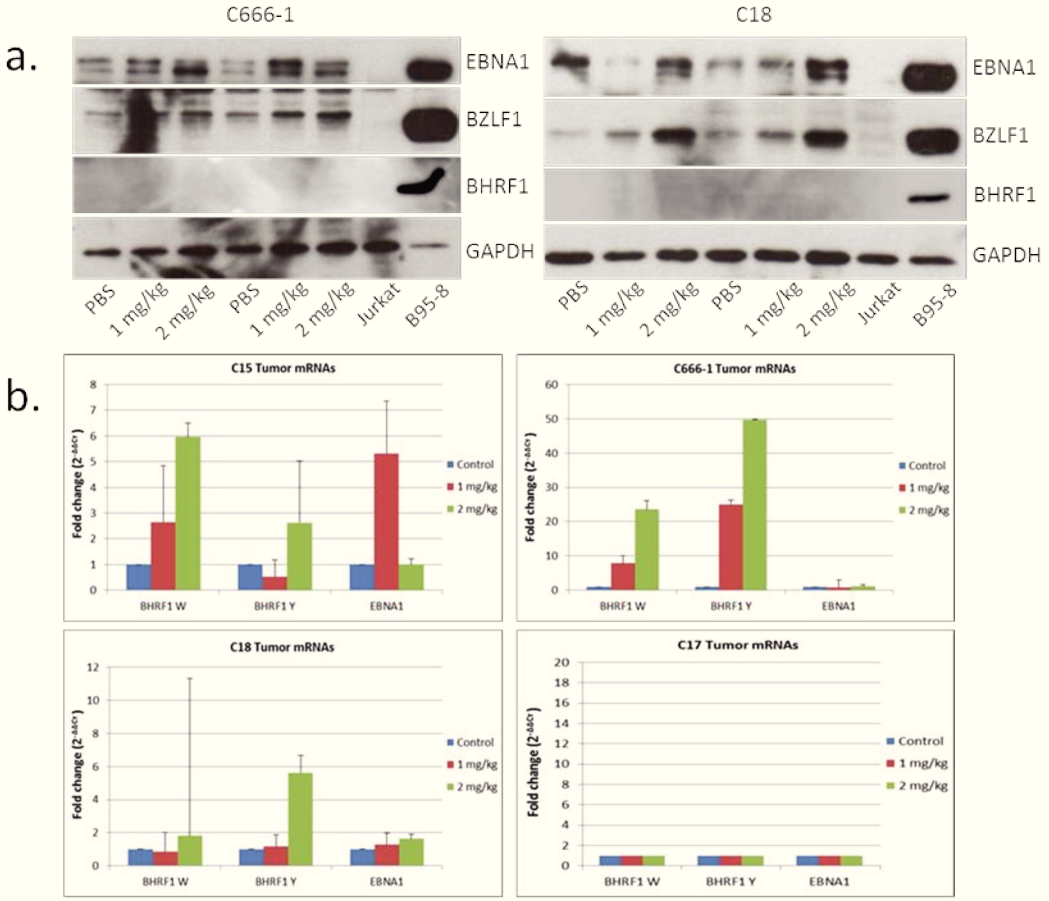

Figure 4a: Protein analysis of C666-1 and C18 tumors treated for two weeks. Protein extracts from Jurkat and the B95-8 cell line treated by TPA were used as negative and positive biomarkers respectively. A dose-dependent induction of BZLF1 protein was seen only in these two tumor models (see supplementary data for the others), without being concordant with the pattern of BHRF1 miRNAs (figure 3). Figure 4b: RT-qPCR analysis of viral messenger RNAs after one week of treatment confirmed no significant change in EBNA1 expression depending on the treatment, but revealed an induction of BHRF1 mRNA in a dose-dependent manner, reflecting the dynamics of the neighboring miRNAs. Normalization was done using the GAPDH mRNA as an endogenous reference.

5-azacytidine alters viral latency

Previous works have shown that 5-azacytidine may cause a switch towards the lytic/productive cycle of EBV, by upregulating the expression of the immediate-early lytic gene BZLF1. This observation was done in the Burkitt's lymphoma (BL) cell line Rael, treated with 5-azacytidine. EBV-associated BL presents a type I latency, where EBNA1 is practically the only expressed viral protein [17]. BZLF1 is a transcription factor, also known as Zta, EB1, or ZEBRA. It mediates the switch from the latent to the

lytic form of viral expression by activating other early lytic genes, thus resulting in the production of new virions through a cascade of viral gene activation [18]. Tempted by the already seen induction of BHRF1 miRNAs, also expressed throughout the lytic cycle, we studied the expression of BZLF1, EBNA1 and BHRF1 at the protein level. BHRF1 is an early lytic gene, producing a Bcl-2 homolog, which acts in an oncogenic way by blocking the induction of apoptosis [19]. Since the transcript coding for BHRF1 contains the precursors of the BHRF1 miRNAs, we hypothesized that a detection of the miRNAs would be accompanied by expression of BHRF1 itself. However, a progressive increase of BZLF1 expression was only detected in the cases of treated C666-1 and C18 tumors, already presenting a weak expression of BZLF1 without treatment (figure 4a). C15 and C17 did not show any expression of BZLF1, with or without 5-azacytidine administration (see figures 2a-2d in supplementary data). Interestingly, only the models with readily detectable baseline expression of BZLF1 were affected by the drug. No specific variation of EBNA1 was seen upon treatment with 5-azacytidine. A de novo expression of the BHRF1 messenger RNA (mRNA) was seen in all treated tumors, in a highly similar way with the previously seen induction of BHRF1 miRNAs. As expected, C17 did not express the transcript neither before, nor after treatment (figure 4b). Intriguingly, we were not able to confirm the induction of BHRF1 at the protein level (figure 4a). These results, taken together with the induction of BHRF1 miRNAs and the homogeneous variation of the BART miRNAs lead to the conclusion that 5-azacytidine alters the established viral latency in NPC tumors, seemingly causing a switch towards type III latency and lytic reactivation. C18 appears to bear a different pattern of latency, as compared to the other tumors. However, the induction of BHRF1 miRNAs seems to be independent from the onset of the viral lytic cycle.

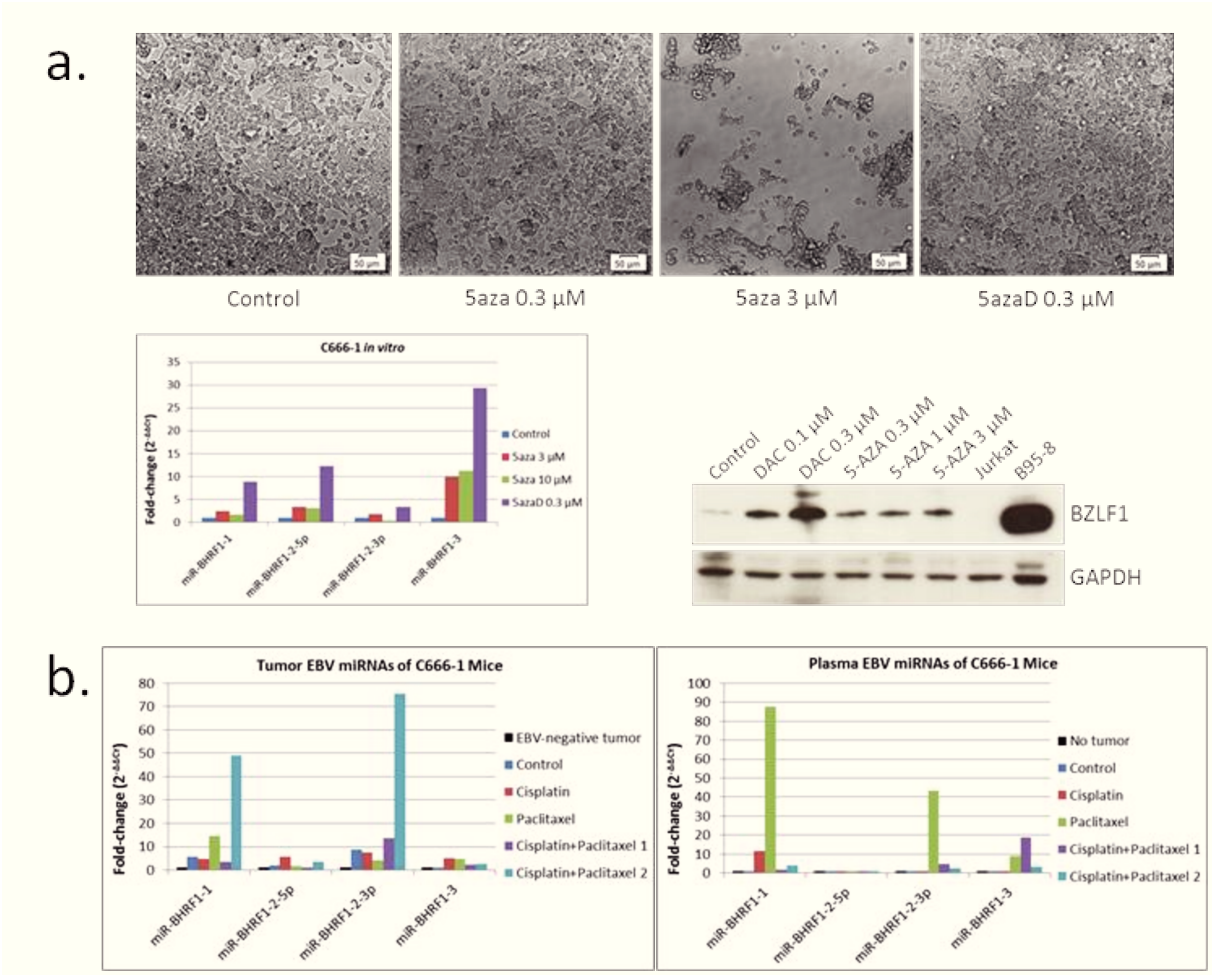

Figure 5a: In vitro treatment of C666-1 cells with different doses of 5aza and 5azaD. The impact of 5azaD on the expression of BHRF1 miRNAs is much stronger (purple bars on the histogram), even at very weak doses with no visible toxicity, compared to 5aza (ass seen in the photos). Treated cells were compared to the control for the in vitro assay. Figure 5b: In vivo two-week treatment of mice xenografted with C666-1 tumors with cisplatin or/and paclitaxel. Untreated C666-1 expressed very low levels of BHRF1 miRNAs, undetected in the plasma, while the use of chemotherapeutic agents induced their expression, leading to their detection in the plasma of the treated mice. All results were normalized with U6 as endogenous reference for each sample. We used an EBV-negative tumor (IGROV1) and the plasma from a tumorless mouse as calibrators for tumor and plasma measurements respectively ($2^{-\Delta\Delta Ct}$).

Induction of BHRF1 miRNAs by other drugs

Prompted by the particular relationship between the clinical aspect of NPC under treatment and the presence of BHRF1 miRNAs in the plasma, we tried to assess the kinetics of this miRNA cluster under treatment by various therapeutic agents. Our aim was to see if this induction is restricted to 5-azacytidine (5aza), or if it can be achieved with other drugs too. Following the example of previous works, we carried out distinct treatments on C666-1, in vitro and in vivo. Yang et al in 2013 compared the expression of C666-1 with biopsies taken from primary NPC tumors of patients and found extensive similarity in viral expression, thus making C666-1 an excellent model for studying EBV dynamics in the context of NPC [5]. At the in vitro level, we compared 5-azacytidine with its deoxy-analog, 5-aza-2'deoxycitidine (5azaD). Unlike 5aza, 5azaD is only incorporated into DNA, with previous publications estimating a 10-fold higher toxicity in treated cell and animal

models, compared to 5aza [20, 21]. As a consequence, we administered lower doses (0.1 and 0.3 μM) of 5azaD to cells and higher doses of 5aza (0.3, 1 and 3 μM). A 72h treatment showed no macroscopic effect of toxicity on the cells, with the exception of 5aza at a concentration of 3 μM (figure 5a). At the molecular level, 5azaD proved to have a much stronger impact on viral expression, as much lower dose generated an induction of BHRF1 miRNAs and an upregulation of BZLF1 protein superior to that caused by 5aza. In the in vivo assay, we treated mice with xenografted C666-1 tumors with chemotherapeutic agents used in the clinic for the standard treatment of nasopharyngeal carcinoma. We administered cisplatin and paclitaxel as monodrugs, at a concentration of 2 mg/kg and 15 mg/kg respectively, as well as a combination of them at the same doses for a total period of two weeks (figure 5b). An ovarian tumor engrafted into nude mice and plasma from a tumorless mouse were used as negative controls for assessment of BHRF1 miRNA expression. An untreated C666-1 tumor presented a low expression, with no detection at all in the plasma of the mouse. Interestingly, increased abundance of BHRF1 miRNAs was seen in treated tumors. Paclitaxel alone and the combination of cisplatin and paclitaxel led to increased expression of miR-BHRF1-1 and miR-BHRF1-2-3p at the level of the tumor. The results of the plasma were not concordant with the ones from the tumors. Cisplatin treatment led to detection of miR-BHRF1-1 alone in the plasma, while the combination treatment led to an expression of miR-BHRF1-2-3p and miR-BHRF1-3 as well. Notably, paclitaxel alone caused a robust expression of miR-BHRF1-1 and miR-BHRF1-2-3p and, to a lesser extent, of miR-BHRF1-3. These results are very limited in terms of treated mice and assessed drug doses and need further validation to generate solid conclusions. However, the preliminary evidence presented here suggests that BHRF1 miRNAs can be induced by other therapeutic modalities and not only demethylating agents. Their detection in the plasma after a limited time of treatment supports the perspective of using them as biomarkers for treatment evaluation in the context of nasopharyngeal carcinoma.

Discussion

Primary tumors C15 and C666-1 showed a strong expression for the majority of BART miRNAs, whereas metastatic tumors C18 (lymph node) and C17 (skin) showed a weaker expression. It is unclear whether the reduction in BART expression could be a result of chronic chemotherapeutic treatment, evolution of the disease and eventual loss of EBV episomes, or reorganization of the viral genome and epigenetic repression. C666-1 and C18 have been shown to contain a similar, if not the same, number of EBV copies [12, 13], exhibiting however contradictive profiles in the expression of EBV miRNAs. 5-azacytidine has not been used for the treatment of nasopharyngeal carcinoma before. However, an orally administered form was recently developed by Celgene and is currently being assessed for a wide variety of cancers, including EBV-positive nasopharyngeal carcinoma. Preliminary results from clinical trials have shown that this drug, as a monodrug, has a positive impact on relapsed refractory NPC for a subset of included patients. Other recent works demonstrate its beneficial action in relapsed NPC in addition to radiotherapy [22]. For a rapid reaction in

case of a negative response, biomarkers for early beneficial effect are greatly needed. Since the drug has been previously shown to bear an impact on the expression of the EBV genome in EBV-associated malignancies, we focused on viral miRNAs, which have the advantage of being detectable in the plasma of NPC patients [16]. As it is already known that 5-azacytidine causes demethylation of EBV DNA in EBV-positive tumors [23] and upregulates BZLF1 in Burkitt's lymphoma cells [18], we were interested to study the general impact of the drug on EBV in the context of type II latency characterizing NPC. Evaluating miRNA expression of the four developed in vivo models of NPC, we confirmed the previously identified robust expression of BART miRNAs and weak or no expression of BHRF1 miRNAs in NPC. Kim and Lee suggested that the expression pattern of EBV miRNAs in tumors reflects differences in the tissue, as well as in the type of the latency [4]. As mentioned, BART miRNAs tend to be more expressed in type II latency and epithelial tumors [5], than in types I and III and lymphomas, while BHRF1 expression is restricted to type III [4]. The primary tumors tested presented a miRNA profile corresponding well to the one of type II latency. On the other hand, metastatic secondary NPC showed an altered type, with a weaker expression of BART and a detection of BHRF1 miRNAs in C18. One possible hypothesis for this observation could be the impact of chronic treatment of these patients with chemotherapy and radiotherapy, which might have had an impact on the status of EBV in these tumors. The treatment proved to be efficient for those primary tumors and insufficient or ineffective for metastatic NPC models. In correlation with the treatment outcome, primary tumors exhibited a general decrease in BART expression and an induction of BHRF1 miRNAs. The detection of the latter in the plasma of positively responding xenografted mice even before any sign of clinical response, suggested a promising tool for early assessment of 5-azacytidine efficacy in nasopharyngeal carcinoma treatment. MiR-BART13-5p, mentioned to present a spectacular decrease upon treatment with 5-azacytidine was recently found to be upregulated in nasopharyngeal carcinoma, with a decreasing variation after effective treatment [24]. Further evaluating the impact of the drug on viral latency, we detected an upregulation of BZLF1, suggesting lytic reactivation of the virus, also supported by the detection of the BHRF1 long transcript after treatment. However, only the tumors with baseline BZLF1 expression showed an upregulation, as a de novo induction was not seen. BZLF1 upregulation matched with an observed downregulation of miR-BART20-5p, mentioned to directly target BZLF1 translation [25]. Li et al (2012) have demonstrated that 5-azacytidine-mediated demethylation of the BZLF1 promoter, often hypermethylated in EBV-associated malignancies, has the ability to induce a lytic cascade [26]. Our findings suggest that when there is no BZLF1 expression at all, other mechanisms may precede DNA demethylation in order to result in activation of the cascade. BHRF1 miRNAs, more precisely miR-BHRF1-1, have also been mentioned to be involved in accumulation of lytic EBV proteins following TPA-induced lytic reactivation, by targeting host p53 [27]. It would be interesting to study the methylation pattern of the viral Wp and Cp promoters, responsible for the production of the

BHRF1 transcript, initially including the BHRF1 miRNAs and the coding sequence of the BHRF1 pro-survival protein, as they have previously been reported to be heavily methylated in latency types I and II, but active in type III [4]. The most original finding of this work is the induction seen in BHRF1 miRNAs in NPC tumors when applying standard chemotherapeutic agents, like cisplatin and paclitaxel, already used. Their detection in the plasma could be a biomarker of good response, thus not being a unique feature of demethylating agents, like 5-azacytidine and 5-aza-2'deoxycitidine. However, it is obvious that further studies have to be conducted towards that aspect and, if validated, this has to be confirmed at the level of plasma coming from patients undergoing treatment.

Acknowledgements

We would like to sincerely thank Celgene for funding the project and providing 5-azacytidine, as well as Exiqon miRNA platform for the custom-made EBV miRNA panels and their contribution to the analysis of the results from the initial two-week treatment. Nikiforos-Ioannis Kapetanakis is the recipient of a PhD scholarship from the French Ministry of Higher Education and Research (MESR).

Conflict of interest

The authors declare no conflict of interest.

References

1. Cancer incidence in five continents. Volume VIII. IARC Sci Publ. 2002; (155):1-781.

2. Chang ET and Adami HO. The enigmatic epidemiology of nasopharyngeal carcinoma. Cancer Epidemiol Biomarkers Prev. 2006; 15(10):1765-1777.

3. Lo KW, Chung GT and To KF. Deciphering the molecular genetic basis of NPC through molecular, cytogenetic, and epigenetic approaches. Semin Cancer Biol. 2012; 22(2):79-86.

4. Kim DN and Lee SK. Biogenesis of Epstein-Barr virus microRNAs. Mol Cell Biochem. 2012; 365(1-2):203-210.

5. Yang HJ, Huang TJ, Yang CF, Peng LX, Liu RY, Yang GD, Chu QQ, Huang JL, Liu N, Huang HB, Zhu ZY, Qian CN and Huang BJ. Comprehensive profiling of Epstein-Barr virus-encoded miRNA species associated with specific latency types in tumor cells. Virol J. 2013; 10:314.

6. Chen HL, Lung MM, Sham JS, Choy DT, Griffin BE and Ng MH. Transcription of BamHI-A region of the EBV genome in NPC tissues and B cells. Virology. 1992; 191(1):193-201.

7. Marquitz AR and Raab-Traub N. The role of miRNAs and EBV BARTs in NPC. Semin Cancer Biol. 2012; 22(2):166-172.

8. Gourzones C, Gelin A, Bombik I, Klibi J, Verillaud B, Guigay J, Lang P, Temam S, Schneider V, Amiel C, Baconnais S, Jimenez AS and Busson P. Extra-cellular release and blood diffusion of BART viral micro-RNAs produced by EBV-infected nasopharyngeal carcinoma cells. Virol J. 2010; 7:271.

9. Xing L and Kieff E. Epstein-Barr virus BHRF1 micro- and stable RNAs during latency III and after induction of replication. J Virol. 2007; 81(18):9967-9975.

10. Oker N, Kapetanakis N-I and Busson P. (2016). Review: Biological and Pharmacological Basis of Cytolytic Viral Activation in EBV-Associated Nasopharyngeal Carcinoma. In: Ongradi J, ed. Herpesviridae. (Rijeka: InTech), pp. Ch. 06.

11. Cheung ST, Huang DP, Hui AB, Lo KW, Ko CW, Tsang YS, Wong N, Whitney BM and Lee JC. Nasopharyngeal carcinoma cell line (C666-1) consistently harbouring Epstein-Barr virus. Int J Cancer. 1999; 83(1):121-126.

12. Xiao K, Yu Z, Li X, Tang K, Tu C, Qi P, Liao Q, Chen P, Zeng Z, Li G and Xiong W. Genome-wide Analysis of Epstein-Barr Virus (EBV) Integration and Strain in C666-1 and Raji Cells. J Cancer. 2016; 7(2):214-224.

13. Busson P, Ganem G, Flores P, Mugneret F, Clausse B, Caillou B, Braham K, Wakasugi H, Lipinski M and Tursz T. Establishment and characterization of three transplantable EBV-containing nasopharyngeal carcinomas. Int J Cancer. 1988; 42(4):599-606.

14. Kelly GL, Long HM, Stylianou J, Thomas WA, Leese A, Bell AI, Bornkamm GW, Mautner J, Rickinson AB and Rowe M. An Epstein-Barr virus anti-apoptotic protein constitutively expressed in transformed cells and implicated in burkitt lymphomagenesis: the Wp/BHRF1 link. PLoS Pathog. 2009; 5(3):e1000341.

15. Livak KJ and Schmittgen TD. Analysis of relative gene expression data using real-time quantitative PCR and the 2(-Delta Delta C(T)) Method. Methods. 2001; 25(4):402-408.

16. Gourzones C, Ferrand FR, Amiel C, Verillaud B, Barat A, Guerin M, Gattolliat CH, Gelin A, Klibi J, Chaaben AB, Schneider V, Guemira F, Guigay J, Lang P, Jimenez-Pailhes AS and Busson P. Consistent high concentration of the viral microRNA BART17 in plasma samples from nasopharyngeal carcinoma patients--evidence of non-exosomal transport. Virol J. 2013; 10:119.

17. Rowe M, Rowe DT, Gregory CD, Young LS, Farrell PJ, Rupani H and Rickinson AB. Differences in B cell growth phenotype reflect novel patterns of Epstein-Barr virus latent gene expression in Burkitt's lymphoma cells. Embo J. 1987; 6(9):2743-2751.

18. Mauser A, Saito S, Appella E, Anderson CW, Seaman WT and Kenney S. The Epstein-Barr virus immediate-early protein BZLF1 regulates p53 function through multiple mechanisms. J Virol. 2002; 76(24):12503-12512.

19. Kvansakul M, Wei AH, Fletcher JI, Willis SN, Chen L, Roberts AW, Huang DC and Colman PM. Structural basis for apoptosis inhibition by Epstein-Barr virus BHRF1. PLoS Pathog. 2010; 6(12):e1001236.

20. Flatau E, Gonzales FA, Michalowsky LA and Jones PA. DNA methylation in 5-aza-2'-deoxycytidine-resistant variants of C3H 10T1/2 C18 cells. Mol Cell Biol. 1984; 4(10):2098-2102.

21. Momparler RL, Rossi M, Bouchard J, Vaccaro C, Momparler LF and Bartolucci S. Kinetic interaction of 5-AZA-2'-deoxycytidine-5'-monophosphate and its 5'-triphosphate with deoxycytidylate deaminase. Mol Pharmacol. 1984; 25(3):436-440.

22. Jiang W, Li YQ, Liu N, Sun Y, He QM, Jiang N, Xu YF, Chen L and Ma J. 5-

Azacytidine enhances the radiosensitivity of CNE2 and SUNE1 cells in vitro and in vivo possibly by altering DNA methylation. PLoS One. 2014; 9(4):e93273.

23. Chan AT, Tao Q, Robertson KD, Flinn IW, Mann RB, Klencke B, Kwan WH, Leung TW, Johnson PJ and Ambinder RF. Azacitidine induces demethylation of the Epstein-Barr virus genome in tumors. J Clin Oncol. 2004; 22(8):1373-1381.

24. Zhang G, Zong J, Lin S, Verhoeven RJ, Tong S, Chen Y, Ji M, Cheng W, Tsao SW, Lung M, Pan J and Chen H. Circulating Epstein-Barr virus microRNAs miR-BART7 and miR-BART13 as biomarkers for nasopharyngeal carcinoma diagnosis and treatment. Int J Cancer. 2015; 136(5):E301-312.

25. Li Y, Long X, Huang L, Yang M, Yuan Y, Wang Y, Delecluse HJ and Kuang E. Epstein-Barr Virus BZLF1-Mediated Downregulation of Proinflammatory Factors Is Essential for Optimal Lytic Viral Replication. J Virol. 2015; 90(2):887-903.

26. Li L, Su X, Choi GC, Cao Y, Ambinder RF and Tao Q. Methylation profiling of Epstein-Barr virus immediate-early gene promoters, BZLF1 and BRLF1 in tumors of epithelial, NK- and B-cell origins. BMC Cancer. 2012; 12:125.

27. Li Z, Chen X, Li L, Liu S, Yang L, Ma X, Tang M, Bode AM, Dong Z, Sun L and Cao Y. EBV encoded miR-BHRF1-1 potentiates viral lytic replication by downregulating host p53 in nasopharyngeal carcinoma. Int J Biochem Cell Biol. 2012; 44(2):275-279.

Supplementary data

Figures 1a-1d: Heat maps showing the variation of all the viral miRNAs studied in the tumor and the plasma after two weeks of treatment with 1 mg/kg and 2 mg/kg of 5-azacytidine, compared to control mice which received the vehicle alone (PBS). Three mice per condition were analyzed. The Ct for a given miRNA target was normalized for each tumor or plasma sample by the mean Ct of 3 human miRNAs with minimal variation among the different conditions (miR-103a-3p, miR-191-5p and miR-200b-3p) for the same sample (ΔCt). The standard deviation of the Ct values of the 3 reference miRNAs did not exceed 0.7. The mean ΔCt of the 3 mice from each condition was calculated and normalized by the mean ΔCt of the control group (ΔΔCt). The presented $2^{-\Delta\Delta Ct}$ values represent the fold-change of the miRNAs based on their baseline expression (control group).

Tumor

Target in Tumor	C15		
$2^{-\Delta\Delta Ct}$ values	Control	1 mg/kg	2 mg/kg
ebv-eber123-5p_2	1	0,98	0,95
ebv-miR-BART10-3p	1	0,77	0,76
ebv-miR-BART10-5p	1	0,86	0,61
ebv-miR-BART11-3p	1	0,87	0,75
ebv-miR-BART11-5p	1	0,91	0,75
ebv-miR-BART12	1	0,80	0,68
ebv-miR-BART13-3p	1	0,87	0,67
ebv-miR-BART13-5p	1	731,60	189,90
ebv-miR-BART1-3p	1	0,94	0,82
ebv-miR-BART14-3p	1	0,87	0,76
ebv-miR-BART14-5p	1	0,87	0,75
ebv-miR-BART15	1	0,96	0,93
ebv-miR-BART1-5p	1	0,95	0,83
ebv-miR-BART16	1	0,80	0,69
ebv-miR-BART17-3p	1	0,94	0,83
ebv-miR-BART17-5p	1	1,00	0,77
ebv-miR-BART18-5p	1	0,87	0,72
ebv-miR-BART19-5p	1	0,91	0,73
ebv-miR-BART20-5p	1	0,57	0,59
ebv-miR-BART21-5p	1	0,89	0,71
ebv-miR-BART22	1	1,00	0,74
ebv-miR-BART2-3p	1	0,86	0,83
ebv-miR-BART2-5p	1	0,86	0,69
ebv-miR-BART3-3p	1	0,86	0,80
ebv-miR-BART3-5p	1	0,90	0,77
ebv-miR-BART4-3p	1	0,98	0,96
ebv-miR-BART4-5p	1	0,90	0,80
ebv-miR-BART5-3p	1	0,85	0,81
ebv-miR-BART5-5p	1	1,00	0,83
ebv-miR-BART6-3p	1	1,10	0,86
ebv-miR-BART6-5p	1	0,99	0,78
ebv-miR-BART7-3p	1	0,93	0,75
ebv-miR-BART7-5p	1	0,90	0,67
ebv-miR-BART8-3p	1	0,80	0,85
ebv-miR-BART8-5p	1	0,80	0,80
ebv-miR-BART9-3p	1	0,94	0,78
ebv-miR-BART9-5p	1	0,88	0,73
ebv-miR-BHRF1-1	1	0,82	2,90
ebv-miR-BHRF1-2-3p	1	3,39	31,20
ebv-miR-BHRF1-2-5p	1	1,06	5,33
ebv-miR-BHRF1-3	1	3,15	9,40

Plasma

Target in Plasma	C15		
$2^{-\Delta\Delta Ct}$ values	Control	1 mg/kg	2 mg/kg
ebv-eber123-5p_2	1	3,09	2,10
ebv-miR-BART10-3p	1	0,51	0,19
ebv-miR-BART10-5p	1	0,20	0,21
ebv-miR-BART11-3p	1	0,60	0,18
ebv-miR-BART11-5p	1	0,49	0,04
ebv-miR-BART12	1	0,43	0,20
ebv-miR-BART13-3p	1	0,56	0,15
ebv-miR-BART13-5p	1	0,44	0,53
ebv-miR-BART1-3p	1	0,84	0,34
ebv-miR-BART14-3p	1	1,03	0,37
ebv-miR-BART14-5p	1	0,69	0,18
ebv-miR-BART15	1	0,72	0,18
ebv-miR-BART1-5p	1	0,74	0,28
ebv-miR-BART16	1	0,61	0,72
ebv-miR-BART17-3p	1	0,83	0,30
ebv-miR-BART17-5p	1	1,02	0,33
ebv-miR-BART18-5p	1	0,89	0,41
ebv-miR-BART19-5p	1	0,61	0,16
ebv-miR-BART20-5p	1	0,43	0,12
ebv-miR-BART21-5p	1	0,80	0,20
ebv-miR-BART22	1	0,01	0,74
ebv-miR-BART2-3p	1	0,59	0,12
ebv-miR-BART2-5p	1	0,70	0,19
ebv-miR-BART3-3p	1	0,59	0,10
ebv-miR-BART3-5p	1	0,51	0,22
ebv-miR-BART4-3p	1	0,77	0,20
ebv-miR-BART4-5p	1	0,60	0,20
ebv-miR-BART5-3p	1	0,58	0,17
ebv-miR-BART5-5p	1	0,66	0,16
ebv-miR-BART6-3p	1	0,66	0,03
ebv-miR-BART6-5p	1	0,73	0,14
ebv-miR-BART7-3p	1	0,62	0,16
ebv-miR-BART7-5p	1	0,98	0,09
ebv-miR-BART8-3p	1	0,76	0,22
ebv-miR-BART8-5p	1	0,57	0,26
ebv-miR-BART9-3p	1	1,13	0,40
ebv-miR-BART9-5p	1	0,73	0,15
ebv-miR-BHRF1-1	1	1,64	0,30
ebv-miR-BHRF1-2-3p	1	1,42	1,38
ebv-miR-BHRF1-2-5p	1	0,58	1,17
ebv-miR-BHRF1-3	1	0,87	2,29

Detection	Reduced	Unchanged	Increased

Figure 1a: Variation of the viral miRNAs in C15 tumors and plasma from the engrafted mice after 2 weeks of treatment.

Tumor

Target in Tumor	C666-1		
$2^{-\Delta\Delta Ct}$ values	Control	1 mg/kg	2 mg/kg
ebv-eber123-5p_2	1	0,62	0,62
ebv-miR-BART10-3p	1	1,01	0,67
ebv-miR-BART10-5p	1	0,75	0,62
ebv-miR-BART11-3p	1	0,91	0,72
ebv-miR-BART11-5p	1	0,87	0,73
ebv-miR-BART12	1	0,86	0,72
ebv-miR-BART13-3p	1	0,75	0,66
ebv-miR-BART13-5p	1	0,02	0,03
ebv-miR-BART1-3p	1	0,83	0,69
ebv-miR-BART14-3p	1	0,92	0,71
ebv-miR-BART14-5p	1	0,93	0,77
ebv-miR-BART15	1	1,03	0,83
ebv-miR-BART1-5p	1	0,84	0,70
ebv-miR-BART16	1	0,78	0,69
ebv-miR-BART17-3p	1	0,81	0,65
ebv-miR-BART17-5p	1	0,78	0,58
ebv-miR-BART18-5p	1	0,81	0,69
ebv-miR-BART19-5p	1	0,74	0,60
ebv-miR-BART20-5p	1	0,76	0,49
ebv-miR-BART21-5p	1	0,96	0,82
ebv-miR-BART22	1	0,94	0,71
ebv-miR-BART2-3p	1	0,82	0,63
ebv-miR-BART2-5p	1	0,77	0,66
ebv-miR-BART3-3p	1	0,89	0,79
ebv-miR-BART3-5p	1	0,86	0,64
ebv-miR-BART4-3p	1	0,93	0,77
ebv-miR-BART4-5p	1	0,87	0,67
ebv-miR-BART5-3p	1	0,70	0,63
ebv-miR-BART5-5p	1	0,90	0,77
ebv-miR-BART6-3p	1	0,81	0,76
ebv-miR-BART6-5p	1	0,93	0,77
ebv-miR-BART7-3p	1	0,72	0,63
ebv-miR-BART7-5p	1	0,78	0,76
ebv-miR-BART8-3p	1	0,97	0,68
ebv-miR-BART8-5p	1	0,98	0,58
ebv-miR-BART9-3p	1	0,81	0,69
ebv-miR-BART9-5p	1	0,73	0,70
ebv-miR-BHRF1-1	1	66,59	120,79
ebv-miR-BHRF1-2-3p	1	36,65	33,81
ebv-miR-BHRF1-2-5p	1	6,93	20,65
ebv-miR-BHRF1-3	1	9,85	33,12

Plasma

Target in Plasma	C666-1		
$2^{-\Delta\Delta Ct}$ values	Control	1 mg/kg	2 mg/kg
ebv-eber123-5p_2	1	3,09	5,11
ebv-miR-BART10-3p	1	0,45	0,27
ebv-miR-BART10-5p	1	0,43	0,19
ebv-miR-BART11-3p	1	0,49	0,32
ebv-miR-BART11-5p	1	0,25	0,10
ebv-miR-BART12	1	0,50	0,33
ebv-miR-BART13-3p	1	0,38	0,21
ebv-miR-BART13-5p	1	0,67	1,46
ebv-miR-BART1-3p	1	0,62	0,48
ebv-miR-BART14-3p	1	0,61	0,37
ebv-miR-BART14-5p	1	0,47	0,29
ebv-miR-BART15	1	0,52	0,28
ebv-miR-BART1-5p	1	0,54	0,33
ebv-miR-BART16	1	0,37	0,22
ebv-miR-BART17-3p	1	0,62	0,40
ebv-miR-BART17-5p	1	0,52	0,35
ebv-miR-BART18-5p	1	0,52	0,22
ebv-miR-BART19-5p	1	0,39	0,16
ebv-miR-BART20-5p	1	0,35	0,18
ebv-miR-BART21-5p	1	0,48	0,31
ebv-miR-BART22	1	23,75	1,95
ebv-miR-BART2-3p	1	0,31	0,18
ebv-miR-BART2-5p	1	0,50	0,27
ebv-miR-BART3-3p	1	0,45	0,32
ebv-miR-BART3-5p	1	1,05	0,30
ebv-miR-BART4-3p	1	0,55	0,35
ebv-miR-BART4-5p	1	0,53	0,33
ebv-miR-BART5-3p	1	0,46	0,17
ebv-miR-BART5-5p	1	0,37	0,21
ebv-miR-BART6-3p	1	0,47	0,21
ebv-miR-BART6-5p	1	0,51	0,30
ebv-miR-BART7-3p	1	0,41	0,20
ebv-miR-BART7-5p	1	0,60	0,20
ebv-miR-BART8-3p	1	0,60	0,32
ebv-miR-BART8-5p	1	0,62	0,23
ebv-miR-BART9-3p	1	0,67	0,39
ebv-miR-BART9-5p	1	0,46	0,22
ebv-miR-BHRF1-1	1	47,59	197,96
ebv-miR-BHRF1-2-3p	1	5,52	12,14
ebv-miR-BHRF1-2-5p	1	2,81	2,25
ebv-miR-BHRF1-3	1	2,27	31,11

Detection	Reduced	Unchanged	Increased

Figure 1b: Variation of the viral miRNAs in C666-1 tumors and plasma from the engrafted mice after 2 weeks of treatment.

Tumor

Target in Tumor	C18		
$2^{-\Delta\Delta Ct}$ values	Control	1 mg/kg	2 mg/kg
ebv-eber123-5p_2	1	1,09	1,43
ebv-miR-BART10-3p	1	1,16	2,45
ebv-miR-BART10-5p	1	1,16	2,07
ebv-miR-BART11-3p	1	1,50	2,61
ebv-miR-BART11-5p	1	1,38	2,66
ebv-miR-BART12	1	1,18	2,29
ebv-miR-BART13-3p	1	0,97	1,82
ebv-miR-BART13-5p	1	1,75	2,04
ebv-miR-BART1-3p	1	1,43	2,95
ebv-miR-BART14-3p	1	1,78	2,51
ebv-miR-BART14-5p	1	1,24	2,74
ebv-miR-BART15	1	1,34	2,68
ebv-miR-BART1-5p	1	1,50	2,55
ebv-miR-BART16	1	1,27	2,21
ebv-miR-BART17-3p	1	1,40	2,96
ebv-miR-BART17-5p	1	1,77	3,26
ebv-miR-BART18-5p	1	1,41	2,94
ebv-miR-BART19-5p	1	1,71	3,42
ebv-miR-BART20-5p	1	1,91	4,29
ebv-miR-BART21-5p	1	1,86	3,51
ebv-miR-BART22	1	1,47	3,09
ebv-miR-BART2-3p	1	1,64	2,53
ebv-miR-BART2-5p	1	1,42	2,66
ebv-miR-BART3-3p	1	1,07	1,66
ebv-miR-BART3-5p	1	1,82	2,84
ebv-miR-BART4-3p	1	1,37	2,33
ebv-miR-BART4-5p	1	1,51	2,92
ebv-miR-BART5-3p	1	0,85	1,72
ebv-miR-BART5-5p	1	1,48	2,75
ebv-miR-BART6-3p	1	1,27	2,64
ebv-miR-BART6-5p	1	1,54	3,07
ebv-miR-BART7-3p	1	1,51	2,75
ebv-miR-BART7-5p	1	1,39	2,33
ebv-miR-BART8-3p	1	1,29	2,64
ebv-miR-BART8-5p	1	1,50	3,31
ebv-miR-BART9-3p	1	1,33	3,22
ebv-miR-BART9-5p	1	1,60	2,96
ebv-miR-BHRF1-1	1	1,25	2,79
ebv-miR-BHRF1-2-3p	1	2,09	5,01
ebv-miR-BHRF1-2-5p	1	4,05	2,41
ebv-miR-BHRF1-3	1	9,60	15,53

Plasma

Target in Plasma	C18		
$2^{-\Delta\Delta Ct}$ values	Control	1 mg/kg	2 mg/kg
ebv-eber123-5p_2	1	1,09	1,69
ebv-miR-BART10-3p	1	0,68	1,86
ebv-miR-BART10-5p	1	2,68	9,66
ebv-miR-BART11-3p	1	0,82	1,46
ebv-miR-BART11-5p	1	0,29	1,17
ebv-miR-BART12	1	1,13	2,29
ebv-miR-BART13-3p	1	0,88	2,15
ebv-miR-BART13-5p	1	1,01	3,39
ebv-miR-BART1-3p	1	0,31	0,79
ebv-miR-BART14-3p	1	1,16	0,91
ebv-miR-BART14-5p	1	3,03	2,83
ebv-miR-BART15	1	1,08	2,51
ebv-miR-BART1-5p	1	0,72	0,92
ebv-miR-BART16	1	1,76	1,26
ebv-miR-BART17-3p	1	2,31	18,68
ebv-miR-BART17-5p	1	0,17	0,93
ebv-miR-BART18-5p	1	0,66	1,33
ebv-miR-BART19-5p	1	0,98	1,86
ebv-miR-BART20-5p	1	1,90	2,58
ebv-miR-BART21-5p	1	0,14	2,30
ebv-miR-BART22	1	0,25	1,42
ebv-miR-BART2-3p	1	1,94	1,34
ebv-miR-BART2-5p	1	0,73	1,47
ebv-miR-BART3-3p	1	0,55	0,93
ebv-miR-BART3-5p	1	0,89	1,87
ebv-miR-BART4-3p	1	0,19	1,37
ebv-miR-BART4-5p	1	1,10	2,08
ebv-miR-BART5-3p	1	0,35	1,43
ebv-miR-BART5-5p	1	1,04	2,57
ebv-miR-BART6-3p	1	0,86	2,03
ebv-miR-BART6-5p	1	1,42	4,02
ebv-miR-BART7-3p	1	0,54	1,92
ebv-miR-BART7-5p	1	2,51	1,68
ebv-miR-BART8-3p	1	1,09	1,03
ebv-miR-BART8-5p	1	1,13	3,01
ebv-miR-BART9-3p	1	1,39	1,47
ebv-miR-BART9-5p	1	2,65	2,36
ebv-miR-BHRF1-1	1	3,25	2,05
ebv-miR-BHRF1-2-3p	1	0,53	1,22
ebv-miR-BHRF1-2-5p	1	2,75	1,29
ebv-miR-BHRF1-3	1	3,56	3,48

Detection	Reduced	Unchanged	Increased

Figure 1c: Variation of the viral miRNAs in C18 tumors and plasma from the engrafted mice after 2 weeks of treatment.

Tumor

Target in Tumor	C17		
$2^{-\Delta\Delta Ct}$ values	Control	1 mg/kg	2 mg/kg
ebv-eber123-5p_2	1	0,87	1,16
ebv-miR-BART10-3p	1	0,89	1,16
ebv-miR-BART10-5p	1	1,14	1,07
ebv-miR-BART11-3p	1	1,23	1,17
ebv-miR-BART11-5p	1	1	0,85
ebv-miR-BART12	1	0,94	0,92
ebv-miR-BART13-3p	1	1,02	0,76
ebv-miR-BART13-5p	1	0,12	0,11
ebv-miR-BART1-3p	1	1,19	1,16
ebv-miR-BART14-3p	1	1,12	1,08
ebv-miR-BART14-5p	1	0,96	1,06
ebv-miR-BART15	1	1,19	1,03
ebv-miR-BART1-5p	1	1,28	1,11
ebv-miR-BART16	1	1,02	0,93
ebv-miR-BART17-3p	1	1,12	1,06
ebv-miR-BART17-5p	1	1,34	1,21
ebv-miR-BART18-5p	1	0,99	1,01
ebv-miR-BART19-5p	1	1,13	0,92
ebv-miR-BART20-5p	1	0,76	0,66
ebv-miR-BART21-5p	1	1,10	1,19
ebv-miR-BART22	1	1,08	0,99
ebv-miR-BART2-3p	1	0,48	1,27
ebv-miR-BART2-5p	1	0,94	0,93
ebv-miR-BART3-3p	1	1,14	0,87
ebv-miR-BART3-5p	1	1,26	1,21
ebv-miR-BART4-3p	1	0,69	1,44
ebv-miR-BART4-5p	1	1,24	1,13
ebv-miR-BART5-3p	1	4,82	0,79
ebv-miR-BART5-5p	1	1,13	1,12
ebv-miR-BART6-3p	1	1,35	1,29
ebv-miR-BART6-5p	1	1,11	1,03
ebv-miR-BART7-3p	1	1,12	1,06
ebv-miR-BART7-5p	1	0,23	1,38
ebv-miR-BART8-3p	1	1,01	1,23
ebv-miR-BART8-5p	1	0,86	0,91
ebv-miR-BART9-3p	1	0,98	0,98
ebv-miR-BART9-5p	1	1,26	1,05
ebv-miR-BHRF1-1	1	1	1
ebv-miR-BHRF1-2-3p	1	1	1
ebv-miR-BHRF1-2-5p	1	2,43	1
ebv-miR-BHRF1-3	1	1	1

Plasma

Target in Plasma	C17		
$2^{-\Delta\Delta Ct}$ values	Control	1 mg/kg	2 mg/kg
ebv-eber123-5p_2	1	5,61	4,19
ebv-miR-BART10-3p	1	3,73	2,70
ebv-miR-BART10-5p	1	2,42	2,39
ebv-miR-BART11-3p	1	2,13	2,02
ebv-miR-BART11-5p	1	2,34	5,78
ebv-miR-BART12	1	1,63	1,76
ebv-miR-BART13-3p	1	1,96	1,30
ebv-miR-BART13-5p	1	1,02	1,08
ebv-miR-BART1-3p	1	6,69	8,20
ebv-miR-BART14-3p	1	1,82	1,25
ebv-miR-BART14-5p	1	1,05	1,09
ebv-miR-BART15	1	2,23	1,58
ebv-miR-BART1-5p	1	2,32	3,15
ebv-miR-BART16	1	0,43	0,46
ebv-miR-BART17-3p	1	5,53	5,48
ebv-miR-BART17-5p	1	2,42	1,32
ebv-miR-BART18-5p	1	2,95	0,94
ebv-miR-BART19-5p	1	1,48	0,81
ebv-miR-BART20-5p	1	0,63	0,96
ebv-miR-BART21-5p	1	1,06	0,51
ebv-miR-BART22	1	0,86	0,74
ebv-miR-BART2-3p	1	1,29	0,41
ebv-miR-BART2-5p	1	2,55	1,90
ebv-miR-BART3-3p	1	3,87	2,81
ebv-miR-BART3-5p	1	1,62	1,52
ebv-miR-BART4-3p	1	1,44	1,36
ebv-miR-BART4-5p	1	2,19	1,58
ebv-miR-BART5-3p	1	0,32	0,43
ebv-miR-BART5-5p	1	1,42	0,81
ebv-miR-BART6-3p	1	1,72	1,40
ebv-miR-BART6-5p	1	9,05	1,91
ebv-miR-BART7-3p	1	1,67	1,17
ebv-miR-BART7-5p	1	0,10	0,71
ebv-miR-BART8-3p	1	2,53	1,54
ebv-miR-BART8-5p	1	5,59	3,84
ebv-miR-BART9-3p	1	2,45	3,10
ebv-miR-BART9-5p	1	1,80	0,95
ebv-miR-BHRF1-1	1	2,32	2,07
ebv-miR-BHRF1-2-3p	1	1	1
ebv-miR-BHRF1-2-5p	1	1,89	2,13
ebv-miR-BHRF1-3	1	1	1

Detection	Reduced	Unchanged	Increased

Figure 1d: Variation of the viral miRNAs in C17 tumors and plasma from the engrafted mice after 2 weeks of treatment.

Figures 2a-2d: Western blot analysis for the expression of viral latent and lytic proteins in tumors of the mice treated for two weeks. As mentioned in figures 1a-d, three mice from each treatment condition (PBS, 1 mg/kg, 2 mg/kg) were selected for analysis. Among the five mice which received a given condition, we selected the smaller, the larger and a medium tumor. For western blot analysis, the results are presented in triplets by tumor size. The triplets of the small tumors were excluded from the study, as in some cases, due to the limited amount of input material, the results of the protein extraction were of low quality. Extract from the EBV-negative Jurkat cell line was used as a negative control, while a marmoset-derived EBV-infected B95-8 cell line treated by TPA for 24hr was chosen as a positive control.

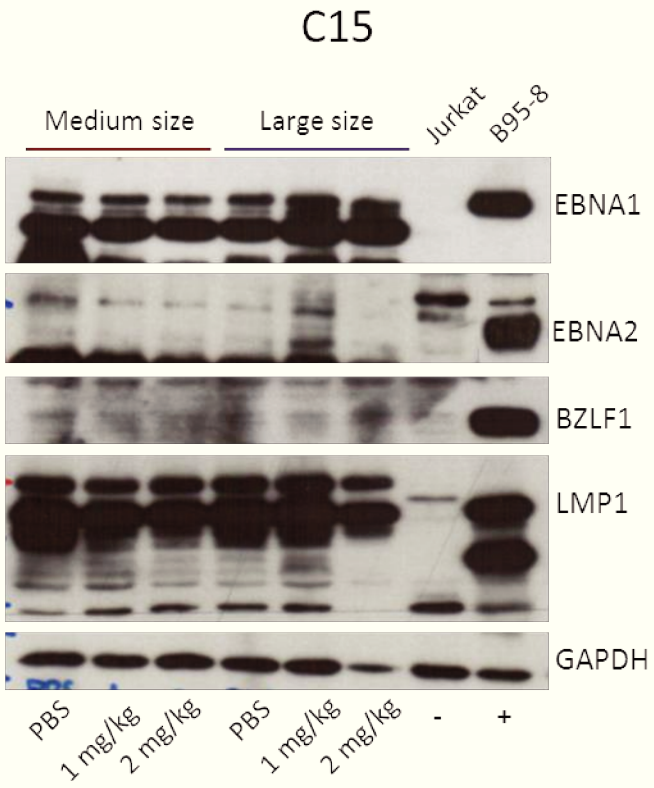

Figure 2a: Expression of latent and lytic EBV proteins in the 3 treatment modalities in C15-engrafted mice, treated for two weeks.

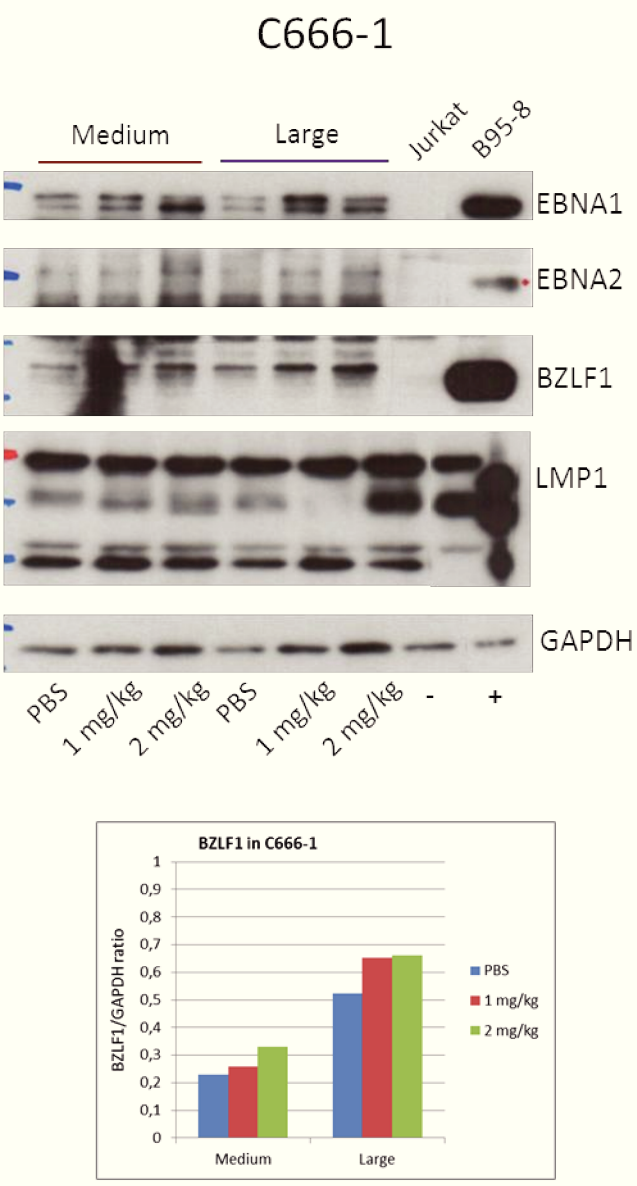

Figure 2b: Expression of latent and lytic EBV proteins in the 3 treatment modalities in C666-1-engrafted mice, treated for two weeks.

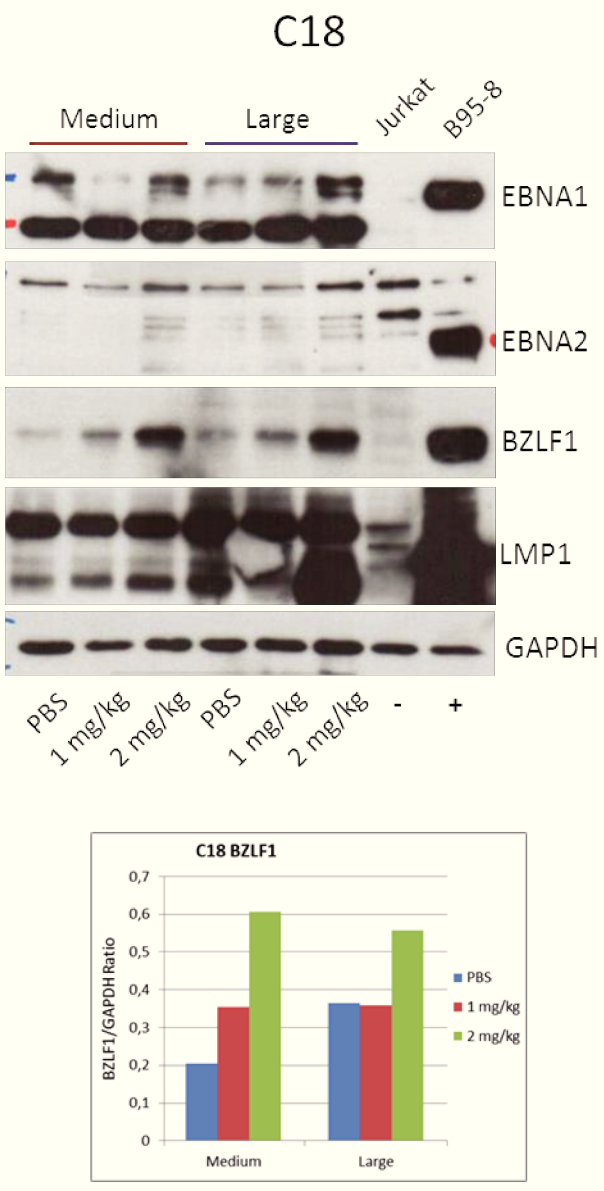

Figure 2c: Expression of latent and lytic EBV proteins in the 3 treatment modalities in C18-engrafted mice, treated for two weeks.

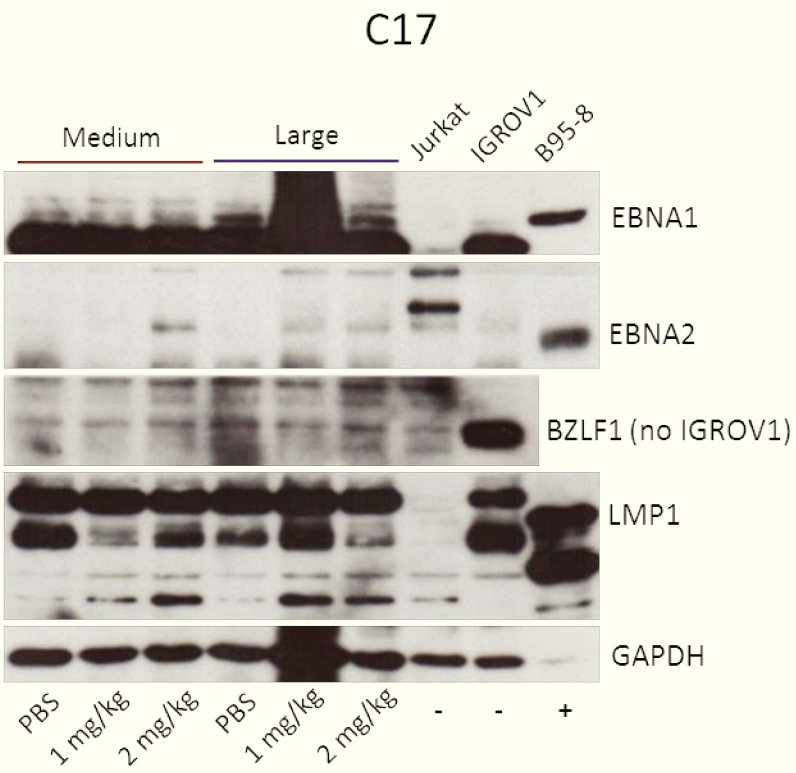

Figure 2d: Expression of latent and lytic EBV proteins in the 3 treatment modalities in C17-engrafted mice, treated for two weeks. For C17 tumors we added one more negative control, derived from an EBV-negative ovarian cell line (IGROV1), engrafted into a nude mouse for 3 weeks without any treatment.

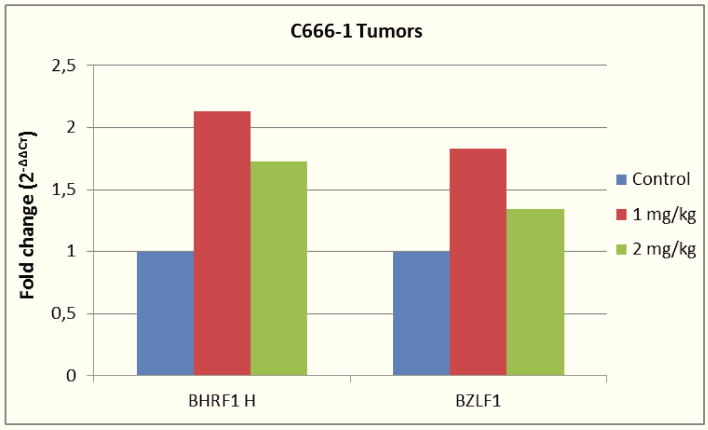

Figure 3: RT-qPCR analysis of the lytic BHRF1 transcript and the mRNA of BZLF1 in the C666-1 tumors treatment for two weeks. For each group, the results were normalized by the expression of GAPDH and compared to the expression of the control group, as explained in the article. The results show a very modest induction of these lytic cycle markers after a two-week treatment with 5-azacytidine.

General discussion and perspectives

Recent works linking circulating miR-200 and ovarian cancer

The first fundamental study on the utility of circulating miRNAs in ovarian cancer diagnosis, prognosis and therapeutics was published by Taylor and Gercel-Taylor back in 2008 [103], having been cited by at least 490 more recent articles (according to PubMed on the 8th of June 2017). This group analyzed exosome-associated miRNAs in the sera of women with various stages of ovarian cancer and women with benign pathologies and reported eight miRNAs to be elevated in ovarian cancer sera, reflecting aberrations at the tumor level, as identified by previous works. The proposed signature consists of miR-21, miR-141, miR-200a, miR-200c, miR-200b, miR-203, miR-205 and miR-214, half of them belonging to the miR-200 family (miR-141, miR-200a, miR-200b, miR-200c). Furthermore, this study was complemented a year later by Xu et al, who profiled the expression of miRNAs in advanced ovarian cancer using a novel PCR-based platform and correlated miRNA expression profiles with disease outcome. This study may not have been on circulating miRNAs, but provided stronger evidence regarding the upregulation of miR-200 members in ovarian cancer. Moreover, they indicated a notable association between one of the two clusters of this family, containing miR-200a, miR-200b and miR-429 and cancer recurrence, as well as overall survival of the patients [308]. Our work confirms these findings concerning miR-200b, suggesting that this deregulation is reflected and detectable in the plasma and could serve as an excellent indicator of imminent recurrence, allowing a quicker reaction. Publications in the last 5 years, many of them simultaneous with our project, further highlight the involvement of miR-200 miRNAs, as well as other miRNAs, in the malignant phenotype of ovarian cancer, suggesting interesting associations with stage, histology and treatment outcome. Regarding their diagnostic potential, Kan et al (2012) presented a signature of four miRNAs (miR-182, miR-200a, miR-200b and miR-200c) which is significantly upregulated in the plasma of serous ovarian cancer patients compared to healthy donors. Taking a step beyond, they suggested a good predictive power of miR-200b and miR-200c together as a discriminative biomarker for serous ovarian cancer [309]. A year later, Zheng et al proposed another miRNA duo in the plasma for diagnosis of early-stage serous ovarian cancer. More precisely, they found that elevated miR-205 and lower let-7f abundance in the plasma compared to healthy subjects were highly consistent with serous epithelial ovarian cancer, even at stage I. Low let-7f was further linked to a poor prognosis at the III-IV stage, as patients with lower levels had a shorter progression-free survival (PFS) that patients with a higher let-7f in their plasma. They

conclude that both miRNAs could complement CA125 for a more accurate diagnosis and a solid prognosis [310]. On the other hand, Zuberi et al (2015) reported that serum miR-200a is significantly upregulated in mucinous ovarian adenocarcinomas rather than in serous [311]. Using a RT-qPCR-based approach and normalizing with U6 RNA serum levels, they demonstrated a 6-fold increase of miR-200a and a 3-fold increase of miR-200b and miR-200c in epithelial ovarian cancer, compared to healthy subjects, highlighting diagnostic and prognostic utility of these miRNAs. Similarly to Zheng et al, Gao et al (2015) started by validating overexpression of miR-141 and miR-200c in the serum of ovarian cancer patients versus disease-free subjects. The group went deeper to suggest that a comparative higher detection of miR-200c and lower detection of miR-141 correlate with an improved short-term and long-term survival rate respectively [312]. Xu et al (2013) focused on miR-21, highlighting that a higher detection in the serum of ovarian cancer patients upon diagnosis is a prognostic indictor of high tumor grade and shorter overall survival (OS) [313].

As soon as a larger cohort is available in order to produce more solid results with a lower risk of biases, a ROC curve and a new Cox regression model should be constructed including the totality of the results, in order to assess the sensitivity, specificity and clinical value of miR-200b as a predictive biomarker and better define the values' width characterizing healthy subjects, benign cases and ovarian carcinomas. In the absence of a new cohort of patients for validation studies, our work on miR-200b has been significantly backed and complemented last year by two highly similar publications from the group of Dr Heidi Schwarzenbach in Hamburg, Germany, in two distinct series of serum samples, coming from ovarian cancer patients, patients with benign ovarian diseases and healthy women [314, 315]. This group followed a workflow similar to ours, regarding the collection of the samples and the organization of their analysis. Their RT-qPCR approach was done using quantitative TaqMan MicroRNA Assays, based on specific reverse transcription of the target of interest and not universal reverse-transcription, as we performed. The subsequent amplification was done on the basis of detected fluorescence emitted by a miRNA-specific probe, attached to the target between the selected primers. As a reminder, SYBR Green fluorescence is not target specific, as it is proportional to the quantity of newly generated DNA during the amplification [316]. In these works, Meng et al compared the abundance of miR-200a, miR-200b, miR-200c and miR-373 in the serum of these three groups, prompted by the previously reported cancer-specific characteristics of the miR-200 family members [317, 318], as well as the suggested association of circulating exosomal miR-373 with aggressive triple-negative breast cancer

[319]. In both publications, they showed the significantly increased detection of these 4 miRNAs in ovarian cancer samples, drawing attention to the triplet miR-200a/b/c, which was able to distinguish malignant from benign cases. Interestingly, they highlighted a selective rise of miR-200b and miR-200c in the serum of patients with advanced disease (FIGO III-IV), compared with early disease (FIGO I-II), suggesting that these two miRNAs may be actively involved in tumor progression. In the end, they provided evidence that miR-200b and miR-200c correlate with CA125 in the serum, as well as with a shorter PFS. MiR-200b was even more significantly linked to the duration of the PFS than miR-200c (p value 0.007 versus 0.017). This work completes our findings, suggesting that, even from the pre-treatment level, miR-200b can provide precious information regarding the evolution of the disease. The reported pre-treatment correlation of miR-200b with CA125 presents a contradiction to our findings, as CA125 reflected disease stage, but we were not able to see a similar correlation for miR-200b. Given the limited capacity of our cohort, one hypothesis could be that a larger cohort could potentially allow exceeding the limits of statistical significance, making the creation of a new collection a priority. Concerning the overexpression mainly of miR-200b and miR-200c in cases of advanced disease, a brilliant review published by Koutsaki et al last month (June 2017) focused on miR-200 in ovarian cancer, suggesting that it reflects the EMT status of tumors at a given stage [320]. As discussed, miR-200 overexpression seems to correlate with disease progression rather that initiation and is linked to the epithelial/mesenchymal balance of the cells (implication and role of miR-200 miRNAs explained in the section "MiRNAs in the tumorigenesis of ovarian cancer" of the introduction). A congruent pattern was observed for E-Cadherin, which was abundant in early stages but low in late-stage tumors. According to their conclusions, in the early stages, malignant cells undergo EMT (low miR-200 expression) in order to acquire a more invasive phenotype. In contrast, "when cells reach their metastatic sites, they tend to lose their invasive characteristics and re-epithelialization occurs". Thus, late-stage disease is characterized by low EMT, potentially replaced by MET (mesenchymal-to-epithelial transition), so with higher levels of miR-200 family members.

It is worth noting that these works focus on the pre-treatment status of miRNAs, not attempting a sequential approach during treatment or follow-up of the disease. Even almost two years after its publication, our work remains original given its alternative approach and the observation of the evolution of a biomarker in parallel with disease surveillance. Benson et al (2015), adopting this approach, shed some light onto another promising aspect of

circulating miRNAs, as they showed that kinetics of miR-148b-5p during a pilot treatment with carboplatin and 5-aza-2'-deoxycytidine (decitabine) was an indicator of tumor response, as a decrease represented a worse clinical outcome with a shorter PFS [321].

Major issues in the research of circulating biomarkers

Up to date, our article has been cited by three groups [322-324], contributing to a better understanding of the power of circulating miRNAs to serve as useful biomarkers. Multiplying publications on circulating miRNAs repeatedly point towards their strength and utility in the clinic when it comes to cancer treatment and monitoring. However, such serum or plasma signatures have not yet entered the clinic. This is mostly due to the lack of reproducibility of the published results. In our work, we were not able to confirm a significant upregulation of miR-21 and miR-205 in the plasma of ovarian cancer patients, despite various works pointing towards the opposite. For instance, Vaksmann et al (2014) reported a significant correlation between elevated circulating miR-21 and a low progression-free and overall survival [325]. In a recent publication, Au Yeung et al (2016) identified significantly higher levels of miR-21 in exosomes of ovarian cancer patients, showing that exosome-delivered miR-21 suppresses ovarian cancer apoptosis and confers chemoresistance by binding to its direct novel target, APAF1, thus actively contributing to the malignant phenotype of metastatic ovarian cancer [326]. MiR-205 on the other hand acts as an oncogene by modulating the expression of multiple cancer-related target genes [327]. Zheng et al (2013), as previously said, suggested that higher plasma concentration of miR-205, along with a lower concentration of let-7f compared to control subjects, could make a reliable biomarker for early-stage ovarian cancer detection [310]. These works were characterized by a larger scale, with a much larger number of inducted patients, making them statistically more solid than our analysis. Given the fact that a considerable part of our tested samples exhibited indeed concordant profiles, it is highly probable that a larger cohort of samples would have added statistical significance to these findings. Other important reasons behind such divergences are the lack of a harmonized method for extraction and quantification, as well as the difficulty to establish a universal reference for data normalization. The fundamental factors to be respected in this field are presented by Marabita et al (2016) in a recent publication [328]. In order to minimize technical variations, one should collect and keep the samples under homogeneous conditions, avoiding repeated freeze-thaw cycles, which favor RNA degradation. Furthermore, batch effects should be reduced, avoiding for example different experiment days, laboratory conditions, reagent lots or operators. Whereas qPCR-based methods are widely used, it is yet

unresolved how the data should be normalized. As a consequence, contradictions are constantly observed among published works. A synthetic RNA for technical normalization could potentially assure minimal technical variation. The efficiency of RNA extraction, complementary DNA synthesis and PCR amplification can be monitored using an exogenous synthetic miRNA (for example, Caenorhabditis elegans cel-miR-39 or Arabidopsis thaliana ath-miR-159a), which are added as spike-in control during processing. When added to the lysis buffer during the extraction step, the synthetic RNA will be put through the same conditions as the endogenous miRNAs, hence providing a process control. Although an exogenous reference could be of great use, it cannot correct other variability parameters, as for example the total concentration of the miRNA fraction in serum/plasma, which is likely changing inter-individually and/or in a disease-associated fashion. For a comprehensive normalization protocol, endogenous controls are required, either using global high-throughput-derived parameters (i.e. mean expression value per sample) or selected, validated stable reference miRNAs for focused assays. Researchers may often use miRNAs supposed to have an unchanged expression profile in the cancer of interest, which is proposed by others as a diagnostic or prognostic biomarker for the same cancer. Examples include miR-16 and miR-191, commonly used as endogenous references, but found in some works to be representative of malignant pathologies, like endometriosis-associated ovarian cancer [329]. Choosing the right reference for data normalization is one of the biggest challenges in circulating biomarker research and discovery. Many groups have proposed different approaches in order to find the proper candidate(s), however we are still far from applying a universal, widely accepted method [328]. In the first article, we attempted to evaluate 3 miRNAs used as endogenous references, after excluding miR-16 and miR-451 because of their already mentioned dependence on the degree of hemolysis in a sample. We evaluated miR-132-3p, miR-23a-5p and miR-191-5p, already used in previous publications [329, 330]. As presented in the supplementary data of the article, the first showed inconsistent detection among the samples, while the second presented a significant variation in the plasma of ovarian cancer patients (based on ANOVA analysis). On the other hand, miR-191-5p had a non-significant variation and a globally stable expression among the tested groups, being the best candidate for normalization. In a wider study, it should be more reliable to combine different candidates for normalization, or even the mean values of the totality of the tested targets to normalize differential variation of the targets. With this idea in mind, we included a limited group of human miRNAs in the analysis of the viral miRnome in the second article, in order to choose the best candidates and eventually combine them. Indeed, miR-103a-3p, miR-191-5p and

miR-200b-3p were the ones to show low variation, which was even lower when the mean values of all three of them were used. These results provided a common normalization tool, independent of the viral expression or the NPC-related characteristics of the models used (C15, C666-1, C17 and C18). Although having found a relatively constant parameter to normalize our data obtained from the two-week treatment, we did not use the same human miRNAs to normalize the results of the one-week treatment. Having a restricted budget, we chose to use a single endogenous reference, the U6 spliceosomal RNA, a small non-coding RNA component of the spliceosome. Although this snRNA yielded excellent results (good detection, insignificant variation among samples), it is obvious that changing of the normalization method affects the reliability and the homogeneity of the presented experimental work. A globally growing trend which might become the golden standard in data normalization in the following years is the use of the average value of all the miRNAs included in a study. This approach bypasses the need to find distinct endogenous references, while directly highlighting the differential expression of a miRNA of interest compared to the entire pool of tested miRNAs [331]. Accumulating results like the ones presented here regarding the miR-200 family and the BHRF1 miRNAs help strengthening the idea of using circulating miRNAs in the clinic, while constantly improving methodologies will definitely offer exciting solutions to the existing problems, accelerating research yield.

Novel quantification technologies

An existing powerful tool for miRNA quantification compatible with serum and plasma samples is the nCounter miRNA assay, developed by Nanostring. This technique, based on a micro-array approach, allows simultaneous profiling of 800 human miRNAs. However, its inability to be adapted for a limited number of target miRNAs maintains its cost at very high levels. Towards this goal of seeking new methodological approaches, our group has initiated a multicenter collaboration aiming to the parallel assessment of newly-developed promising technical approaches. These techniques are designed for the detection and quantification of circulating microRNAs and their efficacy will be compared not only among them, but also with the results of the standard quantitative real-time PCR, routinely used. The common project already launched will involve in the first place 20 pairs of sequential plasma samples, provided by ovarian cancer patients from the Exoplasma initiative (see comment for article 1). The samples were taken before any treatment, at the moment of the diagnostic coelioscopy, and upon completion of the first-line (primary) treatment, including aggressive cytoreductive surgery and chemotherapy (adjuvant and often also neo-adjuvant). The techniques that are

being evaluated are the droplet-digital PCR (ddPCR), the cytometry-based Firefly miRNA assay and a multiplexed miRNA FRET assay currently on development in the group of Niko Hildebrandt (Institut de Biologie Intégrative de la Cellule, Université Paris-Sud). These techniques aim to address and resolve major issues in the detection of circulating nucleic acids, such as the lack of homogeneity, the existence of numerous steps and the normalization of the obtained results.

- Droplet-digital PCR (ddPCR)

In collaboration with Dr Manoel Nunes from the Pharmacogenetics and Translational Medicine Department of Sanofi, we are currently evaluating the sensitivity of ddPCR. This technique has been developed in the last five years and commercialized by Bio-Rad and allows a passage from relative (qPCR) to absolute quantification of nucleic acids, including miRNAs, after a reverse transcription step for RNAs. The basis of ddPCR is the use of a water-oil emulsion allowing the separation of the 20 µl-reaction mix to 20000 nanodroplets, completely uniform in size and volume, of 1 nanoliter each [332]. After the separation step, the emulsified reaction samples are transferred to a 96-well plate and qPCR amplification is performed in every generated droplet, in a similar way to conventional qPCR, using primers and fluorescent probes. After the amplification step, droplets from each sample are streamed in single file on a droplet reader to count positive and negative reactions. Fluorescence measurements for each droplet in two optical channels are used to count the numbers of positive and negative droplets per sample. Positive droplets, containing at least one copy of the target, exhibit increased fluorescence over negative droplets. Results for a given sample are reassembled and the fraction of positive droplets is then fitted to a Poisson distribution to determine the absolute initial copy number of the target molecule in the input reaction mixture in units of copies/µl. The fraction of positive droplets determines the concentration of the target of interest in the initial sample. Each droplet in a sample is plotted on a graph of fluorescence intensity versus droplet number (see figure 15 below). All positive droplets (those above the threshold intensity indicated by the red line) are scored as positive, and each is assigned a value of 1. All negative droplets (those below the threshold) are scored as negative, and each is assigned a value of 0 (zero). This counting technique provides a digital signal from which to calculate the starting target concentration by a statistical analysis of the numbers of positive and negative droplets in a given sample.

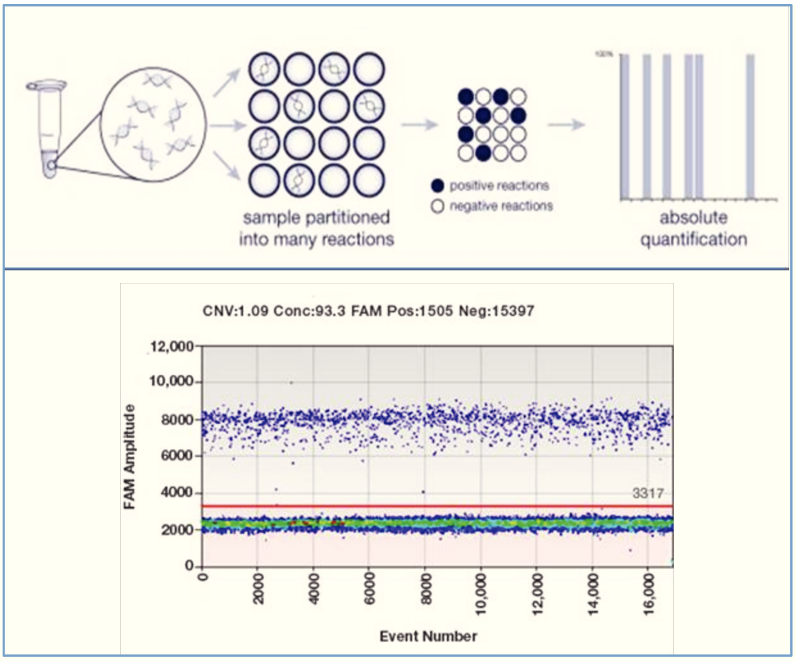

Figure 15: Scheme and data visualization of droplet-digital PCR (ddPCR)

In qPCR, quantitative information is obtained from the cycle threshold (Ct), a point on the analogue fluorescence curve where the signal increases above background. External calibrators or normalization to endogenous controls are required to estimate the concentration of an unknown. Droplet-digital PCR provides the possibility of bypassing error-prone quantification steps like serial dilution and normalization with an endogenous reference by direct transformation of binary end-point PCR data into an absolute number of copies of the target of interest in the template input. This technique has great potential, as it can be applied in a variety of cases. Initially, it was designed to be used to detect rare tumor-specific DNA mutations, present in the form of circulating DNA fragments in the plasma or serum (see introduction, page 28). However, its ability to determine copy-number variation without external calibrators pointed towards its application for the assessment of gene expression levels, including microRNAs [333]. The major limiting factor for now is the high cost of the equipment (distinct machines needed for partitioning, amplification, reassembly and data-reading/processing), thus hampering wide research, or even clinical, use.

- FirePlex miRNA assay

In collaboration with Dr Alessandro Serra of Abcam we are also investigating the potential of the Firefly technology for the detection of miRNAs in body fluids without extraction or processing. This assay is designed to yield relative miRNA expression profiles from direct analysis of crude sample types including serum, plasma, crude exosomes, formalin-fixed

paraffin embedded tissues (FFPEs), cell suspensions, urine and saliva. The core of this technique consists of the specific capture of one or more miRNA targets by Firefly probe-containing particles [334]. When particles are mixed with sample (either crude biofluids after a digest step or purified RNA), target miRNAs bind to their specific probes. The hybridization buffer used for this step is optimized to keep only the right miRNAs bound to the probe, increasing the specificity of the assay. After miRNA capture, particles are rinsed to remove unbound materials and remove potential inhibitors of subsequent steps, such as heparin. Further labeling of the captured miRNA is done with the ligation of universal adaptors.

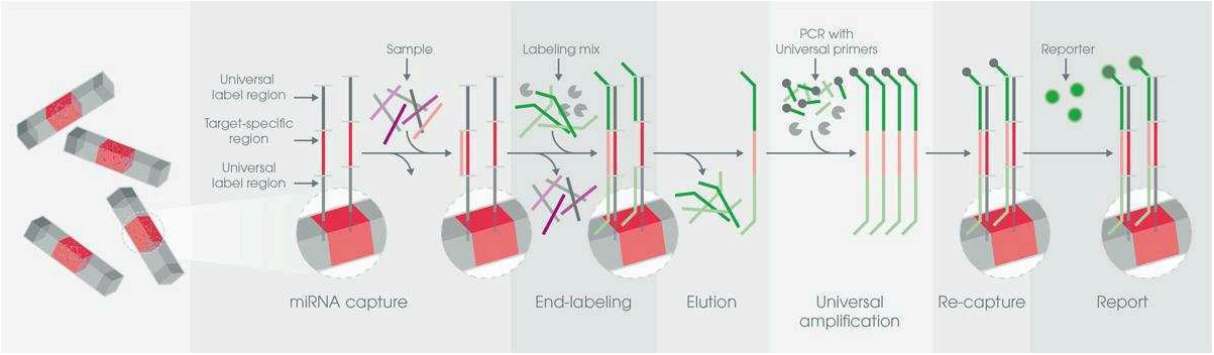

Figure 16: Molecular workflow of the FirePlex miRNA assay (Abcam)

This results to the formation of a DNA-RNA-DNA fusion molecule. After an elution step, these molecules are amplified by universal PCR, using primers specific for the universal adaptors. The reverse primer is labeled with biotin, allowing reporting of the target miRNAs at a later step. After amplification, samples are mixed with particles once more to be recaptured by miRNA-specific probes. A fluorescent reporter is added that binds to the biotin incorporated during amplification. Fluorescence is then measured on the particles by flow cytometry. The whole procedure is described in figure 16. Thus, relative quantification of miRNAs can be done in a direct, homogeneous and much quicker manner. Furthermore, the reaction can contain particles for simultaneous assessment of up to 65 target miRNAs, providing the possibility to study multiplexed panels and not individual targets.

- Multiplexed miRNA RCA-FRET assay

This last method is being assessed in collaboration with the group of Nanobiophotonics, directed by Dr Niko Hildebrandt, member of the Institute of Integrative Biology of the Cell and the Paris-Sud University. This group has been trying to achieve high sensitivity and specificity for short nucleic acid sequences, in order to be able to distinguish molecules of

strong sequence similarities, like miRNAs, without having to amplify the target or apply various temperatures. The detection of the target miRNAs is preceded by rolling circle amplification (RCA) to enhance the emitted fluorescence (figure 17). Different miRNAs are hybridizing to the 5′-PO4 and 3′-OH ends of specific linear ssDNA padlock probes. Ligation of the padlock nick over the miRNA splint creates a circular amplification template. The miRNA target is used as a primer for the polymerase to start an isothermal synthesis of complementary ssDNA around the circular template. The following round of ssDNA synthesis around the circular template replaces the first ssDNA strand and so on. Within a few hours thousands of such tandem sequences can be generated, leading to a long ssDNA (RCP).

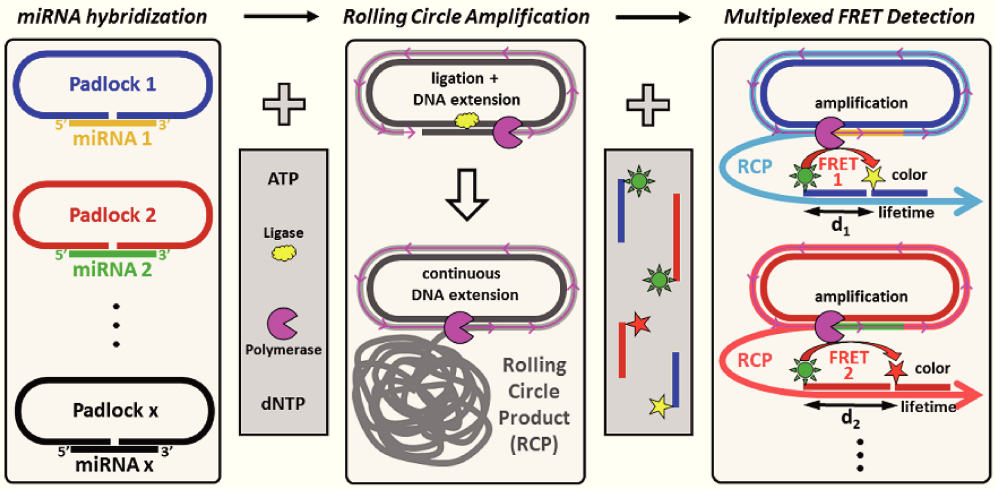

Figure 17: The principle of rolling circle amplification

The detection is based on time-gated Förster resonance energy transfer (TG-FRET) from a luminescent terbium complex (Lumi4-Tb) to different organic dyes [335]. The long excited-state lifetime of terbium secures suppression of background fluorescence upon detection of photoluminescence. The assay relies on the use of specific tetramer probes, consisting of two FRET oligonucleotides and two adaptor oligonucleotides, as seen in the figure below.

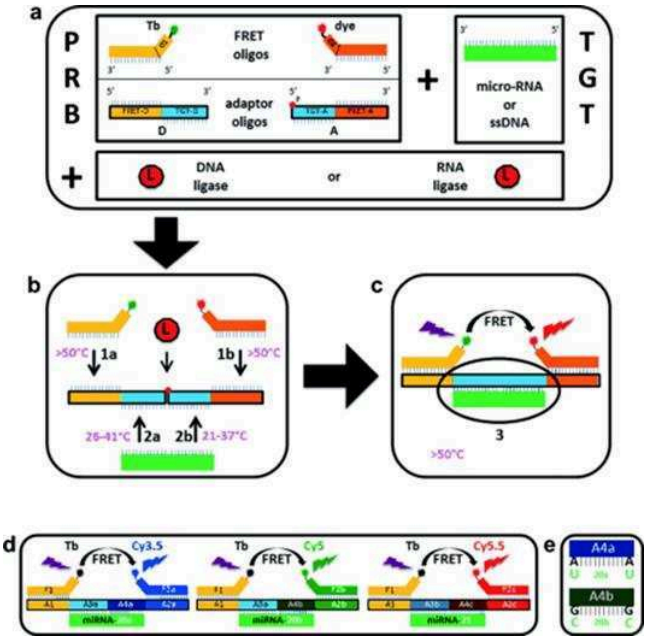

Figure 18: Principle of the multiplexed FRET assay

The FRET oligos have oligonucleotide overhangs, one bearing the terbium and the other bearing a dye (Cy3.5, Cy5, Cy5.5). The adaptor oligos have a part which is perfectly complementary to a part of the target miRNA. A ligase and ATP abundance in the reaction solution are needed for ligation of the two adaptor oligos. Mixing of the probe compartments and the target leads to the formation of stable FRET-adaptor double-strands and semi-stable adaptor-target complexes with an adaptor nick. Ligation of this nick by the added ligase promotes generation of stable probe-target double strands. This formation allows terbium-to-dye FRET, which is detected and measured in a plate reader, depending on the selected sequence and the dye. Selection of specific donor and acceptor labeled oligonucleotides leads to specific hybridization to the tandem repeats of the RCP. FRET from the same type of long-lifetime donor to different dye acceptors can create specific colors (emission wavelength of the acceptor) and lifetimes (distance between donor and acceptor) for multiplexed detection. This technique is expected to offer high sensitivity (picomolar level) and absolute quantification of multiplexed miRNA targets.

Broader perspectives

The published work on miR-200b and its potential clinical use for the surveillance and personalized therapeutic approach in ovarian cancer led to the emergence of two novel projects. The first ongoing project is a collaboration of our group and the group of Dr Alexandra Leary, also based in Gustave Roussy, with the biotechnological miRNA platform

Prestizia, belonging to the Theradiag company. The aim of this collaboration is to take advantage of the samples of the Exoplasma project for a robust simultaneous miRNA profiling of patients' plasma. The short-term goal is the analysis of 30 plasma samples of ovarian cancer before treatment with a TaqMan Array Human MicroRNA Card Set. This assay allows rapid and simultaneous quantification of 754 mature human miRNAs, along with endogenous controls and a negative control and is expected to indicate the miRNAs with the biggest aberrations in the malignancy. The long-term goal of this project, after further validation of the preliminary results from the cohort mentioned above with other cohorts, is to attempt the development of a plasma miRNA-based clinical test for ovarian cancer. This test will be designed to predict response to conventional treatment (see introductory comment for article 1), or eventually evaluate the response of patients with advanced disease upon diagnosis to neo-adjuvant chemotherapy. The first results are encouraging but cannot be presented due to a confidentiality agreement.

Moreover, our group, in collaboration with numerous hospital-based research units has acquired a 3-year funding from the Institut National de Cancer (INCa), for a multicentric project that will attempt a massive parallel analysis of circulating miRNAs in pelvic gynecologic cancers.

BHRF1 miRNA induction independent of viral lytic reactivation?

The obvious question emerging from the work done in the second article is why the induction of the BHRF1 miRNAs, seen especially in the treated C15 and C666-1 models, does not seem to correlate with an induction of the lytic cycle. Indeed, in treated C15 there was no detection of BZLF1, known to be characteristic marker of the lytic cycle reactivation. In C666-1 tumors, the strong induction of BHRF1 miRNAs was accompanied by a very modest increase in the expression of BZLF1, while BHRF1 was not detected at all. On the other hand, C18 tumors exhibiting a spectacular dose-dependent upregulation of BZLF1 (we reproduced the same result later, after only one week of treatment) showed a much lower increase in the expression of the already detected without treatment BHRF1 miRNAs. Furthermore, western blot analysis did not reveal any production of the BHRF1 protein, not even with the dose of 2 mg/kg. These contradictory findings suggest that an induction of these miRNAs may not be connected to lytic reactivation of the viral genome as one would initially expect. In EBV latency, BHRF1 miRNAs are practically expressed only in type III latency, not reported in infected epithelial tissues. The expression of this miRNA cluster draws particular interest, as they seem to have the ability to enhance the expression of each other. Feederle et a1 (2011)

reported that, while miR-BHRF1-1, miR-BHRF1-2 and miR-BHRF1-3 have all the ability to induce B-cell transformation, expression of miR-BHRF1-2 selectively enhances the expression of the other miRNAs of the cluster, indicating the synergistic effect of miRNA clustering [336]. This may explain the simultaneous (but not equal) induction of these miRNAs. However, it is not clear why an increase of their expression, combined with a proportional increase in the expression of the BHRF1 mRNA transcript, does not correlate with a detection of the cis-encoded protein. The explanation may have been provided by an enlightening publication by Xing and Kieff in 2011, supporting the idea of independent regulation of the BHRF1 transcripts, not related to the translation of the mRNA [337]. In fact, in latent infection, EBV expresses the latent BHRF1 RNA, using the latent promoters Wp and Cp, encoding the BHRF1 miRNAs (miR-BHRF1-1, miR-BHRF1-2, and miR-BHRF1-3) and containing the BHRF1 ORF. When the lytic cycle takes place, a distinct transcript is generated, measuring 1.4-kb. This lytic transcript is fully spliced and initiated by the virus replication-activated (lytic) BHRF1 promoter [338]. In this case, the TATA box and transcription start site overlap with the pre-miR-BHRF1-1 sequences [338]. The latent BHRF1 RNA has a long 5′-untranslated region (UTR) and is not spliced [339]. Transcripts from the Cp or Wp promoter initiate alternatively spliced EBNA transcripts in latent infection and can be polyadenylated downstream of the BHRF1 3′-UTR to produce the latent BHRF1 RNA (figure 13A in the introduction). In contrast to miR-BHRF1-1, miR-BHRF1-2 and miR-BHRF1-3 are located in the 3′-UTR. While the BHRF1 miRNAs are produced in type III latent infection [259], BHRF1 protein has not been detected in infected LCLs using effective BHRF1 antibodies [340].

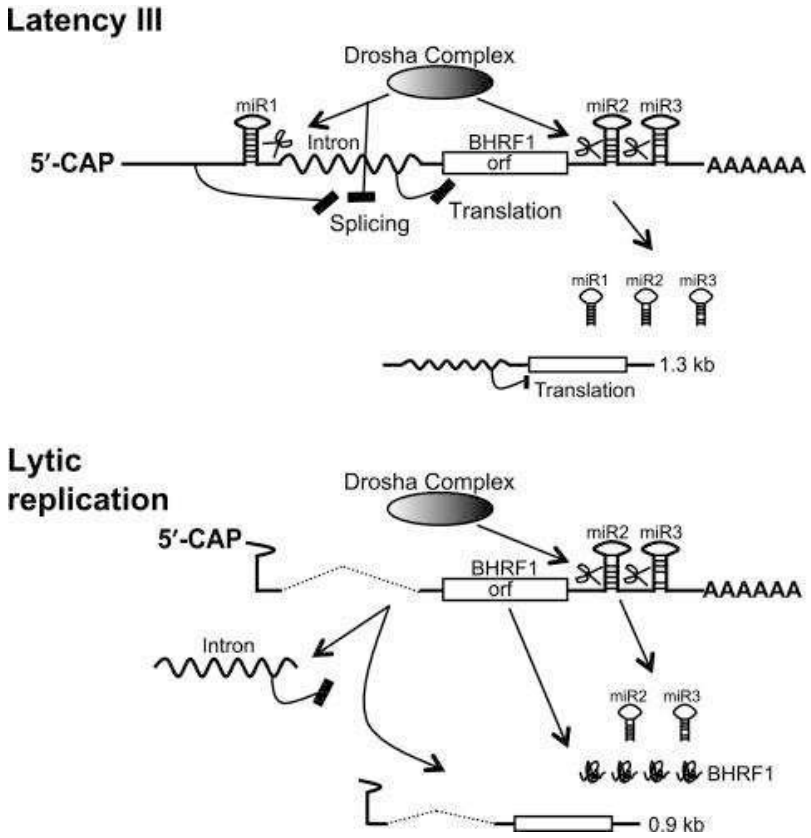

Figure 19: Splicing and Drosha RNA processing controlling the expression of the BHRF1 locus (taken from [337])

Xing and Kieff indicated that Drosha cleavage of the 2.1-kb Wp/Cp-derived BHRF1 RNA generates all BHRF1 miRNAs, as well as a secondary 1.3-kb transcript, which they named dcRNA (latency III in figure 19). Inserting mutations in the miR-BHRF1-1 locus in the 5'UTR of the latent BHRF1 RNA, they abolished site recognition and cleavage by Drosha. In the absence of Drosha activity, none of these derived RNAs was detected. Splicing of the intron preceding the ORF took place, substantially increasing translation and production of the protein. The presence of the intron seems to block the export of the mRNA to the cytoplasm. Summed up, their findings suggested that Drosha cleavage for the excision of miR-BHRF1-1 inhibits downstream RNA splicing and that the remaining intron inhibits potential translation of the latent RNA (figure 19). The lytic transcript, as previously explained, does not contain the miR-BHRF1-1 cleavage site, thus not being subject to Drosha activity. Nevertheless, Drosha-mediated cleavage can take place after splicing, as the lytic mRNA is subsequently cleaved downstream of the ORF, resulting in the production of the BHRF1 protein, miR-BHRF1-2 and miR-BHRF1-3, as well as a 0.9-kb dcRNA.

In figure 3 of the supplementary data of the article, we show that there was no significant change in the detection of the lytic BHRF1 transcript (BHRF1 H) after treatment. Taken together, all these data lead to the hypothesis that 5-azacytidine, at least in C15 and C666-1 models, rather enhanced the expression of the Cp/Wp-related genes than induced the lytic cycle of the virus, explaining the absence of correlation between BZLF1 and BHRF1 miRNA expression. Demethylation of these promoters caused by the drug led to a latency type III-like profile of the BHRF1 miRNAs, whereas there was no change in the profile of the BHRF1 protein, as the accumulated latent BHRF1 transcript was cleaved by Drosha for the generation of the miRNAs, but not spliced, resulting in translation inhibition. A study of the methylation status of the Cp/Wp promoters, as proposed in the discussion of the article, would eventually allow validation of this hypothesis.

Recent advances in EBV biology and nasopharyngeal carcinoma management

Although the management of nasopharyngeal carcinoma has significantly improved in the recent years, due to more effective treatment modalities and combinations, this disease remains challenging in several aspects of its onset and progression. As Wang et al (2017) report in a very recent work, nearly one third of early-stage NPC are estimated to be missed with nasal endoscopy and medical imaging. The onset of symptoms often comes at a later stage, thus adding another negative factor in early diagnosis [341]. NPC carries an excellent prognosis if treated early, but most patients present stage III to IV disease upon diagnosis, which negatively affects the cure rate and increase the mortality rate. The tools that are expected to solve to a certain point this issue could be, as mentioned before, EBV-derived tumor biomarkers. In their work, Romdhoni et al (2014) highlight IgA anti-EBNA1 and VCA-p18 enzyme-linked immunosorbent assay as a diagnostic tool with a positive impact on NPC diagnosis confirmation, although it has a weaker prognostic power after treatment [342]. Other works prove the utility of viral DNA measuring in the blood or in nasopharyngeal brushings for both diagnosis and prognostic evaluation of NPC. Post-treatment, DNA load test in blood and brush proved the best predictor for overall survival and disease-free survival [343]. An interesting article accepted in June 2017 points towards a simultaneous use of EBV serology and EBV DNA load for a better screening of NPC, as in cases of early primary NPC, EBV DNA is not always detectable in the blood of patients. Yao et al, tested the sera of 334 patients with non-metastatic NPC and undetectable pre-treatment EBV DNA and found out that the load of immunoglobulin A (IgA) antibodies against early antigen (EA-IgA) and viral capsid antigen (VCA-IgA) correlated positively with T, N and overall stage of the tumor

[344]. However, as it can be easily understood from this work, the situation is much more complicated for prognosis, as in treated cases of undetectable EBV DNA (before treatment), none of these antibodies, neither their combination achieved a high score as a prognostic factor for remission, relapse or overall survival. In such circumstances, we observe a lack of weapons for an accurate monitoring of the disease.

On the other hand, new treatment combinations are being tested and novel drugs are being developed, hinting at a strong need of accurate response evaluation. Induction chemotherapy consisting of gemcitabine and cisplatin, preceding concurrent chemotherapy and intensity-modulated radiotherapy has exhibited promising clinical efficacy and acceptable toxicity for locoregionally advanced NPC. Fangzheng et al report this year that trials including this modality to the therapeutic approach yielded very satisfying scores [345]. At a median follow-up duration of 48 months (10-59 months), 4-year local relapse-free survival (LRFS) was 86.9%, regional relapse-free survival (RRFS) was 90.6%, distant metastasis-free survival (DMFS) was 79.8%, progression-free survival (PFS) was 77.0%, and overall survival (OS) was 81.9%. Overall, they mentioned that the administration of at least 2 cycles of this induction chemotherapy led to a significantly improved regional relapse-free survival. Another trend concerning treatment of NPC is targeting EBV expression. Stoker et al (2015) applied gemcitabine, valproic acid and ganciclovir (GCV) on 8 NPC patients not responding to conventional treatment, achieving stabilization or regression in 5 of them [346]. The combination of the first two induced viral lytic reactivation, leading to the expression of viral immunogenic proteins and making the tumors a target for antiviral agents, as GCV (see introduction and introductory comment for article 2). However, the toxic side-effects are all but negligible, often complicating regular treatment administration, hampering as a consequence, complete tumor response. Main examples are thrombocytopenia, leukocytopenia, as well as liver dysfunction, which can be really severe. As it can be seen, it is crucial to be able to rapidly distinguish patients who are going to benefit from a specific treatment selection from patients which will not respond. Markers allowing avoiding useless prolongation of a treatment or intensifying it if possible would be of great value in a personalized treatment context.

Utilization of viral miRNAs as tools for disease surveillance

This is where our work draws its significance from. Viral miRNAs present important advantages to serve as potential biomarkers, such as tumor specificity, abundance in NPC cells and detection in plasma and serum. Very few works have been carried out towards this

direction and, more impressively, published works focusing on BHRF1 miRNAs in EBV-associated malignancies are not more than 10 since 2010, as of June 2017. Nevertheless, these works, along with recent data regarding BART miRNAs, reveal very interesting facts. A landmark analysis in 2009 showed that NPC is characterized by a robust expression of BART miRNAs and very low expression of BHRF1 miRNAs [243]. Yang et al (2013) confirmed that pattern in C666-1 cells, in which BART miRNAs account for the impressive 10% of total cellular miRNAs, while BHRF1 miRNAs are hardly detectable [347]. By comparing viral miRNA expression in various EBV-associated tumors and different viral latency types, they demonstrated a higher expression of BARTs in latency II, compared to types I and III. Furthermore, they analyzed viral miRNA expression in tissue samples from primary NPC tumors, proving that they had a practically identical pattern with C666-1. This finding validated this cell line as a model for the study on EBV miRNA dynamics in NPC. The work of Yang et al complemented in an excellent way results published a year before by Kim and Lee [348]. Just for reminder, BHRF1 miRNAs are located within introns of the BHRF1 gene and produced from the long EBNA transcripts (see figure 13 in page 59). BART miRNAs are located in introns contained within the BART transcripts. BHRF1 is an EBV early lytic gene, whose function has already been discussed in the introduction. Kim and Lee showed that distinct EBV miRNA profiles characterize infected epithelial tissues (NPC) and B cells (LCL), suggesting that there may be a relationship between miRNA expression and latency type of the viral infection [348]. Infected epithelial tissues always exhibit type II latency, whereas types I and III are observed in lymphomas. BHRF1 miRNA expression is restricted to latency III-presenting cells. In this type, the BHRF1 transcript has been shown to be transcribed by the Cp and Wp promoters. In types I and II, previous data have proven that Cp and Wp are inactive due to extensive hypermethylation, thus explaining this observation. A very interesting work by Li et al, also from 2012, drew attention to miR-BHRF1-1. Despite induction of all BHRF1 miRNAs upon activation of the lytic cycle [259, 260], miR-BHRF1-1 increase in lymphoid cells is delayed for 48h compared to the other members of the cluster [260], suggesting a potential involvement of this specific miRNA in the late lytic cycle. The NPC cell line SUNE-1 infected by a recombinant EBV strain [349] was treated with TPA (12-O-Tetradecanoylphorbol-13-acetate), an agent known to induce the viral lytic cycle. TPA increased Ea-D and BamHI-W fragment of EBV, as well as BZLF1 expression (markers of lytic activity). Inhibition of miR-BHRF1-1 restored their levels to their pre-treatment status, but subsequent exogenous re-expression of miR-BHRF1-1 increased the expression of BZLF1 and Ea-D and BamHI-W fragment of EBV [350]. Li et al went on to show that miR-BHRF1-1

is involved in viral replication in the late stage of the lytic cycle, by directly targeting and downregulating the p53 tumor suppressor, known to be functionally inhibited by EBV in latent stage [351], transiently elevated in the early lytic stage [352] and declined in late lytic stage to profit viral replication [353]. In the most recent work implicating BHRF1 miRNAs, Tsai et al (2017) compared the expression of different EBV strains found in gastric and nasopharyngeal carcinomas, as well as in lymphomas. The isolated strains were used to infect lymphoblastoid cell lines (LCLs). Their results suggested a wide variation in the expression of BHRF1 miRNAs among the viral strains, with the NPC-derived showing the lowest expression. BHRF1 miRNA expression rate correlated with transformation efficiency of the strain and growth rate of the infected LCLs, without elucidating this observation [354]. BHRF1 variations were mostly pronounced for miR-BHRF1-3.

Conclusion

These 3 years dedicated to the study of circulating miRNAs gave me the chance to acquire a deep knowledge of the field and be fascinated by the dynamics and the possibilities that these tiny molecules possess. MicroRNAs can become a valuable tool and a powerful ally against cancer, contributing to an earlier diagnosis and, thus, to a more effective treatment, as well as to a more sensitive and direct monitoring of the disease during or post-treatment, guaranteeing a quick and better adapted reaction in case of relapse. This doctorate thesis sheds light on important aspects of miRNAs and their relation with the cancer of interest. The first project demonstrates the need to study circulating biomarkers in a time-dependent way, not only focusing on their concentration at a given time-point. Their evolution might hide precious information about a discreet recurrence, or undetectable residual disease and measurable changes could potentially prevent a late reaction with a poorer prognosis and clinical outcome. Of course broader studies, including more patients and a massive panel of miRNAs should be carried out, not only to validate acquired results, but also to draw attention to other miRNA candidates that are missed in a limited study. Nevertheless, accumulated scientific data point towards an imminent entry of circulating nucleic acids, like miRNAs and tumor-derived DNA fragments, into the clinic (see the notion of liquid biopsy in page 28). A first major breakthrough of liquid biopsies on the verge of entering the clinic is the recently proposed detection of circulating tumor cells (CTC) as a tool for early cancer diagnosis. The use of Isolation by Size of Epithelial Tumor cells (ISET) technology has allowed filtering and detection of migrating tumor cells, an early event in carcinogenesis, in patients with a high risk of lung cancer such as subjects with chronic obstructive pulmonary disease. The CTC-

positive subjects under close surveillance went on to develop lung cancer nodes, which were surgically removed at a very early stage, assuring a recurrence-free survival [355]. The second project had its own particular beauty, because of the unique features of nasopharyngeal carcinoma, due to its consistent association with the Epstein-Barr virus and the distinct pattern of expression that EBV presents in the context of infected epithelia. The obtained results indicate the fact that, sometimes, a potential answer to an issue might be found outside cancer (in its strict definition). The de novo induction of the BHRF1 miRNA cluster in treated NPC is a very original discovery, with considerable clinical interest for the management of the disease, highlighting the dynamic nature of the virus, even with a well-established latency in the context of a host. Detection of these miRNAs in circulation could improve selection of treatment modalities and contribute to its fine-tuned tailor-made character. And as science was born just a few moments after the very first expression of human curiosity and will continue to accompany the steps of mankind in its quest to address all emerging or existing questions, I sincerely hope to have added my own small shackle to its never-ending chain.

Bibliography

1. Ambros, V., et al., A uniform system for microRNA annotation. RNA, 2003. **9**(3): p. 277-9.
2. Kim, V.N., Small RNAs: classification, biogenesis, and function. Mol Cells, 2005. **19**(1): p. 1-15.
3. Bartel, D.P., MicroRNAs: genomics, biogenesis, mechanism, and function. Cell, 2004. **116**(2): p. 281-97.
4. Lee, R.C., R.L. Feinbaum, and V. Ambros, The C. elegans heterochronic gene lin-4 encodes small RNAs with antisense complementarity to lin-14. Cell, 1993. **75**(5): p. 843-54.
5. Rodriguez, A., et al., Identification of mammalian microRNA host genes and transcription units. Genome Res, 2004. **14**(10A): p. 1902-10.
6. Sundaram, G.M., et al., 'See-saw' expression of microRNA-198 and FSTL1 from a single transcript in wound healing. Nature, 2013. **495**(7439): p. 103-6.
7. Saini, H.K., S. Griffiths-Jones, and A.J. Enright, Genomic analysis of human microRNA transcripts. Proc Natl Acad Sci U S A, 2007. **104**(45): p. 17719-24.
8. Lee, Y., et al., MicroRNA genes are transcribed by RNA polymerase II. EMBO J, 2004. **23**(20): p. 4051-60.
9. Borchert, G.M., W. Lanier, and B.L. Davidson, RNA polymerase III transcribes human microRNAs. Nat Struct Mol Biol, 2006. **13**(12): p. 1097-101.
10. Faller, M. and F. Guo, MicroRNA biogenesis: there's more than one way to skin a cat. Biochimica et biophysica acta, 2008. **1779**(11): p. 663-7.
11. Lee, Y., et al., The nuclear RNase III Drosha initiates microRNA processing. Nature, 2003. **425**(6956): p. 415-9.
12. Landthaler, M., A. Yalcin, and T. Tuschl, The human DiGeorge syndrome critical region gene 8 and Its D. melanogaster homolog are required for miRNA biogenesis. Curr Biol, 2004. **14**(23): p. 2162-7.
13. Han, J., et al., Molecular basis for the recognition of primary microRNAs by the Drosha-DGCR8 complex. Cell, 2006. **125**(5): p. 887-901.
14. Lee, Y., et al., MicroRNA maturation: stepwise processing and subcellular localization. EMBO J, 2002. **21**(17): p. 4663-70.

15. Bohnsack, M.T., K. Czaplinski, and D. Gorlich, Exportin 5 is a RanGTP-dependent dsRNA-binding protein that mediates nuclear export of pre-miRNAs. RNA, 2004. **10**(2): p. 185-91.
16. Lund, E., et al., Nuclear export of microRNA precursors. Science, 2004. **303**(5654): p. 95-8.
17. Lee, Y.S., et al., Distinct roles for Drosophila Dicer-1 and Dicer-2 in the siRNA/miRNA silencing pathways. Cell, 2004. **117**(1): p. 69-81.
18. Knight, S.W. and B.L. Bass, A role for the RNase III enzyme DCR-1 in RNA interference and germ line development in Caenorhabditis elegans. Science, 2001. **293**(5538): p. 2269-71.
19. Grishok, A., et al., Genes and mechanisms related to RNA interference regulate expression of the small temporal RNAs that control C. elegans developmental timing. Cell, 2001. **106**(1): p. 23-34.
20. Maniataki, E. and Z. Mourelatos, A human, ATP-independent, RISC assembly machine fueled by pre-miRNA. Genes Dev, 2005. **19**(24): p. 2979-90.
21. Kedersha, N., et al., Stress granules and processing bodies are dynamically linked sites of mRNP remodeling. J Cell Biol, 2005. **169**(6): p. 871-84.
22. Diederichs, S. and D.A. Haber, Dual role for argonautes in microRNA processing and posttranscriptional regulation of microRNA expression. Cell, 2007. **131**(6): p. 1097-108.
23. Matranga, C., et al., Passenger-strand cleavage facilitates assembly of siRNA into Ago2-containing RNAi enzyme complexes. Cell, 2005. **123**(4): p. 607-20.
24. Hock, J. and G. Meister, The Argonaute protein family. Genome Biol, 2008. **9**(2): p. 210.
25. Macfarlane, L.A. and P.R. Murphy, MicroRNA: Biogenesis, Function and Role in Cancer. Curr Genomics, 2010. **11**(7): p. 537-61.
26. Wahid, F., et al., MicroRNAs: synthesis, mechanism, function, and recent clinical trials. Biochimica et biophysica acta, 2010. **1803**(11): p. 1231-43.
27. Bartel, D.P., MicroRNAs: target recognition and regulatory functions. Cell, 2009. **136**(2): p. 215-33.
28. Garofalo, M. and C.M. Croce, microRNAs: Master regulators as potential therapeutics in cancer. Annu Rev Pharmacol Toxicol, 2011. **51**: p. 25-43.
29. Jalvy-Delvaille, S., et al., Molecular basis of differential target regulation by miR-96 and miR-182: the Glypican-3 as a model. Nucleic Acids Res, 2012. **40**(3): p. 1356-65.

30. Chendrimada, T.P., et al., MicroRNA silencing through RISC recruitment of eIF6. Nature, 2007. **447**(7146): p. 823-8.
31. Mathonnet, G., et al., MicroRNA inhibition of translation initiation in vitro by targeting the cap-binding complex eIF4F. Science, 2007. **317**(5845): p. 1764-7.
32. Behm-Ansmant, I., et al., mRNA degradation by miRNAs and GW182 requires both CCR4:NOT deadenylase and DCP1:DCP2 decapping complexes. Genes Dev, 2006. **20**(14): p. 1885-98.
33. Valencia-Sanchez, M.A., et al., Control of translation and mRNA degradation by miRNAs and siRNAs. Genes Dev, 2006. **20**(5): p. 515-24.
34. Lewis, B.P., C.B. Burge, and D.P. Bartel, Conserved seed pairing, often flanked by adenosines, indicates that thousands of human genes are microRNA targets. Cell, 2005. **120**(1): p. 15-20.
35. Friedman, R.C., et al., Most mammalian mRNAs are conserved targets of microRNAs. Genome Res, 2009. **19**(1): p. 92-105.
36. Barrey, E., et al., Pre-microRNA and mature microRNA in human mitochondria. PLoS One, 2011. **6**(5): p. e20220.
37. Mercer, T.R., et al., The human mitochondrial transcriptome. Cell, 2011. **146**(4): p. 645-58.
38. Ro, S., et al., The mitochondrial genome encodes abundant small noncoding RNAs. Cell Res, 2013. **23**(6): p. 759-74.
39. Mach, N., et al., Integrated mRNA and miRNA expression profiling in blood reveals candidate biomarkers associated with endurance exercise in the horse. Sci Rep, 2016. **6**: p. 22932.
40. Sripada, L., et al., Systematic analysis of small RNAs associated with human mitochondria by deep sequencing: detailed analysis of mitochondrial associated miRNA. PLoS One, 2012. **7**(9): p. e44873.
41. Bianchessi, V., et al., The mitochondrial lncRNA ASncmtRNA-2 is induced in aging and replicative senescence in Endothelial Cells. J Mol Cell Cardiol, 2015. **81**: p. 62-70.
42. Ernoult-Lange, M., et al., P-bodies and mitochondria: which place in RNA interference? Biochimie, 2012. **94**(7): p. 1572-7.
43. Huang, L., et al., Mitochondria associate with P-bodies and modulate microRNA-mediated RNA interference. J Biol Chem, 2011. **286**(27): p. 24219-30.

44. Jiang, Q., et al., miR2Disease: a manually curated database for microRNA deregulation in human disease. Nucleic Acids Res, 2009. **37**(Database issue): p. D98-104.
45. Luna, J.M., et al., Hepatitis C virus RNA functionally sequesters miR-122. Cell, 2015. **160**(6): p. 1099-110.
46. Melo, S.A., et al., A TARBP2 mutation in human cancer impairs microRNA processing and DICER1 function. Nature genetics, 2009. **41**(3): p. 365-70.
47. Pampalakis, G., et al., Down-regulation of dicer expression in ovarian cancer tissues. Clin Biochem, 2010. **43**(3): p. 324-7.
48. Zhu, D.X., et al., Downregulated Dicer expression predicts poor prognosis in chronic lymphocytic leukemia. Cancer Sci, 2012. **103**(5): p. 875-81.
49. Kumar, M.S., et al., Dicer1 functions as a haploinsufficient tumor suppressor. Genes Dev, 2009. **23**(23): p. 2700-4.
50. Kumar, M.S., et al., Impaired microRNA processing enhances cellular transformation and tumorigenesis. Nature genetics, 2007. **39**(5): p. 673-7.
51. Chiosea, S., et al., Up-regulation of dicer, a component of the MicroRNA machinery, in prostate adenocarcinoma. Am J Pathol, 2006. **169**(5): p. 1812-20.
52. Muralidhar, B., et al., Global microRNA profiles in cervical squamous cell carcinoma depend on Drosha expression levels. J Pathol, 2007. **212**(4): p. 368-77.
53. Suzuki, H.I., et al., Modulation of microRNA processing by p53. Nature, 2009. **460**(7254): p. 529-33.
54. Martello, G., et al., A MicroRNA targeting dicer for metastasis control. Cell, 2010. **141**(7): p. 1195-207.
55. Esquela-Kerscher, A. and F.J. Slack, Oncomirs - microRNAs with a role in cancer. Nat Rev Cancer, 2006. **6**(4): p. 259-69.
56. Calin, G.A., et al., Human microRNA genes are frequently located at fragile sites and genomic regions involved in cancers. Proc Natl Acad Sci U S A, 2004. **101**(9): p. 2999-3004.
57. Lagana, A., et al., Variability in the incidence of miRNAs and genes in fragile sites and the role of repeats and CpG islands in the distribution of genetic material. PLoS One, 2010. **5**(6): p. e11166.
58. Lopez-Serra, P. and M. Esteller, DNA methylation-associated silencing of tumor-suppressor microRNAs in cancer. Oncogene, 2012. **31**(13): p. 1609-22.

59. Weber, M. and D. Schubeler, Genomic patterns of DNA methylation: targets and function of an epigenetic mark. Curr Opin Cell Biol, 2007. **19**(3): p. 273-80.
60. Saito, Y., et al., Specific activation of microRNA-127 with downregulation of the proto-oncogene BCL6 by chromatin-modifying drugs in human cancer cells. Cancer Cell, 2006. **9**(6): p. 435-43.
61. Toyota, M., et al., Epigenetic silencing of microRNA-34b/c and B-cell translocation gene 4 is associated with CpG island methylation in colorectal cancer. Cancer Res, 2008. **68**(11): p. 4123-32.
62. Lehmann, U., et al., Epigenetic inactivation of microRNA gene hsa-mir-9-1 in human breast cancer. J Pathol, 2008. **214**(1): p. 17-24.
63. Bandres, E., et al., Epigenetic regulation of microRNA expression in colorectal cancer. Int J Cancer, 2009. **125**(11): p. 2737-43.
64. Hermeking, H., MicroRNAs in the p53 network: micromanagement of tumour suppression. Nat Rev Cancer, 2012. **12**(9): p. 613-26.
65. Ceppi, P., et al., Loss of miR-200c expression induces an aggressive, invasive, and chemoresistant phenotype in non-small cell lung cancer. Mol Cancer Res, 2010. **8**(9): p. 1207-16.
66. Scott, G.K., et al., Rapid alteration of microRNA levels by histone deacetylase inhibition. Cancer Res, 2006. **66**(3): p. 1277-81.
67. Dews, M., et al., Augmentation of tumor angiogenesis by a Myc-activated microRNA cluster. Nature genetics, 2006. **38**(9): p. 1060-5.
68. Bui, T.V. and J.T. Mendell, Myc: Maestro of MicroRNAs. Genes Cancer, 2010. **1**(6): p. 568-575.
69. Kent, O.A., et al., Repression of the miR-143/145 cluster by oncogenic Ras initiates a tumor-promoting feed-forward pathway. Genes Dev, 2010. **24**(24): p. 2754-9.
70. Chang, T.C., et al., Transactivation of miR-34a by p53 broadly influences gene expression and promotes apoptosis. Mol Cell, 2007. **26**(5): p. 745-52.
71. Matsuzaki, J. and T. Ochiya, Circulating microRNAs and extracellular vesicles as potential cancer biomarkers: a systematic review. Int J Clin Oncol, 2017.
72. Maurel, M., et al., A functional screening identifies five microRNAs controlling glypican-3: role of miR-1271 down-regulation in hepatocellular carcinoma. Hepatology, 2013. **57**(1): p. 195-204.
73. Cartier, F., et al., New tumor suppressor microRNAs target glypican-3 in human liver cancer. Oncotarget, 2017. **8**(25): p. 41211-41226.

74. Maurel, M., et al., MicroRNA-1291-mediated silencing of IRE1alpha enhances Glypican-3 expression. RNA, 2013. **19**(6): p. 778-88.
75. Chim, S.S., et al., Detection and characterization of placental microRNAs in maternal plasma. Clin Chem, 2008. **54**(3): p. 482-90.
76. Lawrie, C.H., et al., Detection of elevated levels of tumour-associated microRNAs in serum of patients with diffuse large B-cell lymphoma. Br J Haematol, 2008. **141**(5): p. 672-5.
77. Mitchell, P.S., et al., Circulating microRNAs as stable blood-based markers for cancer detection. Proc Natl Acad Sci U S A, 2008. **105**(30): p. 10513-8.
78. Valadi, H., et al., Exosome-mediated transfer of mRNAs and microRNAs is a novel mechanism of genetic exchange between cells. Nat Cell Biol, 2007. **9**(6): p. 654-9.
79. Turchinovich, A., L. Weiz, and B. Burwinkel, Extracellular miRNAs: the mystery of their origin and function. Trends Biochem Sci, 2012. **37**(11): p. 460-5.
80. Chen, X., et al., Characterization of microRNAs in serum: a novel class of biomarkers for diagnosis of cancer and other diseases. Cell Res, 2008. **18**(10): p. 997-1006.
81. Turchinovich, A., et al., Characterization of extracellular circulating microRNA. Nucleic Acids Res, 2011. **39**(16): p. 7223-33.
82. Turchinovich, A., et al., Circulating miRNAs: cell-cell communication function? Front Genet, 2013. **4**: p. 119.
83. Hunter, M.P., et al., Detection of microRNA expression in human peripheral blood microvesicles. PLoS One, 2008. **3**(11): p. e3694.
84. Arroyo, J.D., et al., Argonaute2 complexes carry a population of circulating microRNAs independent of vesicles in human plasma. Proc Natl Acad Sci U S A, 2011. **108**(12): p. 5003-8.
85. Wang, K., et al., Export of microRNAs and microRNA-protective protein by mammalian cells. Nucleic Acids Res, 2010. **38**(20): p. 7248-59.
86. Vickers, K.C., et al., MicroRNAs are transported in plasma and delivered to recipient cells by high-density lipoproteins. Nat Cell Biol, 2011. **13**(4): p. 423-33.
87. Wagner, J., et al., Characterization of levels and cellular transfer of circulating lipoprotein-bound microRNAs. Arterioscler Thromb Vasc Biol, 2013. **33**(6): p. 1392-400.
88. Lewis, A.P. and C.L. Jopling, Regulation and biological function of the liver-specific miR-122. Biochem Soc Trans, 2010. **38**(6): p. 1553-7.

89. Pritchard, C.C., H.H. Cheng, and M. Tewari, MicroRNA profiling: approaches and considerations. Nat Rev Genet, 2012. **13**(5): p. 358-69.
90. Gibbings, D.J., et al., Multivesicular bodies associate with components of miRNA effector complexes and modulate miRNA activity. Nat Cell Biol, 2009. **11**(9): p. 1143-9.
91. Pigati, L., et al., Selective release of microRNA species from normal and malignant mammary epithelial cells. PLoS One, 2010. **5**(10): p. e13515.
92. Mittelbrunn, M., et al., Unidirectional transfer of microRNA-loaded exosomes from T cells to antigen-presenting cells. Nature communications, 2011. **2**: p. 282.
93. Thery, C., L. Zitvogel, and S. Amigorena, Exosomes: composition, biogenesis and function. Nat Rev Immunol, 2002. **2**(8): p. 569-79.
94. Cocucci, E., G. Racchetti, and J. Meldolesi, Shedding microvesicles: artefacts no more. Trends Cell Biol, 2009. **19**(2): p. 43-51.
95. Raposo, G. and W. Stoorvogel, Extracellular vesicles: exosomes, microvesicles, and friends. J Cell Biol, 2013. **200**(4): p. 373-83.
96. Collino, F., et al., Microvesicles derived from adult human bone marrow and tissue specific mesenchymal stem cells shuttle selected pattern of miRNAs. PLoS One, 2010. **5**(7): p. e11803.
97. Yang, M., et al., Microvesicles secreted by macrophages shuttle invasion-potentiating microRNAs into breast cancer cells. Mol Cancer, 2011. **10**: p. 117.
98. Kosaka, N., et al., Secretory mechanisms and intercellular transfer of microRNAs in living cells. J Biol Chem, 2010. **285**(23): p. 17442-52.
99. Pegtel, D.M., et al., Functional delivery of viral miRNAs via exosomes. Proc Natl Acad Sci U S A, 2010. **107**(14): p. 6328-33.
100. Fabbri, M., et al., MicroRNAs bind to Toll-like receptors to induce prometastatic inflammatory response. Proc Natl Acad Sci U S A, 2012. **109**(31): p. E2110-6.
101. Lehmann, S.M., et al., An unconventional role for miRNA: let-7 activates Toll-like receptor 7 and causes neurodegeneration. Nat Neurosci, 2012. **15**(6): p. 827-35.
102. Zhang, L., et al., Exogenous plant MIR168a specifically targets mammalian LDLRAP1: evidence of cross-kingdom regulation by microRNA. Cell Res, 2012. **22**(1): p. 107-26.
103. Taylor, D.D. and C. Gercel-Taylor, MicroRNA signatures of tumor-derived exosomes as diagnostic biomarkers of ovarian cancer. Gynecol Oncol, 2008. **110**(1): p. 13-21.

104. Kinoshita, T., et al., MicroRNAs in extracellular vesicles: potential cancer biomarkers. J Hum Genet, 2017. **62**(1): p. 67-74.
105. Krishnamurthy, N., et al., Liquid Biopsies for Cancer: Coming to a Patient near You. J Clin Med, 2017. **6**(1).
106. Toiyama, Y., et al., Serum miR-21 as a diagnostic and prognostic biomarker in colorectal cancer. J Natl Cancer Inst, 2013. **105**(12): p. 849-59.
107. Lin, X.J., et al., A serum microRNA classifier for early detection of hepatocellular carcinoma: a multicentre, retrospective, longitudinal biomarker identification study with a nested case-control study. Lancet Oncol, 2015. **16**(7): p. 804-15.
108. Ertle, J.M., et al., A combination of alpha-fetoprotein and des-gamma-carboxy prothrombin is superior in detection of hepatocellular carcinoma. Digestion, 2013. **87**(2): p. 121-31.
109. Schultz, N.A., et al., MicroRNA biomarkers in whole blood for detection of pancreatic cancer. JAMA, 2014. **311**(4): p. 392-404.
110. Bhat, K., et al., Advances in biomarker research for pancreatic cancer. Curr Pharm Des, 2012. **18**(17): p. 2439-51.
111. Wang, K., et al., Comparing the MicroRNA spectrum between serum and plasma. PLoS One, 2012. **7**(7): p. e41561.
112. Nilsson, R.J., et al., Blood platelets contain tumor-derived RNA biomarkers. Blood, 2011. **118**(13): p. 3680-3.
113. Cheung, Y.F., et al., Plasma high sensitivity troponin T levels in adult survivors of childhood leukaemias: determinants and associations with cardiac function. PLoS One, 2013. **8**(10): p. e77063.
114. Kirschner, M.B., et al., Haemolysis during sample preparation alters microRNA content of plasma. PLoS One, 2011. **6**(9): p. e24145.
115. Piek, J.M., P.J. van Diest, and R.H. Verheijen, Ovarian carcinogenesis: an alternative hypothesis. Adv Exp Med Biol, 2008. **622**: p. 79-87.
116. Parkin, D.M., et al., Global cancer statistics, 2002. CA Cancer J Clin, 2005. **55**(2): p. 74-108.
117. Jemal, A., et al., Cancer statistics, 2010. CA Cancer J Clin, 2010. **60**(5): p. 277-300.
118. Chene, G., et al., [Ovarian carcinogenesis: recent and past hypotheses]. Gynecol Obstet Fertil, 2011. **39**(4): p. 216-23.
119. Seidman, J.D., et al., The histologic type and stage distribution of ovarian carcinomas of surface epithelial origin. Int J Gynecol Pathol, 2004. **23**(1): p. 41-4.

120. Fischerova, D., et al., Diagnosis, treatment, and follow-up of borderline ovarian tumors. Oncologist, 2012. **17**(12): p. 1515-33.
121. Hunn, J. and G.C. Rodriguez, Ovarian cancer: etiology, risk factors, and epidemiology. Clin Obstet Gynecol, 2012. **55**(1): p. 3-23.
122. Pearce, C.L., et al., Association between endometriosis and risk of histological subtypes of ovarian cancer: a pooled analysis of case-control studies. Lancet Oncol, 2012. **13**(4): p. 385-94.
123. Lakhani, S.R., et al., Pathology of ovarian cancers in BRCA1 and BRCA2 carriers. Clin Cancer Res, 2004. **10**(7): p. 2473-81.
124. Antoniou, A., et al., Average risks of breast and ovarian cancer associated with BRCA1 or BRCA2 mutations detected in case Series unselected for family history: a combined analysis of 22 studies. Am J Hum Genet, 2003. **72**(5): p. 1117-30.
125. Shukla, P.C., et al., BRCA1 is an essential regulator of heart function and survival following myocardial infarction. Nature communications, 2011. **2**: p. 593.
126. Bolton, K.L., et al., Association between BRCA1 and BRCA2 mutations and survival in women with invasive epithelial ovarian cancer. JAMA, 2012. **307**(4): p. 382-90.
127. Integrated genomic analyses of ovarian carcinoma. Nature, 2011. **474**(7353): p. 609-15.
128. Ho, C.L., et al., Mutations of BRAF and KRAS precede the development of ovarian serous borderline tumors. Cancer Res, 2004. **64**(19): p. 6915-8.
129. Barsotti, A.M. and C. Prives, Pro-proliferative FoxM1 is a target of p53-mediated repression. Oncogene, 2009. **28**(48): p. 4295-305.
130. Ledermann, J.A., et al., Randomized phase II placebo-controlled trial of maintenance therapy using the oral triple angiokinase inhibitor BIBF 1120 after chemotherapy for relapsed ovarian cancer. J Clin Oncol, 2011. **29**(28): p. 3798-804.
131. Weil, M.K. and A.P. Chen, PARP inhibitor treatment in ovarian and breast cancer. Curr Probl Cancer, 2011. **35**(1): p. 7-50.
132. Los, M., J.M. Roodhart, and E.E. Voest, Target practice: lessons from phase III trials with bevacizumab and vatalanib in the treatment of advanced colorectal cancer. Oncologist, 2007. **12**(4): p. 443-50.
133. Mei, L., et al., Maintenance chemotherapy for ovarian cancer. Cochrane Database Syst Rev, 2013(6): p. CD007414.
134. Suh, K.S., et al., Ovarian cancer biomarkers for molecular biosensors and translational medicine. Expert Rev Mol Diagn, 2010. **10**(8): p. 1069-83.

135. Ferrini, R., Screening asymptomatic women for ovarian cancer: American College of Preventive Medicine practice policy. Am J Prev Med, 1997. **13**(6): p. 444-6.
136. Song, M.J., et al., Diagnostic value of CA125 as a predictor of recurrence in advanced ovarian cancer. Eur J Gynaecol Oncol, 2013. **34**(2): p. 148-51.
137. Di Leva, G. and C.M. Croce, Roles of small RNAs in tumor formation. Trends Mol Med, 2010. **16**(6): p. 257-67.
138. Mateescu, B., et al., miR-141 and miR-200a act on ovarian tumorigenesis by controlling oxidative stress response. Nat Med, 2011. **17**(12): p. 1627-35.
139. Bendoraite, A., et al., Regulation of miR-200 family microRNAs and ZEB transcription factors in ovarian cancer: evidence supporting a mesothelial-to-epithelial transition. Gynecol Oncol, 2010. **116**(1): p. 117-25.
140. Ferlay, J., et al., Cancer incidence and mortality worldwide: sources, methods and major patterns in GLOBOCAN 2012. Int J Cancer, 2015. **136**(5): p. E359-86.
141. Chua, M.L., et al., Nasopharyngeal carcinoma. Lancet, 2016. **387**(10022): p. 1012-24.
142. Chua, M.L., et al., Nasopharyngeal carcinoma. Lancet, 2015.
143. Sham, J.S., et al., Nasopharyngeal carcinoma in young patients. Cancer, 1990. **65**(11): p. 2606-10.
144. Miller, D., The etiology of nasopharyngeal cancer and its management. Otolaryngol Clin North Am, 1980. **13**(3): p. 467-75.
145. Pearson, G.R., et al., Application of Epstein-Barr virus (EBV) serology to the diagnosis of North American nasopharyngeal carcinoma. Cancer, 1983. **51**(2): p. 260-8.
146. Krueger, G.R., et al., Histological types of nasopharyngeal carcinoma as compared to EBV serology. Anticancer research, 1981. **1**(4): p. 187-94.
147. Leung, S.F., et al., Improved accuracy of detection of nasopharyngeal carcinoma by combined application of circulating Epstein-Barr virus DNA and anti-Epstein-Barr viral capsid antigen IgA antibody. Clin Chem, 2004. **50**(2): p. 339-45.
148. Thompson, L.D., Update on nasopharyngeal carcinoma. Head Neck Pathol, 2007. **1**(1): p. 81-6.
149. Li, Y.Y., et al., Exome and genome sequencing of nasopharynx cancer identifies NF-kappaB pathway activating mutations. Nature communications, 2017. **8**: p. 14121.
150. Wei, W.I. and J.S. Sham, Nasopharyngeal carcinoma. Lancet, 2005. **365**(9476): p. 2041-54.

151. Sobin, L.H. and C.C. Compton, TNM seventh edition: what's new, what's changed: communication from the International Union Against Cancer and the American Joint Committee on Cancer. Cancer, 2010. **116**(22): p. 5336-9.
152. Lee, N., et al., Intensity-modulated radiation therapy with or without chemotherapy for nasopharyngeal carcinoma: radiation therapy oncology group phase II trial 0225. J Clin Oncol, 2009. **27**(22): p. 3684-90.
153. Chen, Y., et al., Progress report of a randomized trial comparing long-term survival and late toxicity of concurrent chemoradiotherapy with adjuvant chemotherapy versus radiotherapy alone in patients with stage III to IVB nasopharyngeal carcinoma from endemic regions of China. Cancer, 2013. **119**(12): p. 2230-8.
154. Zhang, A.M., et al., Increased treatment-related mortality with additional cisplatin-based chemotherapy in patients with nasopharyngeal carcinoma treated with standard radiotherapy. Radiother Oncol, 2012. **104**(3): p. 279-85.
155. Tian, R., et al., Use of taxane-containing induction chemotherapy in combination with concurrent chemoradiotherapy in Chinese patients with locally advanced nasopharyngeal carcinoma: a meta-analysis. Onco Targets Ther, 2015. **8**: p. 3255-63.
156. Tan, W.L., et al., Advances in systemic treatment for nasopharyngeal carcinoma. Chin Clin Oncol, 2016. **5**(2): p. 21.
157. Jang-Chun, L., et al., Comparisons of quality of life for patients with nasopharyngeal carcinoma after treatment with different RT technologies. Acta Otorhinolaryngol Ital, 2014. **34**(4): p. 241-6.
158. Bruce, J.P., et al., Nasopharyngeal Cancer: Molecular Landscape. J Clin Oncol, 2015. **33**(29): p. 3346-55.
159. Chang, E.T. and H.O. Adami, The enigmatic epidemiology of nasopharyngeal carcinoma. Cancer Epidemiol Biomarkers Prev, 2006. **15**(10): p. 1765-77.
160. Hsu, W.L., et al., Familial tendency and risk of nasopharyngeal carcinoma in taiwan: effects of covariates on risk. Am J Epidemiol, 2011. **173**(3): p. 292-9.
161. Hildesheim, A. and C.P. Wang, Genetic predisposition factors and nasopharyngeal carcinoma risk: a review of epidemiological association studies, 2000-2011: Rosetta Stone for NPC: genetics, viral infection, and other environmental factors. Seminars in cancer biology, 2012. **22**(2): p. 107-16.
162. Bei, J.X., et al., A genome-wide association study of nasopharyngeal carcinoma identifies three new susceptibility loci. Nature genetics, 2010. **42**(7): p. 599-603.

163. Zhao, M., et al., Further evidence for the existence of major susceptibility of nasopharyngeal carcinoma in the region near HLA-A locus in Southern Chinese. J Transl Med, 2012. **10**: p. 57.
164. Chin, Y.M., et al., HLA-A SNPs and amino acid variants are associated with nasopharyngeal carcinoma in Malaysian Chinese. Int J Cancer, 2015. **136**(3): p. 678-87.
165. Rickinson, A.B. and D.J. Moss, Human cytotoxic T lymphocyte responses to Epstein-Barr virus infection. Annu Rev Immunol, 1997. **15**: p. 405-31.
166. Hsu, W.L., et al., Evaluation of human leukocyte antigen-A (HLA-A), other non-HLA markers on chromosome 6p21 and risk of nasopharyngeal carcinoma. PLoS One, 2012. **7**(8): p. e42767.
167. Skibola, C.F., et al., Genetic variants at 6p21.33 are associated with susceptibility to follicular lymphoma. Nature genetics, 2009. **41**(8): p. 873-5.
168. Tse, K.P., et al., Genome-wide association study reveals multiple nasopharyngeal carcinoma-associated loci within the HLA region at chromosome 6p21.3. Am J Hum Genet, 2009. **85**(2): p. 194-203.
169. Ng, C.C., et al., A genome-wide association study identifies ITGA9 conferring risk of nasopharyngeal carcinoma. J Hum Genet, 2009. **54**(7): p. 392-7.
170. Chou, J., et al., Nasopharyngeal carcinoma--review of the molecular mechanisms of tumorigenesis. Head & neck, 2008. **30**(7): p. 946-63.
171. Yee Ko, J.M., et al., Multigene pathway-based analyses identify nasopharyngeal carcinoma risk associations for cumulative adverse effects of TERT-CLPTM1L and DNA double-strand breaks repair. Int J Cancer, 2014. **135**(7): p. 1634-45.
172. Pathmanathan, R., et al., Clonal proliferations of cells infected with Epstein-Barr virus in preinvasive lesions related to nasopharyngeal carcinoma. The New England journal of medicine, 1995. **333**(11): p. 693-8.
173. Raab-Traub, N. and K. Flynn, The structure of the termini of the Epstein-Barr virus as a marker of clonal cellular proliferation. Cell, 1986. **47**(6): p. 883-9.
174. Sam, C.K., et al., Analysis of Epstein-Barr virus infection in nasopharyngeal biopsies from a group at high risk of nasopharyngeal carcinoma. Int J Cancer, 1993. **53**(6): p. 957-62.
175. Chan, A.S., et al., High frequency of chromosome 3p deletion in histologically normal nasopharyngeal epithelia from southern Chinese. Cancer Res, 2000. **60**(19): p. 5365-70.

176. Chan, A.S., et al., Frequent chromosome 9p losses in histologically normal nasopharyngeal epithelia from southern Chinese. Int J Cancer, 2002. **102**(3): p. 300-3.
177. Knox, P.G., et al., In vitro production of stable Epstein-Barr virus-positive epithelial cell clones which resemble the virus:cell interaction observed in nasopharyngeal carcinoma. Virology, 1996. **215**(1): p. 40-50.
178. Tsang, C.M., et al., Cyclin D1 overexpression supports stable EBV infection in nasopharyngeal epithelial cells. Proceedings of the National Academy of Sciences of the United States of America, 2012. **109**(50): p. E3473-82.
179. Young, L.S. and C.W. Dawson, Epstein-Barr virus and nasopharyngeal carcinoma. Chin J Cancer, 2014. **33**(12): p. 581-90.
180. Li, H.M., et al., Molecular and cytogenetic changes involved in the immortalization of nasopharyngeal epithelial cells by telomerase. Int J Cancer, 2006. **119**(7): p. 1567-76.
181. Chow, L.S., et al., Identification of RASSF1A modulated genes in nasopharyngeal carcinoma. Oncogene, 2006. **25**(2): p. 310-6.
182. Song, S.J., et al., Aurora A regulates prometaphase progression by inhibiting the ability of RASSF1A to suppress APC-Cdc20 activity. Cancer Res, 2009. **69**(6): p. 2314-23.
183. Li, H.M., et al., Epstein-Barr virus latent membrane protein 1 (LMP1) upregulates Id1 expression in nasopharyngeal epithelial cells. Oncogene, 2004. **23**(25): p. 4488-94.
184. Hatzivassiliou, E. and G. Mosialos, Cellular signaling pathways engaged by the Epstein-Barr virus transforming protein LMP1. Front Biosci, 2002. **7**: p. d319-29.
185. Lin, D.C., et al., The genomic landscape of nasopharyngeal carcinoma. Nature genetics, 2014. **46**(8): p. 866-71.
186. Wang, G.L., et al., Inhibiting tumorigenic potential by restoration of p16 in nasopharyngeal carcinoma. Br J Cancer, 1999. **81**(7): p. 1122-6.
187. Chan, S.L., et al., The tumor suppressor Wnt inhibitory factor 1 is frequently methylated in nasopharyngeal and esophageal carcinomas. Lab Invest, 2007. **87**(7): p. 644-50.
188. Hui, A.B., et al., Epigenetic inactivation of TSLC1 gene in nasopharyngeal carcinoma. Mol Carcinog, 2003. **38**(4): p. 170-8.
189. Lung, H.L., et al., TSLC1 is a tumor suppressor gene associated with metastasis in nasopharyngeal carcinoma. Cancer Res, 2006. **66**(19): p. 9385-92.

190. Li, H.P., et al., Silencing of miRNA-148a by hypermethylation activates the integrin-mediated signaling pathway in nasopharyngeal carcinoma. Oncotarget, 2014. **5**(17): p. 7610-24.
191. Alajez, N.M., et al., MiR-218 suppresses nasopharyngeal cancer progression through downregulation of survivin and the SLIT2-ROBO1 pathway. Cancer Res, 2011. **71**(6): p. 2381-91.
192. Cheung, C.C., et al., miR-31 is consistently inactivated in EBV-associated nasopharyngeal carcinoma and contributes to its tumorigenesis. Mol Cancer, 2014. **13**: p. 184.
193. Alajez, N.M., et al., Enhancer of Zeste homolog 2 (EZH2) is overexpressed in recurrent nasopharyngeal carcinoma and is regulated by miR-26a, miR-101, and miR-98. Cell Death Dis, 2010. **1**: p. e85.
194. Tong, Z.T., et al., EZH2 supports nasopharyngeal carcinoma cell aggressiveness by forming a co-repressor complex with HDAC1/HDAC2 and Snail to inhibit E-cadherin. Oncogene, 2012. **31**(5): p. 583-94.
195. Ye, S.B., et al., Exosomal miR-24-3p impedes T-cell function by targeting FGF11 and serves as a potential prognostic biomarker for nasopharyngeal carcinoma. J Pathol, 2016. **240**(3): p. 329-340.
196. Kapetanakis, N.-I., V. Baloche, and P. Busson, Tumor exosomal microRNAs thwarting anti-tumor immune responses in nasopharyngeal carcinomas. Annals of Translational Medicine, 2017. **5**(7).
197. Hui, A.B., et al., Detection of recurrent chromosomal gains and losses in primary nasopharyngeal carcinoma by comparative genomic hybridisation. Int J Cancer, 1999. **82**(4): p. 498-503.
198. Or, Y.Y., et al., PIK3CA mutations in nasopharyngeal carcinoma. Int J Cancer, 2006. **118**(4): p. 1065-7.
199. Or, Y.Y., et al., Identification of a novel 12p13.3 amplicon in nasopharyngeal carcinoma. J Pathol, 2010. **220**(1): p. 97-107.
200. Dittmer, D.P., et al., Multiple pathways for Epstein-Barr virus episome loss from nasopharyngeal carcinoma. Int J Cancer, 2008. **123**(9): p. 2105-12.
201. Cheung, S.T., et al., Nasopharyngeal carcinoma cell line (C666-1) consistently harbouring Epstein-Barr virus. Int J Cancer, 1999. **83**(1): p. 121-6.
202. Busson, P., et al., Establishment and characterization of three transplantable EBV-containing nasopharyngeal carcinomas. Int J Cancer, 1988. **42**(4): p. 599-606.

203. Effert, P., et al., Alterations of the p53 gene in nasopharyngeal carcinoma. J Virol, 1992. **66**(6): p. 3768-75.
204. Feng, W.H., et al., Chemotherapy induces lytic EBV replication and confers ganciclovir susceptibility to EBV-positive epithelial cell tumors. Cancer Res, 2002. **62**(6): p. 1920-6.
205. Chung, G.T., et al., Constitutive activation of distinct NF-kappaB signals in EBV-associated nasopharyngeal carcinoma. J Pathol, 2013. **231**(3): p. 311-22.
206. Old, L.J., et al., Precipitating antibody in human serum to an antigen present in cultured burkitt's lymphoma cells. Proc Natl Acad Sci U S A, 1966. **56**(6): p. 1699-704.
207. Wolf, H., H. zur Hausen, and V. Becker, EB viral genomes in epithelial nasopharyngeal carcinoma cells. Nat New Biol, 1973. **244**(138): p. 245-7.
208. Zeng, Y., et al., Prospective studies on nasopharyngeal carcinoma in Epstein-Barr virus IgA/VCA antibody-positive persons in Wuzhou City, China. Int J Cancer, 1985. **36**(5): p. 545-7.
209. Chan, K.H., et al., Epstein-Barr virus (EBV) infection in infancy. J Clin Virol, 2001. **21**(1): p. 57-62.
210. Tse, E. and Y.L. Kwong, How I treat NK/T-cell lymphomas. Blood, 2013. **121**(25): p. 4997-5005.
211. Flavell, K.J. and P.G. Murray, Hodgkin's disease and the Epstein-Barr virus. Mol Pathol, 2000. **53**(5): p. 262-9.
212. Epstein, M.A. and Y.M. Barr, Cultivation in Vitro of Human Lymphoblasts from Burkitt's Malignant Lymphoma. Lancet, 1964. **1**(7327): p. 252-3.
213. Iizasa, H., et al., Epstein-Barr Virus (EBV)-associated gastric carcinoma. Viruses, 2012. **4**(12): p. 3420-39.
214. Ascherio, A., K.L. Munger, and J.D. Lunemann, The initiation and prevention of multiple sclerosis. Nat Rev Neurol, 2012. **8**(11): p. 602-12.
215. Draborg, A.H., K. Duus, and G. Houen, Epstein-Barr virus in systemic autoimmune diseases. Clin Dev Immunol, 2013. **2013**: p. 535738.
216. Hu, Z. and E.J. Usherwood, Immune escape of gamma-herpesviruses from adaptive immunity. Rev Med Virol, 2014.
217. Miller, G., et al., Lytic cycle switches of oncogenic human gammaherpesviruses. Advances in cancer research, 2007. **97**: p. 81-109.

218. Oker, N., N.-I. Kapetanakis, and P. Busson, Review: Biological and Pharmacological Basis of Cytolytic Viral Activation in EBV-Associated Nasopharyngeal Carcinoma, in Herpesviridae, J. Ongradi, Editor. 2016, InTech: Rijeka. p. Ch. 06.
219. Neitzel, H., A routine method for the establishment of permanent growing lymphoblastoid cell lines. Hum Genet, 1986. **73**(4): p. 320-6.
220. Young, L.S. and A.B. Rickinson, Epstein-Barr virus: 40 years on. Nat Rev Cancer, 2004. **4**(10): p. 757-68.
221. Tao, Q., et al., Epstein-Barr virus (EBV) and its associated human cancers--genetics, epigenetics, pathobiology and novel therapeutics. Front Biosci, 2006. **11**: p. 2672-713.
222. Kelly, G., A. Bell, and A. Rickinson, Epstein-Barr virus-associated Burkitt lymphomagenesis selects for downregulation of the nuclear antigen EBNA2. Nature medicine, 2002. **8**(10): p. 1098-104.
223. Brooks, L., et al., Epstein-Barr virus latent gene transcription in nasopharyngeal carcinoma cells: coexpression of EBNA1, LMP1, and LMP2 transcripts. J Virol, 1992. **66**(5): p. 2689-97.
224. Deacon, E.M., et al., Epstein-Barr virus and Hodgkin's disease: transcriptional analysis of virus latency in the malignant cells. J Exp Med, 1993. **177**(2): p. 339-49.
225. Pallesen, G., et al., Expression of Epstein-Barr virus latent gene products in tumour cells of Hodgkin's disease. Lancet, 1991. **337**(8737): p. 320-2.
226. Young, L.S., et al., Epstein-Barr virus gene expression in nasopharyngeal carcinoma. J Gen Virol, 1988. **69 (Pt 5)**: p. 1051-65.
227. Tempera, I., M. Klichinsky, and P.M. Lieberman, EBV latency types adopt alternative chromatin conformations. PLoS Pathog, 2011. **7**(7): p. e1002180.
228. Chen, H., et al., Linkage between STAT regulation and Epstein-Barr virus gene expression in tumors. J Virol, 2001. **75**(6): p. 2929-37.
229. Frappier, L., Role of EBNA1 in NPC tumourigenesis. Semin Cancer Biol, 2012. **22**(2): p. 154-61.
230. Gruhne, B., et al., The Epstein-Barr virus nuclear antigen-1 promotes genomic instability via induction of reactive oxygen species. Proc Natl Acad Sci U S A, 2009. **106**(7): p. 2313-8.
231. Dawson, C.W., R.J. Port, and L.S. Young, The role of the EBV-encoded latent membrane proteins LMP1 and LMP2 in the pathogenesis of nasopharyngeal carcinoma (NPC). Seminars in cancer biology, 2012. **22**(2): p. 144-53.

232. Dawson, C.W., A.B. Rickinson, and L.S. Young, Epstein-Barr virus latent membrane protein inhibits human epithelial cell differentiation. Nature, 1990. **344**(6268): p. 777-80.
233. Ohtani, N., et al., Epstein-Barr virus LMP1 blocks p16INK4a-RB pathway by promoting nuclear export of E2F4/5. J Cell Biol, 2003. **162**(2): p. 173-83.
234. Zhao, Y., et al., LMP1 expression is positively associated with metastasis of nasopharyngeal carcinoma: evidence from a meta-analysis. J Clin Pathol, 2012. **65**(1): p. 41-5.
235. Longnecker, R., Epstein-Barr virus latency: LMP2, a regulator or means for Epstein-Barr virus persistence? Advances in cancer research, 2000. **79**: p. 175-200.
236. Shah, K.M., et al., The EBV-encoded latent membrane proteins, LMP2A and LMP2B, limit the actions of interferon by targeting interferon receptors for degradation. Oncogene, 2009. **28**(44): p. 3903-14.
237. Li, Q.X., et al., Epstein-Barr virus infection and replication in a human epithelial cell system. Nature, 1992. **356**(6367): p. 347-50.
238. Seto, E., et al., Epstein-Barr virus (EBV)-encoded BARF1 gene is expressed in nasopharyngeal carcinoma and EBV-associated gastric carcinoma tissues in the absence of lytic gene expression. J Med Virol, 2005. **76**(1): p. 82-8.
239. Feederle, R., et al., The Epstein-Barr virus alkaline exonuclease BGLF5 serves pleiotropic functions in virus replication. J Virol, 2009. **83**(10): p. 4952-62.
240. Wu, C.C., et al., Epstein-Barr virus DNase (BGLF5) induces genomic instability in human epithelial cells. Nucleic Acids Res, 2010. **38**(6): p. 1932-49.
241. Liu, M.Y., et al., Expression of the Epstein-Barr virus BHRF1 gene, a homologue of Bcl-2, in nasopharyngeal carcinoma tissue. J Med Virol, 2000. **61**(2): p. 241-50.
242. Takada, K., Role of EBER and BARF1 in nasopharyngeal carcinoma (NPC) tumorigenesis. Seminars in cancer biology, 2012. **22**(2): p. 162-5.
243. Cosmopoulos, K., et al., Comprehensive profiling of Epstein-Barr virus microRNAs in nasopharyngeal carcinoma. J Virol, 2009. **83**(5): p. 2357-67.
244. Gilligan, K., et al., Novel transcription from the Epstein-Barr virus terminal EcoRI fragment, DIJhet, in a nasopharyngeal carcinoma. J Virol, 1990. **64**(10): p. 4948-56.
245. Robertson, E.S., B. Tomkinson, and E. Kieff, An Epstein-Barr virus with a 58-kilobase-pair deletion that includes BARF0 transforms B lymphocytes in vitro. J Virol, 1994. **68**(3): p. 1449-58.

246. Marquitz, A.R. and N. Raab-Traub, The role of miRNAs and EBV BARTs in NPC. Seminars in cancer biology, 2012. **22**(2): p. 166-72.
247. Kim, D.N., Y.J. Song, and S.K. Lee, The role of promoter methylation in Epstein-Barr virus (EBV) microRNA expression in EBV-infected B cell lines. Exp Mol Med, 2011. **43**(7): p. 401-10.
248. Al-Mozaini, M., et al., Epstein-Barr virus BART gene expression. J Gen Virol, 2009. **90**(Pt 2): p. 307-16.
249. Kang, D., R.L. Skalsky, and B.R. Cullen, EBV BART MicroRNAs Target Multiple Pro-apoptotic Cellular Genes to Promote Epithelial Cell Survival. PLoS Pathog, 2015. **11**(6): p. e1004979.
250. Cai, L., et al., Epstein-Barr virus-encoded microRNA BART1 induces tumour metastasis by regulating PTEN-dependent pathways in nasopharyngeal carcinoma. Nature communications, 2015. **6**: p. 7353.
251. Choy, E.Y., et al., An Epstein-Barr virus-encoded microRNA targets PUMA to promote host cell survival. J Exp Med, 2008. **205**(11): p. 2551-60.
252. Marquitz, A.R., et al., The Epstein-Barr Virus BART microRNAs target the pro-apoptotic protein Bim. Virology, 2011. **412**(2): p. 392-400.
253. Dolken, L., et al., Systematic analysis of viral and cellular microRNA targets in cells latently infected with human gamma-herpesviruses by RISC immunoprecipitation assay. Cell Host Microbe, 2010. **7**(4): p. 324-34.
254. Nachmani, D., et al., Diverse herpesvirus microRNAs target the stress-induced immune ligand MICB to escape recognition by natural killer cells. Cell Host Microbe, 2009. **5**(4): p. 376-85.
255. Iizasa, H., et al., Editing of Epstein-Barr virus-encoded BART6 microRNAs controls their dicer targeting and consequently affects viral latency. J Biol Chem, 2010. **285**(43): p. 33358-70.
256. Lo, A.K., et al., Modulation of LMP1 protein expression by EBV-encoded microRNAs. Proc Natl Acad Sci U S A, 2007. **104**(41): p. 16164-9.
257. Lung, R.W., et al., Modulation of LMP2A expression by a newly identified Epstein-Barr virus-encoded microRNA miR-BART22. Neoplasia, 2009. **11**(11): p. 1174-84.
258. Klinke, O., R. Feederle, and H.J. Delecluse, Genetics of Epstein-Barr virus microRNAs. Seminars in cancer biology, 2014. **26**: p. 52-9.
259. Xing, L. and E. Kieff, Epstein-Barr virus BHRF1 micro- and stable RNAs during latency III and after induction of replication. J Virol, 2007. **81**(18): p. 9967-75.

260. Amoroso, R., et al., Quantitative studies of Epstein-Barr virus-encoded microRNAs provide novel insights into their regulation. J Virol, 2011. **85**(2): p. 996-1010.
261. Cai, X., et al., Epstein-Barr virus microRNAs are evolutionarily conserved and differentially expressed. PLoS Pathog, 2006. **2**(3): p. e23.
262. Feederle, R., et al., A viral microRNA cluster strongly potentiates the transforming properties of a human herpesvirus. PLoS Pathog, 2011. **7**(2): p. e1001294.
263. Seto, E., et al., Micro RNAs of Epstein-Barr virus promote cell cycle progression and prevent apoptosis of primary human B cells. PLoS Pathog, 2010. **6**(8): p. e1001063.
264. Bernhardt, K., et al., A Viral microRNA Cluster Regulates the Expression of PTEN, p27 and of a bcl-2 Homolog. PLoS Pathog, 2016. **12**(1): p. e1005405.
265. Milian, E., et al., BHRF1 exerts an antiapoptotic effect and cell cycle arrest via Bcl-2 in murine hybridomas. J Biotechnol, 2015. **209**: p. 58-67.
266. Skalsky, R.L. and B.R. Cullen, EBV Noncoding RNAs. Current topics in microbiology and immunology, 2015. **391**: p. 181-217.
267. Lo, Y.M., et al., Quantitative analysis of cell-free Epstein-Barr virus DNA in plasma of patients with nasopharyngeal carcinoma. Cancer Res, 1999. **59**(6): p. 1188-91.
268. Chan, K.C., et al., Molecular characterization of circulating EBV DNA in the plasma of nasopharyngeal carcinoma and lymphoma patients. Cancer Res, 2003. **63**(9): p. 2028-32.
269. Gourzones, C., et al., Consistent high concentration of the viral microRNA BART17 in plasma samples from nasopharyngeal carcinoma patients--evidence of non-exosomal transport. Virol J, 2013. **10**: p. 119.
270. Presta, L.G., et al., Humanization of an anti-vascular endothelial growth factor monoclonal antibody for the therapy of solid tumors and other disorders. Cancer Res, 1997. **57**(20): p. 4593-9.
271. Burger, R.A., et al., Incorporation of bevacizumab in the primary treatment of ovarian cancer. The New England journal of medicine, 2011. **365**(26): p. 2473-83.
272. Ye, B., A. Gagnon, and S.C. Mok, Recent technical strategies to identify diagnostic biomarkers for ovarian cancer. Expert Rev Proteomics, 2007. **4**(1): p. 121-31.
273. Das, P.M. and R.C. Bast, Jr., Early detection of ovarian cancer. Biomark Med, 2008. **2**(3): p. 291-303.
274. Zurawski, V.R., Jr., et al., Elevated serum CA 125 levels prior to diagnosis of ovarian neoplasia: relevance for early detection of ovarian cancer. Int J Cancer, 1988. **42**(5): p. 677-80.

275. Soletormos, G., et al., Clinical Use of Cancer Biomarkers in Epithelial Ovarian Cancer: Updated Guidelines From the European Group on Tumor Markers. Int J Gynecol Cancer, 2016. **26**(1): p. 43-51.
276. Jacobs, I. and R.C. Bast, Jr., The CA 125 tumour-associated antigen: a review of the literature. Hum Reprod, 1989. **4**(1): p. 1-12.
277. Duffy, M.J., et al., CA125 in ovarian cancer: European Group on Tumor Markers guidelines for clinical use. Int J Gynecol Cancer, 2005. **15**(5): p. 679-91.
278. Bast, R.C., Jr., CA 125 and the detection of recurrent ovarian cancer: a reasonably accurate biomarker for a difficult disease. Cancer, 2010. **116**(12): p. 2850-3.
279. Sorm, F., et al., 5-Azacytidine, a new, highly effective cancerostatic. Experientia, 1964. **20**(4): p. 202-3.
280. Cihak, A., Biological effects of 5-azacytidine in eukaryotes. Oncology, 1974. **30**(5): p. 405-22.
281. Li, L.H., et al., Cytotoxicity and mode of action of 5-azacytidine on L1210 leukemia. Cancer Res, 1970. **30**(11): p. 2760-9.
282. Flatau, E., et al., DNA methylation in 5-aza-2'-deoxycytidine-resistant variants of C3H 10T1/2 C18 cells. Mol Cell Biol, 1984. **4**(10): p. 2098-102.
283. Momparler, R.L., et al., Kinetic interaction of 5-AZA-2'-deoxycytidine-5'-monophosphate and its 5'-triphosphate with deoxycytidylate deaminase. Mol Pharmacol, 1984. **25**(3): p. 436-40.
284. Vesely, J., et al., Radioprotective effect of 5-azacytidine in AKR mice. Z Naturforsch B, 1969. **24**(3): p. 318-20.
285. Choy, M.K., et al., Genome-wide conserved consensus transcription factor binding motifs are hyper-methylated. BMC Genomics, 2010. **11**: p. 519.
286. Christman, J.K., et al., Effect of 5-azacytidine on differentiation and DNA methylation in human promyelocytic leukemia cells (HL-60). Cancer Res, 1983. **43**(2): p. 763-9.
287. Stresemann, C. and F. Lyko, Modes of action of the DNA methyltransferase inhibitors azacytidine and decitabine. Int J Cancer, 2008. **123**(1): p. 8-13.
288. Navada, S.C., et al., Clinical development of demethylating agents in hematology. J Clin Invest, 2014. **124**(1): p. 40-6.
289. Lu, L.J. and K. Randerath, Mechanism of 5-azacytidine-induced transfer RNA cytosine-5-methyltransferase deficiency. Cancer Res, 1980. **40**(8 Pt 1): p. 2701-5.
290. Lee, T.T. and M.R. Karon, Inhibition of protein synthesis in 5-azacytidine-treated HeLa cells. Biochem Pharmacol, 1976. **25**(15): p. 1737-42.

291. Glazer, R.I., et al., The effect of 5-azacytidine and dihydro-5-azacytidine on nuclear ribosomal RNA and poly(A) RNA synthesis in L1210 cells in vitro. Mol Pharmacol, 1980. **17**(1): p. 111-7.
292. Weiss, J.W. and H.C. Pitot, Inhibition of ribosomal ribonucleic acid maturation by 5-azacytidine and 8-azaguanine in Novikoff hepatoma cells. Arch Biochem Biophys, 1974. **160**(1): p. 119-29.
293. Issa, J.P., CpG island methylator phenotype in cancer. Nat Rev Cancer, 2004. **4**(12): p. 988-93.
294. Christman, J.K., 5-Azacytidine and 5-aza-2'-deoxycytidine as inhibitors of DNA methylation: mechanistic studies and their implications for cancer therapy. Oncogene, 2002. **21**(35): p. 5483-95.
295. Savona, M.R., et al., CC-486 (Oral Azacitidine) Monotherapy in Patients with Acute Myeloid Leukemia (AML). Blood, 2015. **126**(23): p. 452-452.
296. Mesia, R., et al., Interim results from a phase II study of CC-486 in previously treated patients (pts) with locally advanced/metastatic nasopharyngeal cancer (NPC). Journal of Clinical Oncology, 2016. **34**(15_suppl): p. 6029-6029.
297. Chan, A.T., et al., Azacitidine induces demethylation of the Epstein-Barr virus genome in tumors. J Clin Oncol, 2004. **22**(8): p. 1373-81.
298. Rodriguez, A., E.J. Jung, and E.K. Flemington, Cell cycle analysis of Epstein-Barr virus-infected cells following treatment with lytic cycle-inducing agents. J Virol, 2001. **75**(10): p. 4482-9.
299. Feederle, R., et al., The Epstein-Barr virus lytic program is controlled by the co-operative functions of two transactivators. EMBO J, 2000. **19**(12): p. 3080-9.
300. Farrell, P.J., et al., Epstein-Barr virus BZLF1 trans-activator specifically binds to a consensus AP-1 site and is related to c-fos. EMBO J, 1989. **8**(1): p. 127-32.
301. Sinclair, A.J., bZIP proteins of human gammaherpesviruses. J Gen Virol, 2003. **84**(Pt 8): p. 1941-9.
302. Yu, X., Z. Wang, and J.E. Mertz, ZEB1 regulates the latent-lytic switch in infection by Epstein-Barr virus. PLoS Pathog, 2007. **3**(12): p. e194.
303. Wille, C.K., et al., 5-hydroxymethylation of the EBV genome regulates the latent to lytic switch. Proc Natl Acad Sci U S A, 2015. **112**(52): p. E7257-65.
304. Wille, C.K., et al., Viral genome methylation differentially affects the ability of BZLF1 versus BRLF1 to activate Epstein-Barr virus lytic gene expression and viral replication. J Virol, 2013. **87**(2): p. 935-50.

305. Cayrol, C. and E.K. Flemington, The Epstein-Barr virus bZIP transcription factor Zta causes G0/G1 cell cycle arrest through induction of cyclin-dependent kinase inhibitors. EMBO J, 1996. **15**(11): p. 2748-59.
306. Feng, W.H., et al., Lytic induction therapy for Epstein-Barr virus-positive B-cell lymphomas. J Virol, 2004. **78**(4): p. 1893-902.
307. Gourzones, C., et al., Extra-cellular release and blood diffusion of BART viral micro-RNAs produced by EBV-infected nasopharyngeal carcinoma cells. Virol J, 2010. **7**: p. 271.
308. Hu, X., et al., A miR-200 microRNA cluster as prognostic marker in advanced ovarian cancer. Gynecol Oncol, 2009. **114**(3): p. 457-64.
309. Kan, C.W., et al., Elevated levels of circulating microRNA-200 family members correlate with serous epithelial ovarian cancer. BMC Cancer, 2012. **12**: p. 627.
310. Zheng, H., et al., Plasma miRNAs as diagnostic and prognostic biomarkers for ovarian cancer. PLoS One, 2013. **8**(11): p. e77853.
311. Zuberi, M., et al., Expression of serum miR-200a, miR-200b, and miR-200c as candidate biomarkers in epithelial ovarian cancer and their association with clinicopathological features. Clin Transl Oncol, 2015. **17**(10): p. 779-87.
312. Gao, Y.C. and J. Wu, MicroRNA-200c and microRNA-141 as potential diagnostic and prognostic biomarkers for ovarian cancer. Tumour Biol, 2015. **36**(6): p. 4843-50.
313. Xu, Y.Z., et al., Identification of serum microRNA-21 as a biomarker for early detection and prognosis in human epithelial ovarian cancer. Asian Pac J Cancer Prev, 2013. **14**(2): p. 1057-60.
314. Meng, X., et al., Circulating Cell-Free miR-373, miR-200a, miR-200b and miR-200c in Patients with Epithelial Ovarian Cancer. Adv Exp Med Biol, 2016. **924**: p. 3-8.
315. Meng, X., et al., Diagnostic and prognostic relevance of circulating exosomal miR-373, miR-200a, miR-200b and miR-200c in patients with epithelial ovarian cancer. Oncotarget, 2016. **7**(13): p. 16923-35.
316. Mackay, I.M., K.E. Arden, and A. Nitsche, Real-time PCR in virology. Nucleic Acids Res, 2002. **30**(6): p. 1292-305.
317. Muralidhar, G.G. and M.V. Barbolina, The miR-200 Family: Versatile Players in Epithelial Ovarian Cancer. Int J Mol Sci, 2015. **16**(8): p. 16833-47.
318. Humphries, B. and C. Yang, The microRNA-200 family: small molecules with novel roles in cancer development, progression and therapy. Oncotarget, 2015. **6**(9): p. 6472-98.

319. Eichelser, C., et al., Increased serum levels of circulating exosomal microRNA-373 in receptor-negative breast cancer patients. Oncotarget, 2014. **5**(20): p. 9650-63.
320. Koutsaki, M., et al., The miR-200 family in ovarian cancer. Oncotarget, 2017.
321. Benson, E.A., et al., Carboplatin with Decitabine Therapy, in Recurrent Platinum Resistant Ovarian Cancer, Alters Circulating miRNAs Concentrations: A Pilot Study. PLoS One, 2015. **10**(10): p. e0141279.
322. Nakamura, K., et al., Clinical relevance of circulating cell-free microRNAs in ovarian cancer. Mol Cancer, 2016. **15**(1): p. 48.
323. Rapisuwon, S., E.E. Vietsch, and A. Wellstein, Circulating biomarkers to monitor cancer progression and treatment. Comput Struct Biotechnol J, 2016. **14**: p. 211-22.
324. Armand-Labit, V. and A. Pradines, Circulating cell-free microRNAs as clinical cancer biomarkers. Biomol Concepts, 2017. **8**(2): p. 61-81.
325. Vaksman, O., et al., Exosome-derived miRNAs and ovarian carcinoma progression. Carcinogenesis, 2014. **35**(9): p. 2113-20.
326. Au Yeung, C.L., et al., Exosomal transfer of stroma-derived miR21 confers paclitaxel resistance in ovarian cancer cells through targeting APAF1. Nature communications, 2016. **7**: p. 11150.
327. Wang, X., et al., Aberrant expression of oncogenic and tumor-suppressive microRNAs in cervical cancer is required for cancer cell growth. PLoS One, 2008. **3**(7): p. e2557.
328. Marabita, F., et al., Normalization of circulating microRNA expression data obtained by quantitative real-time RT-PCR. Brief Bioinform, 2016. **17**(2): p. 204-12.
329. Suryawanshi, S., et al., Plasma microRNAs as novel biomarkers for endometriosis and endometriosis-associated ovarian cancer. Clinical cancer research : an official journal of the American Association for Cancer Research, 2013. **19**(5): p. 1213-24.
330. Shapira, I., et al., Circulating biomarkers for detection of ovarian cancer and predicting cancer outcomes. Br J Cancer, 2014. **110**(4): p. 976-83.
331. Mestdagh, P., et al., A novel and universal method for microRNA RT-qPCR data normalization. Genome Biol, 2009. **10**(6): p. R64.
332. Hindson, B.J., et al., High-throughput droplet digital PCR system for absolute quantitation of DNA copy number. Anal Chem, 2011. **83**(22): p. 8604-10.
333. Campomenosi, P., et al., A comparison between quantitative PCR and droplet digital PCR technologies for circulating microRNA quantification in human lung cancer. BMC Biotechnol, 2016. **16**(1): p. 60.

334. Chapin, S.C., et al., Rapid microRNA profiling on encoded gel microparticles. Angew Chem Int Ed Engl, 2011. **50**(10): p. 2289-93.
335. Jin, Z., et al., A Rapid, Amplification-Free, and Sensitive Diagnostic Assay for Single-Step Multiplexed Fluorescence Detection of MicroRNA. Angew Chem Int Ed Engl, 2015. **54**(34): p. 10024-9.
336. Feederle, R., et al., The members of an Epstein-Barr virus microRNA cluster cooperate to transform B lymphocytes. J Virol, 2011. **85**(19): p. 9801-10.
337. Xing, L. and E. Kieff, cis-Acting effects on RNA processing and Drosha cleavage prevent Epstein-Barr virus latency III BHRF1 expression. J Virol, 2011. **85**(17): p. 8929-39.
338. Cox, M.A., J. Leahy, and J.M. Hardwick, An enhancer within the divergent promoter of Epstein-Barr virus responds synergistically to the R and Z transactivators. J Virol, 1990. **64**(1): p. 313-21.
339. Austin, P.J., et al., Complex transcription of the Epstein-Barr virus BamHI fragment H rightward open reading frame 1 (BHRF1) in latently and lytically infected B lymphocytes. Proc Natl Acad Sci U S A, 1988. **85**(11): p. 3678-82.
340. Alfieri, C., M. Birkenbach, and E. Kieff, Early events in Epstein-Barr virus infection of human B lymphocytes. Virology, 1991. **181**(2): p. 595-608.
341. Wang, K.H., et al., Nasopharyngeal Carcinoma Diagnostic Challenge in a Nonendemic Setting: Our Experience with 101 Patients. Perm J, 2017. **21**.
342. Romdhoni, A.C., N. Wiqoyah, and W.A. Kentjono, Early detection of nasopharyngeal carcinoma using IgA anti-EBNA1 + VCA-p18 serology assay. Ear Nose Throat J, 2014. **93**(3): p. 112-5.
343. Stoker, S.D., et al., Can Epstein-Barr virus DNA load in nasopharyngeal brushings or whole blood predict recurrent nasopharyngeal carcinoma in a non-endemic region? A prospective nationwide study of the Dutch Head and Neck Oncology Cooperative Group. Eur Arch Otorhinolaryngol, 2016. **273**(6): p. 1557-67.
344. Yao, J.J., et al., Prognostic value of serum EBV antibodies in patients with nasopharyngeal carcinoma and undetectable pretreatment EBV DNA. Cancer Sci, 2017.
345. Fangzheng, W., et al., Gemcitabine/cisplatin induction chemotherapy before concurrent chemotherapy and intensity-modulated radiotherapy improves outcomes for locoregionally advanced nasopharyngeal carcinoma. Oncotarget, 2017.

346. Stoker, S.D., et al., Epstein-Barr virus-targeted therapy in nasopharyngeal carcinoma. Journal of cancer research and clinical oncology, 2015. **141**(10): p. 1845-57.
347. Yang, H.J., et al., Comprehensive profiling of Epstein-Barr virus-encoded miRNA species associated with specific latency types in tumor cells. Virol J, 2013. **10**: p. 314.
348. Kim, D.N. and S.K. Lee, Biogenesis of Epstein-Barr virus microRNAs. Mol Cell Biochem, 2012. **365**(1-2): p. 203-10.
349. Wang, Y., et al., Cellular pharmacological properties of gold(III) porphyrin 1a, a potential anticancer drug lead. Eur J Pharmacol, 2007. **554**(2-3): p. 113-22.
350. Li, Z., et al., EBV encoded miR-BHRF1-1 potentiates viral lytic replication by downregulating host p53 in nasopharyngeal carcinoma. Int J Biochem Cell Biol, 2012. **44**(2): p. 275-9.
351. Zhang, Q., D. Gutsch, and S. Kenney, Functional and physical interaction between p53 and BZLF1: implications for Epstein-Barr virus latency. Mol Cell Biol, 1994. **14**(3): p. 1929-38.
352. Sato, Y., et al., Transient increases in p53-responsible gene expression at early stages of Epstein-Barr virus productive replication. Cell Cycle, 2010. **9**(4): p. 807-14.
353. Sato, Y. and T. Tsurumi, Noise cancellation: viral fine tuning of the cellular environment for its own genome replication. PLoS Pathog, 2010. **6**(12): p. e1001158.
354. Tsai, M.H., et al., The biological properties of different Epstein-Barr virus strains explain their association with various types of cancers. Oncotarget, 2017. **8**(6): p. 10238-10254.
355. Ilie, M., et al., "Sentinel" circulating tumor cells allow early diagnosis of lung cancer in patients with chronic obstructive pulmonary disease. PLoS One, 2014. **9**(10): p. e111597.

Appendix

Tumor exosomal microRNAs thwarting anti-tumor immune responses in nasopharyngeal carcinomas

Nikiforos-Ioannis Kapetanakis, Valentin Baloche, Pierre Busson

CNRS UMR8126, Gustave Roussy and Université Paris-Sud/Paris-Saclay, 39 rue Camille Desmoulins, Villejuif, France

Correspondence to: Dr. Pierre Busson. CNRS UMR8126, Gustave Roussy PR1, 39 rue Camille Desmoulins, 94805 Villejuif, France. Email: pierre.busson@gustaveroussy.fr.

Provenance: This is a Guest Editorial commissioned by Section Editor Mingzhu Gao (Department of Laboratory Medicine, Wuxi Second Hospital, Nanjing Medical University, Wuxi, China).

Comment on: Ye SB, Zhang H, Cai TT, *et al.* Exosomal miR-24-3p impedes T-cell function by targeting FGF11 and serves as a potential prognostic biomarker for nasopharyngeal carcinoma. J Pathol 2016;240:329-40.

Submitted Jan 13, 2017. Accepted for publication Jan 21, 2017.

doi: 10.21037/atm.2017.03.57

View this article at: http://dx.doi.org/10.21037/atm.2017.03.57

The considerable progress achieved in the past 10 years in the field of tumor biology and therapeutics has strengthened the idea that cancer is not only a cellular but also a tissue disease. This concept is likely to apply to nasopharyngeal carcinoma (NPC), characterized by the consistent expression of oncogenic viral proteins in a context of inflammation and immune escape (1). In its typical undifferentiated form, NPC is constantly associated with the Epstein-Barr virus, whose genome is contained in the nuclei of all malignant cells, but not in the surrounding tissue. Latency is the predominant mode of virus-cell interactions, meaning that most viral genes are silent in the vast majority of malignant cells. However, a small fraction of them are consistently expressed coding a handful of viral products, both viral proteins and untranslated RNAs, most of them with proven oncogenic properties. The inflammatory context of NPC is obvious for pathologists: almost all NPC primary tumors are heavily infiltrated by non-malignant leucocytes, mainly T-lymphocytes but also B lymphocytes, macrophages, dendritic cells and neutrophils. This inflammatory infiltration often disappears in metastatic lesions. The immune escape is also obvious because of the rapid proliferation of malignant cells despite the consistent expression of EBNA1, LMP1 and LMP2 which are known to be the targets of CD4+ and CD8+ cytotoxic T-cells in EBV-carriers. One interpretation of the paradox of tumor inflammation combined with tumor immune escape is that malignant cells in the primary tumor benefit to some extent from the proximity of leucocytes while developing mechanisms of immune escape.

High-scale genomic studies have brought evidence that the immune escape mechanisms in NPC can be cellular intrinsic alterations, for example defects in the expression of HLA class I molecules (Lo KW, 17th International Symposium on Epstein-Barr virus and associated diseases, Zurich, August 2016, abstract EBV2016-1040). These alterations are probably the most difficult to deal with for the oncologist. However, there is also evidence of a major contribution of extra-cellular "micro-environmental" immunosuppressive factors. Data from previous studies support the role of immunosuppressive proteins either secreted in a soluble form or carried by tumor exosomes, for example CCL20, galectin-9 or IDO (indoleamine 2, 3-dioxygenase) (2-4). One recent elegant publication from Jiang Li's group in Guangzhou provides new insight on the role of tumor exosomes carrying immunosuppressive microRNAs (5) (*Figure 1*). For the sake of brevity, one can distinguish two types of results in this study. Most data are based on *in vitro* experiments. They demonstrate that malignant cells mixed with T-cells from healthy donors can deliver miR-24-3p to these T-cells using exosomes as intercellular carriers. Then it is shown that miR-24-3p decreases the proliferation of target T-cells by down-regulation of FGF11 and subsequent modifications of ERK and STAT protein phosphorylation. Simultaneously, there is a decrease in the expression of interferon-γ and

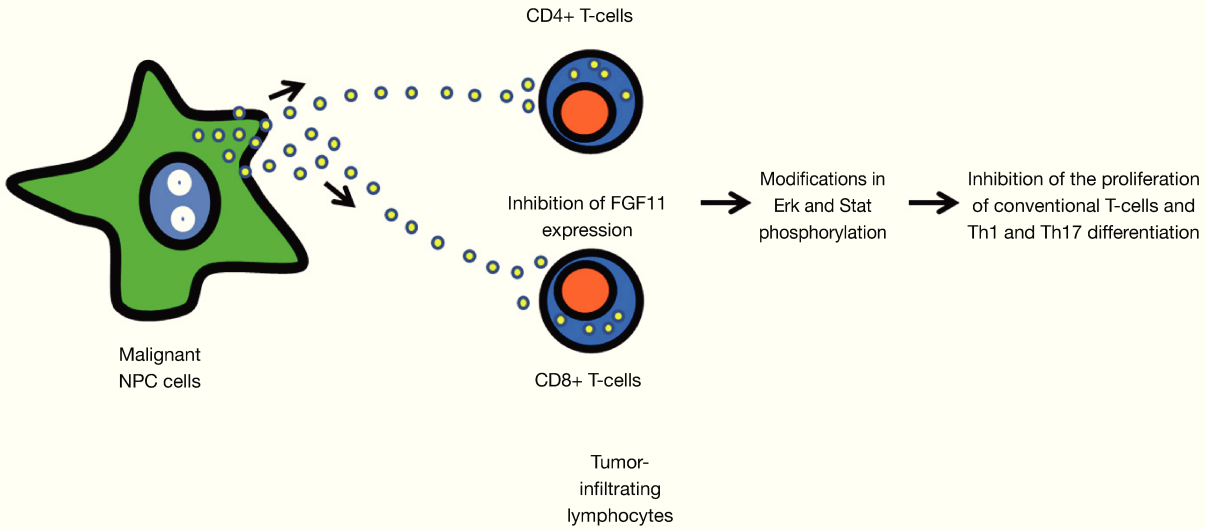

Figure 1 Main steps of the scenario linking the inhibition of the proliferation and differentiation of tumor-infiltrating T-lymphocytes to the release of tumor exosomes carrying miR-24-3p in the microenvironment of nasopharyngeal carcinomas. Exosomes carrying miR-24-3p are released by malignant NPC cells and up-taken by tumor-infiltrating lymphocytes. The internalization of miR-24-3p in target cells results in the downregulation of FGF11 with subsequent modifications in the phosphorylation of Erk and Stat proteins. These signaling events result in the inhibition of the proliferation of conventional T-cells (CD4+ and CD8+) and probably impair Th1 and Th17 differentiation. This scenario is based on *in vitro* and *in vivo* investigations reported by Ye *et al.* (5).

IL-17 expression in CD4 T-cells suggesting the impairment of Th1 and Th17 differentiation. From these data, the authors infer that similar interactions are likely to occur in the tumor microenvironment where malignant cells are in close contact with tumor infiltrating lymphocytes (TILs). Other data, based on investigations of serum samples or tumor tissue sections, support this inference. First, the authors show that the abundance of FGF11 in TILs is inversely correlated with the serum concentration of miR-24-3p. Later, they show on tumor sections that a low abundance of CD4+ and CD8+ TILs correlates with a low abundance of FGF11 in TILS (and in malignant cells as well). Moreover, a high concentration of exosomal miR-24-3p in the serum and a low amount of FGF11 in TILs and malignant cells were associated with a shorter disease-free survival. A few more experiments demonstrated that, at least *in vitro*, hypoxia enhances the concentration of miR-24-3p in tumor exosomes. The data are less consistent with regard to regulatory T-cells (T-regs). Indeed, *in vitro* T-regs' expansion and Fox-P3 expression were enhanced by the uptake of miR-24-3p and FGF11 down-regulation. However, *in vivo*, there was no significant correlation between the abundance of Fox-P3-positive cells among stromal cells and the depletion of FGF11 in TILs and malignant cells. This reminds us that the role of T-regs in NPC remains controversial (3,6).

In terms of methodology, it is important to note that almost all *in vitro* investigations were done using an EBV-negative malignant epithelial cell line, TW03. This approach is likely to have both positive and negative consequences. TW03 cells are easier to handle *in vitro* that genuine NPC cells carrying an endogenous EBV genome. The authors have largely taken advantage of the ease of DNA transfection into these cells to make an intense use of microRNA mimics, microRNA sponges and reporter assays. However, in many respects, TW03 cells lack several major characteristics of NPC cells. For example, NPC cells carry on their surface an array of inflammatory molecules like HLA class II molecules, CD54 and CD70 which are not found on TW03 (1). Moreover, a huge fraction of the total microRNAs produced by NPC cells—often as much as one sixth or even one third of them—are EBV-encoded microRNAs of which some might have an impact on T-cell functions (7). On the other hand, to a large extent, TW03 cells have a phenotype which is reminiscent of the phenotype of malignant cells from squamous cell carcinomas of the upper aero-digestive tract. Therefore, the findings reported by Ye *et al.* may have applications for

non-NPC epithelial malignancies, for example squamous carcinomas of the upper aero-digestive tract where hypoxia is often highly prevalent.

Tumor immunosuppression is usually a multifactorial process. As mentioned previously, other immunosuppressive factors, especially proteins are known to be released by NPC cells either in a soluble form or conveyed by exosomes. Therefore an integrated approach will be required to assess the respective contributions to the immune evasion of NPCs of the various immunosuppressive agents, regardless of their chemical nature, proteins, nucleic acids and probably lipids like prostaglandins. It is noteworthy that in virtually all experiments reported by Ye *et al.*, the reduction of the T-cell proliferation induced by exosomes carrying the miR-24-3p did not exceed 20%. Thus, there is ample room for potential synchronic or non-synchronic cooperation of miR-24-3p with other immunosuppressive factors. In future research, one major challenge will be to identify the predominant mechanisms of immune suppression for each clinical and molecular subtype of NPC or even for a given patient, at each stage of his treatment and surveillance. NPC clearly is a heterogeneous disease, in terms of growth pattern (with either early metastases or predominantly local growth), in terms of malignant cell phenotypes (with more or less epithelio-mesenchymal transition) or in terms of immune "contexture" (variable relative abundance of various types of T-lymphocytes, macrophages, NK cells and dendritic cells) (1,6,8). Although currently there is no consensus on molecular subcategories, it is obvious that the NPC malignant phenotypes can be supported by different genetic and epigenetic alterations as well as different modes of virus-cell interactions, for example a high, low or very low level of LMP1 expression (Lo KW, 17th International Symposium on Epstein-Barr virus and associated diseases, Zurich, august 2016, abstract EBV2016-1040). The work published by Ye *et al.* is also quite exemplary insofar as it shows the importance of combining the investigations on the tumor tissue with investigations on serum or plasma samples (5). One can presume that, in the future, the diagnosis of the immune "contexture" and immune suppressive mechanisms will rely on tumor tissue analysis combined with assays performed on serum or plasma factors including microRNAs and proteins like CCL20 and galectin-9 (8).

What are the consequences of the findings reported by Ye *et al.*, in terms of therapeutics? One option seems to be the use of miR antagonists (antagomiRs or anti-miRs) to neutralize plasma miR-24-3p. Vectorization of these antagonists to the malignant cells or the tumor-infiltrating leucocytes remains a major challenge. Another option is to attempt a capture and depletion of tumor exosomes using systemic injections of therapeutic antibodies. Because exosomes released by endothelial cells or leukocytes are very abundant in plasma and many interstitial fluids, it will be necessary to use antibodies reacting with molecules expressed selectively on the surface of NPC exosomes. Some years ago, we made the empirical and surprising observation that selective capture of tumor exosomes from plasma samples from NPC patients was facilitated by the use of anti-HLA class II antibodies (2). Galectin-9 is another protein present on the surface of NPC tumor exosomes (ibid.). Thus, the use of anti-galectin-9 or anti-HLA II antibodies might play a role in a future strategy of NPC exosome capture and depletion.

Acknowledgements

The authors would like to thank Bristol-Myers Squibb Foundation (2016-2017) for research funding.

Footnote

Conflicts of Interest: The authors have no conflicts of interest to declare.

References

1. Gourzones C, Barjon C, Busson P. Host-tumor interactions in nasopharyngeal carcinomas. Semin Cancer Biol 2012;22:127-36.
2. Klibi J, Niki T, Riedel A, et al. Blood diffusion and Th1-suppressive effects of galectin-9-containing exosomes released by Epstein-Barr virus-infected nasopharyngeal carcinoma cells. Blood 2009;113:1957-66.
3. Mrizak D, Martin N, Barjon C, et al. Effect of nasopharyngeal carcinoma-derived exosomes on human regulatory T cells. J Natl Cancer Inst 2014;107:363.
4. Ben-Haj-Ayed A, Moussa A, Ghedira R, et al. Prognostic value of indoleamine 2,3-dioxygenase activity and expression in nasopharyngeal carcinoma. Immunol Lett 2016;169:23-32.
5. Ye SB, Zhang H, Cai TT, et al. Exosomal miR-24-3p impedes T-cell function by targeting FGF11 and serves as a potential prognostic biomarker for nasopharyngeal carcinoma. J Pathol 2016;240:329-40.

6. Zhang YL, Li J, Mo HY, et al. Different subsets of tumor infiltrating lymphocytes correlate with NPC progression in different ways. Mol Cancer 2010;9:4.
7. Lee KT, Tan JK, Lam AK, et al. MicroRNAs serving as potential biomarkers and therapeutic targets in nasopharyngeal carcinoma: A critical review. Crit Rev Oncol Hematol 2016;103:1-9.
8. Becht E, Giraldo NA, Germain C, et al. Immune Contexture, Immunoscore, and Malignant Cell Molecular Subgroups for Prognostic and Theranostic Classifications of Cancers. Adv Immunol 2016;130:95-190.

Cite this article as: Kapetanakis NI, Baloche V, Busson P. Tumor exosomal microRNAs thwarting anti-tumor immune responses in nasopharyngeal carcinomas. Ann Transl Med 2017;5(7):164. doi: 10.21037/atm.2017.03.57

Chapter 6

Review: Biological and Pharmacological Basis of Cytolytic Viral Activation in EBV-Associated Nasopharyngeal Carcinoma

Natalie Oker, Nikiforos-Ioannis Kapetanakis and Pierre Busson

Additional information is available at the end of the chapter

http://dx.doi.org/10.5772/64738

Abstract

Epstein-Barr virus (EBV) infection contributes to the development of different types of human malignancies, especially nasopharyngeal carcinoma. As a herpesvirus, EBV can establish two major modes of virus-cell interactions: a latent or a lytic infection. Latent infection is prevalent in the vast majority of malignant cells in EBV-related malignancies. Inducing a switch from latent to lytic infection in a substantial fraction of malignant cells has long been considered as a potentially interesting therapeutic approach. Therapeutic benefits are expected from (1) the cytotoxic or cytostatic effects of viral products expressed in the context of the lytic cycle; (2) expression of viral enzymes capable of metabolizing pro-drugs selectively inside these cells and (3) broadening the expression spectrum of antigenic viral proteins. In this chapter, addressing non EBV-specialized readers, we first summarize the main aspects of EBV biology with emphasis on the cellular mechanisms known to control latent and lytic infections. Then, we outline the basic principles and requirements of cytolytic EBV activation performed with a therapeutic intent. Finally, we review the main categories of pharmacological agents reported to be active in the switch from latent to lytic infection, including drugs used for conventional anti-tumour chemotherapy, histone-deacetylase inhibitors and various miscellaneous compounds.

Keywords: nasopharyngeal carcinoma, Epstein-Barr virus, lytic cycle, histone-deacetylase inhibitors, epigenetics, immunotherapy, phenotypic screening, compound library

1. Introduction

Nasopharyngeal carcinomas (NPCs) are consistently associated with the Epstein-Barr virus (EBV) [1] and represent a major public health problem worldwide. In order of frequency, it is the third leading cause of virus-related human malignancies, ranking just behind hepatocellular carcinomas linked to the hepatitis B and C viruses and cervix carcinoma involving human papilloma viruses (HPV) [2]. The incidence of NPC is particularly high in Southern China, especially in the Guangdong province (approximately 25 cases per 100,000 persons per year). In addition, there are areas of intermediate incidence in Southeast Asia and North Africa. Men have been shown to be two to three times more likely to develop NPC than women, the most frequent age of disease occurrence being 50–60 years. Regardless of patient geographical origin, NPCs are constantly associated with EBV (except for a very small number of highly differentiated atypical forms related to tobacco and alcohol and a few cases associated with human papilloma viruses [HPV] mainly observed in Europe and North America) (reviewed in [3]). Like other EBV-associated malignancies, NPC is clearly a multifactorial disease. The non-viral risk factors include germline genetic susceptibility involving alleles of the major histocompatibility complex (MHC) region on chromosome 6 [4]. One example of a susceptibility gene not linked to the MHC region is *MST1R*. It encodes a protein detected in the ciliated epithelial cells in normal nasopharyngeal mucosa, which plays a role in the cilia motility, thus being essential for host defence [5]. The action of diet carcinogens, like salt-preserved fish in South China, probably accounts for multiple acquired cellular genetic and epigenetic alterations detected in malignant cells [4].

Investigations on the mechanisms of NPC oncogenesis and novel therapeutic approaches have long been hampered by a lack of biological resources. It has been proven very difficult to derive tumour lines propagated *in vitro* or even patient-derived xenografts (PDXs), which retain the EBV-genome, using clinical NPC specimens. Currently, there is only one EBV-positive NPC tumour line (C666-1), which is routinely propagated *in vitro*, and a small number of EBV-positive NPC PDXs whose cells are not easily handled *in vitro* [6–9]. There is evidence that malignant NPC cells tend to lose the EBV genome when one attempts their propagation *in vitro*. The resulting EBV-negative cell lines seem to have a phenotype, which does not fit with the NPC cell phenotype *in situ*, especially with regard to immunological characteristics (e.g., HONE1) [10]. They are sometimes artificially reinfected by EBV *in vitro*, but this does not restore a typical NPC cell phenotype.

In addition to the latent EBV-infection, the malignant phenotype of NPC cells is explained by a number of genetic and epigenetic alterations. None of these alterations is constant in all NPC tumours, and few are highly specific of NPCs. In most cases, there are no alterations in the *TP53* gene (it is mutated in less than 10% of the cases; [11]). In contrast, many other tumour suppressor genes (TSGs) are frequently silenced in NPC cells, especially *CDKN2A* (chromosome 9p21.3) and *RASSF1* (chromosome 3p21.3). Their inactivation often results from a combination of hemizygous deletion and promoter hypermethylation on the remaining allele. However, deletions of both alleles and inactivating point mutations have been also reported. Silencing of these TSGs often occurs very early in the carcinogenic process [12]. Many TSGs

http://dx.doi.org/10.5772/64738

like the gene encoding the Wnt inhibitory factor 1 (*WIF*, 12q14.3) or E-cadherin (*CDH*, 16q22.1) are consistently inactivated by methylation of both alleles [13, 14]. One has to keep in mind that prolonged latent—or even transient EBV infection—favours genome-wide hypermethylation of gene promoters [15]. In addition to the silencing of multiple TSGs, NPC cells exhibit alterations of multiple oncogenes, which are often affected by copy number gains, especially *CCND1* (encoding cyclin D1 on chromosome 11q13.3) and *PIK3CA* (3q26.1) [12, 16]. There are also frequent copy-number gains of the gene encoding the lymphotoxin-β receptor (*LTβR*) on chromosome 12p13.31 [12]. This is a rare – or even unique – example of a genetic alteration which is highly specific of NPC tumours. Two oncogenic fusion genes—*UBR5-ZNF423* and *FGFR-TACC3*—have been identified by high-throughput sequencing of tumour mRNAs (RNAseq), but they are only detected in a minority of NPC specimens, mainly among late stage tumours [17, 18]. Whole exome sequencing of 128 NPC specimens has revealed mutations in genes encoding proteins involved in chromatin remodelling, especially *ARID1a* (about 10% of the specimens) and in the process of DNA methylation (*TET1*, *TET2* and *TET3*, altogether in about 9% of the specimens) [11].

On average, NPCs are more radio-sensitive and chemo-sensitive than other head and neck tumours. However, they still raise serious therapeutic issues: (1) NPCs are often discovered at a late stage whereas lymph node and distant organ metastases occur early in tumour evolution; (2) despite remarkable advances in 3D radiotherapy, irradiation often leads to severe functional sequels (subcutaneous and muscular sclerosis and xerostomia); (3) although metastatic lesions are initially sensitive to chemotherapy, they often escape from treatment control after a few months [19, 20]. In summary, despite the remarkable progress achieved in the recent years, there is still an urgent need for better therapeutic modalities. In this context, the idea of using EBV as a kind of endogenous oncolytic virus has been in the air for a very long time. The proof of principle that pharmacological agents can disrupt latent infection and push at least a fraction of EBV-infected malignant cells towards the reactivation of the viral lytic cycle was presented almost 40 years ago. Sodium butyrate was reported as a potent activator of the lytic cycle in EBV-infected human B-lymphocytes in 1979 [21]. However, the progress of this concept towards therapeutic applications has been very slow, especially regarding NPC. The aim of this review is to assemble key information for a public of non-EBV-specialists who want to understand the cellular, molecular and pharmacological basis of translational research on cytolytic viral activation in nasopharyngeal carcinomas.

2. Main aspects of EBV biology and regulation of the latent/lytic modes of infection

2.1. General aspects of EBV biology

EBV is one of the eight human Herpesviridae. It belongs to the subfamily of the γ-herpesvirinae and to the genus of lymphocryptoviruses. Like all Herpesviridae, it is an enveloped double-stranded DNA virus, containing about 80 genes. It is the causative agent of infectious mononucleosis, and it has an etiological role in several human malignant diseases mainly of

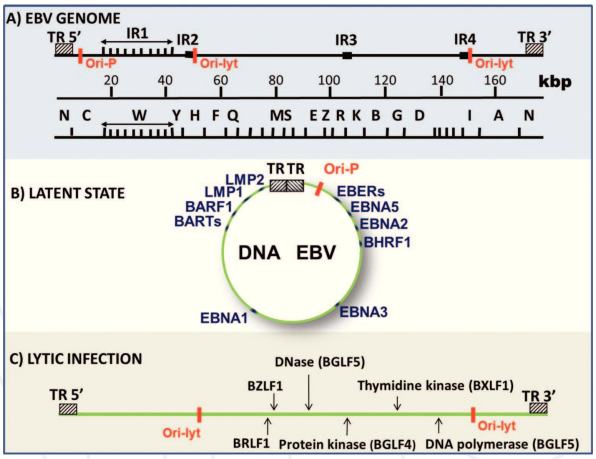

Figure 1. EBV-genome structure and configuration in connection with latent or lytic infection: (A) EBV genome map (linear representation). EBV genome contains about 180 kilobase pairs (kb). Both ends of the viral DNA contain a variable number of repeated non-coding sequences of 500 bp (called TR for terminal repeats). In addition, there are internal repeated sequences called internal repeats (major IR1 and minor IR 2–4). Ori-P is the replication origin of the viral genome used in the latent state of infection. The Ori-lyt are two replication origins used during the lytic infection. The reference restriction map is based on the digestion of the viral DNA by the restriction enzyme BamH1. Restriction fragments are classified from the largest (BamH1A) to the smallest (BamH1Z). Designation of open-reading frames is based on this restriction map. For example, BZLF1 is the first leftward open reading frame in the BamH1 Z fragment (Bam Z leftward open-reading frame 1) (BZLF1 by extension also means the corresponding protein). (B) Configuration of the EBV genome characteristic of the latently infected cells. When the infected cell enters a state of latent infection the viral DNA is circularized probably by recombination of the TRs. This circular form of the genome called episome is contained in the nucleus in combination with cellular chromatin but apart from chromosomes. The episomes are passively replicated by cellular DNA polymerases starting from the Ori-P origin of replication. During latent infection, most viral genes are silent. However, about 10% of them are consistently expressed (in blue). Most of these genes encode final products—viral non-coding RNAs or proteins—with transforming properties. They are called "latent genes" whereas genes expressed only during lytic infection are called "lytic genes". There is no topographical separation between the two categories of genes.(C) Configuration of the EBV-genome characteristic of the lytic infection. As usual in virology, the phase of the lytic cycle which precedes viral DNA replication is called the early phase. As soon as the viral DNA pol starts the autonomous replication of the viral genome, lytically infected cells enter the late phase. Newly synthesized viral genomes are in a linear configuration. Viral proteins expressed at the very beginning of the early phase of the lytic cycle like BZLF1 and BRLF1 are encoded by immediate early genes. Early viral proteins are expressed at a more advanced stage. Many of them are involved in DNA metabolism, for example, the viral thymidine-kinase, DNAse and DNA polymerase. The EBV protein kinase (BGLF4; protein encoded by the Bam G leftward open reading frame 4) can phosphorylate various substrates. It is also one component of the viral particle.

lymphoid and epithelial origin as well as several autoimmune diseases. Examples of EBV-related malignancies are nasopharyngeal carcinomas, several types of lymphomas (endemic Burkitt's Lymphoma (BL), more rarely Hodgkin lymphomas, centro-facial NK-T lymphoma, post-transplant lymphomas and AIDS-associated lymphomas), and approximately 10% of gastric cancers worldwide [22–25]. Examples of autoimmune diseases likely to involve EBV are multiple sclerosis and systemic lupus erythematosus [26, 27]. Like all other herpesviruses, EBV causes lifelong infection following the primo-infection. More than 90% of adult humans are healthy carriers regardless of their geographic origin. Its persistence in healthy carriers is

http://dx.doi.org/10.5772/64738

the result of three types of viral characteristics: (1) its capacity to continuously induce bursts of productive infections in various tissues, especially in the upper aerodigestive tract and more specifically in the tonsils, the salivary glands and possibly gingiva; (2) its capacity to achieve latent infection mainly in B-lymphocytes, especially memory B cells in blood, bone marrow and lymphoid organs; (3) its sophisticated strategies of immune evasion [28].

The distinction between two major modes of virus-cell interactions is a key to understanding EBV biology [29]. (1) Latent infections are cellular infection modalities characterized by the absence of viral particle production, a restricted expression of viral genes (often less than 10 out of 80) and a circular configuration of the viral genome (**Figure 1**). (2) Lytic/productive infections are characterized by sequential or concomitant expression of most viral genes, abundant synthesis of linear viral genomes and finally extracellular release of viral particles or virions in a context of mandatory cell death.

2.2. Latent EBV infection in LCL and NPC cells

One major common characteristic of most EBV-related malignancies is the predominance of latent modes of virus-cell interactions. As a rule in EBV-associated tumours, no EBV particles are detected by electron microscopy on tumour sections, whereas the viral DNA can be visualized in the nuclei of malignant cells by *in situ* hybridization. Consistently, very few malignant cells exhibit expression of viral proteins characteristic of the lytic/productive cycle. This minimal expression of lytic viral proteins in EBV-infected malignant cells favours immune evasion. In most latently infected cells, the virus-cell interactions are bidirectional: a few viral genes often modify the phenotype of the host cell, whereas the cellular context contributes to the repression of most viral genes (see subsequent section B3). For laboratory investigations, a model of latent EBV infection is easily obtained *in vitro* by infection of peripheral blood mononuclear cells (PBMCs) from normal donors, which results in the oncogenic transformation of resting B cells. These EBV-transformed B-cell lines are often called lymphoblastoid cell lines (LCLs). LCLs are immortalized and tumorigenic in SCID (severe combined immune-deficiency) mice [30]. They represent a privileged model for *in vitro* investigations of the molecular basis of latent infections.

During latency, the viral genome is conserved under the form of circular copies, called episomes, from one to several tens, which are present in the nuclei apart from the cell chromosomal DNA but also coated with cellular chromatin and replicated by cellular enzymes at each cell division. Most viral genes expressed in EBV-associated malignancies belong to the category of the latent genes, which are expressed in LCLs *in vitro* and contribute to the maintenance of the transformed phenotype. Their oncogenic effects are summarized in **Table 1**. The latent genes encode nuclear proteins like the EBNAs (Epstein-Barr nuclear antigens), membrane proteins like LMP1, LMP-2A and LMP-2B (latent membrane proteins 1, 2A and 2B) and non-coding RNAs. There are two main categories of non-coding viral RNAs: genuine microRNAs and the EBERs (Epstein-Barr virus encoded small RNAs) [31]. Two families of viral microRNAs, called "BHRF1" and "BART" microRNAs, can be transcribed from two distinct regions of the EBV genome, the Bam-H1 H and Bam-H1 A segments, respectively. The BHRF1 (Bam H rightward open reading frame 1) cluster includes at least

four microRNAs which are transcribed in LCLs but not detectable in most NPC specimens. They have a key role in the inhibition of apoptosis [32]. In contrast, the microRNAs of the BART (Bam A rightward transcripts) family are abundant in most NPC cells and not detected in LCLs. About 40 BART microRNAs have been identified so far [33, 34]. They target a great variety of mRNAs, for example, those encoding the pro-apoptotic protein Puma (miR-BART5), the tumour suppressor protein PTEN (miR-BART1) or the viral DNA polymerase (miR-BART2) [35–37]. The EBERs are single-stranded RNAs of about 170 nucleotides with a complex secondary structure containing double-stranded segments which can react with various cellular receptors of double-stranded RNAs such as the PKR (protein-kinase RNA-dependent), RIG1 (retinoic acid-inducible gene 1) and TLR3 (Toll-like receptor 3) [38]. These interactions stimulate resistance to interferon and production of growth factors like IGF-1 (insulin-like growth factor 1) [38].

	Type	EBV product	Examples of functions
Latency product	Non-coding latent transcripts	**EBERs 1 and 2** (non-coding RNAs)	Inhibit the RNA dependent protein kinase (PKR) activate the Toll-like receptor 3 (TLR3) [38]
		miR-BART (microRNAs)	Inhibit expression of some viral lytic and cellular pro-apoptotic genes, promote metastases [35, 37, 42]
	Non-membrane protein	**EBNA 1** (nuclear protein)	Episome maintenance, contributes to disruption of PML bodies [43]
		BARF1 (secreted protein)	Ligand of the m-CSF or CSF1 receptor [44]
	Membrane latent protein	**LMP1**	Activator of Bcl3/p50/P50 NF-kB complex [1]
		LMP2A	Activator of PI3 kinase/Akt pathway [1]
		LMP2B	Accelerates the degradation of interferon receptors [1]
Lytic cycle products	Immediate early proteins (IE)	**BZLF1**	Act as transactivators, enhancing the expression of later lytic genes [45, 46]
		BRLF1	
	Early proteins (E)	**DNA polymerase**	Lytic replication of the viral genome
		EBV-DNase	Alkaline nuclease with endonuclease and exonuclease activities
		EBV-thymidine kinase (TK)	Phosphokinase with a probable role in the phosphorylation of FIAU [47, 48]
		EBV-protein kinase (PK)	Phosphokinase involved in DNA replication and virion production. Phosphorylates ganciclovir [49, 50]
	Late proteins (L)	**VCA** (viral capsid antigen)	A complex of structural proteins assembled in the viral capsid
		Gp350	Viral envelope glycoprotein binding to the cell membrane receptor CD21 (also known as CR2) [51]

Table 1. Examples of EBV latency and lytic cycle products with clues on their functions.

http://dx.doi.org/10.5772/64738

In comparison to LCLs, latent EBV infection in NPC cells has some specific features. The expression of latent viral proteins is more restricted than in LCLs. Only one latent nuclear protein—EBNA1—is expressed in contrast to six in LCLs. The latent membrane proteins, LMP1 and LMP2, are present in most tumour specimens but often at a low level and with major heterogeneity among tumour cells [39, 40]. Another specific feature of latent EBV-infection in NPCs is the huge abundance of the BART microRNAs which on average account for 20% of total tumour microRNAs [41]).

2.3. The switch from latency to the lytic/productive infection and its regulation

2.3.1. General features of the switch from latent to lytic EBV-infection

Experimental lytic/productive infections by EBV can be achieved in several manners. As explained in the previous section, EBV infection of resting B cells *in vitro* results mostly in transformed cells, which are latently infected. However, EBV-transformed B cells can enter the lytic/productive cycle at a secondary stage triggered by plasmacytic differentiation or treatment with various chemicals (**Table 2**. The experimental systems used for EBV infection of epithelial cells *in vitro* are completely different. First, penetration of viral particles often requires special procedures, as for example, pre-adsorption on B cells [52]. Next, penetration of EBV in epithelial cells often results in direct lytic infection (**Figure 2**) [53, 54]. With most experimental systems, latently infected epithelial cells remain rare, and their isolation usually requires the use of recombinant viruses carrying selectable markers [53]. In some models based on cultured primary epithelial cells, primary lytic infection can be blocked by overexpression of cyclin D1 or inhibition of CDKN2A. So far, most laboratory investigations on EBV lytic/productive infection have been done starting from latently infected cells switching to lytic viral activation (see **Figure 2**). This switch is triggered by external factors and/or modifications of physiological cell conditions, for example, differentiation or senescence. It is the result of a change in the balance of factors either blocking or enhancing the expression of lytic viral genes. As reviewed by Miller et al [29] and more recently by Kenney et al [46] the switch from latent to lytic infection is a sequential process, comprising two main sets of events:

1. Upstream events leading to the expression of the immediate early viral transactivators BZLF1 (also called ZEBRA, Zta or EB-1) and BRLF1 (also called Rta) [29].
2. Downstream events resulting from the interaction of BZLF1 and BRLF1 with a number of viral promoters controlling genes encoding products of the lytic cycle, such as, the EBV DNA-polymerase or EBV-TK (thereafter called lytic promoters) [55].

The genes encoding BZLF1 and BRLF1 are themselves under the control of promoter regions (Zp and Rp), which are regulated by a wide number of cellular factors, either activators or inhibitors. The influence of the inhibitors is predominant in the latently infected cells and vice versa during lytic activation.

Class of drugs	Example
Direct PKC activators	Phorbol-esters [65]
Conventional chemotherapy [30, 60, 74, 88–90]	*cis*-platinum or cisplatin (alkylating agent); paclitaxel (stabilizer of mitotic spindle); 5-fluoro-uracil (pyrimidine analog); gemcitabine (cytidine analog)
Inhibitors of histone deacetylases (HDACi)	Sodium butyrate [21], Trichostatin A [61] Valproic acid [86–88, 104], Panobinostat (LBH-589) [94], Vorinostat (SAHA) [95, 96], Romidepsin [60, 97]
Demethylating agents	5-Azacitidine [100]
Protease inhibitors	Bortezomib [47, 48]
Gamma-secretase inhibitors	Dibenzazepine [101]
Tetrahydrocarbolines and other compounds recently selected by high-throughput assays [103], [102]	
Prodrugs activated by EBV enzymes [59, 80, 105]	Ganciclovir (9-(1,3-dihydroxy-2-propoxyméthyl) guanine or DHPG) FIAU (2′-fluoro-2′-deoxy-β-D-5-iodo-uracil-arabinofuranoside) [47, 48]

Table 2. Summary of the different drugs with reported capacity of lytic EBV activation and prodrugs phosphorylated by EBV-encoded kinases.

BZLF1 and BRLF1 activate one another's promoter and their cooperation is required for optimal activation of many lytic viral promoters [56]. BZLF1 preferentially activates these promoters when they are methylated, whereas BRLF1 is more active on unmethylated promoters [45]. Therefore, they cooperate to induce lytic activation, no matter if the viral genome is methylated or unmethylated. BRLF1 ability to transactivate its target promoters is also dependent on another epigenetic mark, which is the 5-hydroxymethylation of cytosine in promoter CpG islands. Hydroxy-methylation induces an open chromatin conformation, which is critical for optimal action of BRLF1 but not BZLF1 [56].

http://dx.doi.org/10.5772/64738

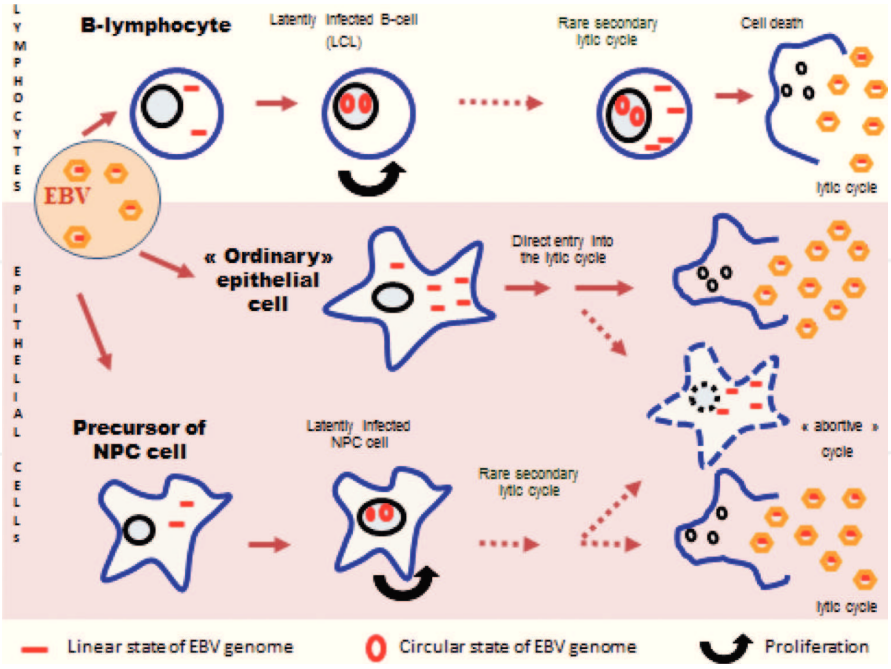

Figure 2. Main modalities of virus-cell interactions in lymphoid and epithelial cells.

– When human resting B-lymphocytes are infected by EBV, a fraction of them enter a state of viral latency requiring the circularization of the EBV genome and the expression of several viral latent genes. Simultaneously, the host cell undergoes an oncogenic transformation driven by the viral latent genes, especially EBNA2, EBNA3A and 3C and LMP1. These transformed B-cells can proliferate indefinitely resulting in LCLs. However, a secondary switch from latency to the lytic cycle can occur in a fraction of them. This fraction is generally very small but it can be increased by some pharmacological agents like HDACi (histone deacetylase inhibitors) or PKC (protein-kinase C) activators.

– EBV infection of epithelial cells *in vitro* requires special experimental systems like co-cultivation with B-cells carrying viral particles . In most of these experiments, penetration of the viral particles results in infections which are directly cytolytic or abortive. There is evidence that the same type of events often occur when epithelial cells are infected *in situ*, for example in the salivary glands or in the tonsil epithelium (normal epithelial cells are depicted by a cell shape named "ordinary epithelial cell") [57, 58].

– However for some reasons, malignant NPC cells undergo a latent infection suggesting a special type of virus-cell interactions at the initial stage of the malignant cell proliferation. There is evidence that the precursor cells have premalignant alterations, especially knock-out of cyclin kinases' inhibitors which make them resistant to virus-induced senescence (cells with pre-malignant lesions are depicted by a cell shape named "precursor of NPC cell"). Obvious-

ly, this is not sufficient for the establishment of latency since it is difficult to establish latency in many epithelial cells which are fully transformed and grown *in vitro*. In latently infected NPC cells secondary lytic or abortive cycle can occur spontaneously in a small fraction of the cells. One important aim of cytolytic activation therapy is to dramatically increase the number of the malignant cells undergoing the lytic cycle.

2.3.2. Overview of the cell physiological conditions and transcription factors involved in the switch from latent to lytic EBV infection

The factors controlling the switch from latent to lytic infection are numerous. They are intricate and highly dependent on the cellular context. **Figure 3** is intended to give a concise overview of these factors. As a first approximation, absence of cellular differentiation, cell proliferation, EMT (epithelial to mesenchymal transition) and inflammation tend to favour the maintenance of a latent infection. In contrast, cell differentiation, senescence, DNA damage response and hypoxia favour the entry into the lytic cycle.

Many signalling pathways which favour lytic EBV activation involve protein-kinases C (PKCs). PKCs phosphorylate hydroxyl groups of serine and threonine in multiple protein substrates, including MAP kinases and MARCK proteins. They are involved in multiple and diverse biological processes including transcriptional regulations, cell growth and immune responses. Physiological activation of "conventional" PKCs (α, β, γ) requires stimulation by diacylglycerol and calcium, whereas activation of "novel" PKCs (δ, ε, H, Θ) requires only diacylglycerol. There is evidence for a special contribution of PKCδ to the control of the switch from latent to lytic infection. For example, as explained in sections C1, D2 and D3, PKCδ plays a critical role downstream of various pharmacological agents inducing lytic EBV activation [59–61]. On the contrary, the intracellular form of the cytokine IL-32 has been shown to prevent lytic activation by sequestration of PKCδ [62]. Several PKC isoforms activate cellular immediate early proteins, for example, the FOS and EGR1 (early growth response) transcription

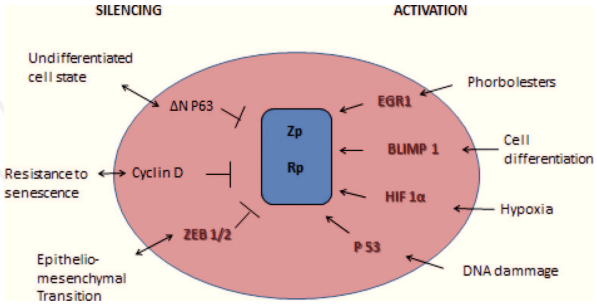

Figure 3. Summary of the physiological cell conditions and transcription factors, which modulate the activity of the *BZLF1* (Zp) and *BRLF1* (Rp) gene promoters in the context of epithelial cells. Both promoters are under the control of inhibitory (left side) and activating (right side) factors. Various physiological cell conditions are enumerated outside the pink circle, whereas the corresponding regulatory proteins are presented inside the pink circle with transcription factors appearing in bold brown letters. Detailed explanations and references are provided in section B3-2.

http://dx.doi.org/10.5772/64738

factors, which have specific binding motifs on the Zp and Rp promoters, respectively [63, 64]. For information, phorbol-esters, which have long been known to induce lytic EBV activation in lymphoid cells, are direct pharmacological agonists of PKCs [65].

The Blimp-1 transcription factor, which is a key player for lymphoid and epithelial cell differentiation, is a strong inducer of lytic EBV activation, especially in epithelial cells; it stimulates the expression of both BZLF1 and BRLF1 [66]. TGF-β has been reported to induce a partial lytic activation in EBV-positive gastric carcinoma cell lines [67]. Various factors, which antagonize senescence, favour the maintenance of EBV latency. As already mentioned, overexpression of cyclin-D1 or loss of CDKN2A, which enhances G0/G1 transition in the cell cycle, prevents lytic activation in some models of EBV latent infection in epithelial cells [53]. Generally speaking, inflammation—for example, inflammation triggered by TNF-α or interferon-γ—is rather seen as a factor which strengthens EBV latency [68]. Activation of NF-κB has been reported to stabilize latency in various γ-herpesviruses [69]. Stat3 is also reported to stabilize latency in EBV-infected cells [63]. However, the influence of inflammatory factors on EBV latency in NPC cells has not been well documented. The ZEB1/ZEB2 transcription factors, which are known to contribute to the EMT in various cell types, have been proven to antagonize EBV lytic activation [46]. Finally, there is evidence that ΔNp63 can contribute to the maintenance of EBV latency. ΔNp63 is a variant of the p63 transcription factor, which is preferentially expressed in undifferentiated basal epithelial cells [46].

The switch of latent to lytic infection is also triggered by various types of cellular stress and adaptive responses. Genotoxic stress and DNA damage response have long been known to favour EBV lytic activation in various cell backgrounds, especially in NPC cells. BRdU treatment was used in one of the oldest reports on lytic EBV activation achieved in an NPC model [70]. Ionizing radiations have been shown to induce lytic activation in LCLs [71]. As explained in details in section D1, many drugs in the arsenal of conventional cancer chemotherapy are inducers of lytic EBV activation in various cellular backgrounds. The ATM (ataxia-telangiectasia mutated) kinase and to a lesser extent TP53 often play a critical role in the sequence of events leading from DNA damage to BZLF1 expression [72, 73]. In addition, there is evidence that ATM is involved in the lytic cascade downstream of BZLF1 [74]. In other words, ATM is apparently involved in the lytic cascade upstream as well as downstream of BZLF1 expression. Endoplasmic reticulum stress, which results from large-scale protein misfolding, has been reported as a condition leading to lytic activation in LCLs [75]. Finally, the cellular stress resulting from hypoxia was reported to favour the switch from latent to lytic infection with a role of the HIF1 transcription factor in the activation of the Zp promoter [46].

2.3.3. Epigenetic factors control the switch from latent to lytic EBV infection

This point will be addressed briefly with focus on two epigenetic processes, which are critical for the switch from latent to lytic EBV infection: DNA methylation and transcriptional control by microRNAs. We have previously mentioned that BZLF1 preferentially interacts with methylated lytic promoters, whereas it is the opposite for BRLF1. Therefore, the net impact of the methylation or the demethylation of the viral genome is not easily predicted and is highly dependent on the cell background [56]. Recent work has shed some light on the role of cellular

microRNAs in the maintenance of EBV latency. Members of the miR-200 family, like miR-200b, target the transcription factors ZEB1 and ZEB2, thus having the ability to reactivate the EBV lytic gene expression when added to EBV-infected cells [76]. This applies not only to endogenous microRNAs but also to members of the miR-200 family conveyed by extracellular vesicles, which can induce lytic EBV activation in recipient cells [77]. In contrast, other microRNAs of cellular and viral origin have the ability to repress viral reactivation by targeting elements of its machinery [78].

3. Basic principles and requirements of therapies based on viral cytolytic activation in EBV-associated malignancies

Like for all Herpesviridae, production of viral particles is automatically associated with the death of cells infected by EBV. This is the reason why the productive cycle—as opposed to the state of latent infection—is often called the lytic cycle [29]. With this in mind, for a long time —going as far as the end of the seventies—many authors have considered reactivation of the lytic cycle as a possible therapeutic strategy. For a long time, the concept has evolved very slowly. One hurdle was the fact that the state of latent infection is generally very stable. In addition, in most cases it is difficult to go beyond partial reactivation with expression of some proteins of the lytic cycle like the immediate-early BZLF1 transactivator. On the other hand it was recognized that, in many cases, even partial reactivation is sufficient to block cell growth [79]. This intrinsic cytotoxic effect of partial reactivation, the possible induction of the expression of viral enzymes capable to of metabolizing a prodrug and the wish to enlarge the range of viral targets for the immune system are currently the main incentives to investigate the induction of the viral lytic activation as a therapeutic approach [30]. One additional perspective is to use precursors of radio-opaque molecules processed by viral enzymes and selectively retained in the malignant cells for specific medical imaging [73, 48]. Two EBV-encoded enzymes are usually cited as having the potential to metabolize and activate prodrugs: the EBV thymidine kinase (TK) and the EBV protein kinase (PK) encoded by the BXLF1 and BGLF4 genes, respectively. Ganciclovir (GCV) and acyclovir (ACV) are not substrates of EBV-TK. Meng et al. have formally demonstrated that among EBV-encoded kinases, EBV-PK is necessary and sufficient to phosphorylate GCV and ACV [49]. Consistent data had been previously reported by Gustafson et al [80]. The phosphorylated active forms of GCV and ACV inhibits cellular and viral replication. Fialuridine or FIAU (2′-fluoro-2′-deoxy-β-D-5-iodouracil-arabinofuranoside) is also a prodrug activated in EBV-infected cells, presumably by the EBV-TK, but its use is limited by its hepatic and metabolic toxicity [47, 48, 81]. However, it can be used occasionally, at least in animal models, for imaging purpose. Indeed, its phosphorylation by EBV-TK results in its selective retention in malignant cells. Thanks to this property, FIAU can be used for imaging in two ways either as a carrier of iodine atoms, which are opaque to X-ray or when the cold iodine atoms are substituted by radioactive isotopes as a tumour-selective radioactive emitter [47, 48, 73].

Induction of the lytic cycle can also have potentially deleterious effects. Several publications have shown that lytic activation in a small fraction of malignant cells can enhance malignant

http://dx.doi.org/10.5772/64738

growth [82]. This is probably due to the increased production of inflammatory cytokines, angiogenic and growth factors in some cells undergoing the lytic cycle [83, 84]. To prevent these deleterious effects, it is important: (a) to ensure that the lytic cycle activation occurs in a large fraction of malignant cells and (b) if possible to combine lytic activation with administration of a cytotoxic prodrug, preferably with a bystander effect (see **Figure 4**).

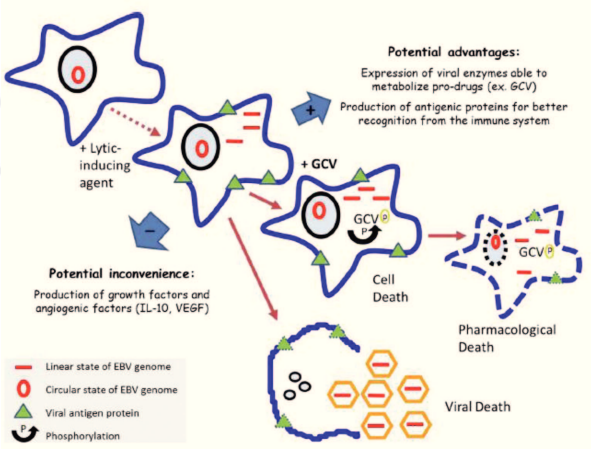

Figure 4. Importance of combining the induction of the lytic cycle with the administration of prodrugs. From a therapeutic point of view, induction of the lytic cycle has both positive and negative consequences. Positive consequences are (1) the expression of viral enzymes, which can activate prodrugs specifically in malignant cells and (2) the broadening of viral antigen expression, which is expected to facilitate specific recognition and destruction of malignant cells by the immune system. One potential drawback is an increase in the production of growth factors and angiogenic factors by malignant cells. Several advantages are expected from the use of a prodrug specifically activated in malignant cells (e.g., ganciclovir or GCV): (1) rapid pharmacological killing of malignant cells including many cells that would not undergo a full lytic cycle and therefore would stay alive for a long time in the absence of the prodrug; (2) reduction in the production of growth and angiogenic factors coming from cells undergoing the lytic cycle; (3) possible bystander killing of cells resistant to lytic cycle induction, for example, by diffusion of phosphorylated GCV through gap junctions.

These experimental approaches will be classified in three categories: (1) one based on drugs used for conventional antitumour chemotherapy; (2) one based on HDAC inhibitors and (3) finally, a miscellaneous category including various agents from PKC activators to demethylating agents.

4. Main categories of pharmacological agents with the potential of cytolytic activation of EBV in the context of NPC cells

4.1. Impact of pharmacological agents used in conventional chemotherapy

A number of drugs used in conventional chemotherapy have the ability to induce the EBV lytic cycle in various lymphoid or epithelial cell backgrounds. The drugs which are the most

active in this process—gemcitabine and to a lesser extent doxorubicin, taxol, *cis*-platinum (CDDP), 5-fluoro-uracil (5-FU) and methotrexate, have been empirically identified (*cis*-platinum and 5-FU are only active in epithelial cells; methotrexate probably only in lymphoid cells) [30, 59, 85]. Regarding NPC cells, initial data on this topic have been published by Shannon Kenney's group in 2002. They showed that CDDP, 5-FU and taxol were able to induce —or to enhance—the expression of the lytic proteins BZLF1, BRLF1 and BMRF1 in a gastric carcinoma cell line artificially infected by EBV (AGS-EBV) [59]. Simultaneously in cytotoxicity assays, synergies were found between GCV and *cis*-platinum or 5-FU. Similar results were obtained using the xenografted NPC tumour line, C18. *De novo* expression of BZLF1 and enhancement of BMRF1 expression were observed after treatment with CDDP or 5-FU. In addition, there was a synergy in tumour growth inhibition when GCV was combined with CDDP or 5-FU in intraperitoneal injections to nude mice bearing C18 xenografts. It is noteworthy that the same agents had no impact on lytic EBV-protein expression in two other NPC xenografts, C15 and C17. One specific feature of C18 shared with AGS-EBV is that, even in the absence of drug treatment, it has a low level of constitutive lytic protein expression. This is not the case for the two other NPC xenografts ([7] and P. Busson, unpublished data).

Subsequently, regardless of the cell background, gemcitabine has been confirmed as the most potent inducer of EBV lytic activation among all drugs routinely used in conventional chemotherapy [30, 73, 86]. Its capacity to contribute to lytic activation in NPC cells has been well documented by Wildeman et al. (2012) and to a lesser extent by Hsu et al. (2015) [86, 87]. In both cases, induction of lytic activation in the C666-1 cell line was stronger when gemcitabine (in the range of 3 μM *in vitro*) was combined with valproic acid (in the range of 300 μM *in vitro*). Valproic acid is a short chain fatty acid typically used as an anti-epileptic drug, which behaves, to some extent, as an HDAC inhibitor. Using the gemcitabine/valproic acid combination *in vitro* more than 80% C666-1 cells were positive for BZLF1 by immunofluorescence [86]. Wildeman's publication also provided substantial clinical data. Objective tumour responses were reported for three end-stage NPC patients subjected to a three-drug regimen combining gemcitabine, valproic acid and GCV [86]. Interestingly, 3 years later, partial tumour responses were again reported by the same group for five out of eight NPC patients refractory to conventional treatments and subjected to the almost same regimen except that GCV was replaced by valganciclovir [88]. The median survival was 9 months (95% confidence interval 7–17 months).

In some epithelial cell backgrounds, the combination of gemcitabine with an HDAC inhibitor is not mandatory for induction of the lytic cycle. Using a naturally EBV-infected gastric carcinoma cell-line, SNU-719, Lee et al. have observed induction of BZLF1 expression by gemcitabine alone at low concentrations (in the 10 nM range *in vitro*) [73]. Consistently, they have observed a synergy of gemcitabine with GCV in the treatment of SCID mice xenografted with SNU-719 gastric carcinoma cells. As pointed by the authors, a synergy between GCV and gemcitabine has also been reported in treatment of non-EBV-related malignant cells but much higher concentrations of gemcitabine were required (about 10 μM) [73, 89].

The mechanisms of lytic activation induced by drugs of conventional chemotherapy are complex and probably diverse. In the case of AGS-EBV cells, Kenney's group has highlight-

http://dx.doi.org/10.5772/64738

ed several signalling pathways suspected to link cell response to *cis*-platinum and 5-FU with the expression of immediate-early viral proteins: the MAPK/ERK, p38 MAPK and PKCδ pathways. However, all these data resulted from experiments based on chemical inhibitors. Therefore, they would probably need verifications by other approaches. As previously mentioned, endoplasmic reticulum (ER) stress is one possible cell alteration leading to lytic activation [75]. However, ER stress markers are not modified in gastric carcinoma cells subjected to lytic activation driven by gemcitabine [73]. Signalling pathways involved in the response to genotoxic stress seem to contribute more consistently to viral lytic activation, especially in epithelial cells. In SNU-719 cells, knocking-down expression of ATM and TP53 by RNA-interference antagonizes BZLF1 induction by gemcitabine [73].

4.2. Impact of HDAC inhibitors

Histone deacetylases (HDAC) belong to a class of enzymes that remove acetyl groups from histones, allowing them to wrap the DNA more tightly and therefore to decrease gene expression in the corresponding part of the genome. Therefore, depending on the cell context, HDAC inhibitors (HDACi) lead to transcriptional activation of a fraction of cellular genes, which are epigenetically silenced. Many HDACi have anti-oncogenic properties. They inhibit cell proliferation and favour cell cycle arrest, differentiation or apoptosis. These effects are at least partially related to re-expression of tumour suppressor genes such as *CDKN2A* or *ATM*. Their use for viral lytic induction is based on the assumption that histone acetylation is one epigenetic mechanism contributing to the silencing of most viral genes in latently infected cells. In addition, they can have less direct effects by increasing the expression of cellular proteins involved in the lytic cycle like the ATM kinase.

The first generation of HDACi includes different categories of compounds, for example, trichostatin A (one member of the hydroxamic acid family) or short chain fatty acids such as butyrate and valproic acid. As mentioned in the introduction of this chapter, as early as 1979, sodium butyrate was shown to induce lytic EBV activation in lymphoid cells [21]. At this date, the capacity of butyrate to inhibit histone deacetylases was not known, and the exact mechanism of the lytic induction remained raveled. It is noteworthy that, much later, in the years 2000, arginine butyrate was used in combination with GCV by Faller et al. in the first clinical trial aiming at lytic EBV activation in a group of patients bearing EBV-associated malignancies. Fifteen patients with refractory EBV-associated lymphoid malignancies were included in this phase I/II trial. Significant clinical responses were obtained for 10 of them including some complete clinical and pathological responses, although with important secondary effects [90].

The impact of valproic acid on lytic EBV gene expression has been mentioned in the previous part (D1) of this chapter. In contrast with more recent HDACi, very high concentrations of valproic acid are required for lytic gene induction, often in the range of 300 μM *in vitro*. In addition, valproic acid often has limited effects on lytic gene expression when it is not combined with another drug acting by a distinct mechanism, like gemcitabine. Recent studies published by G. Miller's group have shown that valproic acid has more complex biological effects than other HDACi. In some circumstances, it behaves as an antagonist of other HDACi and as an inhibitor of EBV lytic reactivation [63, 91]. Trichostatin A has been reported to induce

EBV lytic activation in an epithelial cell line artificially infected by EBV through pathways involving activation of the PKCδ and its phosphorylation of the Sp1 transcription factor (specificity protein 1) [61]. It is noteworthy that trichostatin has also been reported to induce activation of chromosomally integrated genomes of human herpesvirus 6 (HHV6), at least *in vitro* [92, 93].

HDACi of the second generation are compounds, which have been specifically designed to inhibit HDAC enzymes. They include the hydroxamic acids like vorinostat (suberoyl anilide hydroxamic acid or SAHA) and panobinostat (LBH589) and benzamides like entinostat (MS275). Most of them have the ability to inhibit HDAC enzymes of the class I (HDAC-1, HDAC-2, HDAC-3 and HDAC-8) and class II (HDAC-4, HDAC-5, HDAC-6, HDAC-7, HDAC-9 and HDAC-10). In 2012, Faller's group has reported an interesting comparative investigation of a series of HDACi mainly of the second generation, with an assessment of their relative strength in the induction of lytic EBV activation in lymphoid cells [94]. The most potent agent was panobinostat. Entinostat and apicidin, although less effective, were active in the nanomolar range. Vorinostat, which is active in epithelial cells as mentioned below, was not active in the panel of lymphoid cells used by the authors. Panobinostat has obtained approval from the European Medicines Agency and the Food and Drug Administration (USA) for the treatment of multiple myeloma.

Information on the impact of HDACi on epithelial cells, especially NPC cells, is available in a series of reports published by A.K.S. Chiang and collaborators from Hong Kong [95, 96]. Hui et al. reported in 2010 that in AGS-EBV cells, expression of BZLF1, BMRF1 and gp350 and even production of infectious viral particles were induced by Vorinostat used at μM concentrations [96]. As in previous studies, it was observed that the AGS-EBV cells had a certain level of spontaneous lytic activation in basal conditions prior to any drug treatment [59]. It was also confirmed that Vorinostat was a poor inducer of lytic EBV activation in lymphoid cells in contrast with data obtained using epithelial cells. In 2012, the same group has reported *in vitro* induction by Vorinostat (5 μM) of BZLF1 and BMRF1 but not gp350 in the NPC cell line C666-1. The induction of BZLF1 in C666-1 cells needed higher concentration of SAHA and a longer incubation time than for the artificial EBV(+) epithelial cell lines like HK1-EBV and HONE1-EBV. Nevertheless, induction of BZLF1 was achieved using Vorinostat *in vivo* by systemic treatment of C666-1 cells xenografted into nude mice (50 mg/kg, 5 days a week) [95]. Finally, in a report of 2016, Hui et al. have used a more selective HDACi, a bacterial product called romidepsin derived from *Chromobacterium violaceum* [60]. Romidepsin has selective inhibitory action against class I HDAC enzymes (mainly HDAC-1, HDAC-2 and HDAC-3). Romidepsin was shown to induce BZLF1, BRLF1 and BMRF1 in artificially EBV-infected epithelial cells using concentrations ranging from 0.5 to 5 nM. In mice xenografted with C666-1 cells, combined systemic administration of romidepsin (0.375 mg/kg, 2 days a week) and GCV (50 mg/kg, 5 days a week) resulted in a substantial tumour growth reduction [60]. The impact of romidepsin on lytic protein expression was abrogated by a chemical inhibitor of PKCδ but not inhibitors of PI3K, MEK, p38 MAPK, JNK. Interestingly lytic activation was not impaired by an ATM kinase inhibitor in contrast with observations made on SNU-719 gastric carcinoma cells treated with gemcitabine (see part D1 of this chapter and Lee et al.) [73]. Romidepsin is

http://dx.doi.org/10.5772/64738

approved by the FDA (Food and Drug Administration) but not the EMA (European Medicines Agency) for the treatment of cutaneous T-cell lymphomas. Adverse effects are nausea, vomiting, thrombocytopenia and leucopenia [97]. For future research, data on romidepsin underline the potential of novel more selective HDACi whose design is based on now-solved HDAC structures (third generation HDACi, for more information see Stahl et al. [98]).

4.3. Impact of miscellaneous pharmacological agents

In this section, we will briefly introduce other agents that have been used for lytic EBV activation but less consistently than HDAC inhibitors or conventional anti-cancer agents like gemcitabine. Phorbol-esters (like 12-*O*-tetradecanoylphorbol-13-acetate) are compounds, which activate proteins of the PKC family. In the history of EBV research, they have been among the first pharmacological agents along with sodium butyrate and BRdU used for induction of EBV lytic activation. However, to our knowledge, phorbol-esters have not been used in experiments involving NPC cells [65]. Nevertheless, as previously mentioned, one protein of the PKC family, PKCδ was reported to contribute to lytic EBV activation induced in epithelial cells by *cis*-platinum and 5-FU on the one hand and by romidepsin, an inhibitor of class I HDAC enzymes, on the other hand (see sections D1 and D2, respectively) [60, 59].

Bortezomib requires a special mention because it has been selected by a systematic screening of an FDA library of hundreds of chemical compounds to identify novel inducers of the lytic cycle (not published data but quoted by [48]). In Burkit lymphoma cells, the effect of Bortezomib on lytic activation has been reported to be dependent on the b-ZIP transcription factor C-EBP β (CCAAT/enhancer-binding protein β [99]). Bortezomib has proven to induce BZLF1 and EBV-TK expression in EBV-positive Burkitt lymphoma or gastric carcinoma cells xenografted on SCID mice [47, 48]. This process has been exploited for selective accumulation of FIAU in tumour cells expressing EBV-TK. Either for imaging purpose using this iodinated compound labelled with [^{125}I] or with therapeutic intent after labelling FIAU with [^{131}I]. To our knowledge, this approach has not been extended to NPC models. As explained in section C of this chapter, the use of FIAU in patients is compromised by the risk of acute metabolic or hepatic toxicity [81]. In more recent publication, the same group was involved in a new systematic screening of another compound library (John Hopkins Drug Library), which has identified gemcitabine as the best candidate for combination treatment with GCV [73].

Demethylating agents, especially 5-azacytidine, have been considered as potential inducers of EBV lytic activation in NPC cells. As reported by Chan et al., eight NPC patients were treated with 5-aza for one to six cycles: only mild lytic activation was recorded by RT-PCR and immunohistochemistry of lytic EBV products [100]. This relative weakness of 5-azacytidine might be explained by some distinct characteristics of BZLF1 and BRLF1 transactivation, which have been observed in the context of epithelial cells. BZLF1 transactivation of lytic gene promoters is enhanced by DNA methylation whereas it is the opposite for BRLF1 [45]. This is bad news for the impact of demethylating agents since cooperation of BZLF1 and BRLF1 is crucial for the optimal progression of lytic EBV activation.

A Notch2 inhibitor—dibenzazepine—has been shown to induce lytic EBV activation in Burkit and LCL cells by Giunco et al [101]. According to the authors, this effect depends on the

downregulation of the BATF transcription factor, which modulates BZLF1 expression. To our knowledge, lytic induction based on Notch2 inhibitors has not been investigated in NPC cells.

Finally, two groups have recently selected novel inducers of the lytic activation by high-throughput phenotypic screening from large chemical libraries containing several ten thousands of compounds [102, 103]. Tikhmyanova et al. have reported five structurally related tetrahydrocarboline derivatives, which are active in the range of 150–170 nM in various EBV-positive cell-lines including the C666-1 NPC cell line [103]. Choi et al. have published data on five novel compounds, which are distinct from PKC agonists and HDACi, one of which activates the MAPK pathways and bears structural resemblance to iron chelators [102].

5. Conclusions

The idea of inducing EBV lytic activation in malignant NPC cells with a therapeutic intent has been in the air for more than 30 years [21]. However, this therapeutic approach is still facing major obstacles. First, there is evidence that EBV latency is heavily locked in NPC cells, and several locking mechanisms are probably intimately connected with the oncogenic alterations at the levels of genome, epigenome and cell phenotype. For example, there is evidence that the wild-type ATM kinase plays a critical role at several steps of lytic EBV activation (although not under treatment by romidepsin) [60, 72, 74]. In fact, ATM is frequently downregulated in NPC cells [106]. There is also evidence that Stat3 activation prevents EBV lytic activation. Again, constitutive Stat3 activation is a common feature of malignant NPC cells. Hydroxy-methylation marks often disappear from the DNA of NPC cells [107, 108]. In a fraction of tumours, this alteration is a consequence of inactivating mutations in the *TET1*, *TET2* or *TET3* genes [11]. Regardless of its mechanism, the loss of DNA hydroxyl-methylation promotes malignant transformation and simultaneously makes the lytic promoters less sensitive to the action of BRLF1 [56].

Another difficulty is the absence of biomarkers for early identification of NPC tumours that will be responsive to various agents expected to induce the lytic cycle. We suggest that, in general, the most sensitive tumours will be those where there is a spontaneous expression of lytic genes prior to any treatment, a point that would deserve a specific investigation. In spite of all these difficulties, significant progress has been accomplished. Several objective tumour responses have been obtained in NPC patients treated with a combination of gemcitabine, valproic acid and GCV [86, 88]. Since HDACi more effective than valproic acid are now available, there is room for progress using similar patterns of treatment. At a time when the success of immunotherapies based on checkpoint inhibitors has a dramatic impact on our approach of cancer biology and therapy, several authors rightly emphasize the importance of EBV lytic activation as a mean to increase the antigenicity of malignant cells [109]. This trend is even stronger since major changes are taking place at the confluence of epigenetics, virology and tumour immunology: recent publications have shown that demethylating agents can increase tumour cell antigenicity by removing the inhibition of endogenous retroviruses [110].

http://dx.doi.org/10.5772/64738

However, combining the inducers of EBV lytic activation with prodrugs specifically activated by viral enzymes remains a valuable goal. It is striking that while remarkable progress is being made concerning lytic inducers, almost nothing seems to happen regarding the prodrug candidates. So far, most investigators rely on GCV (ganciclovir), which was not designed for EBV-infected cells but is used by default. Nevertheless, a change seems to be in the air in this field too. A recent systematic proteomic analysis of EBV-PK substrates has identified hundreds of cellular proteins involved in DNA damage response, mitosis and cell cycle. More importantly, in terms of pharmacology, the analysis of the phosphosites of these substrates reveals a proline-rich motif signature, which will probably be helpful for the design of artificial substrates [50].

Competing interests

The authors declare no financial or non-financial competing interests.

Acknowledgements

Natalie Oker was the recipient of a fellowship from the "Union des Blessés de la Face et de la Tête—Les Gueules Cassées" (2014).

Author details

Natalie Oker[1,2], Nikiforos-Ioannis Kapetanakis[1] and Pierre Busson[1*]

*Address all correspondence to: pbusson@igr.fr

1 CNRS UMR 8126, Gustave Roussy and University of Paris-Sud/Paris-Saclay, Villejuif, France

2 Department of Otorhinolaryngology, Cervicofacial, Maxillofacial and Plastic Surgery, Lariboisière Hospital (Assistance Publique Hôpitaux de Paris) and University of Denis Diderot, Paris, France

References

[1] Busson P, editor. Nasopharyngeal Carcinoma. Keys for Translational Medicine and Biology. New York/Austin: Landes/Springer; 2012. 205 p.

[2] Busson P, Keryer C, Ooka T, Corbex M. EBV-associated nasopharyngeal carcinomas: from epidemiology to virus-targeting strategies. Trends Microbiol. 2004;12:356–60.

[3] Chua ML, Wee JT, Hui EP, Chan AT. Nasopharyngeal carcinoma. Lancet. 2016 Mar 5;387(10022):1012–24. DOI: 10.1016/S0140-6736(15)00055-0. pii: S0140-6736(15)00055-0.

[4] Feng BJ. Descriptive, environmental and genetic epidemiology of nasopharyngeal carcinoma. In: Bussson P, editor. Nasopharyngeal Carcinoma: Keys for Translational Medicine and Biology. Austin/New York: Landes/Springer; 2013. p. 23–41.

[5] Dai W, Zheng H, Cheung AK, Tang CS, Ko JM, Wong BW, et al. Whole-exome sequencing identifies MST1R as a genetic susceptibility gene in nasopharyngeal carcinoma. Proc Natl Acad Sci USA. 2016;113:3317–22. DOI: 10.1073/pnas.1523436113.

[6] Cheung ST, Huang DP, Hui AB, Lo KW, Ko CW, Tsang YS, et al. Nasopharyngeal carcinoma cell line (C666-1) consistently harbouring Epstein-Barr virus. Int J Cancer. 1999;83:121–6.

[7] Busson P, Ganem G, Flores P, Mugneret F, Clausse B, Caillou B, et al. Establishment and characterization of three transplantable EBV-containing nasopharyngeal carcinomas. Int J Cancer. 1988;42:599–606.

[8] Gressette M, Verillaud B, Jimenez-Pailhes AS, Lelievre H, Lo KW, Ferrand FR, et al. Treatment of nasopharyngeal carcinoma cells with the histone-deacetylase inhibitor abexinostat: cooperative effects with *cis*-platin and radiotherapy on patient-derived xenografts. PLoS One. 2014;9:e91325. DOI: 10.1371/journal.pone.0091325.

[9] Hoe SL, Tan LP, Jamal J, Peh SC, Ng CC, Zhang WC, et al. Evaluation of stem-like side population cells in a recurrent nasopharyngeal carcinoma cell line. Cancer Cell Int. 2014;14:101. DOI: 10.1186/s12935-014-0101-0.

[10] Glaser R, Zhang HY, Yao KT, Zhu HC, Wang FX, Li GY, et al. Two epithelial tumor cell lines (HNE-1 and HONE-1) latently infected with Epstein-Barr virus that were derived from nasopharyngeal carcinomas. Proc Natl Acad Sci USA. 1989;86:9524–8.

[11] Lin DC, Meng X, Hazawa M, Nagata Y, Varela AM, Xu L, et al. The genomic landscape of nasopharyngeal carcinoma. Nat Genet. 2014;46:866–71. DOI: 10.1038/ng.3006.

[12] Lo K, Chung GT, To KF. Acquired genetic and epigenetic alterations in nasophryngeal carcinomas. In: Busson P, editor. Nasopharyngeal Carcinoma—Keys for Translational Medicine and Biology. Austin/New York: Landes/Springer; 2013. p. 61–81.

[13] Ayadi W, Karray-Hakim H, Khabir A, Feki L, Charfi S, Boudawara T, et al. Aberrant methylation of p16, DLEC1, BLU and E-cadherin gene promoters in nasopharyngeal carcinoma biopsies from Tunisian patients. Anticancer Res. 2008;28:2161–7.

[14] Chan SL, Cui Y, van Hasselt A, Li H, Srivastava G, Jin H, et al. The tumor suppressor Wnt inhibitory factor 1 is frequently methylated in nasopharyngeal and esophageal carcinomas. Lab Invest. 2007;87:644–50. DOI: 10.1038/labinvest.3700547.

[15] Birdwell CE, Queen KJ, Kilgore PC, Rollyson P, Trutschl M, Cvek U, et al. Genome-wide DNA methylation as an epigenetic consequence of Epstein-Barr virus infection of immortalized keratinocytes. J Virol. 2014;88:11442–58. DOI: 10.1128/JVI.00972-14.

[16] Hui AB, Or YY, Takano H, Tsang RK, To KF, Guan XY, et al. Array-based comparative genomic hybridization analysis identified cyclin D1 as a target oncogene at 11q13.3 in nasopharyngeal carcinoma. Cancer Res. 2005;65:8125–33.

[17] Chung GT, Lung RW, Hui AB, Yip KY, Woo JK, Chow C, et al. Identification of a recurrent transforming UBR5-ZNF423 fusion gene in EBV-associated nasopharyngeal carcinoma. J Pathol. 2013;231:158–67. DOI: 10.1002/path.4240.

[18] Yuan L, Liu ZH, Lin ZR, Xu LH, Zhong Q, Zeng MS. Recurrent FGFR3-TACC3 fusion gene in nasopharyngeal carcinoma. Cancer Biol Ther. 2014;15:1613–21. DOI: 10.4161/15384047.2014.961874.

[19] Guigay J. Advances in nasopharyngeal carcinoma. Curr Opin Oncol. 2008;20:264–9.

[20] Lee AW, Ma BB, Ng WT, Chan AT. Management of nasopharyngeal carcinoma: current practice and future perspective. J Clin Oncol. 2015 Oct 10;33(29):3356–64.. DOI: 10.1200/JCO.2015.60.9347.

[21] Luka J, Kallin B, Klein G. Induction of the Epstein-Barr virus (EBV) cycle in latently infected cells by *n*-butyrate. Virology. 1979;94:228–31.

[22] Tse E, Kwong YL. How I treat NK/T-cell lymphomas. Blood. 2013;121:4997–5005. DOI: 10.1182/blood-2013-01-453233.

[23] Flavell KJ, Murray PG. Hodgkin's disease and the Epstein-Barr virus. Mol Pathol. 2000;53:262–9.

[24] Epstein MA, Barr YM. Cultivation in vitro of human lymphoblasts from Burkitt's malignant lymphoma. Lancet. 1964;1:252–3.

[25] Iizasa H, Nanbo A, Nishikawa J, Jinushi M, Yoshiyama H. Epstein-Barr virus (EBV)-associated gastric carcinoma. Viruses. 2012;4:3420–39.

[26] Ascherio A, Munger KL, Lunemann JD. The initiation and prevention of multiple sclerosis. Nat Rev Neurol. 2012;8:602–12. DOI: 10.1038/nrneurol.2012.198.

[27] Draborg AH, Duus K, Houen G. Epstein-Barr virus in systemic autoimmune diseases. Clin Dev Immunol. 2013;2013:535738. DOI: 10.1155/2013/535738.

[28] Hu Z, Usherwood EJ. Immune escape of gamma-herpesviruses from adaptive immunity. Rev Med Virol. 2014 Nov;24(6):365–78. DOI: 10.1002/rmv.1791.

[29] Miller G, El-Guindy A, Countryman J, Ye J, Gradoville L. Lytic cycle switches of oncogenic human gammaherpesviruses. Adv Cancer Res. 2007;97:81–109. DOI: 10.1016/S0065-230X(06)97004-3.

[30] Feng WH, Hong G, Delecluse HJ, Kenney SC. Lytic induction therapy for Epstein-Barr virus-positive B-cell lymphomas. J Virol. 2004;78:1893–902.

[31] Skalsky RL, Cullen BR. EBV noncoding RNAs. Curr Top Microbiol Immunol. 2015;391:181–217. DOI: 10.1007/978-3-319-22834-1_6.

[32] Klinke O, Feederle R, Delecluse HJ. Genetics of Epstein-Barr virus microRNAs. Semin Cancer Biol. (Review). 2014;26:52–9. DOI: 10.1016/j.semcancer.2014.02.002.

[33] Amoroso R, Fitzsimmons L, Thomas WA, Kelly GL, Rowe M, Bell AI. Quantitative studies of Epstein-Barr virus-encoded microRNAs provide novel insights into their regulation. J Virol. 2011;85:996–1010. DOI: 10.1128/JVI.01528-10.

[34] Cosmopoulos K, Pegtel M, Hawkins J, Moffett H, Novina C, Middeldorp J, et al. Comprehensive profiling of Epstein-Barr virus microRNAs in nasopharyngeal carcinoma. J Virol. 2009;83:2357–67.

[35] Choy EY, Siu KL, Kok KH, Lung RW, Tsang CM, To KF, et al. An Epstein-Barr virus-encoded microRNA targets PUMA to promote host cell survival. J Exp Med. 2008;205:2551–60.

[36] Barth S, Pfuhl T, Mamiani A, Ehses C, Roemer K, Kremmer E, et al. Epstein-Barr virus-encoded microRNA miR-BART2 down-regulates the viral DNA polymerase BALF5. Nucleic Acids Res. 2008;36:666–75. DOI: 10.1093/nar/gkm1080.

[37] Cai L, Ye Y, Jiang Q, Chen Y, Lyu X, Li J, et al. Epstein-Barr virus-encoded microRNA BART1 induces tumour metastasis by regulating PTEN-dependent pathways in nasopharyngeal carcinoma. Nat Commun. 2015;6:7353. DOI: 10.1038/ncomms8353.

[38] Iwakiri D, Takada K. Role of EBERs in the pathogenesis of EBV infection. Adv Cancer Res. (Review). 2010;107:119–36. DOI: 10.1016/S0065-230X(10)07004-1.

[39] Khabir A, Karray H, Rodriguez S, Rose M, Daoud J, Frikha M, et al. EBV latent membrane protein 1 abundance correlates with patient age but not with metastatic behavior in north African nasopharyngeal carcinomas. Virol J. 2005;2:39.

[40] Heussinger N, Buttner M, Ott G, Brachtel E, Pilch BZ, Kremmer E, et al. Expression of the Epstein-Barr virus (EBV)-encoded latent membrane protein 2A (LMP2A) in EBV-associated nasopharyngeal carcinoma. J Pathol. 2004;203:696–9.

[41] Barth S, Meister G, Grasser FA. EBV-encoded miRNAs. Biochim Biophys Acta. [Research Support, Non-U.S. Gov't]. 2011;1809:631–40. DOI: 10.1016/j.bbagrm.2011.05.010.

[42] Jung YJ, Choi H, Kim H, Lee SK. MicroRNA miR-BART20-5p stabilizes Epstein-Barr virus latency by directly targeting BZLF1 and BRLF1. J Virol. 2014;88:9027–37. DOI: 10.1128/JVI.00721-14.

[43] Frappier L. Role of EBNA1 in NPC tumourigenesis. Semin Cancer Biol. 2012;22:154–61. DOI: 10.1016/j.semcancer.2011.12.002. pii: S1044-579X(11)00103-9.

[44] Strockbine LD, Cohen JI, Farrah T, Lyman SD, Wagener F, DuBose RF, et al. The Epstein-Barr virus BARF1 gene encodes a novel, soluble colony-stimulating factor-1 receptor. J Virol. 1998;72:4015–21.

[45] Wille CK, Nawandar DM, Panfil AR, Ko MM, Hagemeier SR, Kenney SC. Viral genome methylation differentially affects the ability of BZLF1 versus BRLF1 to activate Epstein-Barr virus lytic gene expression and viral replication. J Virol. 2013;87:935–50. DOI: 10.1128/JVI.01790-12.

[46] Kenney SC, Mertz JE. Regulation of the latent-lytic switch in Epstein-Barr virus. Semin Cancer Biol. 2014;26:60–8. DOI: 10.1016/j.semcancer.2014.01.002.

[47] Fu DX, Tanhehco Y, Chen J, Foss CA, Fox JJ, Chong JM, et al. Bortezomib-induced enzyme-targeted radiation therapy in herpesvirus-associated tumors. Nat Med. 2008;14:1118–22. DOI: 10.1038/nm.1864.

[48] Fu DX, Tanhehco YC, Chen J, Foss CA, Fox JJ, Lemas V, et al. Virus-associated tumor imaging by induction of viral gene expression. Clin Cancer Res. 2007;13:1453–8. DOI: 10.1158/1078-0432.CCR-06-2295.

[49] Meng Q, Hagemeier SR, Fingeroth JD, Gershburg E, Pagano JS, Kenney SC. The Epstein-Barr virus (EBV)-encoded protein kinase, EBV-PK, but not the thymidine kinase (EBV-TK), is required for ganciclovir and acyclovir inhibition of lytic viral production. J Virol. 2010;84:4534–42. DOI: 10.1128/JVI.02487-09.

[50] Li R, Liao G, Nirujogi RS, Pinto SM, Shaw PG, Huang TC, et al. Phosphoproteomic profiling reveals Epstein-Barr virus protein kinase integration of DNA damage response and mitotic signaling. PLoS Pathog. 2015;11:e1005346. DOI: 10.1371/journal.ppat.1005346. pii: PPATHOGENS-D-15-01981.

[51] Coghill AE, Bu W, Nguyen H, Hsu WL, Yu KJ, Lou PJ, et al. High levels of antibody that neutralize B-cell infection of Epstein-Barr virus and that bind EBV gp350 are associated with a lower risk of nasopharyngeal carcinoma. Clin Cancer Res. 2016 Jul 15;22(14):3451–7. DOI: 10.1158/1078-0432.CCR-15-2299. pii: clincanres.2299.2015.

[52] Shannon-Lowe CD, Neuhierl B, Baldwin G, Rickinson AB, Delecluse HJ. Resting B cells as a transfer vehicle for Epstein-Barr virus infection of epithelial cells. Proc Natl Acad Sci USA. 2006 May 2;103(18):7065–70.

[53] Tsang CM, Yip YL, Lo KW, Deng W, To KF, Hau PM, et al. Cyclin D1 overexpression supports stable EBV infection in nasopharyngeal epithelial cells. Proc Natl Acad Sci USA. 2012;109:E3473–82. DOI: 10.1073/pnas.1202637109.

[54] Feederle R, Neuhierl B, Bannert H, Geletneky K, Shannon-Lowe C, Delecluse HJ. Epstein-Barr virus B95.8 produced in 293 cells shows marked tropism for differentiat-

ed primary epithelial cells and reveals interindividual variation in susceptibility to viral infection. Int J Cancer. 2007;121:588–94. DOI: 10.1002/ijc.22727.

[55] Quinlivan EB, Holley-Guthrie EA, Norris M, Gutsch D, Bachenheimer SL, Kenney SC. Direct BRLF1 binding is required for cooperative BZLF1/BRLF1 activation of the Epstein-Barr virus early promoter, BMRF1. Nucleic Acids Res. 1993;21:1999–2007.

[56] Wille CK, Nawandar DM, Henning AN, Ma S, Oetting KM, Lee D, et al. 5-Hydroxymethylation of the EBV genome regulates the latent to lytic switch. Proc Natl Acad Sci USA. 2015;112:E7257–65. DOI: 10.1073/pnas.1513432112.

[57] Temple RM, Zhu J, Budgeon L, Christensen ND, Meyers C, Sample CE. Efficient replication of Epstein-Barr virus in stratified epithelium in vitro. Proc Natl Acad Sci USA. 2014;111:16544–9. DOI: 10.1073/pnas.1400818111.

[58] Hadinoto V, Shapiro M, Sun CC, Thorley-Lawson DA. The dynamics of EBV shedding implicate a central role for epithelial cells in amplifying viral output. PLoS Pathog. 2009;5:e1000496. DOI: 10.1371/journal.ppat.1000496.

[59] Feng WH, Israel B, Raab-Traub N, Busson P, Kenney SC. Chemotherapy induces lytic EBV replication and confers ganciclovir susceptibility to EBV-positive epithelial cell tumors. Cancer Res. 2002;62:1920–6.

[60] Hui KF, Cheung AK, Choi CK, Yeung PL, Middeldorp JM, Lung ML, et al. Inhibition of class I histone deacetylases by romidepsin potently induces Epstein-Barr virus lytic cycle and mediates enhanced cell death with ganciclovir. Int J Cancer. 2016;138:125–36. DOI: 10.1002/ijc.29698.

[61] Tsai PF, Lin SJ, Weng PL, Tsai SC, Lin JH, Chou YC, et al. Interplay between PKCdelta and Sp1 on histone deacetylase inhibitor-mediated Epstein-Barr virus reactivation. J Virol. 2011;85:2373–85. DOI: 10.1128/JVI.01602-10.

[62] Lai KY, Chou YC, Lin JH, Liu Y, Lin KM, Doong SL, et al. Maintenance of Epstein-Barr Virus latent status by a novel mechanism, latent membrane protein 1-induced interleukin-32, via the protein kinase c-delta pathway. J Virol. 2015;89:5968–80. DOI: 10.1128/JVI.00168-15.

[63] Gorres KL, Daigle D, Mohanram S, McInerney GE, Lyons DE, Miller G. Valpromide inhibits lytic cycle reactivation of Epstein-Barr virus. MBio. 2016 Mar 1;7(2):e00113;7. DOI: 10.1128/mBio.00113-16 e00113-16.

[64] Ye J, Gradoville L, Miller G. Cellular immediate-early gene expression occurs kinetically upstream of Epstein-Barr virus bzlf1 and brlf1 following cross-linking of the B cell antigen receptor in the Akata Burkitt lymphoma cell line. J Virol. 2010;84:12405–18. DOI: 10.1128/JVI.01415-10.

[65] Nutter LM, Grill SP, Li JS, Tan RS, Cheng YC. Induction of virus enzymes by phorbol esters and *n*-butyrate in Epstein-Barr virus genome-carrying Raji cells. Cancer Res. 1987;47:4407–12.

[66] Vrzalikova K, Vockerodt M, Leonard S, Bell A, Wei W, Schrader A, et al. Down-regulation of BLIMP1alpha by the EBV oncogene, LMP-1, disrupts the plasma cell differentiation program and prevents viral replication in B cells: implications for the pathogenesis of EBV-associated B-cell lymphomas. Blood. 2011;117:5907–17. DOI: 10.1182/blood-2010-09-307710.

[67] Fukuda M, Ikuta K, Yanagihara K, Tajima M, Kuratsune H, Kurata T, et al. Effect of transforming growth factor-beta1 on the cell growth and Epstein-Barr virus reactivation in EBV-infected epithelial cell lines. Virology. 2001;288:109–18. DOI: 10.1006/viro.2001.1071. pii: S0042-6822(01)91071-2.

[68] Li Y, Long X, Huang L, Yang M, Yuan Y, Wang Y, et al. Epstein-Barr Virus BZLF1-mediated downregulation of proinflammatory factors is essential for optimal lytic viral replication. J Virol. 2015;90:887–903. DOI: 10.1128/JVI.01921-15.

[69] Brown HJ, Song MJ, Deng H, Wu TT, Cheng G, Sun R. NF-kappaB inhibits gammaherpesvirus lytic replication. J Virol. 2003;77:8532–40.

[70] Trumper PA, Epstein MA, Giovanella BC. Activation in vitro by BUdR of a productive EB virus infection in the epithelial cells of nasopharyngeal carcinoma. Int J Cancer. 1976;17:578–87.

[71] Westphal EM, Blackstock W, Feng W, Israel B, Kenney SC. Activation of lytic Epstein-Barr virus (EBV) infection by radiation and sodium butyrate in vitro and in vivo: a potential method for treating EBV-positive malignancies. Cancer Res. 2000;60:5781–8.

[72] Hagemeier SR, Barlow EA, Meng Q, Kenney SC. The cellular ataxia telangiectasia-mutated kinase promotes Epstein-Barr virus lytic reactivation in response to multiple different types of lytic reactivation-inducing stimuli. J Virol. 2012;86:13360–70. DOI: 10.1128/JVI.01850-12.

[73] Lee HG, Kim H, Kim EJ, Park PG, Dong SM, Choi TH, et al. Targeted therapy for Epstein-Barr virus-associated gastric carcinoma using low-dose gemcitabine-induced lytic activation. Oncotarget. 2015;6:31018–29. DOI: 10.18632/oncotarget.5041.

[74] Hau PM, Deng W, Jia L, Yang J, Tsurumi T, Chiang AK, et al. Role of ATM in the formation of the replication compartment during lytic replication of Epstein-Barr virus in nasopharyngeal epithelial cells. J Virol. 2015;89:652–68. DOI: 10.1128/JVI.01437-14.

[75] Taylor GM, Raghuwanshi SK, Rowe DT, Wadowsky RM, Rosendorff A. Endoplasmic reticulum stress causes EBV lytic replication. Blood. 2011;118:5528–39. DOI: 10.1182/blood-2011-04-347112.

[76] Lin Z, Flemington EK. miRNAs in the pathogenesis of oncogenic human viruses. Cancer Lett. 2011;305:186–99. DOI: 10.1016/j.canlet.2010.08.018.

[77] Lin Z, Swan K, Zhang X, Cao S, Brett Z, Drury S, et al. Secreted oral epithelial cell membrane vesicles induce Epstein-Barr virus reactivation in latently infected B cells. J Virol. 2016;90:3469–79. DOI: 10.1128/JVI.02830-15.

[78] Forte E, Luftig MA. The role of microRNAs in Epstein-Barr virus latency and lytic reactivation. Microbes Infect/Institut Pasteur. 2011;13:1156–67. DOI: 10.1016/j.micinf.2011.07.007.

[79] Cayrol C, Flemington EK. The Epstein-Barr virus bZIP transcription factor Zta causes G0/G1 cell cycle arrest through induction of cyclin-dependent kinase inhibitors. EMBO J. 1996;15:2748–59.

[80] Gustafson EA, Chillemi AC, Sage DR, Fingeroth JD. The Epstein-Barr virus thymidine kinase does not phosphorylate ganciclovir or acyclovir and demonstrates a narrow substrate specificity compared to the herpes simplex virus type 1 thymidine kinase. Antimicrob Agents Chemother. 1998;42:2923–31.

[81] McKenzie R, Fried MW, Sallie R, Conjeevaram H, Di Bisceglie AM, Park Y, et al. Hepatic failure and lactic acidosis due to fialuridine (FIAU), an investigational nucleoside analogue for chronic hepatitis B. N Engl J Med. 1995;333:1099–105. DOI: 10.1056/NEJM199510263331702.

[82] Hong GK, Gulley ML, Feng WH, Delecluse HJ, Holley-Guthrie E, Kenney SC. Epstein-Barr virus lytic infection contributes to lymphoproliferative disease in a SCID mouse model. J Virol. 2005;79:13993–4003.

[83] Hsu M, Wu SY, Chang SS, Su IJ, Tsai CH, Lai SJ, et al. Epstein-Barr virus lytic transactivator Zta enhances chemotactic activity through induction of interleukin-8 in nasopharyngeal carcinoma cells. J Virol. 2008;82:3679–88. DOI: 10.1128/JVI.02301-07.

[84] Lee CH, Yeh TH, Lai HC, Wu SY, Su IJ, Takada K, et al. Epstein-Barr virus Zta-induced immunomodulators from nasopharyngeal carcinoma cells upregulate interleukin-10 production from monocytes. J Virol. 2011;85:7333–42. DOI: 10.1128/JVI.00182-11.

[85] Feng WH, Cohen JI, Fischer S, Li L, Sneller M, Goldbach-Mansky R, et al. Reactivation of latent Epstein-Barr virus by methotrexate: a potential contributor to methotrexate-associated lymphomas. J Natl Cancer Inst. 2004;96:1691–702. DOI: 10.1093/jnci/djh313.

[86] Wildeman MA, Novalic Z, Verkuijlen SA, Juwana H, Huitema AD, Tan IB, et al. Cytolytic virus activation therapy for Epstein-Barr virus-driven tumors. Clin Cancer Res. 2012;18:5061–70. DOI: 10.1158/1078-0432.CCR-12-0574.

[87] Hsu CL, Kuo YC, Huang Y, Huang YC, Lui KW, Chang KP, et al. Application of a patient-derived xenograft model in cytolytic viral activation therapy for nasopharyngeal carcinoma. Oncotarget. 2015;6:31323–34. DOI: 10.18632/oncotarget.5544.

[88] Stoker SD, Novalic Z, Wildeman MA, Huitema AD, Verkuijlen SA, Juwana H, et al. Epstein-Barr virus-targeted therapy in nasopharyngeal carcinoma. J Cancer Res Clin Oncol. 2015;141:1845–57. DOI: 10.1007/s00432-015-1969-3.

[89] Boucher PD, Shewach DS. In vitro and in vivo enhancement of ganciclovir-mediated bystander cytotoxicity with gemcitabine. Mol Ther. 2005;12:1064–71. DOI: 10.1016/j.ymthe.2005.07.643. pii: S1525-0016(05)01254-2.

[90] Perrine SP, Hermine O, Small T, Suarez F, O'Reilly R, Boulad F, et al. A phase 1/2 trial of arginine butyrate and ganciclovir in patients with Epstein-Barr virus-associated lymphoid malignancies. Blood. 2007;109:2571–8. DOI: 10.1182/blood-2006-01-024703.

[91] Daigle D, Gradoville L, Tuck D, Schulz V, Wang'ondu R, Ye J, et al. Valproic acid antagonizes the capacity of other histone deacetylase inhibitors to activate the Epstein-barr virus lytic cycle. J Virol. 2011;85:5628–43. DOI: 10.1128/JVI.02659-10.

[92] Arbuckle JH, Medveczky MM, Luka J, Hadley SH, Luegmayr A, Ablashi D, et al. The latent human herpesvirus-6A genome specifically integrates in telomeres of human chromosomes in vivo and in vitro. Proc Natl Acad Sci USA. 2010;107:5563–8. DOI: 10.1073/pnas.0913586107.

[93] Pellett PE, Ablashi DV, Ambros PF, Agut H, Caserta MT, Descamps V, et al. Chromosomally integrated human herpesvirus 6: questions and answers. Rev Med Virol. 2012;22:144–55. DOI: 10.1002/rmv.715.

[94] Ghosh SK, Perrine SP, Williams RM, Faller DV. Histone deacetylase inhibitors are potent inducers of gene expression in latent EBV and sensitize lymphoma cells to nucleoside antiviral agents. Blood. 2012;119:1008–17. DOI: 10.1182/blood-2011-06-362434.

[95] Hui KF, Ho DN, Tsang CM, Middeldorp JM, Tsao GS, Chiang AK. Activation of lytic cycle of Epstein-Barr virus by suberoylanilide hydroxamic acid leads to apoptosis and tumor growth suppression of nasopharyngeal carcinoma. Int J Cancer. 2012;131:1930–40. DOI: 10.1002/ijc.27439.

[96] Hui KF, Chiang AK. Suberoylanilide hydroxamic acid induces viral lytic cycle in Epstein-Barr virus-positive epithelial malignancies and mediates enhanced cell death. Int J Cancer. 2010;126:2479–89. DOI: 10.1002/ijc.24945.

[97] Martinez-Escala ME, Kuzel TM, Kaplan JB, Petrich A, Nardone B, Rosen ST, et al. Durable responses with maintenance dose-sparing regimens of romidepsin in cutaneous T-cell lymphoma. JAMA Oncol. 2016 Jun 1;2(6):790–3.. DOI: 10.1001/jamaoncol.2016.0004.

[98] Stahl M, Gore SD, Vey N, Prebet T. Lost in translation? Ten years of development of histone deacetylase inhibitors in acute myeloid leukemia and myelodysplastic syndromes. Expert Opin Investig Drugs. 2016;25:307–17. DOI: 10.1517/13543784.2016.1146251.

[99] Shirley CM, Chen J, Shamay M, Li H, Zahnow CA, Hayward SD, et al. Bortezomib induction of C/EBPbeta mediates Epstein-Barr virus lytic activation in Burkitt lymphoma. Blood. 2011;117:6297–303. DOI: 10.1182/blood-2011-01-332379.

[100] Chan AT, Tao Q, Robertson KD, Flinn IW, Mann RB, Klencke B, et al. Azacitidine induces demethylation of the Epstein-Barr virus genome in tumors. J Clin Oncol. 2004;22:1373–81. DOI: 10.1200/JCO.2004.04.185.

[101] Giunco S, Celeghin A, Gianesin K, Dolcetti R, Indraccolo S, De Rossi A. Cross talk between EBV and telomerase: the role of TERT and NOTCH2 in the switch of latent/lytic cycle of the virus. Cell Death Dis. 2015;6:e1774. DOI: 10.1038/cddis.2015.145.

[102] Choi CK, Ho DN, Hui KF, Kao RY, Chiang AK. Identification of novel small organic compounds with diverse structures for the induction of Epstein-Barr virus (EBV) lytic cycle in EBV-positive epithelial malignancies. PLoS One. 2015;10:e0145994. DOI: 10.1371/journal.pone.0145994. pii: PONE-D-15-43595.

[103] Tikhmyanova N, Schultz DC, Lee T, Salvino JM, Lieberman PM. Identification of a new class of small molecules that efficiently reactivate latent Epstein-Barr Virus. ACS Chem Biol. 2014;9:785–95. DOI: 10.1021/cb4006326.

[104] Stevens SJ, Zwaan CM, Verkuijlen SA, Middeldorp JM. Epstein-Barr virus (EBV) serology for predicting distant metastases in a white juvenile patient with nasopharyngeal carcinoma and no clinical response to EBV lytic induction therapy. Head Neck. (Case Reports) 2006;28:1040–5. DOI: 10.1002/hed.20466.

[105] Chen MR, Chang SJ, Huang H, Chen JY. A protein kinase activity associated with Epstein-Barr virus BGLF4 phosphorylates the viral early antigen EA-D in vitro. J Virol. 2000;74:3093–104.

[106] Bose S, Yap LF, Fung M, Starzcynski J, Saleh A, Morgan S, et al. The ATM tumour suppressor gene is down-regulated in EBV-associated nasopharyngeal carcinoma. J Pathol. 2009;217:345–52.

[107] Ho Y, Tsao SW, Zeng M, Lui VW. STAT3 as a therapeutic target for Epstein-Barr virus (EBV): associated nasopharyngeal carcinoma. Cancer Lett. 2013;330:141–9. DOI: 10.1016/j.canlet.2012.11.052.

[108] Kung CP, Meckes DG, Jr., Raab-Traub N. Epstein-Barr virus LMP1 activates EGFR, STAT3, and ERK through effects on PKCdelta. J Virol. 2011;85:4399–408. DOI: 10.1128/JVI.01703-10.

[109] Hutajulu SH, Kurnianda J, Tan IB, Middeldorp JM. Therapeutic implications of Epstein-Barr virus infection for the treatment of nasopharyngeal carcinoma. Ther Clin Risk Manag. 2014;10:721–36. DOI: 10.2147/TCRM.S47434.

[110] Chiappinelli KB, Strissel PL, Desrichard A, Li H, Henke C, Akman B, et al. Inhibiting DNA methylation causes an interferon response in cancer via dsRNA including endogenous retroviruses. Cell. 2015;162:974–86. DOI: 10.1016/j.cell.2015.07.011. pii: S0092-8674(15)00848-X.

www.impactjournals.com/oncotarget/ Oncotarget, 2016, Vol. 7, (No. 50), pp: 82580-82593

Research Paper

Stimulation of the toll-like receptor 3 promotes metabolic reprogramming in head and neck carcinoma cells

Mathieu Veyrat[1], Sylvère Durand[2], Marion Classe[3], Tanja Matijevic Glavan[4], Natalie Oker[1,5], Nikiforos-Ioannis Kapetanakis[1], Xiaojun Jiang[1], Aurore Gelin[1], Philippe Herman[5], Odile Casiraghi[6], David Zagzag[7], David Enot[2], Pierre Busson[1], Benjamin Vérillaud[1,5]

[1]University Paris-Sud (Paris 11), CNRS-UMR 8126, Gustave Roussy, Villejuif, France

[2]Equipe 11 Labélisée par la Ligue Nationale Contre le Cancer, INSERM U1138, Centre de Recherche des Cordeliers, Paris, France, Metabolomics and Molecular Cell Biology Platforms, Gustave Roussy, Villejuif, France

[3]Department of Pathology, Lariboisière Hospital, AP-HP, University Paris-Diderot Paris 7, Paris, France

[4]Division of Molecular Medicine, Rudjer Boskovic Institute, Zagreb, Croatia

[5]Department of Head and Neck surgery, Lariboisière Hospital, AP-HP, University Paris-Diderot Paris 7, Paris, France

[6]Department of Biopathology, Gustave Roussy, Villejuif, France

[7]Department of Neuropathology, New York University School of Medicine, New York, NY, USA

Correspondence to: Benjamin Vérillaud, **email:** benjamin.verillaud@gmail.com

Keywords: *toll-like receptor 3, innate immunity, warburg effect, HIF, metabolomics*

Received: *February 12, 2015* ***Accepted:*** *October 19, 2016* ***Published:*** *October 25, 2016*

ABSTRACT

In this study, a possible link between the innate immune recognition receptor TLR3 and metabolic reprogramming in Head and Neck carcinoma (HNC) cells was investigated. The effects of TLR3 stimulation/knock-down were assessed under several culture conditions in 4 HNC cell-lines by cell growth assays, targeted metabolomics, and glycolysis assays based on time-resolved analysis of proton release (Seahorse analyzer). The stimulation of TLR3 by its synthetic agonist Poly(A:U) resulted in a faster growth of HNC cells under low foetal calf serum conditions. Targeted analysis of glucose metabolism pathways demonstrated a tendency towards a shift from tricarboxylic acid cycle (Krebs cycle) to glycolysis and anabolic reactions in cells treated with Poly(A:U). Glycolysis assays confirmed that TLR3 stimulation enhanced the capacity of malignant cells to switch from oxidative phosphorylation to extra-mitochondrial glycolysis. We found evidence that HIF-1α is involved in this process: addition of the TLR3 agonist resulted in a higher cell concentration of the HIF-1α protein, even in normoxia, whereas knocking-down TLR3 resulted in a lower concentration, even in hypoxia. Finally, we assessed TLR3 expression by immunohistochemistry in a series of 7 HNSCC specimens and found that TLR3 was detected at higher levels in tumors displaying a hypoxic staining pattern. Overall, our results demonstrate that TLR3 stimulation induces the Warburg effect in HNC cells *in vitro*, and suggest that TLR3 may play a role in tumor adaptation to hypoxia.

INTRODUCTION

Head and Neck squamous cell carcinoma (HNSCC) is the 6th most frequent type of cancer worldwide, and affects all ethnic groups [1]. It is mainly related to chronic exposure to tobacco and alcohol, though Human Papilloma Virus (HPV) appears to be implicated in an increasing number of cases [2, 3]. A particular form of virus-related Head and Neck carcinoma is Nasopharyngeal Carcinoma (NPC) which is consistently associated to the Epstein-Barr virus and often displays a lympho-epithelial pattern with minimal squamous cell differentiation [4, 5].

We and others have previously reported substantial expression of TLR3 in HNSCC as well as in NPC [6–8]. The toll-like receptors (TLRs) are mammalian orthologs of the Toll cell surface receptor of drosophila. They were first studied for their role in innate immunity [9]. TLRs are specifically triggered by Pathogen-Associated Molecular Patterns (PAMPs): for example, TLR3 is activated by double-stranded RNA [10]. It has been shown more recently that TLRs could also be implicated in non-immune processes, such as tissue homeostasis, and cancer [11]. A strong and consistent expression of TLR3 has been reported not only in head and neck carcinoma, but in a variety of human cancers, such as melanoma, breast cancer, clear cell renal carcinoma and neuroblastoma [12–15].

The consistent expression of TLR3 by malignant cells raises the question of its potential role in oncogenesis and tumor progression. In a somehow paradoxical manner, many investigators have emphasized the role of TLR3 as a factor of vulnerability for malignant cells. Initially Poly(I:C) was used as an artificial ligand of TLR3 and was shown in several studies to induce apoptosis of various types of malignant cells *in vitro* [12, 14, 16, 17]. However, these studies have met two limitations. First, Poly(I:C) is also a ligand for receptors distinct from TLR3, especially RIG-I and MDA5 [18]. Next, Poly(I:C) was used by most investigators at very high concentrations (often reaching 50 mg/ml). Poly(A:U) which is specific for TLR3 was used in more recent works but still at high concentrations [19]. Finally using concentrations of Poly(A:U) in the range of 200–300 ng/ml we have found pro-apoptotic effects only when this ligand was used in combination with an inhibitor of c-IAP2 [20]. It means that, in natural conditions, the Poly(A:U) by itself is not pro-apoptotic. Moreover, Paone et al. have shown that the stimulation of TLR3 by low doses of Poly(I:C) (0.05–5 μg/mL) in the prostate cancer cell line PC3 resulted in reduced apoptosis and in secretion of functional vascular endothelial growth factor (VEGF) induced by an increased expression of hypoxia-inducible factor-1α (HIF-1α) [21]. More recently, Shengwei et al. described a positive feed-back loop between TLR3-4/NFκB/HIF-1α in 2 oral squamous cell carcinoma cell lines [22]. These observations prompted us to further investigate the oncogenic effects of TLR3 in head and neck carcinoma.

Indeed, most HNSCC display a hypoxic profile [23], often associated to necrotic foci within the tumor or the metastatic lymph nodes. The shortage of oxygen and nutrients in large tumor areas is mainly a consequence of quantitative and/or qualitative inadequacy of tumor angiogenesis [24]. One important aspect of the adaptation of malignant cells to hypoxia is a metabolic reprogramming with a major impact on glucose metabolism. In contrast with most normal tissues, the extra-mitochondrial degradation of glucose tends to predominate over mitochondrial glycolysis based on oxidative phosphorylation. This change in the balance of glucose metabolic pathways often called the Warburg effect is believed to improve the energy supply of malignant cells in hypoxic conditions. In this system, glucose is also used as a carbon source for anabolic reactions [25, 26]. HIF-1α is a pivotal transcription factor that regulates most genes involved in metabolic reprogramming in response to hypoxia [27]. The recent description of a crosstalk between TLR3 and HIF-1α in 2 oral squamous cell carcinoma cell lines [22] raises the issue of the potential relationship between TLR3 and metabolic reprogramming in cancer cells.

The initial aim of this study was to determine whether TLR3 ligands were able to promote malignant cell growth *in vitro* using a panel of HNSCC cell lines. We found a growth-promoting effect of Poly(A:U) which was only apparent when cells were cultured in a low volume of medium and in low fetal calf serum conditions and abolished when TLR3 was knocked down. These observations suggest that TLR3 and its ligands induce a metabolic reprogramming, facilitating resistance to a shortage of oxygen and/or nutrients. This hypothesis was confirmed by the combination of two approaches: targeted analysis of cell metabolites and assessment of the extra-mitochondrial glycolytic capacity by real-time measurement of proton release from live cells. Overall, these data indicate that the TLR3 has the capacity to induce a metabolic reprogramming in HNSCC cells. The pathological relevance of these findings was also investigated by an immunohistochemical (IHC) study in a small series of 7 HNSCC samples.

RESULTS

TLR3 promotes head and neck carcinoma cells growth *in vitro*

To address the potential role of TLR3 in malignant cells growth, we stimulated several head and neck carcinoma cell lines, namely CNE1, SQ20B, FaDu and HONE1 (which had previously been tested for TLR3 expression [8]), with the synthetic TLR3 agonist Poly(A:U) and assessed their growth ratio by repeated cell counts. In normal culture conditions, there was no effect of TLR3 stimulation on cell growth (data not shown). However, when the cells were grown in low foetal calf serum conditions (0.1 to 1% FCS medium) in a low volume of medium (3 mL in a 25 cm^2 flask), we observed a modest but consistent growth promoting effect of TLR3 stimulation by Poly(A:U) in all cell lines (Figure 1A, 1B). This was observed even for doses of Poly(A:U) as low as 0.25 to 1 μg/mL. To further study the role of TLR3 in cancer cell growth, we established 2 cell lines derived from CNE1 and SQ20B and stably transfected with a plasmid encoding a shRNA directed against TLR3, driven by a doxycyclin-inducible promoter (Tet-on system). As shown in Figure 1C and 1D, invalidation of TLR3 resulted in a reduced growth capacity for both cell lines.

The stimulation of TLR3 by Poly(A:U) induces significant metabolic changes in CNE1 and SQ20B head and neck carcinoma cell lines

During the cell counts experiments, we observed a faster acidification of the culture media of cells treated by Poly(A:U), suggesting that TLR3 stimulation might have an effect on malignant cells' metabolism. We therefore decided to assess the impact of TLR3 stimulation on the metabolic profile of the 4 head and neck carcinoma cell lines HONE1, FaDU, CNE1 and SQ20B cells using a metabolomics approach targeted on glucose metabolism pathways. We assessed the level of metabolites involved in glycolysis, TCA (tricarboxylic acid cycle) /OXPHOS (oxidative phosphorylation), amino acid synthesis, PPP (pentose phosphate pathway, which branches off glycolysis to generate precursors for the synthesis of nucleotides), and cataplerosis (a process in which intermediates are removed from the TCA cycle and converted to amino acids, glucose, or fatty acids [28]). The level of ATP/AMP was also evaluated in this metabolomics approach. HONE1, FaDu, CNE1 and SQ20B cells were treated

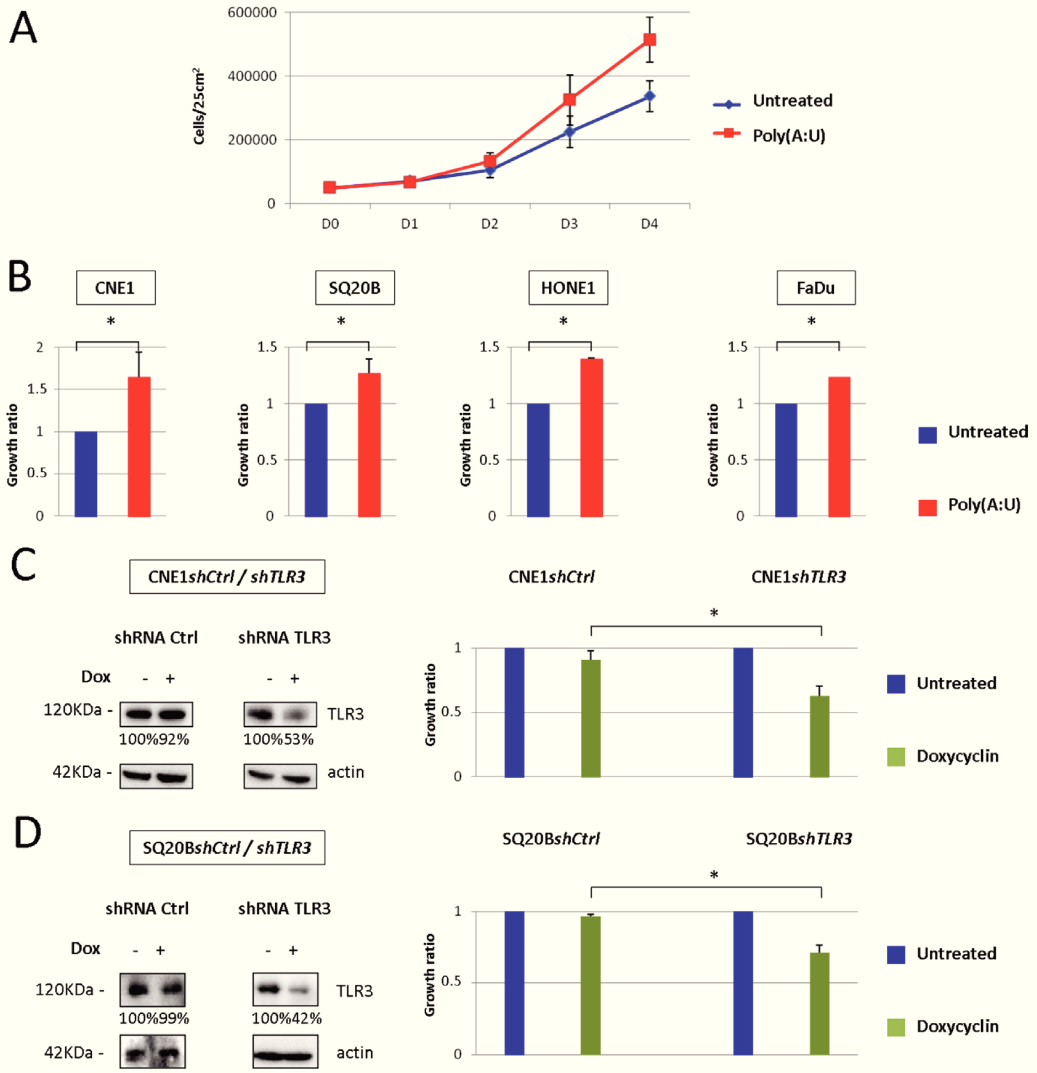

Figure 1: Impact of TLR3 stimulation/invalidation on Head and Neck carcinoma cells growth *in vitro*. (**A**) *In vitro* growth of CNE1 nasopharyngeal carcinoma cells was measured by daily cell count, in basal conditions or under TLR3 stimulation by its synthetic agonist Poly(A:U) at 0.25 µg/mL For this experiment, 5×10^4 cells were plated at day 0 in 25 cm^2 flasks with 3 mL of 0.1 % FCS medium, and cells were counted from day 0 to day 4. (**B**) The same experiment was repeated with SQ20B, HONE1 and FaDu head and neck carcinoma cell lines under the same conditions (except for FaDu: Poly(A:U) was used at 1 µg/mL, in 1%FCS medium). Cell counts were normalized to the cell numbers recorded in basal conditions and arbitrarily set at 1. (**C**), (**D**) CNE1 and SQ20B cell lines were stably transfected with a plasmid carrying a shRNA directed against TLR3, and inducible by doxycyclin. TLR3 invalidation under doxycyclin was controlled by Western blot (left panel; the same blotted membranes were stained with anti-actin for protein loading controls), and its growth inhibitory effect was evaluated by cell counts at day 4 in cells cultured in 25 cm^2 flasks under regular FCS conditions (right panel). The data are presented as mean ± standard deviation, and p values < 0.05 were considered statistically significant. Similar results were obtained in three independent experiments. *$p < 0.05$.

with Poly(A:U) at 0.25 μg/mL and collected after 4 hours. Targeted LC/MS profiling revealed a difference between the metabolic profile of untreated cells and cells stimulated by Poly(A:U): indeed, the level of several metabolites involved in glucose metabolism pathways was modified after 4 hours of Poly(A:U). Overall, there was a global increase in anabolic pathways such as PPP, amino acid synthesis, and cataplerosis. Conversely, there was a decrease in the level of TCA cycle metabolites (Figure 2). Although the results did not reach statistical significance, there was also a tendency to an increase in the metabolic activity of malignant cells (reflected by the ATP/AMP ratio) and in the level of glycolysis (with an increase in lactates levels). Of note, the results obtained in SQ20B cells after 4 hours of Poly(A:U) treatment were less significant than in the other cell lines. However, the same trend in metabolites levels was observed after 24H of exposure to Poly(A:U) (Supplementary Figure S1).

TLR3 mediates changes in the glycolytic capacity of head and neck carcinoma cells, and contributes to the Warburg effect

To better understand the influence of TLR3 on glucose metabolism, we used a dynamic and integrated mode of exploration based on time-resolved analysis of proton release from live cells using a Seahorse analyzer (Figure 3). This device allows a precise and continuous monitoring of a parameter called Extracellular Acidification Rate or ECAR, which reflects pH variations in the medium surrounding live cells grown in microplates and subjected to complete isolation from the ambient atmosphere for the time of the assay (about 2 h). Then, continuous real-time measurement of ECAR takes place while the cells are subjected to a series of standardized and sequential manipulations of glucose metabolism. Following glucose loading, a key step is the addition of oligomycin which blocks oxidative phosphorylation inducing a rapid and steep increase of the ECAR. This modification is a direct reflection of the forced shift of glucose metabolism towards extra-mitochondrial degradation which is accompanied by lactate production and rapid acidification of the extra-cellular medium. At the final step, glycolysis is totally inhibited by addition of 2D-glucose, a glucose analog which blocks glucose hexokinase, the first enzyme in the glycolytic pathway. The resulting immediate and drastic reduction of the ECAR provides a confirmation of the direct relationship between extra-mitochondrial glycolysis and medium acidification. A very interesting parameter called "glycolytic reserve" is the difference between ECAR measured just prior to oligomycin addition and the plateau following the steep increase resulting from the blockade of oxidative phosphorylation. As shown in Figure 3A, the glycolytic reserve was markedly increased in FaDu, CNE1 and SQ20B cells subjected to a stimulation by the TLR3 agonist Poly(A:U) at 0.25 μg/mL for 4 hours prior to the assay. This glycolysis promoting effect was abrogated when the Poly(A:U) stimulation and the glycolysis assay were preceded by the inhibition of TLR3 expression in both CNE1*shTLR3* and SQ20B*shTLR3* cell lines (Figure 3B and 3C, respectively). Moreover, independently of the effect of Poly(A:U), the basal glycolytic capacity was reduced in SQ20B following inhibition of TLR3 expression. Overall, these results confirm that TLR3 plays a role in the metabolic regulation of HNSCC cells, and specifically favours a switch from oxidative phosphorylation to extra-mitochondrial glycolysis.

TLR3 regulates the level of HIF-1α protein in CNE1 and SQ20B head and neck carcinoma cell lines

We investigated the possible role of the key transcription factor HIF-1α in the metabolic response mediated by TLR3 in CNE1 and SQ20B cell lines. In normoxic conditions, HIF-1α is recognized and ubiquitinated by the VHL E3 ubiquitin ligase and degraded by the proteasome: it is therefore usually not detected (or at extremely low levels) by Western blot analysis in cells cultured in normoxia. In other models [21, 22], it has been shown that Poly(I:C) treatment can induce an increase in the level of HIF-1α. Accordingly, HIF-1α was detected in CNE1 and SQ20B cells even in normoxia when they were treated for 24 hours with Poly(A:U) at 0.25 μg/mL (Figure 4A). This increase was even stronger when cells were cultured in low FCS conditions. Conversely, invalidation of TLR3 by RNA interference was associated to a lower concentration of HIF-1α protein in CNE1*shTLR3* and SQ20B*shTLR3* cells cultured in hypoxia (Figure 4B).

Preferential detection and distinct pattern of TLR3 in tumors expressing the hypoxic markers CAIX and HIF-1α

We further investigated the pathological relevance of these *in vitro* findings by an immunohistochemical (IHC) study on human HNSCC tissues. The expression of TLR3 and of the hypoxia markers CAIX and HIF-1α was assessed in 7 samples of HNSCC, and in 1 benign lymph node as a control. The samples were obtained from the primary tumor site in 2 cases, and from a metastatic lymph node in 5 cases. The primary tumors were HPV positive and HPV negative in 4 and 3 cases, respectively. Control staining were performed with an isotype control matched with the primary antibodies. There was a strong staining for TLR3 protein in tumors expressing CAIX and HIF-1α (Figure 5A, Supplementary Figure S2). In these samples, the hypoxic markers were expressed just adjacent to the necrotic areas of the tumor, whereas TLR3 was expressed at higher levels in the periphery of the

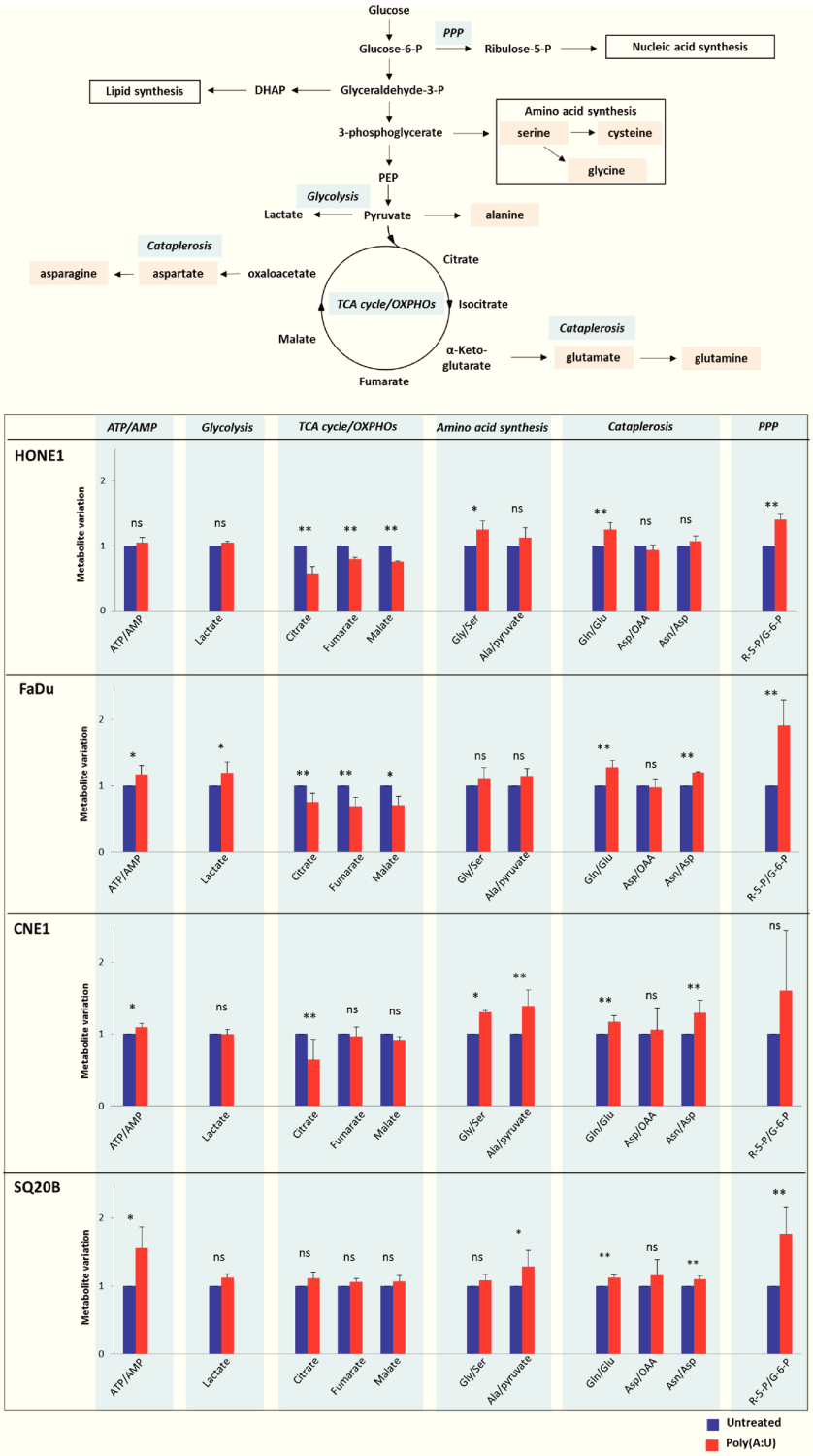

Figure 2: Changes in the metabolic profile of HONE1, FaDu, CNE1 and SQ20B carcinoma cells upon TLR3 stimulation by Poly(A:U). HONE1, FaDu, CNE1 and SQ20B cells were plated in 6-well plates and treated with Poly(A:U) (0.25 µg/mL). One million cells were harvested after 4H incubation and samples were prepared for targeted analysis in a single LC/MS profiling as described in the material and methods section. A summary of the main glucose metabolism pathways, including TCA cycle/OXPHOs, glycolysis, pentose phosphate pathway (PPP), aminoacid synthesis and cataplerosis is displayed in the upper panel. Targeted analysis revealed that TLR3 stimulation by Poly(A:U) induced variations in the level of several metabolites/metabolites ratio involved in these pathways (lower panel). Areas under curve (AUC) were normalized on AUC recorded in basal conditions and arbitrarily set at 1.The data are presented as mean ± standard deviation, and in this experiment p values < 0.1 were considered statistically significant. Similar results were obtained in three independent experiments. *$p < 0.1$; **$p < 0.05$; ns: not significant; Gly: glycine; Ser: serine; Gln: glutamine; Glu: glutamine; Asp: aspartate; Asn: asparagine; R-5-P: ribulose-5-Phosphate; G-6-P: glucose-6-Phosphate.

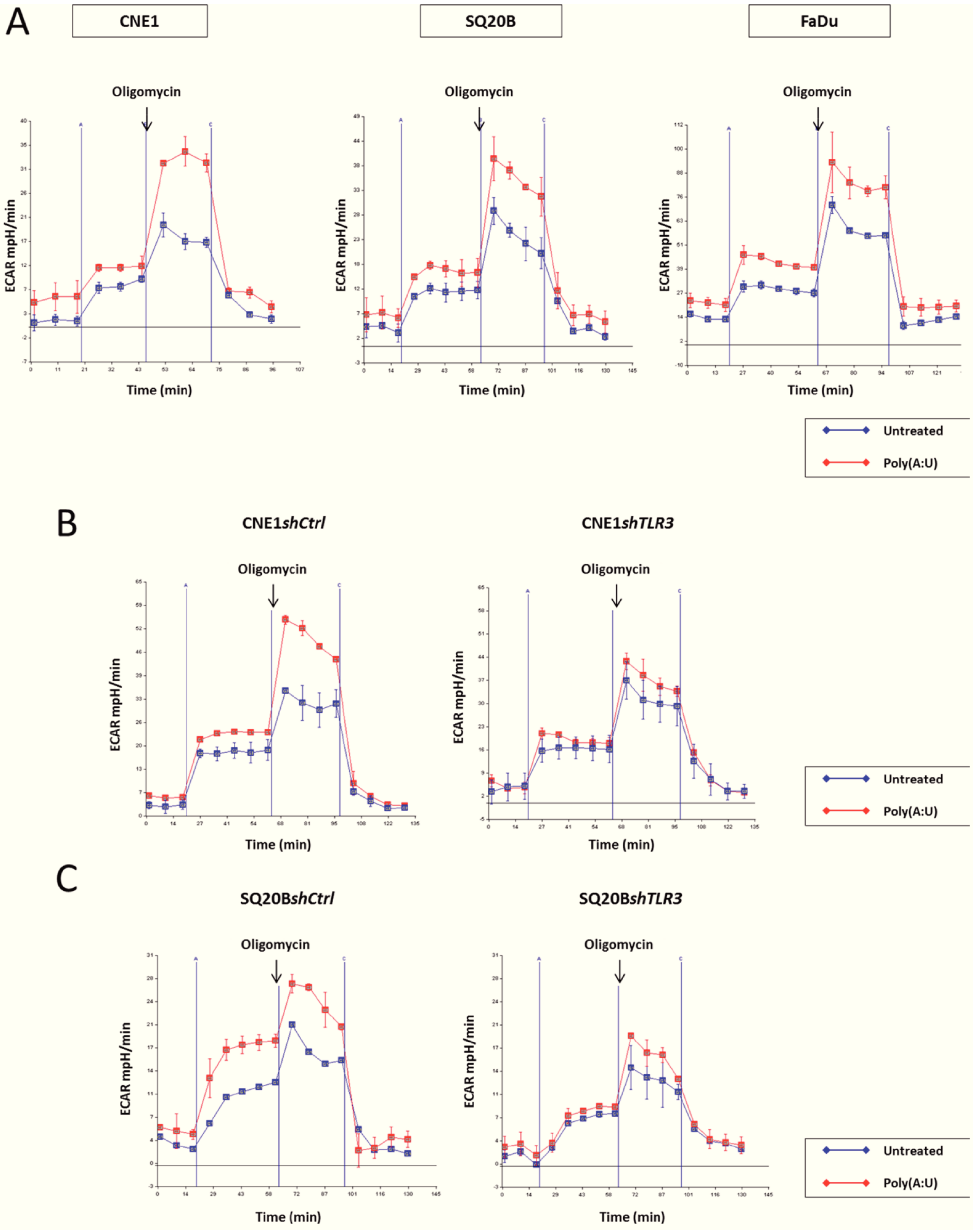

Figure 3: Implication of TLR3 in the onset of the warburg effect in HN carcinoma cells. The glycolytic capacity of the cells was assessed in various experimental conditions using the Seahorse XF24 extracellular flux analyzer as described in the material and methods section. This device allows real-time monitoring of proton release from live cells seeded in microplates and isolated from the ambient atmosphere. We used the ECAR (extra-cellular acidification rate measured in mpH/min) as our main output parameter. The actual glycolysis assay included 4 phases. In phase 1, cells were maintained in glucose starvation conditions for 20 min. In phase 2, following glucose addition, they were incubated for 35 min with glucose at a saturating concentration. Entry in phase 3 was triggered by addition of oligomycin which induced a blockade of the respiratory chain and a forced shift towards extra-mitochondrial glycolysis. Entry in phase 4 was due to the addition of 2D-glucose resulting in the complete blockade of glycolysis. The glycolytic reserve was assessed as the difference in the ECAR measured just prior to oligomycin addition and at the plateau following the rapid increase of medium acidification. This acidification was due to the forced shift towards extra-mitochondrial glycolysis accompanied by intense lactate production. The dramatic reduction of ECAR resulting from 2D-glucose addition was a confirmation that the acidification was directly related to extra-mitochondrial glycolysis. (**A**) The day before the assay, FaDu, CNE1 and SQ20B cells were plated at 4×10^4 cells per well in XF24 plates and treated with Poly(A:U) (0.25 µg/mL) for 4 hours prior to the actual assay. There was a strong increase in the glycolytic reserve in all three cell types pre-treated with Poly(A:U). Consistent with the idea of the promotion of extra-mitochondrial glycolysis by TLR3, the increase in ECAR following glucose addition at the end of phase 1 was greater in cells treated with Poly(A:U) especially for SQ20B. (**B**), (**C**) The same experiment was repeated with CNE1*shTLR3* and SQ20B*shTLR3* cell lines, and their counterparts CNE1*shCtrl* and SQ20B*shCtrl*, transfected with a plasmid encoding a non-specific shRNA. Invalidation of TLR3 by RNA interference abrogated the increase of the glycolytic reserve induced by Poly(A:U). Moreover, independently of Poly(A:U) treatment, there was a reduction of the basal glycolytic capacity following TLR3 inhibition in SQ20B cells.

tumor, on the invasion front. On the other hand, TLR3 was detected at much lower levels in tumor samples displaying a low level of CAIX/HIF-1α (Figure 5B). Neither TLR3 nor CAIX/HIF-1α were detected in the tissue sample of benign lymph node. A summary of the staining pattern for TLR3, CAIX and HIF-1α is presented in Table 1. Of note, the tumors with a "hypoxic" profile were all HPV positive in our series.

DISCUSSION

The initial aim of this study was to investigate a possible growth promoting effect in head and neck carcinoma cells treated *in vitro* with low concentrations of a specific TLR3 ligand, Poly(A:U). Using various experimental conditions in an empirical approach, we found a modest enhancement of cell growth which was only apparent under the following conditions: 1) cultivation in a low volume of medium and in low foetal calf serum conditions; 2) monitoring of cell growth based on direct cell counting instead of MTT assays. These observations led us to hypothesize that metabolic changes were part of the malignant cell response to the stimulation of TLR3. This was confirmed by two different approaches: 1) targeted metabolic analysis of stimulated and unstimulated cells done by mass spectrometry; 2) assessment of the extra-mitochondrial glycolytic capacity by time-resolved analysis of proton release from live cells. Our data demonstrate that TLR3 stimulation results in a metabolic reprogramming characterized by an increase in the cell capacity of extra-mitochondrial glycolysis and a concomitant increase in the concentration of the metabolites involved in anabolic reactions such as amino acid synthesis, pentose phosphate pathway, and cataplerosis. Overall, the changes induced by TLR3 stimulation were characteristic of a form of metabolic reprogramming consistently associated with the malignant phenotype and often designated as the tumor Warburg effect [25, 26]. Finally, immunostaining experiments in HNSCC samples showed that TLR3 was detected at higher levels in hypoxic tumors, with an enhancement of the staining in the periphery of the tumor, on the invasive front.

We noticed an apparent discrepancy between the data resulting from the metabolomics analyses (mass spectrometry) and the glycolysis assays (Seahorse): indeed, the former revealed only a slight increase in lactate levels, whereas the latter showed a strong increase of ECAR upon Poly(A:U) treatment. This is not so puzzling if one keeps in mind that the metabolomics analyses are performed on cell extracts whereas the ECAR measurements are performed exclusively on the culture medium. It has been shown that in malignant cells, the lactate generated by glycolysis is rapidly exported in the extra-cellular medium by monocarboxylate transporters [29]: the metabolomics analyses may therefore underestimate the lactate production..

The elucidation of the cellular and molecular events linking TLR3 and the onset of the Warburg effect will require further investigation. Presently, it is interesting to note that we have found a strong impact of TLR3 knock-

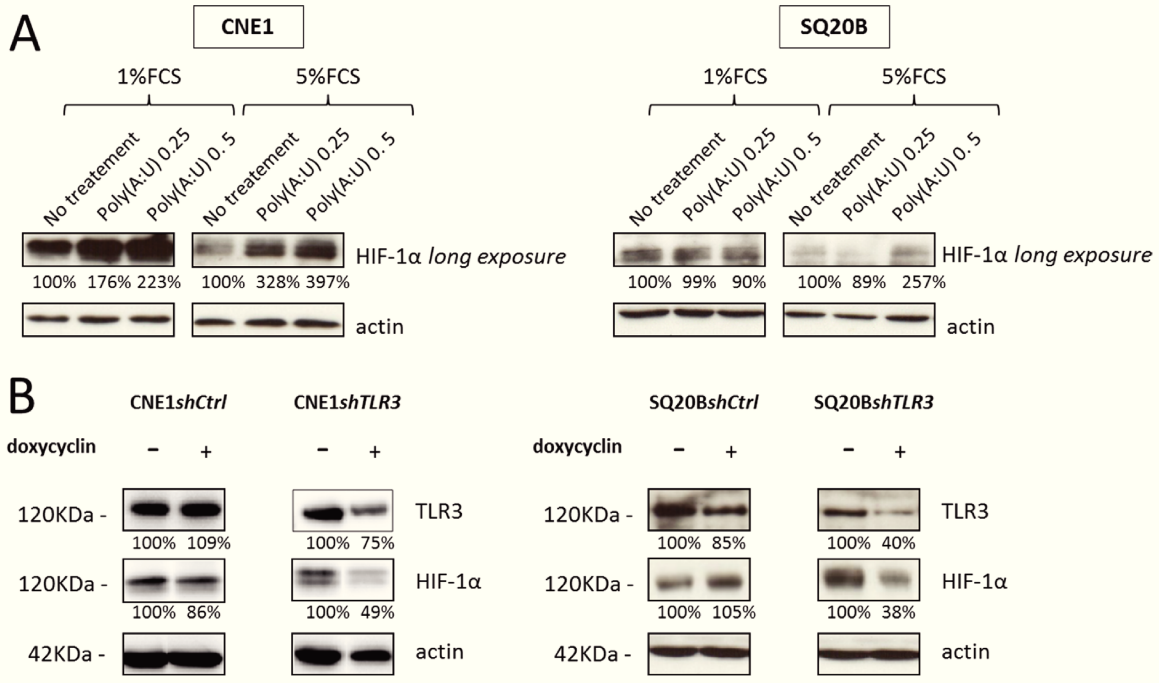

Figure 4: Impact of TLR3 on the level of HIF-1α protein. (**A**) The level of HIF-1α protein was assessed by Western blot analysis in CNE1 and SQ20B cells treated for 24H by Poly(A:U) at 0.25 and 0.5 μg/mL in normoxia under low (1%) and normal (5%) FCS conditions. (**B**) The same experiment was performed with CNE1 and SQ20B subclones invalidated for TLR3 cultured for 24H in hypoxic conditions (0.1% oxygen, 5% FCS). The same blotted membranes were stained with anti-actin for protein loading controls.

Table 1: Detection of TLR3, CAIX and HIF-1α proteins by immunohistochemistry on tissue sections from HNSCC samples

Patient #	Primary tumor site (origin of the sample)	HPV status	HES	TLR3 staining	CAIX staining	HIF-1α staining
1	Oropharynx (primary tumor site)	Positive	Large areas of necrosis	Strong staining of the invasion front	Strong perinecrotic staining	Strong perinecrotic staining
2	Oral cavity (primary tumor site)	Negative	No necrosis	Faint staining of the surface epithelium	Faint staining with homogenous repartition	Negative
3	Oropharynx (Metastatic lymph node)	Positive	Large areas of necrosis	Strong staining of the invasion front	Strong perinecrotic staining	Moderate perinecrotic staining
4	Oropharynx (Metastatic lymph node)	Positive	Large areas of necrosis	Strong staining of the invasion front	Strong perinecrotic staining	Strong perinecrotic staining
5	Hypopharynx (Metastatic lymph node)	Negative	No necrosis	Negative	Faint staining of few cells in the core of the tumor	Faint staining of few cells on the periphery of the tumor
6	Oropharynx (Metastatic lymph node)	Positive	No necrosis	Faint staining of the invasion front	Faint staining with homogenous repartition	Negative
7	Hypopharynx (Metastatic lymph node)	Negative	No necrosis	Faint staining of inflammatory cells	Negative	Negative
8	Nonmalignant lymph node	–	–	Negative	Faint staining of germinative centers	Negative

Images for cases 1 and 7 are displayed in Figure 5A and 5B, respectively. Images for cases 3 and 4 are displayed in Supplementary Figure S2A and S2B, respectively. HPV: human papilloma virus; HES: haematoxylin eosin safran.

down on the expression of HIF-1α even in normoxia (Figure 4). This is consistent with a report by Paone et al. based on a model of prostate cancer [21]. These authors have reported an increase in the expression of HIF-1α and a nuclear accumulation of the HIF-1 complex in response to TLR3 stimulation, even in normoxia. This process resulted in vascular endothelial growth factor (VEGF) secretion and in apoptosis reduction. Similarly, Shengwei et al. recently described a positive regulation of HIF-1α upon TLR3 stimulation in 2 oral squamous cell carcinoma cell lines, mediated at least in part by NF-κB [22]. It is noteworthy that the authors used Poly(I:C) at high concentrations (10 μg/mL) for these experiments. They also showed that HIF-1α increased TLR3 and TLR4 expression through direct promoter binding. However, the authors didn't investigate the metabolic impact of TLR3 stimulation, as we could do in this report. Further investigations are warranted to formally demonstrate that HIF-1α is needed to trigger the metabolic reprogramming in HNSCC cancer cells. Another aspect of the correlation between TLR3 and cell metabolism was explored by some of us (Matijevic et al.) through a proteomic approach, also in an *in vitro* HNSCC model: stimulation of TLR3 by its synthetic ligand Poly(I:C) resulted in a differential expression of 15 proteins, of which 10 were involved in protein metabolic processes [30]. The authors mostly focused on the downregulation of calreticulin and the upregulation of profilin 1, as these variations are associated with tumor aggressiveness, but they also reported an upregulation of PKM2, i.e. the embryonic form of pyruvate kinase: this isoform is frequently re-expressed in tumor cells, and gives them a proliferative advantage in hypoxic conditions [31]. PKM2 is one of the numerous genes upregulated by HIF-1α, and it would also be interesting to determine if HIF-1α is involved in PKM2 induction in response to Poly(I:C) or Poly(A:U). Beside HIF-1α one can suspect the activation of the interferon pathway by TLR3 to contribute to metabolic reprogramming, especially through up-regulation of STAT1 [32].

To a large extent, the nature of the TLR3 ligands in epithelial malignancies remains hypothetical. To our knowledge, there is no report of a direct stimulation of TLR3 by viral products in HPV-related HNSCC. On the other hand, NPCs appear as a peculiar entity with regards to TLR3 function because they produce very large amounts of small untranslated RNAs encoded by the EBV genome which are called EBERs (EBV-encoded small RNAs) [5]. The EBERs are ligands of TLR3 and there is evidence that their stimulation supports tumor growth through an increase in insulin-like growth factor 1 (IGF-1) expression [33, 34]. However, the Head and Neck carcinoma cell lines used in this study were all EBV-negative. Still, as shown in Figure 4B, TLR3 inhibition had a negative impact on HIF-1α expression in CNE1 and SQ20B cells independently of Poly(A:U) stimulation. This observation supports the hypothesis of a low-intensity, permanent stimulation of SQ20B cells by unknown endogenous TLR3 ligands. A possible source of TLR3 ligands for malignant HNSCC cells *in vivo* and maybe even *in vitro* might be necrotic cells releasing double-stranded RNA fragments. Indeed, stimulation of TLR3 by such "DAMPs" (damage-associated molecular patterns) has been reported in several *in vitro* and *in vivo*

models [35–37]. In our preliminary study on a small series of 7 HNSCC samples, we found that in necrotic tumors the hypoxic markers CAIX and HIF-1α were expressed adjacent to the necrotic areas, whereas TLR3 was detected in the periphery of the tumor, on the invasion front. Both our findings and these publications suggest a model according to which dying cells of the necrotic core of the tumor nodules release fragments of dsRNA that

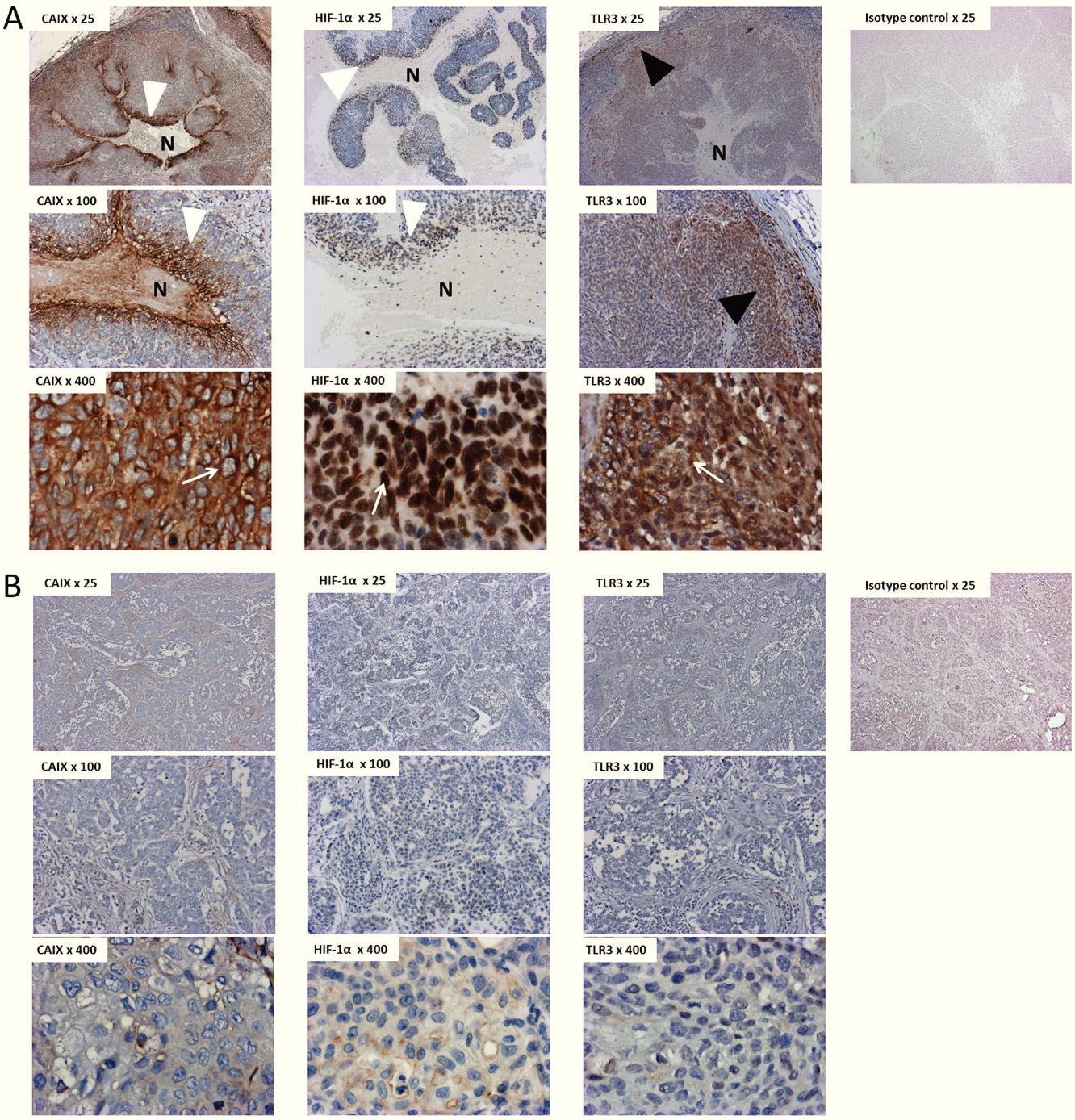

Figure 5: Immunostaining of TLR3, HIF-1α and CAIX in tissue samples of HNSCC. HNSCC sections (A = patient#1; B = patient#7) were immunostained with antihuman CAIX, HIF-1α and TLR3 antibodies, or with an isotype control matched with the primary antibody. TLR3 was detected at higher levels in tumors displaying a hypoxic pattern (**A**) than in non-hypoxic tumors (**B**). Note the repartition of the staining in panel A, with a strong perinecrotic staining for HIF-1α and CAIX (white arrowheads) and a stronger staining for TLR3 on the periphery of the tumor, next to the invasive front (black arrowhead). Note the specific staining pattern of CAIX, HIF-1α and TLR3, within malignant cells (white arrows): CAIX was detected on the membrane of the cells, whereas the staining was nuclear for HIF-1α and cytoplasmic for TLR3. This is concurrent with the cell surface, cell nuclei and endosomal expression of CAIX, HIF-1α and TLR3, respectively. N: Necrosis. Overall magnification ×25/×100/×400.

are internalized by the cells which survive and proliferate in the invasion front. Through TLR3 stimulation, these double-stranded RNA fragments might support metabolic reprogramming, cell survival and possibly cell growth of cells facing a partial shortage of oxygen and nutrients. In other words they might be involved in a dialog between necrotic and invasive live cells within the tumor microenvironment. Confirmation of this hypothesis will require additional IHC studies on a larger series. Other investigations performed *in vitro* will be based on cellular reporter systems to determine which fractions of the DAMPs behave as agonists of TLR3.

Our findings have several implications for future developments in clinical tumor assessment and therapeutics. Although hypovascularization and low oxygen pressure have long been reported to favour resistance to radiotherapy, it remains difficult to assess the negative impact of hypoxia and to base a therapeutic decision on this evaluation [38–41]. Moreover, it is necessary to assess not only the level of oxygen deprivation but also how malignant cells react to this shortage: in this context, *in situ* detection of TLR3 might be useful in addition to classical "hypoxic tissue markers", like HIF1-α, carbonic anhydrase IX or osteopontin [39].

A number of studies have emphasized the therapeutic anti-tumor potential of TLR3 stimulation by synthetic ligands. These synthetic ligands are expected not only to boost the effector cells of the innate immune system but also to favour tumor cell death and tumor regression. This strategy has been apparently supported by encouraging results obtained in clinical trials [42, 43]. However, in the light of our results, artificial stimulation of TLR3 should be considered with caution. Our findings regarding TLR3 and resistance to hypoxia are consistent with the negative results obtained in another clinical trial. Indeed, in a phase III study of Poly(A:U) vs placebo – used as an adjuvant therapy after surgical resection in colorectal cancer - survival was shorter for the patients who were given the Poly(A:U) [44]. On the other hand, we have previously reported a dramatic induction of apoptosis in a variety of malignant epithelial cells subjected *in vitro* to combinations of TLR3 ligands with an inhibitor of c-IAP2 [20, 45]. This type of combined treatments which neutralize the growth promoting effects of the TLR3 ligands might be beneficial for some categories of patients.

MATERIALS AND METHODS

Cell lines and pharmacological reagents

EBV-negative NPC cell lines CNE1 and HONE1 were grown in RPMI 1640 medium (Gibco-Invitrogen, Carlsbad, CA) supplemented with 5% fetal calf serum (FCS). FaDu and SQ20B (hypopharyngeal and laryngeal squamous cell carcinoma, respectively) were grown in Minimum Essential Medium (MEM, Invitrogen) and Dulbecco's Modified Eagle's Medium (DMEM, Gibco-Invitrogen), respectively, supplemented with 5% FCS. The CNE1 cell line was a gift from Pr Yi Zeng (Chinese Academy of Preventive Medicine, Beijing). The HONE 1 cell line was provided by Dr Véronique Boyer and Pr Patrice Morand (Grenoble – Alpes university, France). The Fadu and SQ20B lines were provided by Pr Eric Deutsch (Gustave Roussy, Villejuif, France). These cell lines have not yet been investigated for polymorphic markers based on small tandem repeats. The TLR3 agonist Poly(A:U) was obtained from InvivoGen (San Diego, CA). Doxycyclin was purchased from Sigma Aldrich (St Quentin-Fallavier, France).

Stable transfection of CNE1 and SQ20B cell lines

To study the role of TLR3 in cancer cell growth, we established subclones of CNE1 and SQ20B cell lines transfected with a plasmid carrying a shRNA directed against TLR3 and inducible by doxycyclin (TET-on system), thus allowing conditional knock-down of TLR3. Four plasmids (V2THS171345, V3THS370036, V3THS370035, V3THS370032) with independent non-overlapping shRNA sequences (TATCAGAAAGTTGAGATAG, TGAACTGCATGATGTACCT, TGAGATAGCTCATTG TGCT, TAAATCCTACATCCAAGCT, respectively) were tested, and for each cell line the one with the best amplitude of TLR3 silencing was used for subsequent experiments (V3THS370032 and V3THS370035 for CNE1 and SQ20B, respectively). Prior to transfection, 1×10^5 cells were seeded into 6-well plates in 2 ml complete medium; they were ~70–80% confluent at the time of transfection. The pTRIPZ (Thermo Scientific and Open Biosystems, Pittsburgh PA) expression vector was transfected using Lipofectamine 2000 (Invitrogen) according to the manufacturer's instructions. Briefly, 0.5 µg of pTRIPZ plasmid in Opti-MEM reduced serum medium (Gibco Life Technologies) were mixed with 5 µl of Lipofectamine for 20 min at room temperature. The DNA/Lipofectamine complexes were then incubated with the cells for 5 h, and the medium was then renewed with 2 ml fresh complete medium. After 24 h, puromycin was added to the medium at 0.35 µg/mL. The selective medium was replenished every 3–4 days until discrete foci of puromycin-resistant cells were evident after two to three weeks of selection. These clones were isolated, expanded and tested by Western blotting in order to select those with the best amplitude of TLR3 silencing.

Cell growth assays

Repeated cell counts were performed using a Vi-Cell XR analyzer (Beckman Coulter, Brea, CA).

Sample preparation for metabolomics assays and targeted analysis by HPLC coupled to a triple quadruple (QQQ) mass spectrometer

Cells were cultured in 6-well plates being at an approximate 80% of confluence the day of the experiment. After the corresponding treatment, plates were placed upon ice under chemical hood and processed. Wells were softly and quickly (< 2s) rinced with cold milliQ water (+4°C). Cells were then lysed with 500 µl of cold methanol/water (9/1, v/v, −20°C), scrapped and pooled (2 wells per conditions) in microcentrifuge tubes. Cold chloroform (100 µl, −20°C) was added to the lysate. Solution was vortexed for 30s and centrifuged at 15000 rpm for 10 min at +4°C. Supernatant was collected and evaporated in microcentrifuge tubes at 40°C in a pneumatically-assisted concentrator (Techne DB3). 300 µl of methanol were added on dried extract and split in two parts of 150 µl: the first one used for the GC-MS experiment, the second one used for the LC-MS experimentation. Analytical methods and data processing were performed as previously described [46]. Standards and reagents were all obtained from Sigma Aldrich.

Glycolysis assays

The modalities of glucose metabolism in cells stimulated or not by Poly(A:U) were explored using the Seahorse XF24 extracellular flux analyzer in combination with the XF Glycolysis Stress kit (Seahorse Biosciences, North Billerica, MA). The Seahorse device allows precise, continuous measurement of pH variations in the culture medium surrounding cells grown in proprietary XF24 microplates. While cells of each microwell are completely isolated from the ambient atmosphere, a microfluidic system allows sequential addition of various reagents in the culture medium. These reagents are injected simultaneously in all wells corresponding to a given experimental condition. We used ECAR (extracellular acidification rate measured in mpH/min) as the main output parameter. ECAR is a direct reflection of proton release in the culture medium of each microwell. It was monitored through a cycle of sequential manipulations of glucose metabolism. After a first step of glucose starvation conditions lasting 20 min, glucose was added at a saturating concentration. Oligomycin was added 35 min later. Finally 2D glucose was added 30 min later. The day before the assay, cells were plated at $4x10^4$ cells per well in XF24 plates and incubated with regular cell culture medium in a 5% CO2 atmosphere at 37°C for 24 hours. On the day of the assay, the cells were treated with 0.25 µg/mL Poly(A:U) - or mock-treated - for 4 hours. The medium was then replaced with DMEM XF assay medium (pH adjusted to 7.35 using 1 N sodium hydroxide) supplemented with 2 mM L-glutamine with or without 0.25 µg/mL Poly(A:U). After media changes, the cells were placed in a 37°C CO^2-free incubator for 1 hour and finally in the airtight Seahorse XF24 plate reader for the actual glycolysis assay.

Cell protein extraction and western blot analysis

Proteins from cultured cells were extracted by lysis in RIPA buffer (50 mM Tris, 150 mM NaCl, 5 mM EDTA, 0.5% sodium deoxycholic acid, 0.5% NP-40, 0.1% SDS) supplemented with a protease inhibitor cocktail (Complete; Roche Molecular, Neuilly sur Seine, France). They were separated by SDS-PAGE and transferred to polyvinylidene difluoride membranes (Immobilon, Millipore, Billerica, CA) by electroblot at 4°C for 90 minutes at 90 V or overnight at 45 V. The antibodies used for Western blot analysis were mouse monoclonal antibodies directed against the human TLR3 (clone 512505, ref. MAB1487, R&D Systems, Minneapolis, MN), HIF-1α (610958; BD Biosciences, Bedford, MA), β-Actin (AC-74; Sigma Aldrich) and α-Tubulin (B-5-1-2; Sigma Aldrich). Blotted membranes were incubated with a secondary peroxidase-conjugated antibody, and chemiluminescent detection was done using the Immobilon Western Chemiluminescent HRP Substrate (Millipore, Billerica, CA). The acquisition was performed with ImageQuant LAS 4000 mini biomolecular imager (GE Healthcare Bio-Sciences AB) and specific protein bands were quantified using ImageQuant TL software (GE Healthcare Bio-Sciences AB, Uppsala, Sweden).

Clinical specimens and immunohistochemistry

Samples were obtained from 8 patients referred to the Lariboisière hospital (Paris, France). All patients had HNSCC. All the clinical samples were obtained and processed according to the guidelines of Lariboisière hospital institutional review board, and all patients gave their informed consent to this study. Biopsies were fixed in formaldehyde and paraffin-embedded. For TLR3 and CAIX, tissue sections were microwaved at 98°C for 30 minutes in citrate buffer (10 mM, pH 7.3) and then incubated with the primary antibody (antihuman TLR3 rabbit polyclonal antibody at 1:5000 PK-AB718-3643, PromoCell, Heidelberg, Germany; antihuman CAIX rabbit polyclonal antibody at 1:500 Ab15086, AbCam, Cambridge, MA). Binding of the primary antibody was detected with the CSA II kit from DAKO (based on a tyramide amplification system; DAKO, Carpinteria, CA). For HIF-1α, slides were treated with target retrieval solution (DAKO) at 97°C for 45 min and then incubated with primary antibody (antihuman HIF-1α rabbit polyclonal antibody at 1:300, Bethyl Laboratories, Montgomery, TX). Binding of the primary antibody was detected with the Catalyzed Signal Amplification System (DAKO, Carpinteria, CA). For all cases nuclei were counterstained with hematoxylin.

Statistical analysis

Statistical analyses were performed using R 3.3.0 statistical software. We used the Student *t*-test for quantitative data. *P*-values were two-tailed.

ACKNOWLEDGMENTS

We are grateful to people serving the Gustave Roussy platform of metabolomics: Marie Scoazec, Alexis Chéry and Nazanine Modjtahedi. We thank Olivia Bawa for her help in IHC studies.

We thank the Proteigene company for lending the Sea Horse device, providing valuable reagents and advice, especially Alain Omasson and Sofia Vikstrom.

CONFLICTS OF INTEREST

All authors certify that they have no conflicts of interest.

FINANCIAL SUPPORT

BV was supported by a fellowship from the Institut National du Cancer and from the APHP-CNRS. NO and MV were the recipients of a fellowship from the Fondation des Gueules Cassées and from the Institut National du Cancer, respectively. All the metabolomics experiments were financed by the "Taxe d'apprentissage" program (Gustave Roussy-Cancer Campus).

REFERENCES

1. IARC. Estimated cancer incidence, mortality and prevalence worldwide in 2012. http://globocan.iarc.fr/. Globocan.
2. Brownson RC, Chang JC. Exposure to alcohol and tobacco and the risk of laryngeal cancer. Archives of environmental health. 1987; 42:192–196.
3. Gillison ML. Human papillomavirus-associated head and neck cancer is a distinct epidemiologic, clinical, and molecular entity. Semin Oncol. 2004; 31:744–754.
4. Gourzones C, Barjon C, Busson P. Host-tumor interactions in nasopharyngeal carcinomas. Semin Cancer Biol. 2012; 22:127–136.
5. Gourzones C, Busson P, Raab-Traub N. Epstein-Barr Virus and the Pathogenesis of Nasopharyngeal Carcinomas. In: Busson P, ed. Nasopharyngeal Carcinoma : Keys for Translational Medicine and Biology. 2013. (Austin/New-York: Landes/Springer), 42–60.
6. Rydberg C, Mansson A, Uddman R, Riesbeck K, Cardell LO. Toll-like receptor agonists induce inflammation and cell death in a model of head and neck squamous cell carcinomas. Immunology. 2009; 128:e600–611.
7. Pries R, Hogrefe L, Xie L, Frenzel H, Brocks C, Ditz C, Wollenberg B. Induction of c-Myc-dependent cell proliferation through toll-like receptor 3 in head and neck cancer. Int J Mol Med. 2008; 21:209–215.
8. Verillaud B, Gressette M, Morel Y, Paturel C, Herman P, Lo KW, Tsao SW, Wassef M, Jimenez-Pailhes AS, Busson P. Toll-like receptor 3 in Epstein-Barr virus-associated nasopharyngeal carcinomas: consistent expression and cytotoxic effects of its synthetic ligand poly(A:U) combined to a Smac-mimetic. Infect Agent Cancer. 2012; 7:36.
9. Lemaitre B, Nicolas E, Michaut L, Reichhart JM, Hoffmann JA. The dorsoventral regulatory gene cassette spatzle/Toll/cactus controls the potent antifungal response in Drosophila adults. Cell. 1996; 86:973–983.
10. Alexopoulou L, Holt AC, Medzhitov R, Flavell RA. Recognition of double-stranded RNA and activation of NF-kappaB by Toll-like receptor 3. Nature. 2001; 413:732–738.
11. Lin Q, Wang L, Lin Y, Liu X, Ren X, Wen S, Du X, Lu T, Su SY, Yang X, Huang W, Zhou S, Wen F, et al. Toll-Like Receptor 3 Ligand Polyinosinic:Polycytidylic Acid Promotes Wound Healing in Human and Murine Skin. J Invest Dermatol. 2012.
12. Salaun N, Delyfer MN, Rougier MB, Korobelnik JF. [Assessment of risk factors for retinal vein occlusions in patients under 60 years of age]. J Fr Ophtalmol. 2007; 30:918–923.
13. Salaun B, Zitvogel L, Asselin-Paturel C, Morel Y, Chemin K, Dubois C, Massacrier C, Conforti R, Chenard MP, Sabourin JC, Goubar A, Lebecque S, Pierres M, et al. TLR3 as a biomarker for the therapeutic efficacy of double-stranded RNA in breast cancer. Cancer Res. 2011; 71:1607–1614.
14. Morikawa T, Sugiyama A, Kume H, Ota S, Kashima T, Tomita K, Kitamura T, Kodama T, Fukayama M, Aburatani H. Identification of Toll-like receptor 3 as a potential therapeutic target in clear cell renal cell carcinoma. Clin Cancer Res. 2007; 13:5703–5709.
15. Chuang JH, Chuang HC, Huang CC, Wu CL, Du YY, Kung ML, Chen CH, Chen SC, Tai MH. Differential toll-like receptor 3 (TLR3) expression and apoptotic response to TLR3 agonist in human neuroblastoma cells. J Biomed Sci. 2011; 18:65.
16. Matijevic T, Marjanovic M, Pavelic J. Functionally active toll-like receptor 3 on human primary and metastatic cancer cells. Scandinavian journal of immunology. 2009; 70:18–24.
17. Matijevic T, Kirinec G, Pavelic J. Antitumor activity from the combined application of poly(I:C) and chemotherapeutics in human metastatic pharyngeal cell lines. Chemotherapy. 2011; 57:460–467.
18. Perrot I, Deauvieau F, Massacrier C, Hughes N, Garrone P, Durand I, Demaria O, Viaud N, Gauthier L, Blery M, Bonnefoy-Berard N, Morel Y, Tschopp J, et al. TLR3 and Rig-like receptor on myeloid dendritic cells and Rig-like receptor on human NK cells are both mandatory for

production of IFN-gamma in response to double-stranded RNA. Journal of immunology. 2010; 185:2080–2088.

19. Conforti R, Ma Y, Morel Y, Paturel C, Terme M, Viaud S, Ryffel B, Ferrantini M, Uppaluri R, Schreiber R, Combadiere C, Chaput N, Andre F, et al. Opposing effects of toll-like receptor (TLR3) signaling in tumors can be therapeutically uncoupled to optimize the anticancer efficacy of TLR3 ligands. Cancer Res. 2010; 70:490–500.
20. Verillaud B, Gressette M, Morel Y, Paturel C, Herman P, Lo KW, Tsao SW, Wassef M, Jimenez-Pailhes AS, Busson P. Toll-like receptor 3 in Epstein-Barr virus-associated nasopharyngeal carcinomas: consistent expression and cytotoxic effects of its synthetic ligand poly(A:U) combined to a Smac-mimetic. Infectious agents and cancer. 2012; 7:36.
21. Paone A, Galli R, Gabellini C, Lukashev D, Starace D, Gorlach A, De Cesaris P, Ziparo E, Del Bufalo D, Sitkovsky MV, Filippini A, Riccioli A. Toll-like receptor 3 regulates angiogenesis and apoptosis in prostate cancer cell lines through hypoxia-inducible factor 1 alpha. Neoplasia. 12:539–549.
22. Shengwei H, Wenguang X, Zhiyong W, Xiaofeng Q, Yufeng W, Yanhong N, Hao S, Qingang H, Wei H. Crosstalk between the HIF-1 and toll-like receptor/nuclear factor-kappaB pathways in the oral squamous cell carcinoma microenvironment. Oncotarget. 2016; 7:37773–37789. doi: 10.18632/oncotarget.9329.
23. Hoogsteen IJ, Marres HA, Bussink J, van der Kogel AJ, Kaanders JH. Tumor microenvironment in head and neck squamous cell carcinomas: predictive value and clinical relevance of hypoxic markers. A review. Head Neck. 2007; 29:591–604.
24. Weinberg RA. Dialogue Replaces Monologue : Heterotypic Interactions and the Biology of Angiogenesis. In: Weinberg RA, ed. The biology of cancer. (New-York and Abingdon: Garland Science - Taylor & Francis group). 2007. 527–586.
25. Kroemer G, Pouyssegur J. Tumor cell metabolism: cancer's Achilles' heel. Cancer Cell. 2008; 13:472–482.
26. Vander Heiden MG, Cantley LC, Thompson CB. Understanding the Warburg effect: the metabolic requirements of cell proliferation. Science. 2009; 324:1029–1033.
27. Semenza GL, Nejfelt MK, Chi SM, Antonarakis SE. Hypoxia-inducible nuclear factors bind to an enhancer element located 3' to the human erythropoietin gene. Proc Natl Acad Sci U S A. 1991; 88:5680–5684.
28. Owen OE, Kalhan SC, Hanson RW. The key role of anaplerosis and cataplerosis for citric acid cycle function. J Biol Chem. 2002; 277:30409–30412.
29. Le Floch R, Chiche J, Marchiq I, Naiken T, Ilc K, Murray CM, Critchlow SE, Roux D, Simon MP, Pouyssegur J. CD147 subunit of lactate/H+ symporters MCT1 and hypoxia-inducible MCT4 is critical for energetics and growth of glycolytic tumors. Proc Natl Acad Sci USA. 2011; 108:16663–16668.
30. Matijevic T, Pavelic J. Poly(I:C) treatment influences the expression of calreticulin and profilin-1 in a human HNSCC cell line: a proteomic study. Tumour Biol. 2012; 33:1201–1208.
31. Christofk HR, Vander Heiden MG, Harris MH, Ramanathan A, Gerszten RE, Wei R, Fleming MD, Schreiber SL, Cantley LC. The M2 splice isoform of pyruvate kinase is important for cancer metabolism and tumour growth. Nature. 2008; 452:230–233.
32. Pitroda SP, Wakim BT, Sood RF, Beveridge MG, Beckett MA, MacDermed DM, Weichselbaum RR, Khodarev NN. STAT1-dependent expression of energy metabolic pathways links tumour growth and radioresistance to the Warburg effect. BMC Med. 2009; 7:68.
33. Iwakiri D, Zhou L, Samanta M, Matsumoto M, Ebihara T, Seya T, Imai S, Fujieda M, Kawa K, Takada K. Epstein-Barr virus (EBV)-encoded small RNA is released from EBV-infected cells and activates signaling from Toll-like receptor 3. J Exp Med. 2009; 206:2091–2099.
34. Iwakiri D, Sheen TS, Chen JY, Huang DP, Takada K. Epstein-Barr virus-encoded small RNA induces insulin-like growth factor 1 and supports growth of nasopharyngeal carcinoma-derived cell lines. Oncogene. 2005; 24:1767–1773.
35. Kariko K, Ni H, Capodici J, Lamphier M, Weissman D. mRNA is an endogenous ligand for Toll-like receptor 3. J Biol Chem. 2004; 279:12542–12550.
36. Cavassani KA, Ishii M, Wen H, Schaller MA, Lincoln PM, Lukacs NW, Hogaboam CM, Kunkel SL. TLR3 is an endogenous sensor of tissue necrosis during acute inflammatory events. J Exp Med. 2008; 205:2609–2621.
37. Biswas I, Singh B, Sharma M, Agrawala PK, Khan GA. Extracellular RNA facilitates hypoxia-induced leukocyte adhesion and infiltration in the lung through TLR3-IFN-gamma-STAT1 signaling pathway. Eur J Immunol. 45:3158–3173.
38. Nordsmark M, Overgaard M, Overgaard J. Pretreatment oxygenation predicts radiation response in advanced squamous cell carcinoma of the head and neck. Radiotherapy and oncology. 1996; 41:31–39.
39. De Schutter H, Landuyt W, Verbeken E, Goethals L, Hermans R, Nuyts S. The prognostic value of the hypoxia markers CA IX and GLUT 1 and the cytokines VEGF and IL 6 in head and neck squamous cell carcinoma treated by radiotherapy +/- chemotherapy. BMC cancer. 2005; 5:42.
40. Schrijvers ML, van der Laan BF, de Bock GH, Pattje WJ, Mastik MF, Menkema L, Langendijk JA, Kluin PM, Schuuring E and van der Wal JE. Overexpression of intrinsic hypoxia markers HIF1alpha and CA-IX predict for local recurrence in stage T1-T2 glottic laryngeal carcinoma treated with radiotherapy. International journal of radiation oncology, biology, physics. 2008; 72:161–169.
41. Wachters JE, Schrijvers ML, Slagter-Menkema L, Mastik M, de Bock GH, Langendijk JA, Kluin PM, Schuuring E, van der Laan BF and van der Wal JE. Prognostic significance of HIF-1a, CA-IX, and OPN in

T1-T2 laryngeal carcinoma treated with radiotherapy. Laryngoscope. 2013; 123:2154–2160.

42. Salaun B, Coste I, Rissoan MC, Lebecque SJ, Renno T. TLR3 can directly trigger apoptosis in human cancer cells. J Immunol. 2006; 176:4894–4901.

43. Butowski N, Chang SM, Junck L, DeAngelis LM, Abrey L, Fink K, Cloughesy T, Lamborn KR, Salazar AM, Prados MD. A phase II clinical trial of poly-ICLC with radiation for adult patients with newly diagnosed supratentorial glioblastoma: a North American Brain Tumor Consortium (NABTC01–05). J Neurooncol. 2009; 91:175–182.

44. Lacour J, Laplanche A, Malafosse M, Gallot D, Julien M, Rotman N, Guivarc'h M, Roullet-Audy JC, Lasser P, Hautefeuille P and et al. Polyadenylic-polyuridylic acid as an adjuvant in resectable colorectal carcinoma: a 6 1/2 year follow-up analysis of a multicentric double blind randomized trial. Eur J Surg Oncol. 1992; 18:599–604.

45. Friboulet L, Gourzones C, Tsao SW, Morel Y, Paturel C, Temam S, Uzan C, Busson P. Poly(I:C) induces intense expression of c-IAP2 and cooperates with an IAP inhibitor in induction of apoptosis in cancer cells. BMC cancer. 2010; 10:327.

46. Enot DP, Niso-Santano M, Durand S, Chery A, Pietrocola F, Vacchelli E, Madeo F, Galluzzi L, Kroemer G. Metabolomic analyses reveal that anti-aging metabolites are depleted by palmitate but increased by oleate *in vivo*. Cell Cycle. 14:2399–2407.

université PARIS-SACLAY | ÉCOLE DOCTORALE Cancérologie, biologie, médecine, santé (CBMS)

Titre : MicroARN circulants associés aux tumeurs solides: étude de leur potentiel comme biomarqueurs pour l'évaluation du pronostique et de la réponse au traitement

Mots clés : miARN, plasma, biomarqueurs, cancer ovarien, carcinome nasopharyngé

Résumé : Ce travail se focalise sur la biologie et la dynamique des miARN circulants, démontrant leur potentiel comme biomarqueurs précieux pour une meilleure évaluation du pronostique et de la réponse au traitement dans le cancer. Ces molécules minuscules simple-brin jouent un rôle crucial dans la régulation post-transcriptionnelle de l'expression génomique, ciblant et réprimant la traduction des ARNm par complémentarité de séquence. Leur libération extracellulaire et leur stabilité dans la circulation ont attiré l'attention sur eux, en tant que fournisseurs potentiels d'informations concernant leurs cellules d'origine dans diverses maladies, y compris le cancer. Travaillant sur deux projets distincts, nous avons étudié la dynamique et l'évolution des miARN plasmatiques chez des patients atteints de cancer ovarien en cours de traitement, ainsi que des changements dans l'expression des miARN viraux dans des modèles in vitro et in vivo de carcinome nasopharyngé associé à l'EBV. Chez le cancer de l'ovaire, nos résultats suggèrent une utilité du miR-200b dans la surveillance de la maladie, sa variation pendant le traitement étant prédictive de la survie sans progression des patients et pouvant être utilisée complémentairement au biomarqueur standard CA125 pour un suivi plus efficace. D'ailleurs, le traitement des carcinomes nasopharyngés par divers agents thérapeutiques a induit l'expression des miARN BHRF1 préalablement réprimés au génome latent de l'EBV dans les cellules malignes. Ces miARN étaient également détectables dans le plasma des souris traitées avant une réponse clinique visible, proposant un nouveau mode d'évaluation précoce du traitement.

Title: Circulating microRNAs associated to solid tumors: study of their potential as biomarkers for evaluation of prognosis and treatment response

Keywords: miRNA, plasma, biomarkers, ovarian cancer, nasopharyngeal carcinoma

Abstract: This work focuses on the biology and dynamics of circulating miRNAs, demonstrating their potential to become valuable biomarkers for better evaluation of prognosis and treatment outcome in cancer. These tiny single-stranded molecules play a crucial role in post-transcriptional regulation of gene expression, targeting and repressing mRNA translation via base complementarity. Their extracellular liberation and stability in circulation have attracted attention on them, as potential providers of information regarding their cells of origin in various diseases, including cancer. Working on two distinct projects, we studied the dynamics and evolution of plasma miRNAs in patients with ovarian cancer undergoing treatment, as well as changes in viral miRNA expression in treated vitro and vivo models of EBV-associated nasopharyngeal carcinoma. In ovarian cancer, our results suggest a special utility of miR-200b in the surveillance of the disease, as its variation throughout treatment proved to be predictive of the progression-free survival of the patients and could be used along with the standard biomarker CA125 for a more efficient follow-up. On the other hand, treatment of nasopharyngeal carcinoma with various therapeutic agents induced the expression of the previously silent BHRF1 miRNAs of the latent EBV genome found in the malignant cells. These miRNAs were even detectable in the plasma of treated mice before the onset of clinical response, providing potential for treatment evaluation at a very early stage.